

2000

DEVELOPMENT AND INVESTIGATION OF THE PROPERTIES OF AN ELECTROCHEMICALLY REGENERABLE CHEMICALLY MODIFIED ELECTRODE FOR CHEMELUMINESCENCE DETECTION OF ANALYTES IN SOLUTION

WILLIAMS, CLAIRE ELIZABETH

<http://hdl.handle.net/10026.1/1713>

<http://dx.doi.org/10.24382/1616>

University of Plymouth

All content in PEARL is protected by copyright law. Author manuscripts are made available in accordance with publisher policies. Please cite only the published version using the details provided on the item record or document. In the absence of an open licence (e.g. Creative Commons), permissions for further reuse of content should be sought from the publisher or author.

**DEVELOPMENT AND INVESTIGATION OF THE PROPERTIES OF AN
ELECTROCHEMICALLY REGENERABLE CHEMICALLY MODIFIED
ELECTRODE FOR CHEMILUMINESCENCE DETECTION OF ANALYTES
IN SOLUTION**

by

CLAIRE ELIZABETH WILLIAMS

A thesis submitted to the University of Plymouth
in partial fulfilment for the degree of

DOCTOR OF PHILOSOPHY

Department of Environmental Sciences,
Faculty of Science,
University of Plymouth, Drake Circus,
Plymouth, Devon PL4 8AA

December 2000

90 0453176 8



UNIVERSITY OF PLYMOUTH	
Item No.	900 4531768
Date	22 JAN 2001 S
Class No.	7 543.0871 WIL
Contl. No.	X 70419 1902
LIBRARY SERVICES	
REFERENCE ONLY	

LIBRARY STORE

ABSTRACT

DEVELOPMENT AND INVESTIGATION OF THE PROPERTIES OF AN ELECTROCHEMICALLY REGENERABLE CHEMICALLY MODIFIED ELECTRODE FOR CHEMILUMINESCENCE DETECTION OF ANALYTES IN SOLUTION

by

CLAIRE ELIZABETH WILLIAMS

The aim of this study was to exploit the sensitivity of the chemiluminescent ruthenium tris(2,2'-bipyridine) redox system for analytical purposes by producing electrochemically regenerable electrodes modified with a polymer derivative of this complex. Ruthenium tris(4-methyl-4'-vinyl-2,2'-bipyridine) bis(hexafluorophosphate) was synthesised and subsequently polymerised onto an electrode surface using the technique of cyclic voltammetry.

A potential was applied to the resulting Chemically Modified Electrode (CME) and upon reaction of the ruthenium centres with an analyte in solution, chemiluminescence was observed. Measurement of the emission intensity was used for the determination of the analyte concentration. The ruthenium centres were subsequently regenerated by the reversal of the applied potential. Very little environmentally unfriendly and expensive waste results from this process. This is in direct contrast with current methods which traditionally use the ruthenium tris(2,2'-bipyridine) complex either in solution or immobilised within a membrane for analyses of this type.

Attention was focused upon detection of the oxalate ion and the ruthenium tris(2,2'-bipyridine)/oxalate redox system reported in the literature was used as a model to investigate the capabilities of the CME's produced. A scan rate of 10 V/s between the potential limits of + 0.5 to + 1.5 V at pH 6.5 was established as the optimum conditions. A linear working range for oxalate was observed from 1.9×10^{-2} M to the limit of detection, 1.1×10^{-3} M. The lifetime of a CME was investigated and although the chemiluminescent signal diminished with time, the electrode was still functioning after 24 weeks, a total of over 200 regenerations. A series of amines and valine were also successfully detected using CME's.

In addition, a similar sensor was fabricated from the electropolymerization of a novel ruthenium complex, ruthenium tris(4-methyl-4'-(*E*-prop-2-enyl)-2,2'-bipyridine) bis(hexafluorophosphate). This was also shown to be capable of chemiluminescence emission and was successfully regenerated.

Two electrochemically regenerable CME's were therefore produced and this research is a valuable advance in the field of chemiluminescent detectors.

CONTENTS

	<u>Page Number</u>
Copyright Statement	i
Title Page	ii
Abstract	iii
Contents	iv
Tables	xiii
Figures	xv
Schemes	xx
Plates	xxi
Acknowledgments	xxii
Author's Declaration	xxiv
<u>CHAPTER 1: INTRODUCTION</u>	1
(1.1) Chemiluminescence	1
(1.1.1) Introduction	1
(1.1.2) Theory and Mechanism of Chemiluminescence	2
(1.1.3) Chemiluminescence Systems and Their Analytical Applications	6
(1.1.4) Electrochemiluminescence and Electrogenenerated Chemiluminescence	8
(1.2) The Ruthenium tris(2,2'-Bipyridine) Complex	10
(1.2.1) Introduction	10
(1.2.2) The Rôle of Ru(bpy) ₃ ²⁺ as a Light Absorption and Light Emission Sensitizer	11

	<u>Page Number</u>
(1.2.3) Chemiluminescence of Ru(bpy) ₃ ²⁺	12
(1.2.4) The Nature of the Ru(bpy) ₃ ²⁺ Excited State	13
(1.2.5) Generation of Chemiluminescence from Ru(bpy) ₃ ²⁺	14
(1.2.6) Use of Ru(bpy) ₃ ²⁺ for the Chemiluminescence Detection of Analytes	18
(1.2.6.1) The Oxalate Redox System	19
(1.2.6.1.1) <i>Detection Methods for Oxalate</i>	20
(1.2.6.1.2) <i>Detection of Oxalate Using the Ruthenium</i> <i>tris(2,2'-bipyridine) Complex</i>	21
(1.2.6.2) Detection of Amines and Amine-Based Pharmaceutical Products	23
(1.2.6.3) Detection of Amino Acids, Peptides and Proteins	24
(1.2.6.4) Detection of Other Analytes	25
(1.2.6.5) Uses of Ru(bpy) ₃ ²⁺ as a Chemiluminescent Label	26
(1.2.6.6) Methods of Utilising the Ruthenium tris(2,2'-bipyridine) Complex for Analyte Detection	26
(1.3) Chemically Modified Electrodes	31
(1.3.1) Introduction	31
(1.3.2) Applications of Chemically Modified Electrodes	32
(1.3.3) Methods for Preparation of Chemically Modified Electrodes	34
(1.4) Search for a Suitable CME for the Present Study	36
(1.4.1) Chemical Modification of an Electrode Surface Using the Ruthenium tris(2,2'-bipyridine) Complex	36
(1.4.2) Synthesis of a Monomer for Electropolymerization	39

	<u>Page Number</u>
(1.4.3) Electropolymerization of Ruthenium tris(4-methyl-4'-vinyl-2,2'-bipyridine) bis(hexafluorophosphate)	40
(1.5) Techniques Used in the Present Study	44
(1.5.1) Electropolymerization	44
(1.5.1.1) Formation of Polymer Films of Different Monomers and Their Applications	46
(1.5.1.2) The Structure of Polymer Films Formed from poly-[Ruthenium tris(4-methyl-4'-vinyl-2,2'-bipyridine) bis(hexafluorophosphate)]	47
(1.5.1.3) Mechanism of Formation of poly-[Ru(vbpy) ₃ ²⁺] and its Conduction	50
(1.5.2) Methods Used to Study the Formation of Chemically Modified Electrodes	52
(1.5.2.1) Cyclic Voltammetry	52
(1.6) Aim of the Present Study	55
<u>CHAPTER 2: SYNTHESIS OF RUTHENIUM TRIS(BIPYRIDINE) COMPLEXES</u>	56
(2.1) Critical Review of Methods for Synthesis of 4-methyl-4'-vinyl-2,2'-bipyridine	56
(2.2) Synthesis of 4-hydroxyethyl-4-methyl-2,2'-bipyridine using the Ghosh & Spiro method	65

	<u>Page Number</u>
(2.2.1) Introduction	65
(2.2.2) Experimental Procedure	67
(2.2.3) Results & Discussion	70
(2.2.4) Investigation of Paraformaldehyde Decomposition	75
(2.2.5) Investigation of Carbanion Production	78
(2.2.5.1) Use of Deuterated Water to Quantify Carbanion Production	79
(2.2.5.2) Investigation of the Effect of Using Excess Amounts of D ₂ O and Lithium Diisopropylamide on the Percentage of Deuterated Product	83
(2.2.5.3) Effect of Using Excess Lithium Diisopropylamide on the Yield of the Ghosh & Spiro Reaction	86
(2.2.6) Analogous Reaction Using 4-methylpyridine; Synthesis of 4-hydroxyethylpyridine	87
(2.2.7) Excerpts of Personal Communications Related to the Ghosh & Spiro Method	88
(2.3) Synthesis of 4-methoxy-4'-methyl-2,2'-bipyridine from 4,4'-dimethyl-2,2'-bipyridine	89
(2.3.1) Experimental Procedure	89
(2.3.2) Results	91
(2.3.3) Discussion	93
(2.4) Synthesis of 4-methyl-4'-vinyl-2,2'-bipyridine from 4-methoxyethyl-4'-methyl-2,2'-bipyridine	95

	<u>Page Number</u>
(2.4.1) Introduction	95
(2.4.2) Experimental Procedure	96
(2.4.3) Results	97
(2.4.4) Discussion	98
(2.5) Synthesis of Ruthenium tris(4-methyl-4'-vinyl-2,2'-bipyridine) bis(hexafluorophosphate)	101
(2.5.1) Introduction	101
(2.5.2) Experimental Procedure	102
(2.5.3) Results	102
(2.5.4) Discussion	103
(2.5.4.1) Calculation of the Ratio of Tris and Bis Complexes	108
(2.5.4.2) Mathematical Model for Prediction of Percentage Composition in a Mixture of Ruthenium tris(vinylbipyridine) Complexes	111
(2.6) Synthesis of Ruthenium tris(4-methyl-4'-(<i>E</i>-prop-2-enyl)- 2,2'-bipyridine) bis(hexafluorophosphate)	115
(2.6.1) Introduction	115
(2.6.2) Synthesis of 4-(2-hydroxypropyl)-4'-methyl-2,2'- bipyridine from 4,4'-dimethyl-2,2'-bipyridine	116
(2.6.2.1) Experimental Procedure	116
(2.6.2.2) Results	117
(2.6.2.3) Discussion	120

	<u>Page Number</u>
(2.6.3) Synthesis of 4-methyl-4'-(<i>E</i> -prop-2-enyl)-2,2'-bipyridine from 4-(2-hydroxypropyl)-4'-methyl-2,2'-bipyridine	120
(2.6.3.1) Experimental Procedure	120
(2.6.3.2) Results	121
(2.6.3.3) Discussion	123
(2.6.4) Synthesis of Ruthenium tris(4-methyl-4'-(<i>E</i> -prop-2-enyl) -2,2'-bipyridine) bis(hexafluorophosphate)	124
(2.6.4.1) Experimental Procedure	124
(2.6.4.2) Results	124
(2.6.4.3) Discussion	125
(2.7) Experimental Appendix	128
(2.7.1) Instrumentation and Techniques Used for Analysis	128
(2.7.2) Chemicals Used in this Study	130
 <u>CHAPTER 3: PREPARATION, DEVELOPMENT AND</u>	
<u>INVESTIGATION OF CHEMICALLY MODIFIED ELECTRODES</u>	
<u>COATED WITH RUTHENIUM TRIS(BIPYRIDINE) RELATED</u>	
<u>POLYMERS</u>	133
 (3.1) Electropolymerization	 133
(3.1.1) Introduction	133
(3.1.2) Initial Electropolymerization Procedure	133
(3.1.3) Electropolymerization Within a Glove Box	141

	<u>Page Number</u>
(3.1.4) Final Modifications of the Electropolymerization Procedure	142
(3.1.5) Electropolymerization of Ruthenium tris(4-methyl-4'-(<i>E</i> -prop-2-enyl)-2,2'-bipyridine) bis(hexafluorophosphate)	146
(3.1.6) Overall Discussion of the Electropolymerization Procedure	148
(3.2) Microscope Images of Chemically Modified Electrodes	149
(3.2.1) Microscopy	149
(3.2.2) Scanning Electron Microscopy	149
(3.3) Electrochemical Properties & Analytical Applications of Ruthenium tris(2,2'-Bipyridine) Solution (Ru(bpy)₃²⁺)	153
(3.3.1) Investigation of Chemiluminescence Emission from 0 mM, 0.1 mM and 0.1 M Oxalate Solutions	153
(3.3.2) Investigation of Chemiluminescence Emission from 0 mM, 0.1 mM and 0.1 M Oxalate Solutions Using a Reduced Potential Range	159
(3.4) Electrochemical Properties & Analytical Applications of Chemically Modified Electrodes	162
(3.4.1) Electrochemiluminescence of poly-[Ru(vbpy) ₃ ²⁺]	162
(3.4.2) Effect of Film Quality upon Electrochemical Properties	162
(3.4.3) Investigation and Optimization of the Electrochemical Properties of Chemically Modified Electrodes Using The Oxalate Redox System	163
(3.4.4) Effect of pH on Intensity of Chemiluminescence Emission	168
(3.4.4.1) Effect of pH on Intensity of Chemiluminescence Emission Using a Narrow pH Range	170

	<u>Page Number</u>
(3.4.5) Calibration & Limit of Detection Results	171
(3.4.5.1) Ru(bpy) ₃ ²⁺ Solution Calibration Data	171
(3.4.5.2) CME Calibration Data	174
(3.4.5.2.1) Investigation of a Preliminary CME	174
(3.4.5.2.2) Investigation of a More Developed CME	177
(3.4.6) Electrode Lifetime Study	178
(3.4.7) Detection of a Range of Analytes	181
(3.4.7.1) Introduction	181
(3.4.7.2) Experimental Procedure	181
(3.4.7.3) Results & Discussion	183
(3.4.7.3.1) Detection of Ascorbic and Citric Acid	183
(3.4.7.3.2) Detection of Amines	184
(3.4.7.3.3) Detection of Amino Acids	186
(3.5) Chemiluminescence of poly-[Ruthenium tris(4-methyl-4'-(<i>E</i> -prop-2-enyl)-2,2'-bipyridine) bis(hexafluorophosphate)]	188
(3.6) Experimental Appendix	190
(3.6.1) Instrumentation and Techniques Used for Analysis	190
(3.6.2) Chemicals Used in this Study	191
<u>CHAPTER 4: CONCLUSIONS AND FUTURE WORK</u>	193
(4.1) Summary	193
(4.2) Future Work	194

	<u>Page Number</u>
<u>REFERENCES</u>	201
<u>BIBLIOGRAPHY</u>	230

TABLES

	<u>Page number</u>
(1.1) The three electronic states arising from the $(\pi^*)^2$ electronic configuration of molecular oxygen.	4
(1.2) Analytical figures of merit for the detection of various analytes using ruthenium complex based sensors	30
(1.3) Applications of electrodes modified with poly-[Ru(vbpy) ₃ ²⁺]	41
(2.1) Comparison of efficiency of literature methods for the synthesis of 4-methyl-4'-vinyl-2,2'-bipyridine	65
(2.2) Percentage intensity values for the ¹³ C NMR methyl carbon signal at 20.4 - 20.9 ppm	82
(2.3) Percentage intensity values for the ¹³ C NMR methyl group signal at 20.5 - 21.0 ppm for the experiment using excess D ₂ O and Lithium Diisopropylamine	84
(2.4) Full NMR interpretation for 4-methyl-4'-vinyl-2,2'-bipyridine	99
(2.5) Full NMR interpretation for Ru(vbpy) ₃ ²⁺	104
(2.6) Proton ratios in a mixture of tris and bis complexes	109
(2.7) Proton ratios for the mixture of the ruthenium vinylbipyridine complexes	110
(2.8) Composition of a ruthenium vinylbipyridine complex based upon varying percentages of ligands 4-methyl-4'-vinyl-2,2'-bipyridine and 4,4'-dimethyl-2,2'-bipyridine	113
(2.9) Full NMR interpretation for Ru(ppbpy) ₃ ²⁺	126
(2.10) Table of chemicals and their preparation for use in this study	130

	<u>Page Number</u>
(3.1) Parameters used for the detection of the analytes determined in this study	182
(3.2) Variation of parameters for the detection of ascorbic acid	183
(3.3) Chemiluminescence observed for the detection of amines	185
(3.4) Chemiluminescence observed for the detection of the amino acids	187
Tryptophan and Valine	
(3.5) Table of chemicals and their preparation for use in this study	191

FIGURES

	<u>Page number</u>
(1.1) Equation showing the relationship between photochemistry and chemiluminescence	1
(1.2) A molecular orbital diagram for the oxygen molecule, O ₂	3
(1.3) The luminol reaction	5
(1.4) Mechanism of peroxide decomposition resulting in chemiluminescence	5
(1.5) A typical electron transfer reaction	6
(1.6) Ruthenium tris(2,2'-bipyridine) complex, Ru(bpy) ₃ ²⁺	10
(1.7) Use of Ru(bpy) ₃ ²⁺ for the photochemical decomposition of water	12
(1.8) Reaction showing chemiluminescence from the Ruthenium tris(2,2'-bipyridine) complex	13
(1.9) Generation of chemiluminescence from the Ru(bpy) ₃ ²⁺ system by reaction of the +3 state with the +1 state	14
(1.10) Generation of chemiluminescence from the Ru(bpy) ₃ ²⁺ system by reaction of the +3 state with a reducing agent	15
(1.11) Generation of chemiluminescence from the Ru(bpy) ₃ ²⁺ system by reaction of the +1 state with an oxidising agent	15
(1.12) Redox potentials for the ground and lowest excited states of Ru(bpy) ₃ ²⁺	17
(1.13) The oxalate anion	19
(1.14) Alternative mechanisms of the reaction of Ru(bpy) ₃ ²⁺ with oxalate	21
(1.15) Summary of the mechanism of the reaction of Ru(bpy) ₃ ²⁺ with oxalate	22
(1.16) Mechanism of the reaction of Ru(bpy) ₃ ²⁺ with peroxydisulphate	25
(1.17) Structure of the cation-exchange polymer, Nafion	27

	<u>Page Number</u>
(1.18) Regeneration of the ruthenium complex after the chemiluminescence reaction has taken place	28
(1.19) Methods for preparation of chemically modified electrodes	35
(1.20) Formation of polymer modified electrodes from redox polymers	38
(1.21) Proposed use of poly-[Ru(vbpy) ₃ ²⁺]-coated electrodes	43
(1.22) Mechanism of the proposed use of poly-[Ru(vbpy) ₃ ²⁺]-coated electrodes in terms of a simple molecular orbital diagram	44
(1.23) Schematic drawing of poly-[Ru(vbpy) ₃ ²⁺] assuming (A) linear vinyl coupling and (B) dimer-bridge vinyl coupling	48
(1.24) Electron transfer through the conjugated polymer system to the electrode	51
(1.25) Waveform for a potential sweep experiment	52
(1.26) IUPAC convention for cyclic voltammograms	53
(1.27) A typical cyclic voltammogram	54
(2.1) Enlargement of ¹³ C NMR signal at 20 - 21 ppm	82
(2.2) Enlargement of DEPT NMR signal at 20 - 21 ppm	82
(2.3) The four possible ruthenium complexes obtained by complexing a mixture of the ligands 4-methyl-4'-vinyl-2,2'-bipyridine (ii) and 4,4'-dimethyl-2,2'-bipyridine (vi)	107
(2.4) Graph of relative percentages of ruthenium vinylbipyridine complexes based upon relative percentages of ligands 4-methyl-4'-vinyl-2,2'-bipyridine and 4,4'-dimethyl-2,2'-bipyridine	112

	<u>Page Number</u>
(2.5) Facial (Fac) & meridional (Mer) isomers of Ruthenium tris(4-methyl-4'-vinyl-2,2'-bipyridine) bis(hexafluorophosphate)	114
(3.1) Initial experimental arrangement for electropolymerization	134
(3.2) Cyclic Voltammogram obtained from the electropolymerization of 0.1 mM Ru(vbpy) ₃ ²⁺ in 0.1 M tetraethylammonium perchlorate in acetonitrile	139
(3.3) Cyclic Voltammogram of the conductance of the CME produced in figure (3.2), placed in 0.1 M tetraethylammonium perchlorate	140
(3.4) Cyclic Voltammogram obtained from the electropolymerization of 0.1 mM Ru(vbpy) ₃ ²⁺ in 0.1 M tetrabutylammonium perchlorate in acetonitrile	144
(3.5) Cyclic Voltammogram of the conductance of the CME produced, (figure 3.4) in fresh 0.1 M tetrabutylammonium perchlorate	145
(3.6) Cyclic Voltammogram obtained from the electropolymerization of 0.1 mM Ru(ppbpy) ₃ ²⁺ in 0.1 M tetrabutylammonium perchlorate	147
(3.7) Experimental arrangement for chemiluminescence detection	154
(3.8) Comparison of chemiluminescence emission obtained using solutions of 1 mM Ru(bpy) ₃ ²⁺ in 0.1 M acetate buffer using different scan rates [0 M oxalate]	156
(3.9) Comparison of chemiluminescence emission obtained using solutions of 0.1 mM oxalate in 1 mM Ru(bpy) ₃ ²⁺ /0.1 M acetate buffer using different scan rates	157

	<u>Page Number</u>
(3.10) Comparison of chemiluminescence emission obtained using solutions of 0.1 M oxalate in 1 mM Ru(bpy) ₃ ²⁺ /0.1 M acetate buffer using different scan rates	158
(3.11) Comparison of chemiluminescence emission obtained using solutions of 0.1 mM oxalate in 1 mM Ru(bpy) ₃ ²⁺ /0.1 M acetate buffer using different scan rates and a reduced potential range	160
(3.12) Comparison of chemiluminescence emission obtained using solutions of 0.1 M oxalate in 1 mM Ru(bpy) ₃ ²⁺ /0.1 M acetate buffer using different scan rates and a reduced potential range	161
(3.13) Comparison of chemiluminescence emission obtained using a CME in 0.1 M acetate buffer using different scan rates [0 M oxalate]	165
(3.14) Comparison of chemiluminescence emission obtained using a CME in a solution of 0.1 mM oxalate in 0.1 M acetate buffer using different scan rates	166
(3.15) Comparison of chemiluminescence emission obtained using a CME in a solution of 0.1 M oxalate in 0.1 M acetate buffer using different scan rates	167
(3.16) Change in chemiluminescence emission with varying pH	169
(3.17) Change in chemiluminescence emission with varying pH (narrow range)	170
(3.18) Calibration graph for Ru(bpy) ₃ ²⁺ /oxalate system, scan measurements performed at 0.1 V/s	173
(3.19) Calibration graph for Ru(bpy) ₃ ²⁺ /oxalate system, scan measurements performed at 10 V/s	173
(3.20) Calibration graph for a preliminary CME, scan measurements performed at 0.1 V/s	176

	<u>Page Number</u>
(3.21) Calibration graph for a preliminary CME, scan measurements performed at 10 V/s	176
(3.22) Graph of electrode performance over a period of time	179
(3.23) Average chemiluminescence response over a period of days	180
(3.24) Structure of two amino acids, valine (Val) and tryptophan (Trp)	186
(3.25) Chemiluminescent response of CME coated with poly-[Ru(ppbpy) ₃ ²⁺] in a solution containing 0 M oxalate	188
(3.26) Chemiluminescent response of CME coated with poly-[Ru(ppbpy) ₃ ²⁺] in a solution containing 0.1 M oxalate	189

SCHEMES

	<u>Page number</u>
(2.1) Ghosh & Spiro synthesis of 4-methyl-4'-vinyl-2,2'-bipyridine	57
(2.2) Synthesis of 4-methyl-4'-vinyl-2,2'-bipyridine using the method reported by Furue <i>et al.</i>	58
(2.3) Synthesis of 4-methyl-4'-vinyl-2,2'-bipyridine using the method reported by Kaschig & Lohmann	60
(2.4) Synthesis of 4-methyl-4'-vinyl-2,2'-bipyridine using the method reported by Pitt <i>et al.</i>	62
(2.5) Synthesis of 4-methyl-4'-vinyl-2,2'-bipyridine using the method reported by Abruña <i>et al.</i>	63
(2.6) Synthesis of 4-methyl-4'-vinyl-2,2'-bipyridine using the method reported by Leasure <i>et al.</i>	64
(2.7) Synthesis of Ruthenium tris(4-methyl-4'-vinyl-2,2'-bipyridine) bis(hexafluorophosphate) using the method reported by Bommarito <i>et al.</i>	102
(2.8) Probabilities of formation of ruthenium vinylbipyridine complexes	111
(2.9) Synthesis of 4-methyl-4'-(<i>E</i> -prop-2-enyl)-2,2'-bipyridine using the method reported by Ghosh & Spiro	116

PLATES

	<u>Page number</u>
(2.1) The paraformaldehyde unit	68
(3.1) Empty electrochemical cell used for electropolymerization, horizontal position	136
(3.2) Electrochemical cell used for electropolymerization, vertical position	137
(3.3) Microscope image of a preliminary CME	150
(3.4) Microscope image of a more developed CME	150
(3.5) Scanning Electron Microscope image of poly-[Ruthenium tris(4-methyl-4'-vinyl-2,2'-bipyridine) bis(hexafluorophosphate)], x 5500 magnification, accelerating voltage of the electron beam, 20 kV	151
(3.6) Scanning Electron Microscope image of poly-[Ruthenium tris(4-methyl-4'-(<i>E</i> -prop-2-enyl)-2,2'-bipyridine) bis(hexafluorophosphate)], x 5500 magnification, accelerating voltage of the electron beam, 15 kV	152

ACKNOWLEDGMENTS

I would like to thank the University of Plymouth for funding this research. In particular, I would like to express my sincere and grateful thanks to the following people:

Firstly, to my main supervisor, Dr Roy Lowry, for his patience and encouragement over the course of my research. His enthusiasm and reassurance have been much appreciated. I would also like to thank my second supervisor, Dr Jim Braven, for all his help and advice, particularly in the early stages of the synthetic work. Thank you both for your support and guidance.

My thanks to Dr Simon Belt, my unofficial third supervisor, for all his help with NMR interpretation and to all other members of staff for useful discussions.

I would like to acknowledge the excellent support from the technical staff; Dr Roger Evens, Mr Roger Srodzinski, Dr Jeremy Clark, Mr Ian Doidge, Miss Sally Madgwick, Mr Andrew Tonkin and Mr Andy Arnold. Their help with use and repair of instrumentation and with general practical work has made my work easier and is much appreciated.

Many thanks to Mr Ron Neale and Mr David Johns from SECEE for the loan of the PMT equipment, Mr Paul Russell and Mr Mike Hockings for use of the optical microscope, Dr Roy Moate and Mr Peter Bond of the Electron Microscopy Unit and Mr Roger Bowers for production of the electrochemical cell and electrodes.

I would like to acknowledge past and present friends and colleagues of the Department of Environmental Sciences. Thanks to Dr. Pete Sutton for helpful discussions and to Mr. Joe Morrish for his help. In particular, a big thank you to 'Uncle' Neil Chilcott Ph.D for his help with computer-related matters. I also wish to thank him for

being a true friend over the last few years. Never have I owed one person so many pints of cider. Also a big '*merci beaucoup*' to *mon ami* Dr Thierry Le Goff. I would like to thank my long-suffering French co-worker for being there, particularly in times of darkness (and there were many). Cheers mate! Thanks also to Mark 'Cedric' Williams for mad excursions around Dartmoor and laughs about bunnies, bay leaves, fishing and marrows. Thank you to James Murphy for helpful advice, to Eileen Smith for girly chats and to all those friends not mentioned here but not forgotten.

I would like to acknowledge Stafford-Miller Ltd. for employing me on a part-time basis and for their understanding attitude regarding my need for flexible working hours. Thanks also to all my friends and colleagues at the company for their support.

Finally, I would like to thank my family for their unending support over the past few years. In particular, to Mum and Dad for their constant love and support. Couldn't have done it without you, love you both lots xxxx. My student days are nearly over, honest!

*'...I have seen that in any great undertaking it is not enough
for a man to depend simply upon himself.'*

Lone Man [Isna la-wica] (late 19th century)

Teton Sioux, Native American Indian

AUTHOR'S DECLARATION

At no time during the registration for the degree of Doctor of Philosophy has the author been registered for any other University award.

This study was financed with the aid of a studentship from the University of Plymouth.

A programme of advanced study was undertaken which included supervised training in advanced techniques for organic synthesis, NMR, GC, GC-MS, IR and cyclic voltammetry, advanced organic chemistry tutorials (Disconnection approach) and presentation skills.

Relevant scientific seminars and conferences were attended and work presented on two occasions. A paper has been prepared for publication.

Publications:

Williams, C.E., Lowry, R.B., Braven, J. & Belt, S.T.; *In press*:

'Novel Synthesis and Characterisation of Ruthenium tris(4-methyl-4'-vinyl-2,2'-bipyridine) Complexes.'

Presentation and Conferences Attended:

Department of Environmental Sciences weekly research seminars.

University of Plymouth, September 1996 - September 1999 (term-time)

Royal Society of Chemistry (Penninsula Section) lectures.

University of Plymouth, September 1996 - September 1999.

'Water, Water Everywhere! Sensing and Making Sense of the Aquatic Environment.'

The Western Region of the Analytical Division joint with the Electroanalytical Group and Zeneca Ltd. Brixham Environmental Laboratory, Zeneca Ltd. April 1998

'The Fourth Bill Carruthers' Half-Day Symposium.'

University of Exeter, April 1998

'Electrochem '99'

University of Portsmouth, September 1999

Oral presentation given; 'Immobilisation of Electrochemically Regenerable Compounds for Chemiluminescence Analysis.'

'Thin Solid Films'

Nottingham University, September 1999

Poster presented.

Signed... *C.E. Williams*

Date... *11/01/01*

CHAPTER 1

INTRODUCTION

(1.1) CHEMILUMINESCENCE

(1.1.1) Introduction

Man has always held a fascination for the phenomenon of light, its sources and its effects on his surroundings¹. Luminescence is a generic term that covers a range of processes which produce light. These processes have been discussed in a review by Robards & Worsfold². Over a century ago, it was discovered that several simple organic compounds were capable of exhibiting chemiluminescence (CL). This has been defined simply as the luminescence that arises during the course of a chemical reaction³. Bioluminescence is a special type of CL found in biological systems; it is the natural emission of light from various living plants and animals, such as the fire-fly, marine organisms and bacteria.

A substantial fraction of chemical literature deals with reactions involving light. This general area is known as photochemistry. A CL process is simply the reverse of a photochemical process, as shown in Figure 1.1:

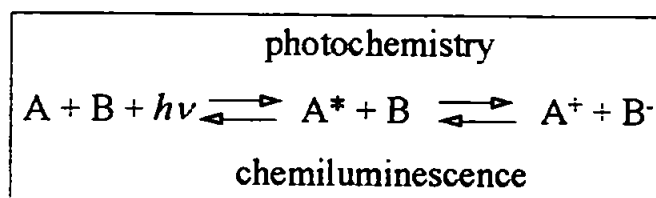


Figure 1.1: Equation showing the relationship between photochemistry and chemiluminescence

(1.1.2) Theory and Mechanism of Chemiluminescence

A detailed introduction to CL may be found in the Encyclopaedia of Analytical Science^{4,5}.

Reactions that produce CL are relatively uncommon as most chemical reactions release energy as heat via vibrational excitation of ground-state products. A CL reaction produces light which is not accompanied by the release of heat.

The first step of the CL process is electron transfer. In the example shown below, the cation and anion of compounds A and B react and chemical energy is converted to electronic excitation energy. The result is the formation of an excited state intermediate A* and B is converted to its uncharged state:



If the decay of an excited product to its ground state occurs radiatively, then the electron transfer may be accompanied by emission of a photon. This is the second stage of the CL process:



The wavelength of the light emitted lies usually within the visible region of the electromagnetic spectrum, for example, the luminol reaction emits blue light at 425 nm.⁵ However, this is not always the case. The light emitted from the reaction of ozone with nitric oxide lies in the infrared region and reaction of ozone with sulfur monoxide extends into the ultra-violet region.⁵

The intensity of the light emission varies for each individual CL system and is sensitive to environmental conditions, such as the solvent used or the presence of quenchers. The rate of production depends on the rate and efficiency of the CL reaction.

This efficiency is known as the quantum yield (ϕ_{CL}). It is defined as the number (or rate) of molecules emitting light divided by the number (or rate) of molecules reacting³. The quantum yield is expressed either as a value between 0 and 1 or as a percentage. It is generally in the range 1 - 5 % for CL reactions, in contrast to the more efficient bioluminescent systems, where quantum yields approach 100 %.

CL requires the prior or simultaneous presence of an oxidant. There are three basic mechanisms for producing CL.

(1) Oxygen as an Oxidant in CL Reactions.

This is the most common mechanism. The molecular orbital diagram of oxygen is shown in Figure 1.2 below.

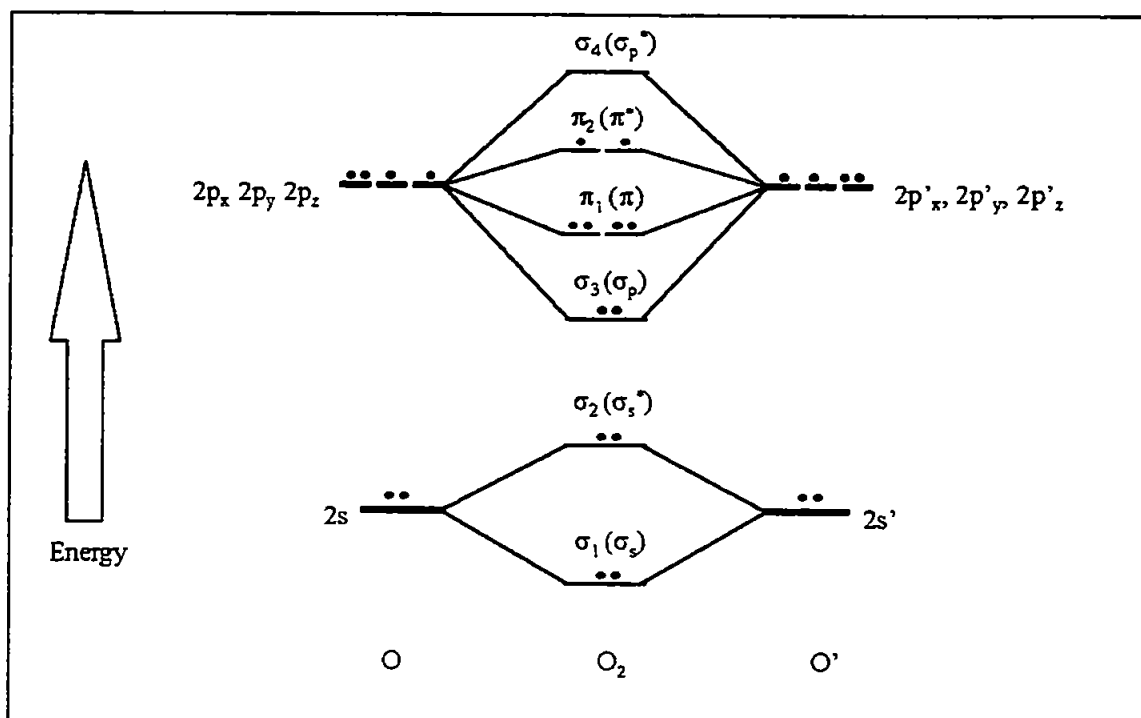


Figure 1.2: A molecular orbital diagram for the oxygen molecule, O_2 . Adapted from ref.⁶

The oxygen molecule contains two unpaired electrons in the π^* molecular orbitals. Three electronic states are therefore possible and are shown in Table 1.1 overleaf. A triplet state

(T_0) is in the ground state and two singlet excited states (S_1 and S_2) are available at higher energies. A triplet state has two unpaired electrons with the same spin, a singlet state may or may not have all its electrons paired but the total spin is zero.

STATE	π_x^*	π_y^*	ENERGY
S_2	↑	↓	155 kJ (~ 13000 cm^{-1})
S_1	↑↓		92 kJ (~ 8000 cm^{-1})
T_0	↑	↑	0 (Ground state)

Table 1.1: The three electronic states arising from the $(\pi)^2$ electronic configuration of molecular oxygen. Taken from ref.⁶

Generation of an excited singlet state from a triplet state is 'forbidden' according to the selection rule which states that the spin must not change during an electronic transition. However, in some cases this is known to occur, as with singlet oxygen. When either the S_1 or S_2 states is generated, because the transition is forbidden, the promoted electron spends an extended period of time in the excited state before falling to the ground state. The long lifetimes of these excited states S_1 and S_2 allow them to be useful for reactions with a variety of substrates. The energy can be transferred to another molecule (e.g. a fluorescent compound) where transition from its excited state to the ground state is allowed. The lifetime of this excited state is short and results in the emission of a photon. This type of reaction is called a sensitized CL reaction.

Perhaps the best known example of the use of oxygen in a CL process is the oxidation of luminol (5-amino-2,3-dihydrophthalazine-1,4-dione). In basic aqueous solution and in the presence of oxygen, this gives rise to the emission of an intense blue light. This is shown in Figure 1.3 overleaf.

(3) Electron Transfer Reactions Involving Other Oxidants

Electron transfer reactions play a fundamental rôle in chemistry and are very important in the connections between chemistry and light. In a typical electron transfer reaction, an electron is withdrawn from the Highest Occupied Molecular Orbital (HOMO). However, in CL reactions, an electron is taken from a lower orbital and an electron from a higher orbital fills its place, releasing a photon of light. The initial electron is removed using an oxidizing agent with a lower lying molecular orbital than that of the reactant. An example of an electron transfer reaction involves 9,10-diphenylanthracene (DPA) and the Wurster's Blue cation (the cation radical of N,N,N',N'-tetramethyl-p-phenylenediamine (TMPD)) as an oxidant:

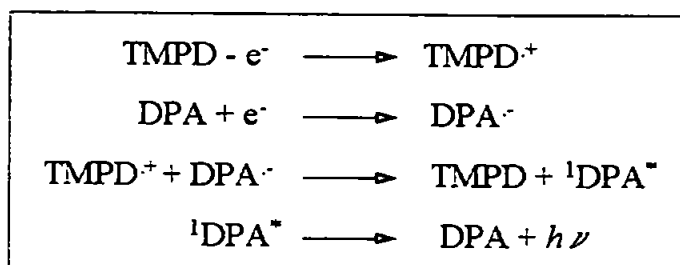


Figure 1.5: A typical electron transfer reaction

The use of an oxidizing agent can be replaced by an electrode. Electrons can be electrochemically added or removed from the orbitals by applying a potential. This is discussed fully in section 1.1.4 (page 8).

(1.1.3) Chemiluminescence Svstems and Their Analytical Applications

CL has for a long time been established as a method for the analysis of a wide range of compounds in both the liquid and the gas phase. Solid-state CL is more recent - CL from polymers has a history covering only three decades. Analytical use of CL first began in the 1970s and the applications are far-reaching, spanning toxicological,

environmental and biochemical areas. Many species can be detected using this method, including metal ions, inorganic anions and pharmaceutical drugs and organic compounds. CL intensity is dependent on the rate of the CL reaction, which in turn is dependent upon the concentration of the species present and can therefore be used quantitatively to determine the concentration of the analyte of interest. Emission intensity can be maximised by optimising parameters such as concentration and pH.

Flow Injection Analysis (FIA) often utilises liquid phase CL reactions. High Performance Liquid Chromatography (HPLC), and more recently, capillary electrophoresis (CE) and supercritical fluid chromatography (SFC) are other methods with which CL detection can be coupled.

Although much less widely applicable than absorption methods because of the relatively limited number of CL systems, there are several advantages of using CL detection as an analytical method;

- **Radiation source not required** - this reduces or eliminates Raman and Rayleigh scattering.
- **Simple and inexpensive instrumentation** required for CL measurement
- **No source or background noise** (however, chemical and background noise are present, thus reagents and solvents used must be of high purity)
- **Speed of response** - in many cases, light is produced almost instantaneously
- **Wide linear dynamic ranges**
- **Extreme sensitivity** - limits of detection can be sub-femtomoles in some cases, due to the ability to detect single photons

Another application of CL includes the production of 'cold light' sources, e.g. lightsticks based on CL reactions which provide a source of light when camping or in similar situations.

Comprehensive reviews of the details of many CL systems have been published^{2-5,9}. Some of the most popular reactions are based upon cyclic acyl hydrazides (e.g. luminol, as discussed previously) and acridine derivatives (e.g. lucigenin).

(1.1.4) Electrochemiluminescence and Electrogenerated Chemiluminescence

In many analytically useful CL systems, one or more of the reactants can be generated electrochemically. This can be termed either as electrochemiluminescence or electrogenerated chemiluminescence. These terms are very similar and many literature sources often use the two terms interchangeably. Robards & Worsfold² gave distinct definitions for each, whereas Knight¹⁰ reported that the two terms are general and describe a variety of different mechanisms. For the purposes of this current study, the term electrochemiluminescence (ECL) as defined by Jirka & Nieman¹¹ for electrogenerated chemiluminescence will be used:

*'the reaction is initiated either by direct reaction of a CL reagent at the electrode or by electrogeneration of a requisite reagent which then reacts with other species in solution.'*¹¹

An ECL reaction is initiated by application of a potential to an electrode and the reagent(s) are produced *in situ*, whereas for CL, the reaction is begun by simple mixing. Rozhitskii discussed the principles of the technique of ECL, reviewed systematically the publications on ECL analysis and considered the prospects for further use of the method¹². The occurrence, mechanisms and analytical applications of a wide range of

electrogenerated CL reactions have been reviewed¹³, followed by a review of recent trends in the analytical applications⁷.

Many of the analytical characteristics and advantages of the use of the CL technique also apply to ECL. Further advantages include¹⁰:

- **The CL can be controlled by alterations to the applied potential.** A potentiostat can be used to modulate the potential of a working electrode which generates a key species in the ECL reaction.
- **Active reagents can be produced *in situ*.** This reduces the number of reagents required.
- **Spatial control of CL emission.** This can be controlled because of the rôle of the electrode in initiating the reaction.
- **Temporal control.** The ECL reaction can be turned 'on' and 'off' as desired.
- **Some CL reagents can be electrochemically regenerated at the electrode.** This allows them to take part in the CL reaction with the analyte once again, reducing the need for fresh reagent.

As with any technique, there are disadvantages and problems¹⁰. These include the presence of species which interfere either constructively or destructively in the ECL reaction or the fouling of an electrode surface leading to problems in reproducibility. The fact that the exact mechanisms of many reactions are not known can also be a problem when trying to investigate structure-activity relationships.

Despite these problems, the number of papers which describe the use of the technique of ECL is ever-increasing.

There are four main systems which have been investigated analytically¹³:

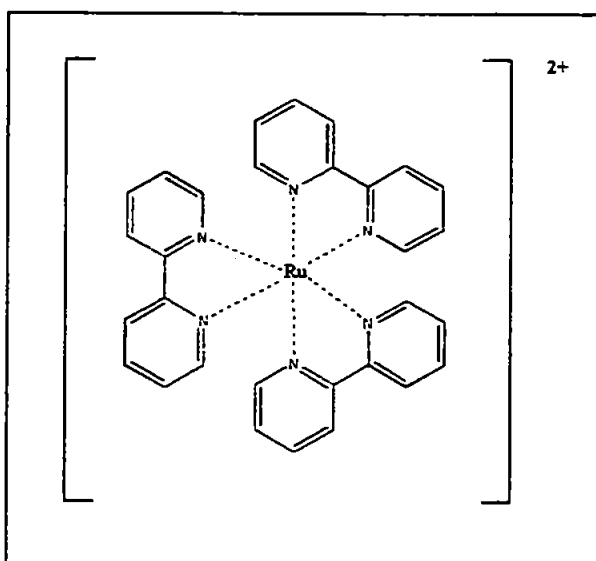
- (1) ECL of polyaromatic hydrocarbons
- (2) Methods based on the luminol reaction
- (3) Ruthenium tris(2,2'-bipyridine)
- (4) Cathodic luminescence at an oxide covered aluminium electrode.

This study will focus upon the third category which is discussed in the following section.

(1.2) THE RUTHENIUM TRIS(2,2'-BIPYRIDINE) COMPLEX

(1.2.1) Introduction

Ruthenium, a second-row transition element, is one of the platinum-group metals and is capable of forming complexes with many different ligand types. Amongst these, the 2,2'-bipyridine molecule is a well-known chelating agent¹⁴. The focus of this current study is the ruthenium tris(2,2'-bipyridine) complex, (i), shown below in Figure 1.6. In this complex, three bipyridine ligands surround a ruthenium centre in an octahedral arrangement.



(i)

Figure 1.6: Ruthenium tris(2,2'-bipyridine) complex, $\text{Ru}(\text{bpy})_3^{2+}$

The general chemistry of complexes containing 2,2'-bipyridine ligands can be found in a number of texts¹⁴⁻¹⁶.

Ruthenium tris(2,2'-bipyridine) chloride hexahydrate was first synthesised by Burstall¹⁷ in 1936. The structural details of this complex have since been recorded¹⁸ and further spectroscopic data is given in a review by Krausz & Ferguson¹⁹.

The chemical stability of the ruthenium complex in the +2 and +3 oxidation states and its redox activity are of particular interest. These characteristics have been the subject of a number of comprehensive reviews¹⁸⁻²¹. Ruthenium polypyridine complexes play a key rôle in many important areas, including photochemistry, photocatalysis and electron and energy transfer²²⁻²⁴.

(1.2.2) The Rôle of Ru(bpy)₃²⁺ as a Light Absorption and Light Emission Sensitizer

The ruthenium tris(2,2'-bipyridine) complex is used as an excited-state reactant in energy and electron-transfer processes and as a mediator in the interconversion of light and chemical energy. Considerable research has centred around its use as a photosensitizer in the photochemical decomposition of water, using visible light, into oxygen and hydrogen^{18,22}. This is depicted in Figure 1.7 overleaf.

The splitting of water into its constituents would not occur ordinarily as water cannot absorb visible radiation. However, use of Ru(bpy)₃²⁺ as a photosensitizer makes this possible as it is thermodynamically capable of both oxidizing and reducing water at pH 7. Photosensitizers are molecules which absorb radiation from a source and transfer the energy absorbed to other acceptor molecules. This is a very attractive route for the conversion of solar energy into chemical energy. Further details can also be found in various texts²²⁻²⁶.

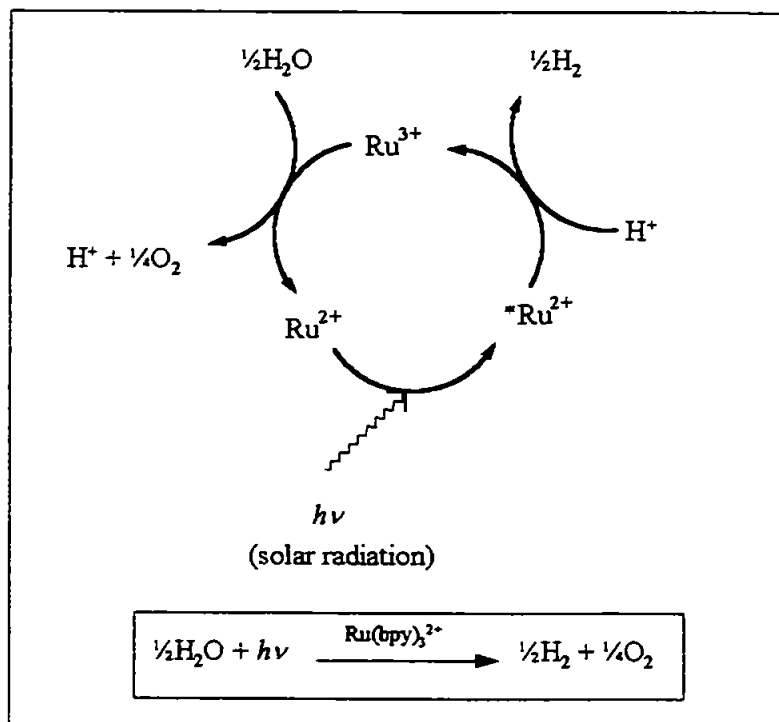
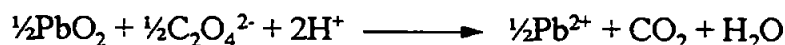


Figure 1.7: Use of $\text{Ru}(\text{bpy})_3^{2+}$ for the photochemical decomposition of water. Taken from ref.²²

The ruthenium complex can also act as a light emission sensitizer to transform potential CL reactions into effective CL reactions²². For example, the reduction of lead dioxide by oxalate ions in acid medium has the potential to generate visible light but instead produces heat because the reaction products are unable to emit light.



However, if the reaction is carried out in the presence of $\text{Ru}(\text{bpy})_3^{2+}$, it becomes the emitting species and CL is observed.

(1.2.3) Chemiluminescence of $\text{Ru}(\text{bpy})_3^{2+}$

CL has been observed from the reactions of many transition metal complexes (ruthenium, osmium, rhodium, platinum, palladium and iridium) containing bipyridine or related ligands. The photoluminescent properties of $\text{Ru}(\text{bpy})_3^{2+}$ were not discovered until

1959 by Paris & Brandt²⁷, 23 years after its initial synthesis. The first account of chemically induced luminescence from $\text{Ru}(\text{bpy})_3^{2+}$ was reported by Hercules & Lytle²⁸ in 1966. An aqueous, acidic solution of the ruthenium complex was oxidized from the more stable +2 state to the +3 state by lead dioxide and subsequently reacted with aqueous base. A bright orange CL emission at 610 nm, lasting less than a second, was observed.

Figure 1.8 shows this reaction:

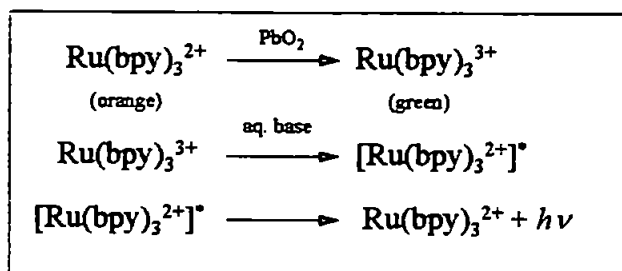


Figure 1.8: Reaction showing chemiluminescence from the ruthenium tris(2,2'-bipyridine) complex

The first example of ECL derived from the electrogenerated species of $\text{Ru}(\text{bpy})_3^{2+}$ in acetonitrile solution was reported²⁹ in 1972 and since then, $\text{Ru}(\text{bpy})_3^{2+}$ has been the most widely studied inorganic ECL to date. In comparison with systems such as luminol, it is a useful CL reagent because it does not decompose or undergo molecular rearrangement during the reaction.

(1.2.4) The Nature of the $\text{Ru}(\text{bpy})_3^{2+}$ Excited State

An electronically excited state usually differs from the corresponding ground state molecule by having an electron in a high energy (anti-bonding or non-bonding) orbital and a hole in a low energy (bonding) orbital. Since the discovery of CL emission from the ruthenium tris(2,2'-bipyridine) complex, the nature of the mechanism of the formation of the excited state $[\text{Ru}(\text{bpy})_3^{2+}]^*$ has been the subject of much discussion³⁰. The conclusion

reached is that the excited state is a very short-lived triplet which arises from a localised metal to ligand charge transfer (MLCT) process. An electron is promoted from the t_{2g} (d^6) orbital on the ruthenium to the vacant, low-lying π^* antibonding orbital on the ligand. This $d\pi^*$ charge transfer state has a reported lifetime of between 0.6×10^{-6} and 5×10^{-6} seconds³¹. Details of the properties and reactivity of the luminescent excited state of polypyridine complexes of Ru(II) have been reported by Sutin & Creutz³².

The excited state is very useful as its lifetime is long enough to be exploited in chemical reactions. The reactive species $\text{Ru}(\text{bpy})_3^+$ and $\text{Ru}(\text{bpy})_3^{3+}$ can be obtained easily from $[\text{Ru}(\text{bpy})_3^{2+}]^*$ as electron transfer is rapid and structural differences are small.

(1.2.5) Generation of Chemiluminescence from $\text{Ru}(\text{bpy})_3^{2+}$

The excited state and hence CL can be generated by using any of the following three methods³:

(1) Reaction of the +3 with the +1 oxidation state

By pulsing the potential between the oxidation and reduction potentials of $\text{Ru}(\text{bpy})_3^{2+}$, the oxidized and reduced forms can be created easily. Both can subsequently undergo a comproportionation reaction. Of the two $\text{Ru}(\text{bpy})_3^{2+}$ species produced, one is in the ground state and the other is in the excited state. The latter species subsequently decays, resulting in the emission of a photon. This is shown in Figure 1.9 below:

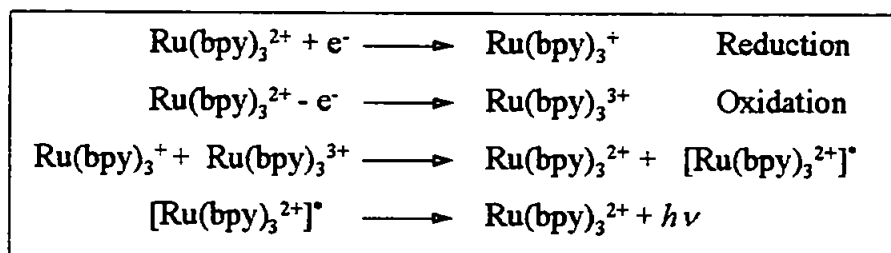


Figure 1.9: Generation of chemiluminescence from the $\text{Ru}(\text{bpy})_3^{2+}$ system by reaction of the +3 state with the +1 state.

This mechanism was investigated^{33,34} and the quantum yield was estimated to be 0.05 in acetonitrile at 25 °C. This is a relatively high yield compared with other CL systems.

(2) Reaction of the +3 oxidation state with reducing agents.

The substrate S is initially oxidized by the ruthenium complex in the +3 oxidation state to form a strong reductant R[·] and another molecule X. Reaction of R[·] with the ruthenium (III) complex generates the excited state which then decays and light emission is observed.

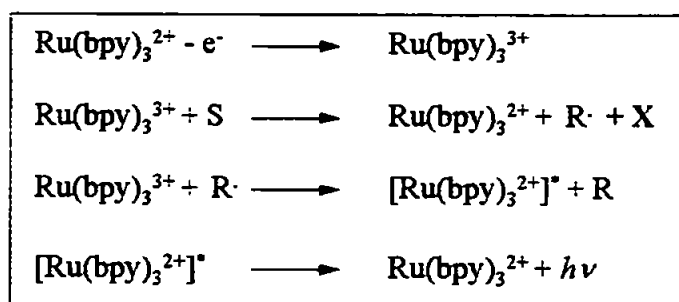


Figure 1.10: Generation of chemiluminescence from the $\text{Ru}(\text{bpy})_3^{2+}$ system by reaction of the +3 state with a reducing agent.

An example of this mechanism is discussed in section 1.2.6.1.2 (page 21).

(3) Reaction of the +1 oxidation state with oxidising agents

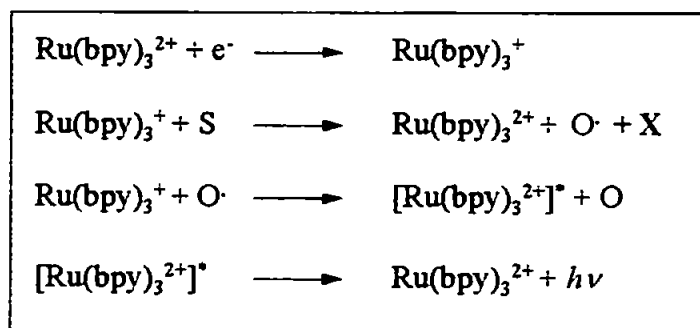


Figure 1.11: Generation of chemiluminescence from the $\text{Ru}(\text{bpy})_3^{2+}$ system by reaction of the +1 state with an oxidising agent.

In this case, the substrate S is reduced by the ruthenium complex in the +1 oxidation state to form a strong oxidant O' . This reacts with further ruthenium (I) complex to produce to the excited state. The +2 state is regenerated upon decay of this excited state to produce a photon of light. An example of this mechanism is discussed in section 1.2.6.4 (page 25).

Methods (1) and (2) are more common than method (3) and both involve production of the ruthenium +3 state. This state is unstable and therefore has to be freshly generated from ruthenium 2+ just before use, employing one of three possible methods. Each method, together with its advantages and disadvantages, is described in detail in Gerardi *et al.*³⁰. A table comparing the intensities of CL emission resulting from the detection of several different analytes using each of the three methods has been published³⁵. The merits each of these methods are discussed below.

(i) Chemical/Photochemical Generation

The +3 oxidation state can be generated by a number of oxidants, for example, lead dioxide:



This was first used by Hercules & Lytle²⁸ in 1966 and is still utilised today due to its speed and simplicity. Despite these advantages, the temporal stability of the $\text{Ru}(\text{bpy})_3^{3+}$ is limited and as a result, this has not been the predominant method for its production. However, two methods have been reported³⁶ which increased the stability of the +3 oxidation state from several hours to days. This was accomplished by either optimising the acidity or by continually passing the ruthenium solution through a lead dioxide filter

system. A constant, stable source of reagent was obtained in both cases. Other chemical methods included the use of oxidants such as concentrated nitric acid¹⁷, chlorine gas³⁷ or cerium (IV) salts³⁸.

The majority of analytical applications employ some form of electrochemical means to produce $\text{Ru}(\text{bpy})_3^{3+}$. This is particularly successful because of the simple interconversion of the three key oxidation states. Figure 1.12 shows the redox potentials for the ground and lowest excited states of $\text{Ru}(\text{bpy})_3^{2+}$. These are independent of the solvent employed.

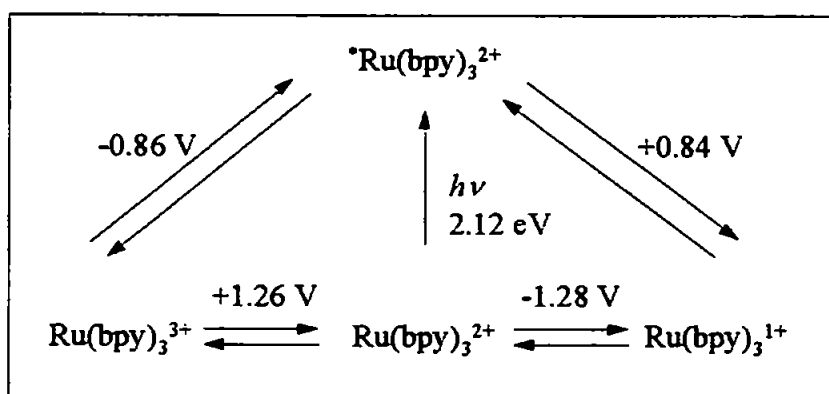


Figure 1.12: Redox potentials for the ground and lowest excited states of $\text{Ru}(\text{bpy})_3^{2+}$. Taken from ref.²²

The technique of ECL of $\text{Ru}(\text{bpy})_3^{2+}$ is increasing in popularity because the unstable +3 oxidation state can be electrochemically generated *in situ*.

(ii) Electrochemical Oxidation

The reagent can be generated in a cell which is remote from the site of its interaction with the analyte(s). Nonidez & Leyden³⁹ first reported the production of the reagent in this way. The oxidized state was produced by controlled potential electrolysis and then pumped into the flow cell. This method was effective but time-consuming.

Brune & Bobbitt^{40,41} used a similar method but continuously pumped the reagent into the electrochemical cell. This enabled large volumes of stable reagent to be used.

(iii) *In situ* Generated Electrochemiluminescence

Over two thirds of the applications which use electrochemical means to produce the ruthenium +3 oxidation state utilise *in situ* electrochemiluminescence. The numerous advantages of ECL have previously been described in section 1.1.4 (page 8). Production of the ruthenium +3 state is instantaneous by application of a potential to the reagent solution, and because it is produced *in situ*, it can react straight away. This method of generation was first reported²⁹ in 1972 and used for the analytical detection of oxalate⁴² in 1983. Since then, it has become the most popular method of generation of Ru(bpy)₃³⁺.

(1.2.6) Use of Ru(bpy)₃²⁺ for the Chemiluminescent Detection of Analytes

Ru(bpy)₃²⁺ has been shown to exhibit excellent properties as an electron transfer reactant in CL processes. It has been used for the sensitive detection of an exceptionally wide range of analytes and this has been the subject of a series of comprehensive reviews^{10,13,30,35,43}. The advantages of using this system include the following:

- The complex can undergo simple, reversible one-electron transfer processes leading to sufficiently stable reduced or oxidized species
- The excited state has a moderate lifetime
- Unlike systems such as the luminol reaction, CL emission occurs without bond cleavage or rearrangement
- Reactions can be carried out in a variety of solvents (acetonitrile or methanol are widely used)

- The complex can undergo ECL in aqueous buffered solutions at a wide range of pH values, often in the presence of dissolved oxygen and other impurities, at room temperature, at easily attainable potentials and with very high efficiency.
- Many analytes can be detected without the need for derivatization.

Some examples of each of the main classes of analytes are discussed in the following sections.

(1.2.6.1) The Oxalate Redox System

The ruthenium tris(2,2'-bipyridine)/oxalate redox system has been widely studied as it gives the most intense CL emission of all the analytes investigated.

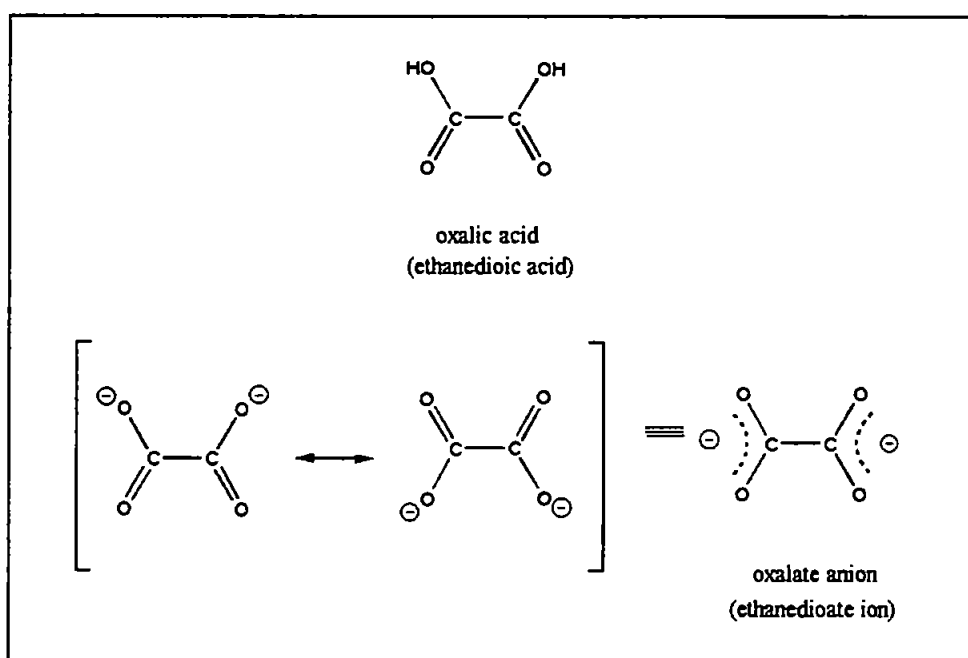


Figure 1.13: The oxalate anion

Detection of oxalate has applications in clinical, food and industrial chemistry. High oxalate concentrations in bodily fluids can be indicative of clinical disorders such as

renal failure, vitamin deficiencies and intestinal diseases. It is also implicated in the formation of kidney stones. A specific, accurate and reliable method for detection of oxalate in urine, blood plasma and blood serum is therefore required to diagnose the condition and prevent complications. Since the treatment of diseases such as these involves a low oxalate diet, an assay is also required for determination of levels in foodstuffs. Oxalic acid is commonly found in spinach leaves and is present as potassium hydrogen oxalate in rhubarb.

Oxalate is also found in Bayer liquor, the process liquor stream from the Bayer Process for production of aluminium hydroxide. The removal of oxalate for the prevention of problems in the production of high quality alumina also requires a sensitive method for oxalate detection.

(1.2.6.1.1) Detection Methods for Oxalate

Sharma *et al.*⁴⁴ have reviewed the methods for detection of oxalate in biological materials, including enzymatic techniques, isotope dilution and ion chromatography. Each has its advantages but many of these methods suffer from lack of sensitivity or extensive sample preparation is required. The measurement of oxalate in biological fluids is still a major problem for clinical biochemists, particularly because of the much higher concentrations of other anions such as chloride, sulfate and phosphate in the samples and/or specific interferences from proteinaceous materials and metal cations. Many methods are not suitable to detect oxalate in both urine and blood. Various methods have been used for determination of oxalate levels in Bayer liquor but as with clinical methods, there are problems with accuracy and precision.

(1.2.6.1.2) Detection of Oxalate Using the Ruthenium tris(2,2'-bipyridine) Complex

The CL emission from this system was first reported⁴⁵ in 1977 and the full mechanistic details were proposed⁴⁶ by Rubinstein *et al.* in 1981. The key features of this mechanism are as shown in Figure 1.14:

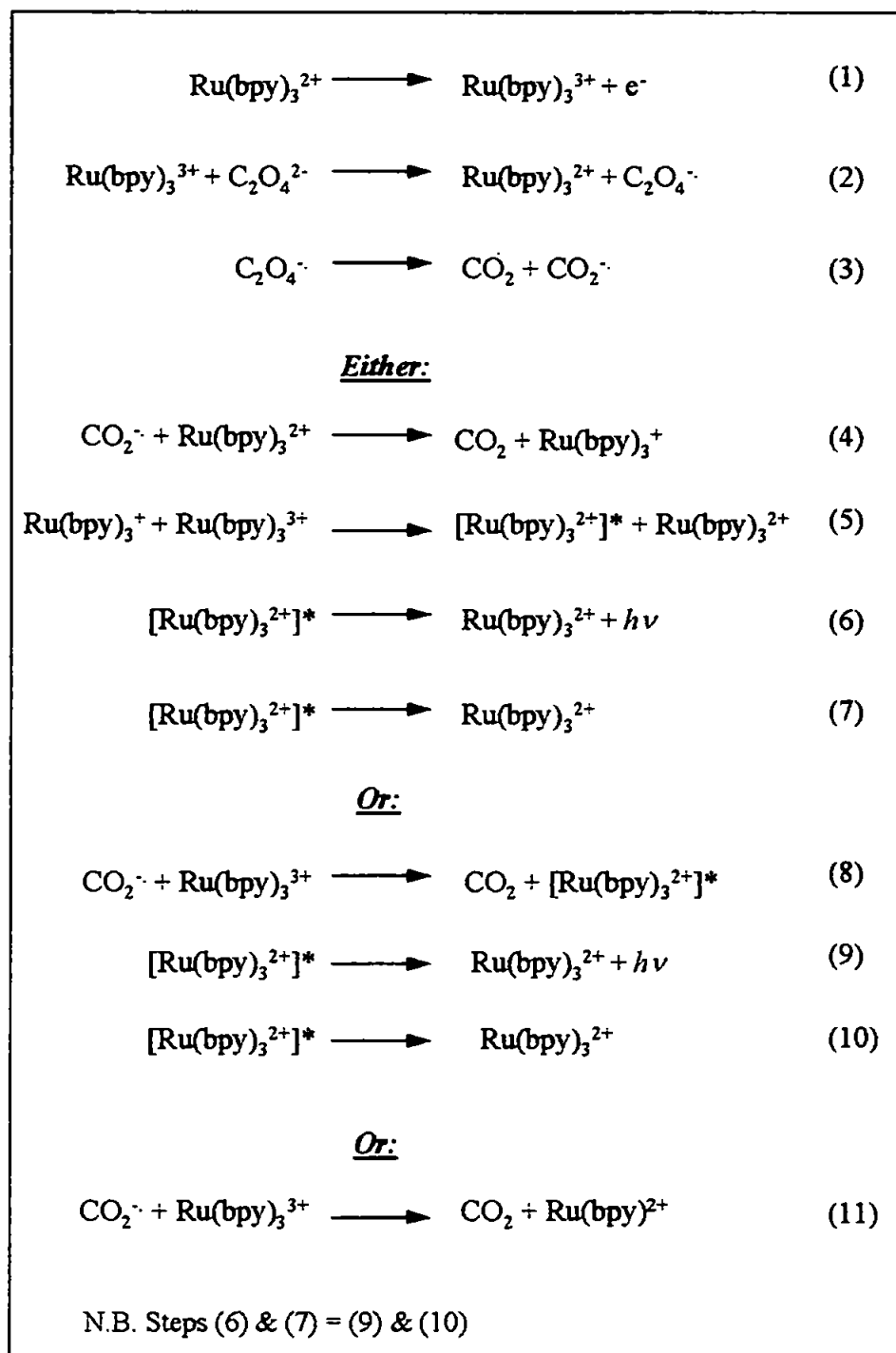


Figure 1.14: Alternative mechanisms of the reaction of Ru(bpy)_3^{2+} with oxalate. Adapted from ref.⁴⁶

Firstly, the ruthenium complex is oxidized to the +3 state, either chemically or electrochemically (1). The reaction with oxalate (2) generates the radical anion which then disproportionates to carbon dioxide and $\text{CO}_2^{\cdot-}$ (3). The $\text{CO}_2^{\cdot-}$ radical anion is a strong reductant which can react with either the +2 or +3 state of the ruthenium complex in three different ways. (4) shows the reduction of the +2 state complex to the +1 state. An annihilation reaction between the +1 and the +3 state generates two molecules of the +2 state, one in the excited state, the other in the ground state (5). Decay of the excited state may (6) or may not (7) result in the emission of CL.

The $\text{CO}_2^{\cdot-}$ species can also react with the +3 state of the ruthenium complex to form the +2 excited state (8). As before, this state decays with (9) or without (10) the emission of a photon. Alternatively, the $\text{CO}_2^{\cdot-}$ species can react with the +3 state to generate the +2 state which is not in the excited state and therefore no CL emission is observed (11).

The intensity of CL produced is directly proportional to the yield of excited state products, which in turn is proportional to oxalate concentration.

This complex mechanism has been summarised by Jirka & Nieman¹¹:

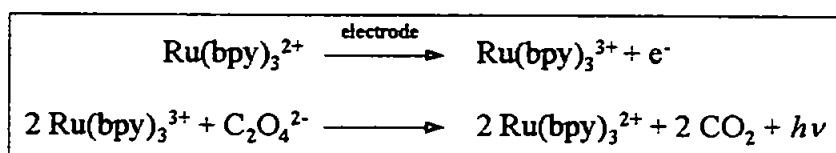


Figure 1.15: Summary of the mechanism of the reaction of $\text{Ru}(\text{bpy})_3^{2+}$ with oxalate.

It was not until 1983 that the system was used analytically⁴². As with most of the subsequent investigations, the +3 oxidation state of the complex was generated electrochemically. The reaction was carried out in purely aqueous solutions and a linear relationship between oxalate concentration and CL emission intensity was observed for

the range 10^{-6} - 10^{-4} M oxalate. However, more recent work has extended the limit of detection to 0.3×10^{-12} M⁴⁷. Typical oxalate levels are 1.7×10^{-5} - 3.9×10^{-5} M in normal blood and 1.6×10^{-4} - 5.5×10^{-4} M for normal urine⁴². In normal human serum, oxalate concentrations range from 1×10^{-5} - 2×10^{-5} M⁴⁸. The Ru(bpy)₃²⁺ system has been shown to be a sensitive method for oxalate detection and this analyte has been detected successfully in urine and blood plasma^{49,50} and Bayer liquor⁵¹.

(1.2.6.2) Detection of Amines and Amine-Based Pharmaceutical Products

As direct determination of aliphatic amines is difficult due to their low molar absorptivity in the UV spectrum, some sort of derivatization is generally employed for their detection. However, there are very few derivatization methods for tertiary amines. As a result of this, research has been conducted⁵² into the reaction of amines with Ru(bpy)₃²⁺. The results showed that CL intensity for tertiary amines was 100 and 1000 times greater than that for secondary and primary amines, respectively. No CL was observed for aromatic substituted amines such as aniline, diphenylamine and triphenylamine. However, some primary aromatic amines, including benzylamine and phenethylamine, have been detected by on-line photochemical derivatization prior to detection⁵³. CL response was enhanced by irradiation of these compounds with UV light. A whole range of aliphatic, aromatic and cyclic amines have since been detected, generally at picomolar levels. These are tabulated in a review by Knight and Greenway⁵⁴, who investigated the relationship between the structural attributes of various amines, such as the size and nature of substituent groups, upon the CL response.

The detection of these analytes via this CL method is of particular importance as many products, including pesticides, surfactants and especially pharmaceuticals, contain amine functional groups. As a result of this, Ru(bpy)₃²⁺ has been used for the

determination of many drugs at picomolar levels. These range from antihistamines, such as pheniramine and pyrilamine⁵⁵ to antibiotics such as clindamycin⁵⁶ and erythromycin⁵⁷ and its derivatives⁵⁸. Codeine also contains a tertiary amino group and has been detected, together with related alkaloids such as morphine and heroin, using this method^{31,59,60}. The detection of these various compounds has potential clinical and forensic applications.

(1.2.6.3) Detection of Amino Acids, Peptides and Proteins

The determination of levels of amino acids, proteins and peptides is a very important area. As with amines, many modern techniques require derivatization of these species to enhance detection. However, CL methods which do not require prior derivatization have been developed. In 1990, He *et al.* determined the relative signals and LOD's of 21 amino acids, some peptides and a few proteins⁶¹. The method used was Flow Injection Analysis (FIA) coupled with CL detection using $\text{Ru}(\text{bpy})_3^{2+}$. Further investigations of amino acids were conducted and the rôle of electron-donating/withdrawing character, pH and stoichiometry on the CL reaction of $\text{Ru}(\text{bpy})_3^{2+}$ with amino acids was investigated^{40,41}. The results showed that analytes with electron-withdrawing groups tend to diminish ECL intensity while electron-donating groups enhance ECL intensity.

Of all the amino acids, tryptophan (Trp) in particular has received much attention. A selective and sensitive method for the analysis of Trp (down to picomolar levels) using both FIA⁶² and liquid chromatography⁶³ has been developed. Trp is an essential amino acid and is a constituent of protein. There are connections between Trp levels and hepatic encephalopathy⁶⁴. Methods for the analysis of Trp, particularly in blood plasma, clearly have important biomedical applications.

(1.2.6.4) Detection of Other Analytes

There are many other analytes which can be detected using the ruthenium tris(2,2'-bipyridine) system which do not fit into the categories discussed so far. For example, the luminescence intensities of both mono- and polyhydric alcohols and other compounds containing hydroxyl groups, including glucose, sucrose and glycerol have been studied^{65,66}. The ECL reaction of $\text{Ru}(\text{bpy})_3^{2+}$ has been used to determine the presence of ascorbic acid in soft drinks and apple juice⁶⁷. Citric acid was the subject of an investigation which detected its presence in human urine and orange juice⁶⁸.

All of the examples considered so far have investigated the effects of reducing agents upon the ruthenium complex in the +3 state. In contrast, White & Bard looked at the effect of $\text{SO}_4^{\cdot-}$, an oxidizing agent produced from peroxydisulphate ($\text{S}_2\text{O}_8^{2-}$) upon the ruthenium tris(2,2'-bipyridine) system⁶⁹. The proposed mechanism for this reaction was as shown in Figure 1.16:

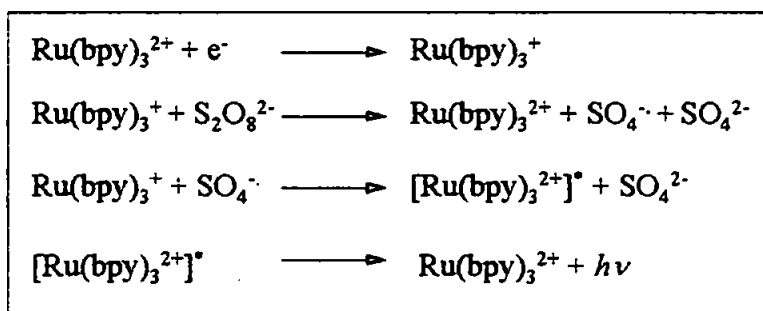


Figure 1.16: Mechanism of the reaction of $\text{Ru}(\text{bpy})_3^{2+}$ with peroxydisulphate

$\text{SO}_4^{\cdot-}$ is the only known oxidant for this CL reaction. Despite the fact that conditions had to be optimized in order to prevent quenching of the CL by $\text{S}_2\text{O}_8^{2-}$, early investigations showed that the ECL intensity of this system was several times larger than that of previously reported systems of $\text{Ru}(\text{bpy})_3^{2+}$.

(1.2.6.5) Uses of Ru(bpy)₃²⁺ as a Chemiluminescent Label

Detection of proteins and oligonucleotides in immunoassay and DNA probe assays (e.g. DNA fingerprinting) is of great importance in today's world. Many biologically important compounds can be labelled with molecules which have a certain distinct feature that allows detection and quantification at a low concentration level. CL labels have many advantages, including high sensitivity, dynamic range, simple instrumentation, long shelf-life and low cost and avoid the problems of storage, handling and disposal associated with radioactive labelling. Further advantages have been discussed by Blackburn *et al.*⁷⁰

Ru(bpy)₃²⁺ has been attached to various compounds as a CL label and can be continuously recycled and re-excited. The first reported use of (i) as a tag for protein binding reactions was in 1984 when the complex was determined in the presence of liver tissue extract⁷¹. Hsueh *et al.*⁷² performed a quantitative analysis of DNA by labelling with Ru(bpy)₃²⁺ and detecting the ECL and Blackburn *et al.*⁷⁰ modified Ru(bpy)₃²⁺ by attaching a group on to one of the bipyridine ligands to create an activated species which was used to label proteins and nucleic acids. An ECL method has also been successfully developed for the detection of β-lactam antibiotics and their inactivation by β-lactamases by using ruthenium-labelled penicillin substrates^{73,74}.

(1.2.6.6) Methods of Utilising the Ruthenium tris(2,2'-bipyridine) Complex for Analyte Detection

Ru(bpy)₃²⁺ can be employed in different forms for analyte detection. The most common method uses a solution of the complex in buffer and is either mixed directly with the analyte solution (as in the detection of oxalate⁴²) or after the analyte has passed

through a separation column. An example of the latter method is the determination of ascorbic acid in soft drinks and apple juice after separation of the ascorbic acid by HPLC⁶⁷. However, although the complex does not decompose or rearrange during solution phase reactions such as these, it can be only used once. It is mixed with the products of the reaction and thus fresh solution is required for further analysis. This results in the continuous generation of waste. Ruthenium and its compounds are toxic to the environment and are expensive as the abundance of this metal in the earth's crust is quite low (1mg/tonne, about one-tenth of the abundance of platinum)⁷⁵. This has resulted in efforts to conserve this expensive reagent.

To alleviate this problem, regenerable sensors have been developed by a number of authors^{43,76-79}. Ru(bpy)₃²⁺ has been successfully immobilized into the sulfonated polyfluorocarbon cation-exchange polymer, Nafion:

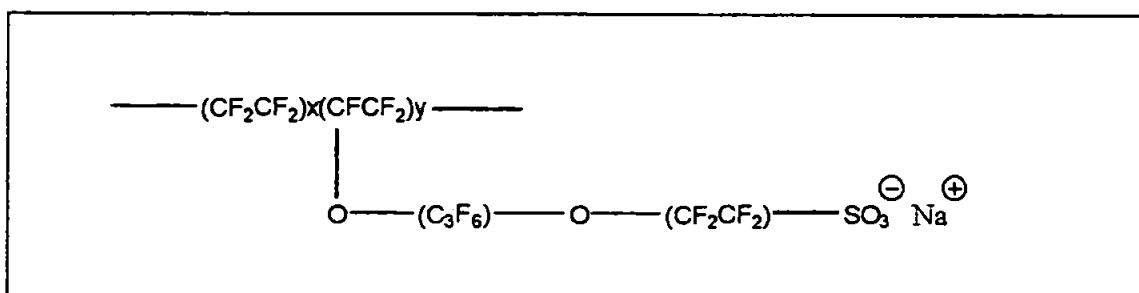


Figure 1.17: Structure of the cation-exchange polymer, Nafion
Taken from ref.⁸⁰

This is an ion-exchange polymer which is very resistant to chemical attack, even by strong oxidants at elevated temperatures and has good ionic transport properties. It is mechanically stable and adheres well to electrode surfaces leading to stable films. The structure is composed of hydrophobic fluorocarbon regions with hydrophilic polysulfonate pockets distributed amongst them. Cations such as Ru(bpy)₃²⁺ can be taken up into these pockets, which maintain access to the electrode surface. In 1993, Martin

and Nieman prepared an electrode by casting the Nafion film and then loading it with the ruthenium complex for the determination of glucose by CL detection of NADH⁷⁷.

In all the reactions discussed so far, the ruthenium +2 oxidation state is regenerated, as shown in Figure 1.18;

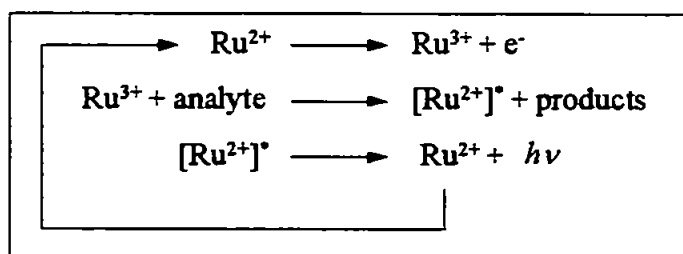


Figure 1.18: Regeneration of the ruthenium complex after the chemiluminescence reaction has taken place.

If the ruthenium complex is in the solution phase, then this cannot be reused due to the presence of products from the reaction. However, if $\text{Ru}(\text{bpy})_3^{2+}$ is immobilised in a Nafion film, it is separate from the analyte solution and is able to be recycled. The sensor produced is therefore regenerable and reduces the consumption of this expensive reagent.

A study was performed in 1995 to compare the use of the immobilized complex in Nafion with external and *in situ* generation of $\text{Ru}(\text{bpy})_3^{3+}$ in solution⁴³. Several analytes including oxalate and amines were detected using these methods. The immobilized mode showed the wider dynamic range and was the most conservative of reagent.

However, there are a number of disadvantages of these Nafion-coated electrodes, mainly, their stability. Knight⁶⁰ reported that when electrodes of this type were stored overnight in buffer, the ECL intensity dropped to approximately 15% of that observed with a freshly prepared sensor. This was possibly due to migration of $\text{Ru}(\text{bpy})_3^{2+}$ into hydrophobic regions of the film which can result in very slow transport rates. It has also been reported that a fresh sensor is required on a daily basis⁷⁷. This work also highlights

the additional problem of the lengthy preparation time. It took between 2 - 3 hours to immobilize the complex in a Nafion film. Also, the sensor is limited to chromatographic separations which use mobile phases having < 30 % organic modifier⁴³. Nafion films are slowly destroyed upon exposure to mobile phases with a higher organic content. Limits of detection using this method were in the nanomolar range, which is not as low as for the solution phase. In terms of time, convenience and reliability of the experiment, the *in situ* solution mode is superior.

A vast range of ECL sensors have been fabricated using compounds based on a modification of the ruthenium tris(bipyridine) complex. For example, Zhang & Bard were the first to observe electrogenerated CL from a monolayer of a Ru(bpy)₃²⁺-based surfactant on semiconductor and metal electrodes upon its reaction with oxalate⁸¹. A heptyl-thiol derivative of Ru(bpy)₃²⁺ has been prepared, which was adsorbed through the thiol functionality onto indium tin oxide substrates⁸². A study of the voltammetric and CL characterization of this electrode was performed and it was assessed for analytical utility. Many of these Ru(bpy)₃²⁺ based sensors, however, are not suitable for detecting a wide range of analyte concentrations or even for analytical applications at all. Reasons for this are that the selectivities are not high enough to apply to practical samples or that the stability of the electrode coating was limited. Table 1.2 overleaf shows ECL sensors which have been successfully used for detection of varying concentrations of an analyte. In the majority of the cases, CL emission was most intense for oxalate and oxalic acid. In general, the dynamic range of the sensors were only one or two orders of magnitude and limits of detection were micromolar concentrations at best.

ELECTRODE MODIFIED WITH Ru(bpy) ₃ ²⁺ OR RELATED COMPLEXES	ANALYTE DETECTED	LINEAR CALIB'N RANGE	L.O.D.	REF.
Langmuir-Blodgett Monolayer of ruthenium (II) bis(2,2'-bipyridine)(4,4'-dinonadecyl-2,2'-bipyridine) perchlorate on Sb-Doped SnO ₂ Electrode	Oxalate	10 ⁻⁶ - 10 ⁻⁴ M	Not given	(83)
Fibre-Optic ECL Sensor equipped with a carbon paste electrode modified with Bis(2,2'-bipyridine)(4,4'-dinonadecyl-2,2'-bipyridine) Ru(II)	Oxalate	10 ⁻⁴ - 10 ⁻³ M	2 x 10 ⁻⁵ mol dm ⁻³ (when S/N = 3)	(84)
Pt electrode coated with tris(2,2'-bipyridine) ruthenium (II)(Ru(II) complex)-modified chitosan	Oxalic Acid	0.1 - 10 mM	3 x 10 ⁻⁵ M (with S/N = 3)	(85)
Pt electrode coated with Ru(bpy) ₃ ²⁺ complex-modified chitosan / silica gel membrane	Oxalic Acid & Ascorbic Acid	0.1 - 10 mM (oxalic acid), 0.5 - 5 mM (ascorbic acid)	0.02 mM (S/N = 3), 0.05 mM	(86)
Tris(4,7-diphenyl-1,10-phenanthroline)disulfonic acid ruthenium (II) immobilized in a cationic polypyrrole membrane	Oxalate	0.1 - 100 μM	0.06 μM (3 x s.d. of blank)	(87)

Table 1.2: Analytical figures of merit for the detection of various analytes using ruthenium complex based sensors.

The electrode fabricated by Blanchard *et al.* was the most sensitive and the linear calibration range spanned three orders of magnitude, however, there were problems with the long term stability of the electrode coating⁸⁷.

It has been stated that the $\text{Ru}(\text{bpy})_3^{2+}$ ECL in analytical science has not reached its full potential and further work is required so that the inherent sensitivity of the techniques can be explored³⁵. There is a demand for a simple, robust chemical sensor which can be regenerated repeatedly and at the same time, its sensitivity is maintained. If $\text{Ru}(\text{bpy})_3^{2+}$ were able to be immobilized directly onto an electrode surface, without the need for a membrane, yet were still capable of electron transfer, this could prove to be a valuable asset to methods for CL detection. The next section discusses the ways of attaching compounds to an electrode surface for various purposes. These types of electrodes are known as 'Chemically Modified Electrodes.'

(1.3) CHEMICALLY MODIFIED ELECTRODES

(1.3.1) Introduction

The considerable amount of work done in this field has been extensively reviewed⁸⁸⁻⁹⁷.

A Chemically Modified Electrode (CME) has been defined as:

'an electrode made of a conducting or semiconducting material that is coated with a selected monomolecular, multimolecular, ionic, or polymeric film of a chemical modifier and that by means of faradaic (charge-transfer) reactions or interfacial potential differences (no net charge transfer) exhibits chemical, electrochemical, and/or optical properties of the film.'
(IUPAC Recommendations 1997)⁹⁸

Further terminology and definitions pertaining to this expansive area of chemistry can be found in the literature⁹⁸.

All electrode processes involve an electronic interaction between reactants and the electrode surface. Thus, modification of the electrode surface can dramatically change the

properties of the electrode. CME's have been produced as a result of the desire to control the chemical nature and the reactivity at the electrode/solution interface. The electrode can be successfully tailor-made to exhibit the chemical, electrochemical, optical and other properties that the reagent displayed whilst in solution. Ideally, the immobilized film should be stable upon repeated oxidation and reduction and should have good chemical and electrochemical reversibility.

(1.3.2) Applications of Chemically Modified Electrodes

The applications of CME's have been reviewed by Dong & Wang⁹⁹. Further details can be found in other texts^{88,91-94,96,97,100-102}. Some of the major applications are listed below:

- electrocatalysis
- selective preconcentration and separation
- incorporation of biocomponents
- energy conversion and storage
- microstructured electrodes
- display devices (e.g. electrochromic surfaces)
- chemical sensors
- inhibition of surface fouling
- investigation of the kinetics and mechanisms of redox reactions
- analytical applications (electroanalysis)

One of the biggest attractions of CME research is the application to electrocatalysis. Reactions which are kinetically unfavourable at an unmodified surface can take place by incorporation of catalytic sites at the electrode-solution interface. As

with any catalytic process, the aim is to reduce the energy of activation of a reaction by provision of a low-energy pathway between reactants and products. An immobilized redox-catalyst reagent acts as a fast electron transfer mediator for the oxidation or reduction of solution substrates. Although only small amounts of material are needed, the concentration of electroactive material on the electrode surface can reach much higher levels in comparison with those attained in homogeneous solution. The reaction can be controlled by the applied potential and at the end of the experiment, separation of the electrocatalyst from the reaction medium is easy.

In the present study, a CME is produced for application in the field of electroanalysis. The signal from the electrode can be related to the concentration of the species of interest. CME's can be combined with sensitive instrumental techniques such as FIA and HPLC to create a highly selective analytical measurement. Important characteristics of a CME for analytical applications involving continuous, long-term operation in a flowing system include the following¹⁰³:

- good mechanical and chemical stability
- good short-term reproducibility and long-term stability of the modifier's activity towards the analyte
- flexible modifier loading levels
- a wide dynamic range (ideally linear) of response
- low and stable background currents over the potential required
- compatibility with a wide range of aqueous and organic matrices
- simple and reliable fabrication that results in consistency of response from one electrode to another

(1.3.3) Methods for Preparation of Chemically Modified Electrodes

Although not an exhaustive study, the most important methods of preparation of CME's are shown in Figure 1.19 overleaf. A brief discussion of each method will be given, together with examples.

Coatings can be deposited onto a wide range of electrode surfaces, from the traditional platinum, carbon and gold electrodes to semiconductors such as tin dioxide and silicon. Four main methods of preparation have been used¹⁰⁰. Adsorption is the oldest technique and was used by Lane & Hubbard^{104,105} in 1973. This first example of deliberate surface modification saw a variety of olefinic-bearing species chemisorbed to platinum surfaces. The majority of adsorption studies have utilised physisorption and have been carried out on carbon surfaces. The technique is simple, yet suffers from the disadvantage that only a limited amount of material can be adsorbed. In addition, the electrodes have limited lifetime because of gradual desorption of the coating.

As a result of this problem, studies were conducted into chemically binding the coating to the electrode. For example, ferrocenes have been studied whilst covalently linked to a platinum surface¹⁰¹. Although coatings are much more firmly bound to the electrode using this method, more steps are usually required in the synthesis.

Most of the early work on CME's focused on monolayers. Recent research has been centered upon attachment of a whole range of conducting polymers of different thicknesses from between about ten nanometers to a few micrometers. This is a simpler, more effective and more versatile method than those already discussed. Polymer films are generally attached to electrode surfaces by chemisorption forces or by being insoluble in the contacting solvent but can also be surface-bonded e.g. polymerized organosilane reagents¹⁰⁷.

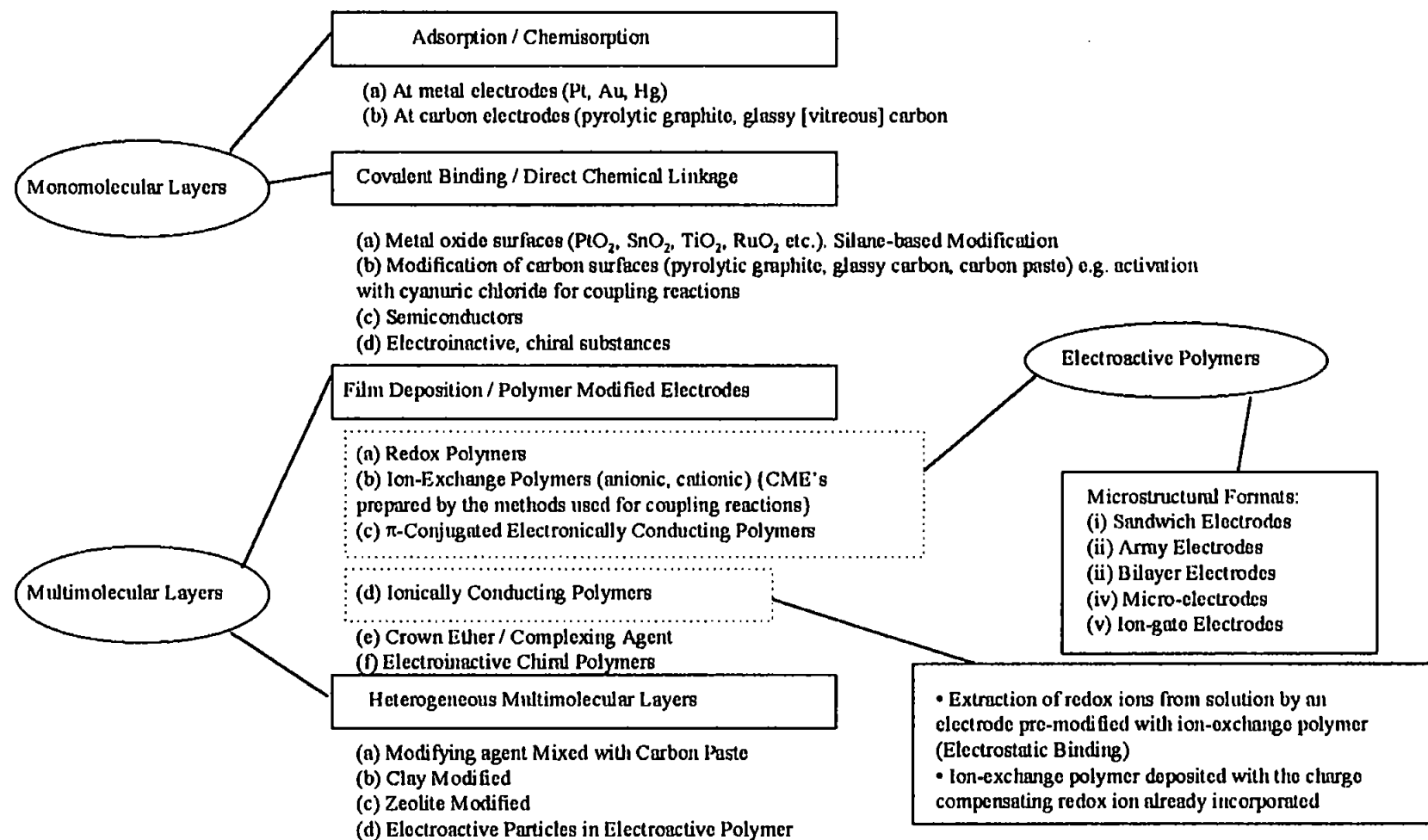


Figure 1.19: Methods for preparation of chemically modified electrodes. Adapted from ref.¹⁰⁰.

There are certain advantages of using Polymer Modified Electrodes (PME's):

- greater physical, chemical and electrochemical stability than monolayers
- increased concentration of active sites about 10^{-10} - 10^{-6} mol/cm² corresponding to 1 - 10^5 monolayers
- signals obtained are greatly amplified in comparison with monolayer coverages; higher electronic conductivity often leads to a different electrochemical response
- a great diversity and complexity of immobilized chemical microstructures
- use of functionalized polymer films allows for many synthetic variations, thus permitting reagents for a particular application to be tailored with relatively simple procedures.

(1.4) SEARCH FOR A SUITABLE CME FOR THE PRESENT STUDY

(1.4.1) Chemical Modification of an Electrode Surface Using the Ruthenium tris(2,2'-bipyridine) Complex

As described in section 1.2.6.6 (page 26), current methods using the ruthenium tris(2,2'-bipyridine) complex for analyte detection are either not reusable (resulting in environmentally unfriendly and expensive waste) or are not robust. There is a need for a compound to be capable of electron transfer when immobilised on an electrode surface. The resulting sensor should be electrochemically regenerable, stable, rugged and cheap. Having considered all the methods for preparation of a CME, a polymer modified electrode was chosen. A conducting polymer was considered to be essential for the electrochemical regeneration of the ruthenium centres.

The three main types of electroactive polymers are:

- Redox polymers (polymers containing redox active centres e.g. poly(vinylferrocene))
- Ion-exchange polymers e.g. $\text{Fe}(\text{CN})_6^{3-/4-}$ in protonated poly(4-vinylpyridine)
- π -conjugated electronically conducting polymers e.g. poly(acetylene), poly(pyrrole), poly(aniline) and their derivatives.

Of these three types, the first two contain redox centres. The ruthenium complex is redox active and could therefore be used in either of these two types of redox polymer. Ion exchange polymers have the redox active groups as counterions to the poly-ionic film. A Nafion-coated electrode, discussed in section 1.2.6.6 (page 26), containing the ruthenium complex immobilized within the polymer, is an example of a cationic ion-exchange polymer. However, there are many disadvantages of using these films.

In comparison, if a redox centre is part of the polymer backbone, it is called a redox polymer. Figure 1.20 overleaf shows methods of formation of PME's from redox polymers. Many of these methods also apply to the formation of ion-exchange polymers. Further details can be found in a review by Murray¹⁰⁸.

A conducting redox polymer was chosen to modify the electrode surface. The electrochemically active centres can therefore undergo electron transfer reactions with the electrode. The ruthenium complex needed to be incorporated into the conducting polymer. Redox polymers can be reaction-modified, i.e. the redox centre is attached as a pendant group to a suitably functionalised polymer, itself already attached to the electrode surface. For example, Kaneko *et al.* prepared a co-polymer-pendant $\text{Ru}(\text{bpy})_3^{2+}$ based on the copolymer of 4-methyl-4'-vinyl-2,2'-bipyridine and styrene¹⁰⁹. However, this method is not without its disadvantages as binding of transition-metal complexes to polymers can result in incomplete metalation of the polymeric ligand sites.

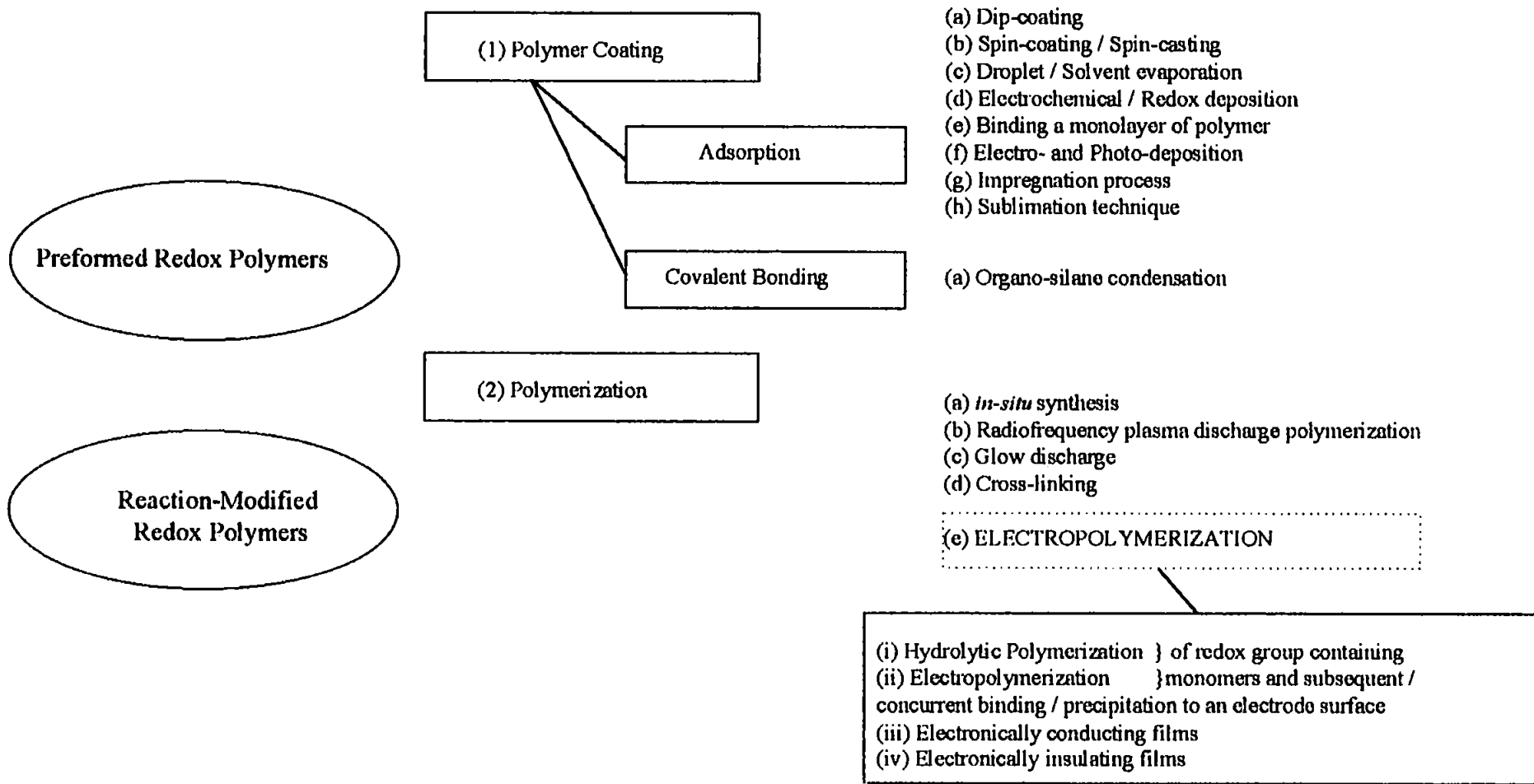


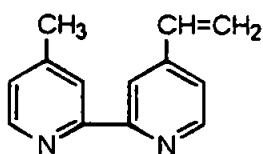
Figure 1.20: Formation of polymer modified electrodes from redox polymers

In contrast, the redox polymer can be pre-formed, i.e. the polymer already contains a redox-active centre before its application to the electrode. The polymer can either be coated onto the electrode or directly deposited by polymerization - *in situ* preparation of a polymer film from monomers. Electropolymerization is the most widely used polymerization technique. It offers a fixed redox centre present in each repeating unit of the polymer. This method is advantageous as it enables deposition of insoluble polymers, uniform coatings on irregular surfaces and film thickness can easily be controlled electrochemically. Further advantages are discussed in section 1.5.1 (page 44).

It has been shown that reduction of $\text{Ru}(\text{bpy})_3^{2+}$ does not yield a polymer film¹¹⁰. This is attributed to the lack of any group on the bipyridine ligands capable of taking part in the polymerization process. However, the presence of a vinyl group facilitates polymer formation. Therefore, for the purposes of the present study, the ruthenium complex had to be modified prior to electropolymerization.

(1.4.2) Synthesis of a Monomer for Electropolymerization

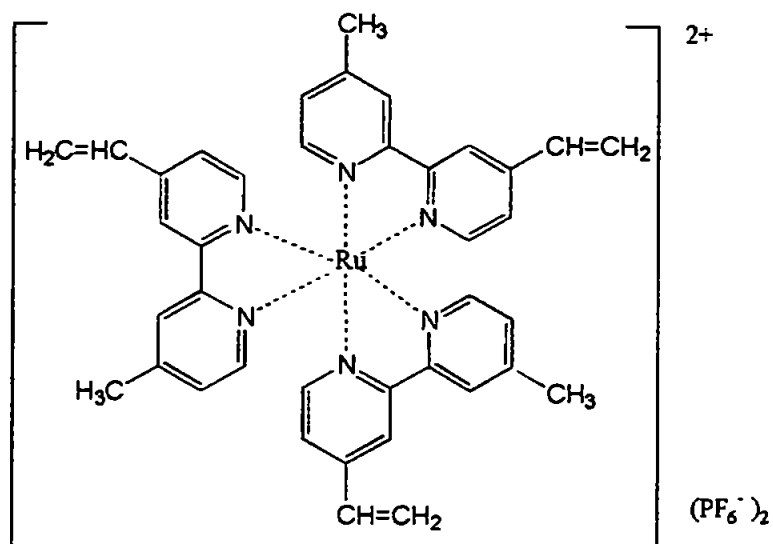
In the current study, a vinyl group was to be attached to one of the bipyridine ligands of $\text{Ru}(\text{bpy})_3^{2+}$. Chapter 2 gives details of a critical review of all the methods for synthesis of the ligand 4-methyl-4'-vinyl-2,2'-bipyridine;



(ii)

The original idea was to then find a suitable synthetic route for incorporation of one vinylbipyridine ligand into a ruthenium complex. However, a study of the literature showed that polymer formation was far more successful with three vinyl ligands¹¹⁰. This is

discussed more fully, in section 1.5.1.2 (page 47). The target molecule for this research subsequently became ruthenium tris(4-methyl-4'-vinyl-2,2'-bipyridine) bis(hexafluorophosphate), $[\text{Ru}(\text{vbpy})_3]^{2+}$:



(iii)

(1.4.3) Electropolymerization of ruthenium tris(4-methyl-4'-vinyl-2,2'-bipyridine) bis(hexafluorophosphate)

Examples of electrodes coated with polymeric films formed from the above monomer can be found in the literature¹¹¹⁻¹¹⁹. Some of these are listed in Table 1.3 overleaf. The tris-vinylbipyridine complex (iii) is capable of undergoing electropolymerization at the vinyl substituent on the bipyridine ligand to form stable, adherent, intractably insoluble electrochemically active films of poly-ruthenium tris (4-methyl-4'-vinyl-2,2'-bipyridine) bis(hexafluorophosphate), (poly- $[\text{Ru}(\text{vbpy})_3]^{2+}$) with a high density of redox sites. Elemental analysis of the polymer film and the agreement of formal potentials of the monomer and its corresponding polymer has indicated that the ruthenium co-ordination sphere remains essentially intact upon electropolymerization and

ELECTRODE PREPARATION	APPLICATION	REF.
Formation of bilayer (and co-polymer) films on electrodes using poly-[Ru(vbpy) ₃ ²⁺] with other Ru and Fe vinylpyridine and vinylbipyridine complexes.	The properties of electrodes such as these were considered to be potentially useful for mimicking electronic device behaviours such as Zener diodes, transistors, optical switches and solar collectors.	(111)
Electropolymerization of Ru(vbpy) ₃ ²⁺ on a Pt electrode.	Long-lived display device based on ECL observed from the sequential oxidation and reduction of the immobilized redox centres.	(112)
Incorporation of 2,9-dimethyl sulfonated bathophenanthroline by ion-exchange into electrodes modified with poly-[Ru(vbpy) ₃ ²⁺] and subsequent incorporation of a Cu(I) complex by immersion.	Measurement of peak current from the C.V. of the electrode for detection of copper levels with the potential of extending the utility of the electrode for detection of other metal ions.	(113)
Electrodes modified with poly-[Ru(vbpy) ₃ ²⁺] immersed in an aqueous solution of one of a number of ligands followed by immersion in a solution of Cu(I)	Measurement of current (or area under the voltammetric wave) from the voltammogram produced by the electrode. Used analytically for determination of copper levels in solution. Investigation of the potential of this type of electrode for speciation studies.	(114)
Poly-[Ru(vbpy) ₃ ²⁺] coated electrodes modified with Chromotrope 2B incorporated by ion-exchange. Subsequent immersion of the electrode in a solution of the Cu(I) complex.	Measurement of normalized current from voltammograms of the electrode for the detection of copper with the potential of use of an electrode of this type for speciation studies.	(115)

Table 1.3: Applications of electrodes modified with poly-[Ru(vbpy)₃²⁺]

ELECTRODE PREPARATION	APPLICATION	REF.
Modification of poly-[Ru(vbpy) ₃ ²⁺] coated electrodes with amino acids (incorporation by ion-exchange)	Measurement of normalized current from voltammograms for the determination of mercury in solutions, leading to the potential investigations of the bioavailability and thus toxicity of mercury and other heavy metals. Further use for speciation studies.	(116)
Incorporation of electroactive ions by ion exchange into electrodes modified with poly-[Ru(vbpy) ₃ ²⁺]	Investigation of ion exchange and charge transport properties of poly-[Ru(vbpy) ₃ ²⁺] films and the electrochemical behaviour of the electroactive ions IrCl ₆ ²⁻ , Fe(CN) ₆ ³⁻ and W(CN) ₈ ⁴⁻ within the polymer film.	(117)
Immobilization of heteropolyoxometalates (PMo ₁₂ O ₄₀ ³⁻ , PW ₁₂ O ₄₀ ³⁻ , SiW ₁₂ O ₄₀ ⁴⁻ in films of poly-[Ru(vbpy) ₃ ²⁺]	Investigation of the electrochemistry of these incorporated ions and their ability to act as electrocatalysts for the electrochemical reduction of hydrogen ion.	(118)
Electropolymerization of Ru(vbpy) ₃ ²⁺ on a Pt electrode and co-polymer electrodes of poly-[Ru(vbpy) ₃ ²⁺] doped with <i>p</i> -vinylbenzoic acid.	Use of electrodes coated with poly-[Ru(vbpy) ₃ ²⁺] as active catalysts for the electro-oxidation of guanine and DNA. Co-polymers used to prepare site specifically assembled loci for DNA detection.	(119)

cont...

Table 1.3: Applications of electrodes modified with poly-[Ru(vbpy)₃²⁺]

that the resulting polymer can be regarded as fully metalated. These films are generally uniform and free from imperfections such as large channels or pinholes¹¹⁰. The characteristics of the monomer complex, such as its spectroscopic and electrochemical properties, redox activity and ability to emit CL are maintained in the surface-confined environment on the electrode. Table 1.3 gives details of a few applications of these electrodes. The poly-[Ru(vbpy)₃²⁺]-coated electrode was first fabricated in 1981 by Abruña and co-workers¹¹¹, who have since investigated various applications of this electrode. Considerable research has been performed on determining the electrochemical properties of these and similar types of films. For example, the Surface Extended X-Ray Absorption Fine Structure and near edge structure of these electropolymerized films has been studied¹²⁰. The permeation of various compounds such as electroactive solutes and neutral, cationic and anionic electrode reagents through the films have been studied^{121,122} together with the conductivity of these and other transition metal co-ordination polymers¹²³. Leidner *et al.* refer to other properties of these types of films which have been investigated¹²⁴⁻¹²⁵.

Of all the studies performed on electrodes of this type, few have considered the ECL ability and none have investigated the analytical applications. The proposed use of the poly-[Ru(vbpy)₃²⁺]-coated electrode is very simply summarised in Figure 1.21 below:

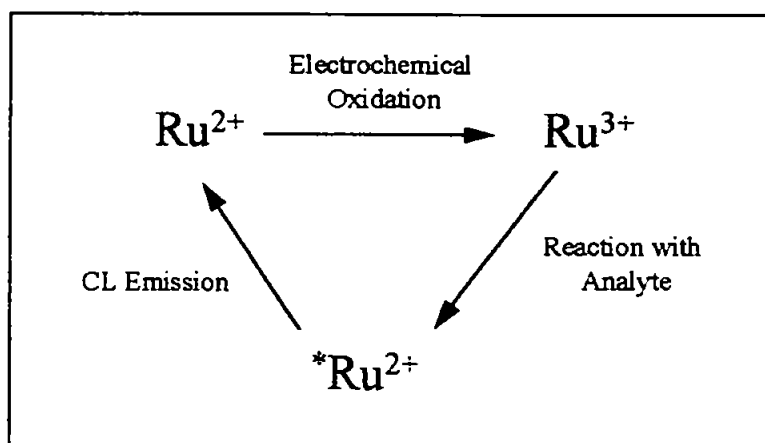


Figure 1.21: Proposed use of poly-[Ru(vbpy)₃²⁺]-coated electrodes

The importance of this cycle is that it can be repeated many times, illustrating the regenerability of the electrode. In terms of a simple molecular orbital diagram, the mechanism, known as an EC (electrochemical-chemical) mechanism is as shown in Figure 1.22:

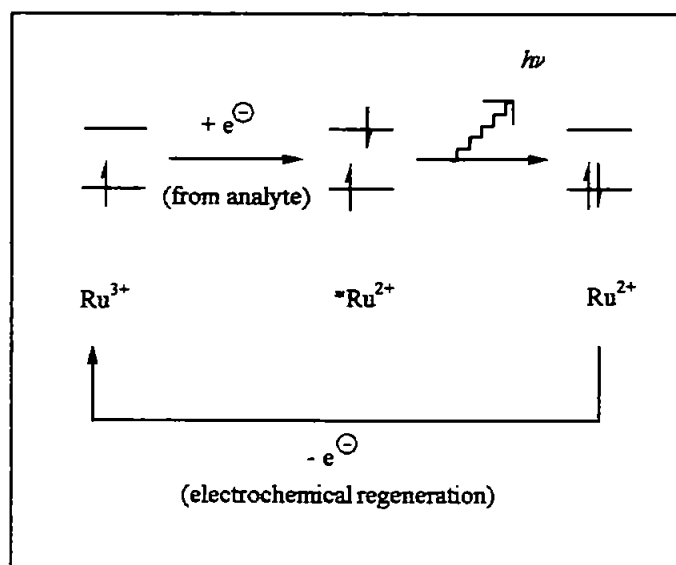


Figure 1.22: Mechanism of the proposed use of poly-[Ru(vbpy)₃²⁺]-coated electrodes in terms of a simple molecular orbital diagram.

An electron is removed electrochemically from the Ru(II) centre, producing the Ru(III) state. An electron is re-introduced by an analyte into the ruthenium centre but into a higher unoccupied molecular orbital. The Ru(II) excited state then decays, emitting a photon in the process. The electron is now back in the ground state and can be once again removed electrochemically to repeat the cycle.

(1.5) TECHNIQUES USED IN THE PRESENT STUDY

(1.5.1) Electropolymerization

Polymerization is usually initiated by use of a radical-forming compound, for example, peroxides are used in the polymerization of alkenes. Electropolymerization is

initiated electrochemically and proceeds by polymerization of an appropriate electroactive monomer. The result is a polymer-modified electrode.

Electropolymerization has been reported extensively in the literature as a simple method for obtaining a wide variety of stable, uniform, electrochemically active films.

Advantages of this technique include the following:

- Easy assembly
- Films can be deposited upon a wide range of supports, including platinum, gold, silver, TiO_2 , vitreous (glassy carbon) or highly oriented pyrolytic graphite and optically transparent electrodes of SnO_2 or In_2O_3
- Surface coverage (Γ) can be systematically and reproducibly controlled from submonolayer to layers hundreds of nanometres thick by varying scan times and scan rates. Permeability and other physicochemical properties of films can be explored as a function of Γ .
- The accumulating polymer film retains electrochemical reactivity at the potentials required for sustained reduction or oxidation of fresh monomer by redox sites at the polymer/solution boundary. Further growth can occur on the outer (solution) surface of the polymer film even if the electrode is later re-immersed in the monomer solution after having been removed
- Straightforward co-polymerization
- The interaction with the electrode surface occurs without appreciable electronic and structural change. Films retain many of their intrinsic properties, eg redox properties, spectral features, light absorbance and reactivity characteristics of the related monomer complexes in solution.
- Good reproducibility

(1.5.1.1) Formation of Polymer Films of Different Monomers and Their Applications

Abruña *et al.* reported the production of the first examples of redox-polymer modified electrodes by electropolymerizing vinylpyridine and vinylbipyridine complexes of ruthenium and iron¹¹¹. The properties of the resulting electrodes were considered to be potentially useful for applications such as transistors, optical switches and solar collectors. This paper was followed a year later by another published by the same group¹¹⁰. Studies were carried out in an attempt to understand the electropolymerization process involving the ruthenium vinylpyridine and vinylbipyridine complexes.

Following this early work¹¹¹, there was a swift development in the range of different complexes which could be electropolymerized; most commonly, those containing alkynyl and vinyl linkages. A vast number of vinyl-substituted pyridine and polypyridine complexes of transition metals have since been prepared and studied⁸⁸. Ghosh & Spiro attached vinyl derivatives of tris(bipyridine)- and tris(*o*-phenanthroline)-ruthenium (II) complexes to platinum electrodes using two different methods, hydrosilylation and electropolymerization¹⁰⁷. The electrochemical characteristics of these electrodes were studied under a variety of conditions.

A series of papers on the synthesis, characterization and electropolymerization of novel derivatives of the 4-methyl-4'-vinyl-2,2'-bipyridine ligand for various applications, including spectrochemical recognition of group 1A and 2A metal cations have been published¹²⁶⁻¹³³.

The iron and osmium vinylbipyridine complexes, analogous to the ruthenium complexes, have been investigated. The mechanism of formation of poly-[Fe(vbpy)₃]²⁺ was studied¹³⁴ using the technique of laser desorption Fourier transform mass

spectrometry and the Surface Extended X-ray Absorption Fine Structure (EXAFS) of polymer films of $\text{Os}(\text{vbpy})_3^{2+}$ has also been investigated¹²⁰. Mixed ligand complexes are also possible, for example, electrode coatings of a ruthenium complex containing two 1,10-phenanthroline ligands¹³⁵.

Ligands do not necessarily need to contain vinyl or alkynyl linkages. The electropolymerization of an aldehyde-substituted derivative of 2,2'-bipyridine has been studied¹³⁶, together with bromomethyl-substituted derivatives¹³⁷. Fussa-Rydel *et al.* studied the electropolymerization of iron, ruthenium and osmium complexes containing 5-chlorophenanthroline ligands¹³⁸. The advantages of using the latter ligand compared with vinylated ligands include its commercial availability of the ligand and photostability of the monomers.

Electropolymerization has been extended to larger structures. Moss *et al.* investigated the polymerization of molecular assemblies¹³⁹. As with simple monomers, there is retention of the often complex mixed-valence and photochemical properties in the film environment.

In conclusion, electropolymerization of complexes to form thin, redox-active films has provided one of the most versatile routes for the modification of metallic and semiconductor electrode surfaces.

(1.5.1.2) The Structure of Polymer Films Formed from poly-[Ruthenium tris(4-methyl-4'-vinyl-2,2'-bipyridine) bis(hexafluorophosphate)].

The initial aim of this current study had been to synthesise the complex ruthenium (4-methyl-4'-vinyl-2,2'-bipyridine) bis(2,2'-bipyridine) bis(hexafluorophosphate), i.e. the ruthenium complex with just one vinyl-containing ligand. However, previous workers

reported that 'as a general rule, ruthenium complexes bearing only one vinyl substituent deposit poorly'¹¹⁰. Monomers with a single polymerizable group generally form films 20 - 50 times less rapidly than similar complexes having two vinyl-containing ligands¹⁴⁰. Monomeric metal complexes containing at least two electropolymerizable vinyl groups are necessary to produce layers of adequate thickness and stability¹⁴¹ and optimum films are produced with three vinyl groups¹¹⁰.

The theory behind this is best visualised diagrammatically and is shown below in Figure 1.23. It has been suggested that the reluctance of mono-vinyl complexes to polymerize is steric in origin¹¹⁰. The repeated addition of monomer units to a growing polyvinyl backbone requires the close approach of the very bulky bipyridine complexes. Linear chain growth requires (sterically) a helical spiral with little flexibility. However, if two or more vinyl groups are present in the metal complex monomer, at the very least, only two vinyl groups in a chain are needed for coupling to occur during polymerization. Subsequent units can attach themselves to the other vinyl groups of the monomer. In essence, the more vinyl-containing ligands per complex, the better. A sterically-favoured network as opposed to a linear helical spiral of monomers is formed.

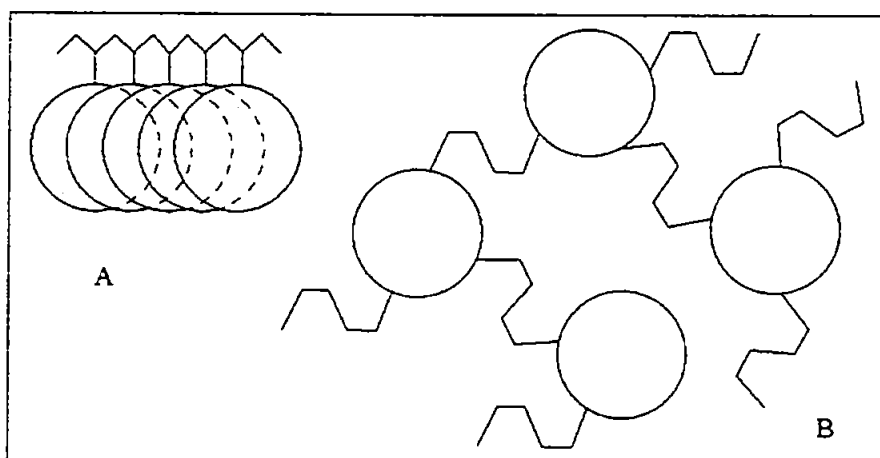


Figure 1.23: Schematic drawing of poly-[Ru(vbpy)₃²⁺] assuming (A) linear vinyl coupling and (B) dimer-bridge vinyl coupling
Taken from ref.¹¹⁰

Other work has supported this theory¹³⁴. Using $\text{Ru}(\text{Me}_2\text{bpy})_2(\text{vbpy})]^{2+}$ for electropolymerization, it was stated that linear polymers are formed which most likely contain seven or fewer monomer units. The lack of cross-linking would probably result in material that is soluble and that would not deposit on the electrode. From this body of work^{110,134}, it became apparent that electropolymerization of the tris-vinylated complex could best serve the purposes of this study.

For complexes containing vinylpyridine and vinylbipyridine ligands, electropolymerization is more rapid and efficient (often by a factor of ten) if two-electron as opposed to one-electron reduction is performed. This has been attributed to a diminution of electrostatic repulsion^{134,142}. The existence of a net electrostatic charge on polymerizing vinylbipyridine metal monomer complexes reduces the rate of electrochemically induced polymer formation.

Film deposition can be controlled by varying monomer concentration (generally, concentrations from 0.02 mM - 2 mM are used), the potential limits, the scan rate and the number of polymerization cycles. If deposition is carried out for too long, very thick films are formed, which are visibly rough and mechanically fragile¹¹⁰. Thinner films tend to be more adherent. Stirring of the solution accelerates film growth. Alternative methods of electropolymerization are available. For example, films can be produced by electroreduction at constant negative potentials, ie potentiostatically. The quantity of polymer deposited on the electrode is controlled by the time of electrolysis and by the negative potential limit. However, this is also thought to affect the morphology of the deposited film. Denisevich *et al.* stated that while substantive differences in the electrochemistry of potential scanning and potentiostatically deposited films were not detected, some structural differences may nevertheless exist¹¹⁰. Calvert *et al.* did detect

that growth rate was faster and the resulting films were clearly less uniform in appearance when electropolymerization was performed by reduction at constant negative potentials¹⁴⁰.

(1.5.1.3) Mechanism of Formation of poly-[Ru(vbpy)₃²⁺] and its Conduction

The mechanism of the polymerization of Ru(vbpy)₃²⁺ has not been fully established. However, the proposed mechanism of polymer formation in similar compounds is quite complex¹⁴⁰ and is summarised as follows. Initiation of polymerization, rather than involving metal localized reduction of the complex, involves reduction at the π^* levels of the vinylbipyridine group. Addition of electrons to π^* orbitals primarily localized on the bipyridine ligands results in generation of a ligand-based radical anion, which appears to act as the initiator. There are a number of mechanistic pathways which can then lead to polymer chain growth. Two of these mechanisms are predominant. It was shown that hydrodimerization, a radical-radical coupling process involving pairs of vinyl groups, was an important pathway. In addition, polymer growth can also occur by chain propagation of radical anions. The dimers formed by the first method can also participate in the second method.

Investigation of the mechanism provides further insight into why complexes with only one vinyl group per molecule do not polymerize very well. In addition to the steric problems explained previously, it can be seen that if radical-radical coupling of the two vinyl moieties occurs, the final product can only be a dimer, which will probably be soluble in the monomer solution, unlike a long chain polymer which would deposit on the electrode surface.

In addition to mechanistic studies, Calvert *et al.* also investigated steric and electronic factors of various monomers and their effects on polymerizability and film formation¹⁴⁰.

Monomers with vinyl groups present result in polymers composed of metal centres distributed along the saturated four-carbon chains which originating from the vinyl groups attached to the aromatic ring systems. Although, in theory, carbon atom backbones will not conduct, poly-[Ru(vbpy)₃]²⁺ is capable of electron transfer. Conduction of the polymer film can occur by electron self-exchange reactions between the immobilised redox sites of the otherwise highly conjugated polymer system. This has been termed in the literature as a 'hopping' process, or electron 'bucket brigade' and is shown in Figure 1.24 below. A flow of counterions also occurs to compensate for alternations in the electrical charges of the fixed redox sites. This combination of ion and electron motions is termed electrochemical charge transport. Charge transport in electroactive polymers is discussed in detail in Dalton *et al.*¹⁴³ The presence of the hydrocarbon backbone also explains why the polymer films are photo-inert, in comparison with the monomer which is photo-sensitive because of the vinyl linkages.

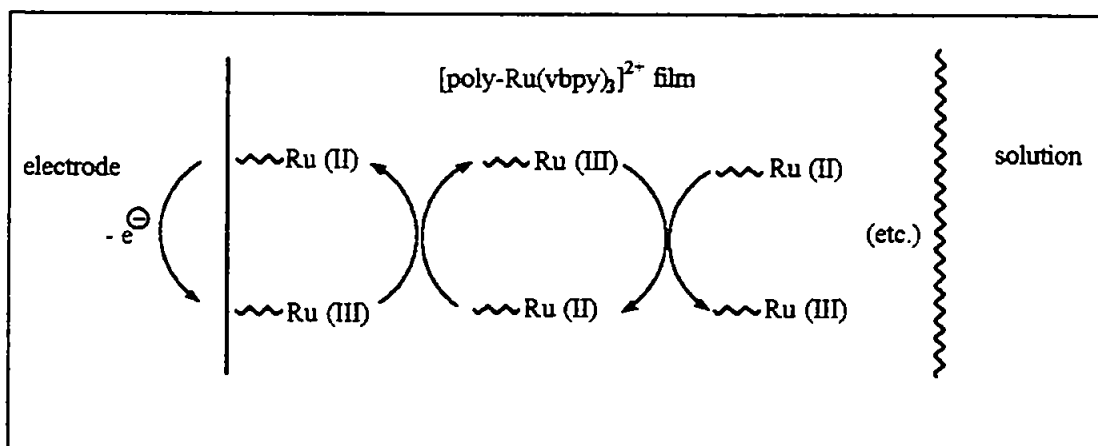


Figure 1.24: Electron transfer through the conjugated polymer system to the electrode.
Taken from ref.⁹⁷

(1.5.2) Methods Used to Study the Formation of CME's

Many different methods are available for monitoring the success and progress of film formation. Of these, the most direct methods are based on electrochemical analysis. These include cyclic voltammetry, ac voltammetry, chronoamperometry, chronocoulometry or rotating disk voltammetry. These techniques measure macroscopic properties of the film such as the number of redox centres, the conductivity and the thickness. Spectroscopic techniques such as scanning electron microscopy, secondary-ion mass spectrometry, absorption and X-ray photoelectron spectroscopy are less direct but provide structural information. All of the above techniques are discussed in detail in reviews by Albery & Hillman⁹⁰ and Murray⁹⁶.

Of all the methods mentioned, one of the most important is cyclic voltammetry.

(1.5.2.1) Cyclic Voltammetry

Voltammetry studies the relationship between potential and current. Working, reference and secondary electrodes are placed in an unstirred solution of supporting electrolyte and a redox species. The potential of the working electrode is controlled relative to the reference electrode by a potentiostat and the resultant current is measured.

Figure 1.25 shows the variation of potential with time, which is a triangular waveform:

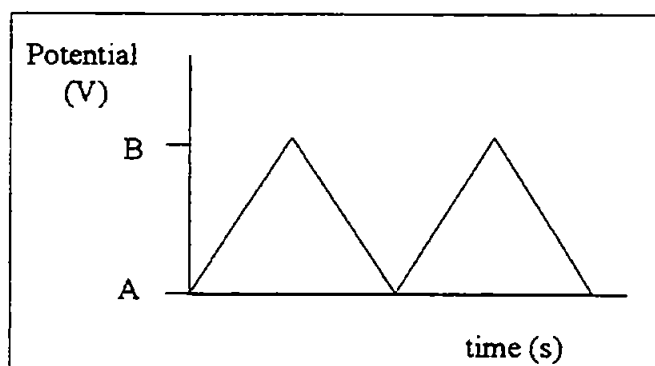


Figure 1.25: Waveform for a potential sweep experiment

The potential is varied linearly with time beginning at a potential where no electrode reaction occurs (A) and moving to a potential (B) where reduction or oxidation occurs. When the potential limit B is reached, the potential ramp is reversed. The scan or sweep rate can be varied typically from a few millivolts to a few volts per second.

During the scan, various intermediates and products are formed, resulting in a change in the current. This can be plotted against potential and the result is a cyclic voltammogram (CV). The axes of this current-voltage plot may be oriented in 8 different ways. The IUPAC convention¹⁴⁴, which is used in the current study, is shown in Figure 1.26 below:

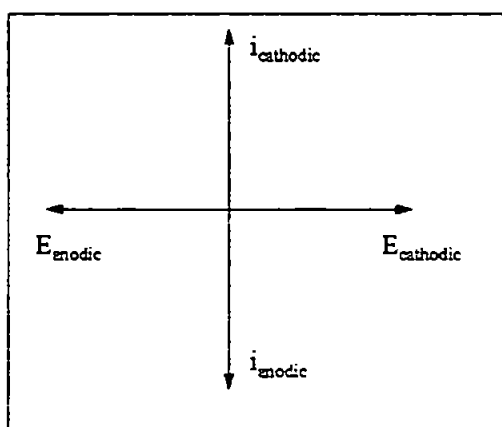
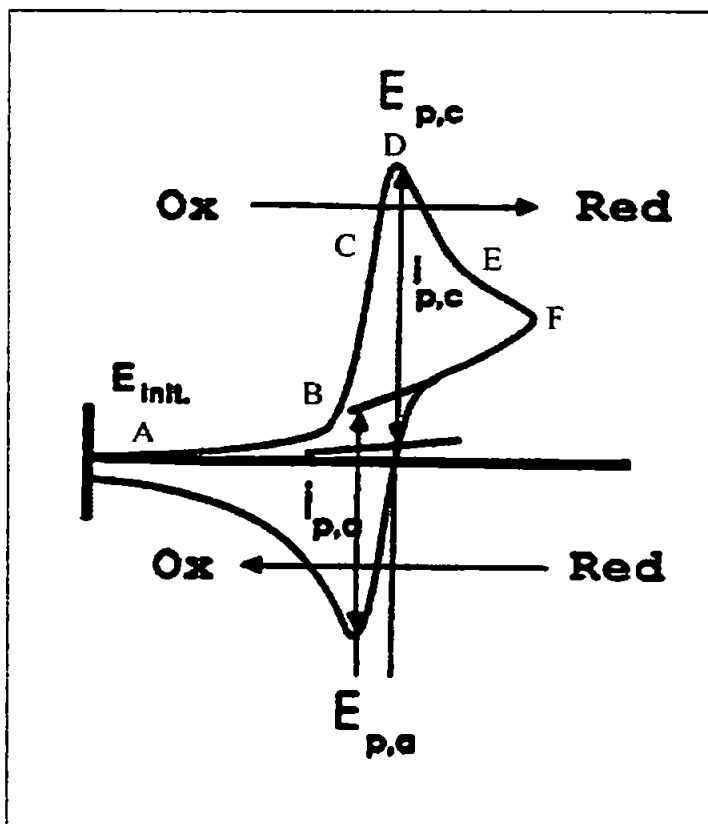


Figure 1.26: IUPAC convention for cyclic voltammograms¹⁴⁴

Analysis of a typical CV, shown overleaf in Figure 1.27, can be found in the review by Abruña⁸⁸. The CV results from the reduction of a solution of species Ox to Red. The characteristic potential for the process is represented on the diagram as $E_{p,c}$ and $E_{p,a}$. At point A, an initial potential E_{init} is applied. As it is removed from $E_{p,c}$, essentially no current flows. The potential is then altered with time and upon scanning cathodically, the species Ox close to the electrode surface is reduced to Red. Current begins to flow (B) and continues to do so (C) until the peak potential $E_{p,c}$ is reached (D). The surface concentration of Ox becomes gradually less until it is exhausted and so the flow of current

falls. Further current will only flow as fresh Ox diffuses to the electrode surface from the solution. This is reflected in the characteristic 'tailing' of the peak (E).

At point F, the potential limit is reached and the sweep direction is reversed. At this stage, the potential is considerably different from the potential $E_{p,a}$ required for electrochemistry to occur. As was observed when scanning cathodically, very little current flows initially. However, as the potential approaches $E_{p,c}$, the reduced material generated in the forward sweep is re-oxidized and current flows once again. The peak potential $E_{p,c}$ represents the maximum current flow, followed by tailing of the peak as the rate of conversion of Red to Ox is less than the rate of diffusion of fresh Red to the electrode-solution interface.



KEY

E_{init} = initial potential, $E_{p,c}$ = cathodic peak potential, $E_{p,a}$ = anodic peak potential, $i_{p,c}$ = cathodic peak current, $i_{p,a}$ = anodic peak current

Figure 1.27: A typical cyclic voltammogram. Taken from ref.⁸³.

Further details of the technique and the interpretation of CV's can be found in any standard electrochemistry text, in particular, the text by Baizer¹⁴⁴.

(1.6) AIM OF THE PRESENT STUDY

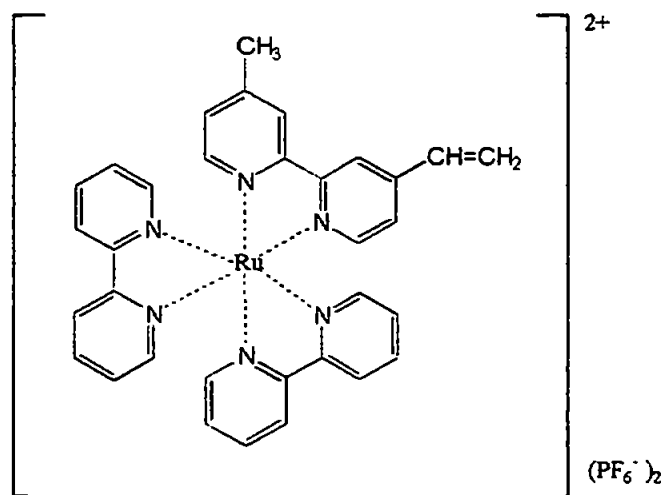
Various concepts have so far been introduced. The aim of this present study draws together all these areas and can be summarised as follows. Due to the lack of a reusable and robust sensor based upon the ruthenium tris(bipyridine) complex for the CL detection of various analytes, the fabrication of an electrochemically regenerable Chemically Modified Electrode was proposed. Synthesis of a vinyl derivative of the ruthenium complex is required which can then polymerized onto an electrode surface. It is proposed that this electrode is used analytically for the repeated CL determination of a range of analytes. The regenerability of this immobilised complex would eliminate the need for extra equipment such as pumps, reagent reservoirs and mixing devices. In addition, there would be a large reduction in the the consumption of the expensive ruthenium complex and the waste of decomposition products and solvents which typically must be pumped continuously during analyses would be diminished.

CHAPTER 2

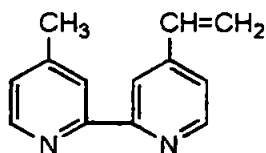
SYNTHESIS OF RUTHENIUM TRIS(BIPYRIDINE) COMPLEXES

(2.1) CRITICAL REVIEW OF METHODS FOR THE SYNTHESIS OF 4-METHYL-4'-VINYL-2,2'-BIPYRIDINE

The initial target molecule for this project was the complex ruthenium (4-methyl-4'-vinyl-2,2'-bipyridine) bis(2,2'-bipyridine) bis(hexafluorophosphate), (iv);



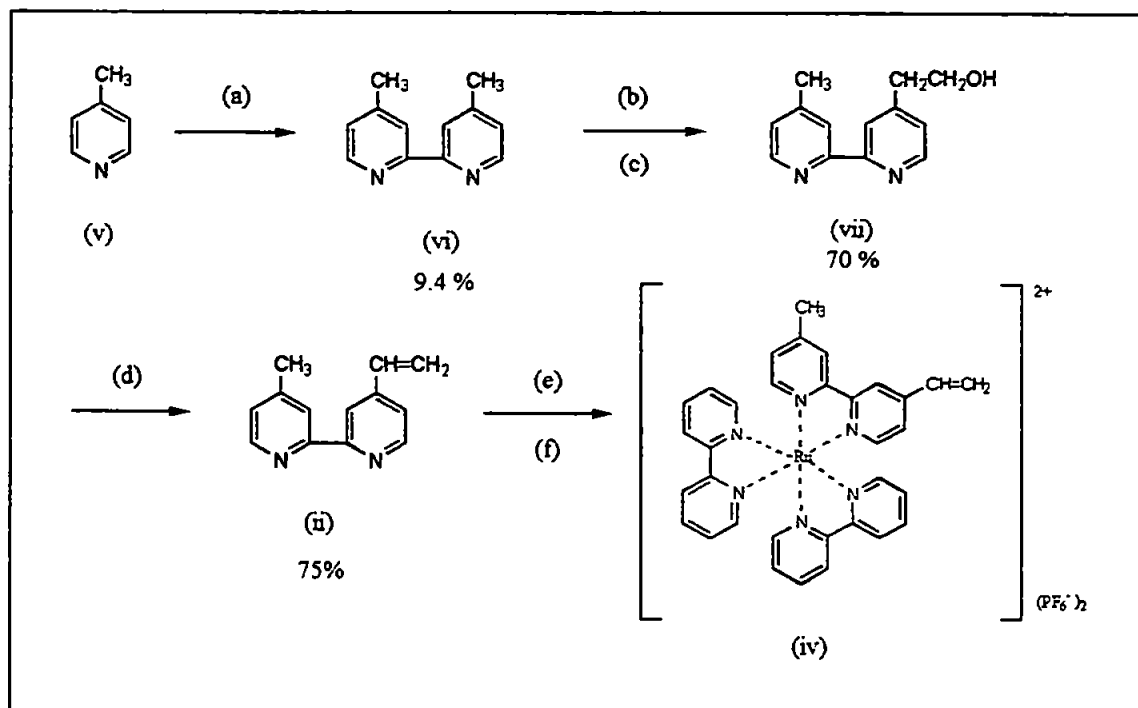
The immediate precursor to (iv) was the ligand 4-methyl-4'-vinyl-2,2'-bipyridine (ii);



The various methods reported in the literature for the synthesis of (ii) are described below.

(a) Ghosh & Spiro, 1980¹⁴⁵

This was one of the earliest reported methods. The synthetic route is shown in Scheme 2.1;



KEY

(a) 5% Pd / C, reflux, 72 hrs, (b) LDA / THF, (c) HCHO, 1 eq., (d) P₂O₅ / Xylene, reflux, (e) Ru(bpy)₂Cl₂ (cis-Dichlorobis(bipyridine) ruthenium), CH₃OH / H₂O, reflux, (f) NH₄PF₆

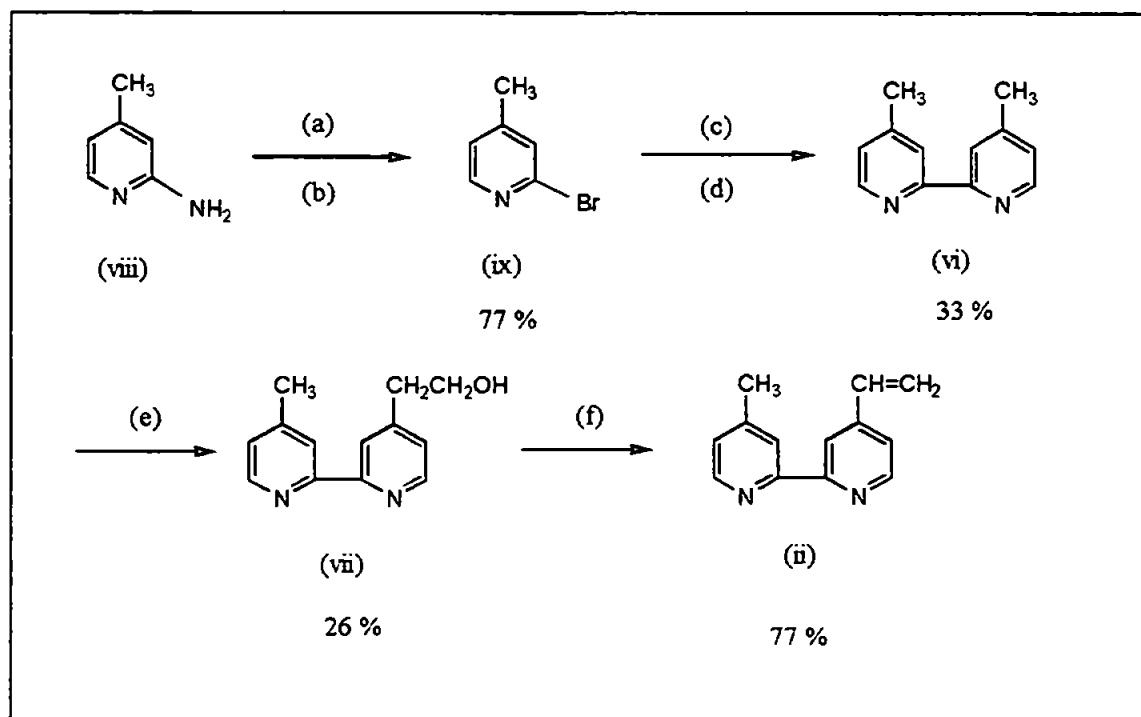
(ii) 4-methyl-4'-vinyl-2,2'-bipyridine [4-ethenyl-4'-methyl-2,2'-bipyridine], (iv) Ruthenium (4-methyl-4'-vinyl-2,2'-bipyridine) bis(2,2'-bipyridine) bis(hexafluorophosphate), (v) 4-methylpyridine, (vi) 4,4'-dimethyl-2,2'-bipyridine, (vii) 4-hydroxyethyl-4'-methyl-2,2'-bipyridine

Scheme 2.1: Ghosh & Spiro¹⁴⁵ synthesis of (ii)

The first step was the coupling of two molecules of 4-methylpyridine (v), using palladium on activated carbon as a catalyst, to synthesise 4,4'-dimethyl-2,2'-bipyridine (vi). The next stage involved formation of the bipyridine carbanion using a strong base, lithium diisopropylamine (LDA), prepared *in situ* from diisopropylamine and

n-butyllithium. Hydroxyethylation to produce (vii) in a yield of 70 % was performed using gaseous formaldehyde generated by heating the polymer paraformaldehyde. Dehydration of (vii) using phosphorus pentoxide gave the product (ii). The final step was the complexation of (ii) with *cis*-dichlorobis(bipyridine)ruthenium to form (iv).

(b) Furue *et al.*, 1982¹⁴⁶



KEY

(a) 47 % HBr soln., Br₂ (b) NaNO₂ soln. at < 5 °C, NaOH soln. added, < 25 °C (c) Cu powder, 220 °C (d) gradual increase to 240 °C over 45 min (e) 35 % aq. formalin, piperidine (cat.), under N₂ pressure at 160-170 °C, (f) *p*-*tert*-butylpyrocatechol (trace amount), NaOH powder, 0.4 Torr, 120 °C

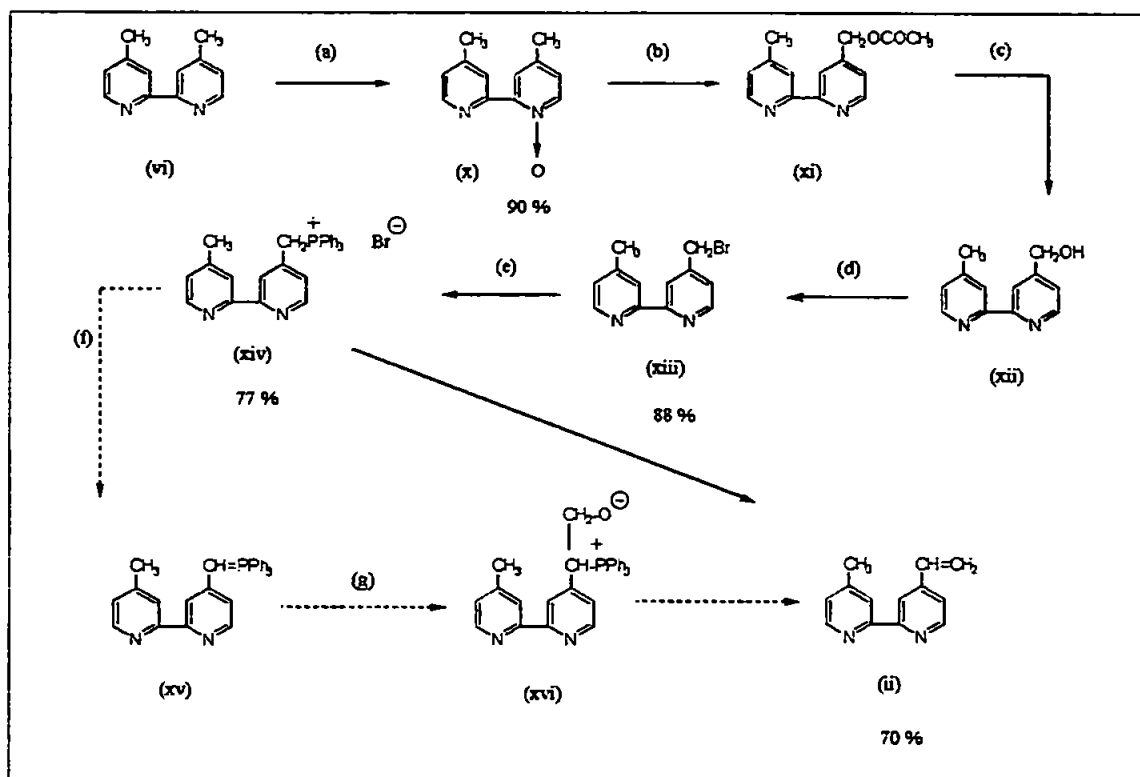
(ii) 4-methyl-4'-vinyl-2,2'-bipyridine, (vi) 4,4'-dimethyl-2,2'-bipyridine, (vii) 4-hydroxyethyl-4'-methyl-2,2'-bipyridine, (viii) 2-amino-4-methylpyridine, (ix) 2-bromo-4-methylpyridine,

Scheme 2.2: Synthesis of (ii) using the method reported by Furue *et al.*¹⁴⁶

Synthesis of (vi) was accomplished using the method described by Case¹⁴⁷. Furue *et al.*¹⁴⁶ then produced (ii) via a similar synthetic route to the Ghosh & Spiro method¹⁴⁵. Hydroxyethylation of (vi) was carried out using aqueous formalin and a catalytic amount of the weak base, piperidine. This stage was performed using a magnetic stirring autoclave and under nitrogen pressure to prevent the aqueous formalin from boiling. (ii) was produced by treatment of a mixture of (vii) and p-tert-butylpyrocatechol (a radical inhibitor) with powdered sodium hydroxide under reduced pressure in a Kugelrohr distillation apparatus.

(c) Kaschig & Lohmann, 1984¹⁴⁸

Kaschig & Lohmann¹⁴⁸ patented a multi-step route for the synthesis of (ii), shown overleaf in Scheme 2.3. Conversion of (vi) to the bipyridine mono-N-oxide (x) was effected by use of peracetic acid in the presence of an inert solvent. The electron-withdrawing effect of the N-oxide group increased the acidity of the methyl group attached to this pyridine ring and facilitated proton abstraction in the next stage. Excess acetic anhydride in chloroform converted the methyl group to the acetoxy group. Saponification of the resulting ester (xi) in the presence of a base was carried out in an aqueous-alcoholic medium, producing the hydroxymethyl compound (xii) in a yield of 5.3 % relative to (vi). (xii) was then treated with conc. aqueous hydrobromic acid under reflux. The corresponding bromomethyl compound (xiii), produced in 88 % yield from (xii), underwent a Wittig reaction to produce the target molecule (ii). Details of this final stage included treatment of (xiii) with triphenylphosphine to afford the phosphonium salt (xiv) in 77 % yield. The ylid (xv) was produced by base abstraction of a proton.



KEY

(a) 1.8 M peracetic acid soln. in ethyl acetate added dropwise at 23 - 28 °C to (vi) in DCM. Stir for 50 hrs,
 (b) 2:1 acetic anhydride : chloroform, 20 hours stirring at 60 - 65 °C, (c) 10 % NaOH, EtOH, reflux for 30 mins,
 (d) 62 % HBr acid, reflux 6 hrs, (e) Ph_3P in N,N -DMF at 80 °C for 3 hrs, (f) NaOH soln, (g) 35 % HCHO soln, DCM, di-tert-butyl-p-cresol, Bu_4NCN , stir for 1 hr at 23 °C

(x) 4,4'-dimethyl-2,2'-bipyridine mono-N-oxide, (xi) 4-methyl-4'-acetoxymethyl-2,2'-bipyridine, (xii) 4-methyl-4'-hydroxymethyl-2,2'-bipyridine, (xiii) 4-methyl-4'-bromomethyl-2,2'-bipyridine, (xiv) [4-methyl-2,2'-bipyridin-4'-yl-(methylene)]triphenylphosphonium bromide, (xv) [4-methyl-2,2'-bipyridin-4'-yl-(methylene)]triphenylphosphorane, (xvi) Betaine intermediate

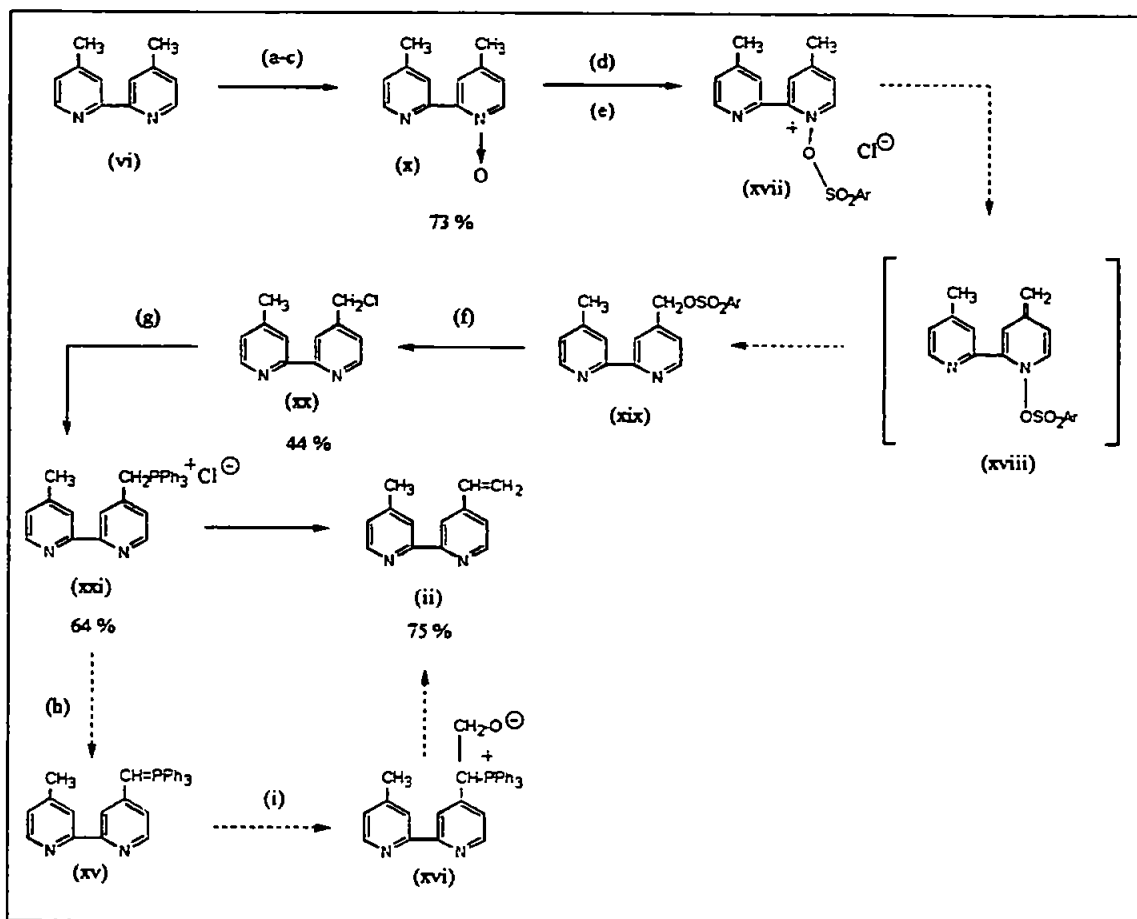
Scheme 2.3: Synthesis of (ii) using the method reported by Kaschig & Lohmann¹⁴⁸

Addition of aqueous formalin solution, together with tetra-n-butylammonium cyanide present as a phase transfer catalyst and di-tert.-butyl-p-cresol as a polymerization inhibitor resulted in the betaine (xvi), which spontaneously underwent elimination to yield the product (ii).

Kaschig & Lohmann¹⁴⁸ also mentioned two other methods for synthesis of (ii) but not in any great synthetic detail. The first was based upon that already published by Ghosh and Spiro¹⁴⁵ in 1980. The second was similar to that later published by Abruña *et al.* in 1985 (part e of the present study)¹⁴⁹.

(d) Pitt *et al.*, 1986¹⁵⁰

A similar route was recorded by Pitt *et al.*¹⁴⁴ in 1986, as shown in Scheme 2.4 overleaf. Once again, a peracid was used in the first stage to synthesise the N-oxide (x). However, whereas the route reported previously involved three steps to produce the bromomethyl-bipyridine compound, Pitt *et al.* obtained the analogous chloromethyl compound (xx) in two steps¹⁵⁰. This was achieved by protecting the N-oxide group using *p*-toluenesulfonyl chloride, producing (xvii). The intermediate (xviii) formed, underwent a rearrangement¹⁵¹ to (xix) and the CH₂OSO₂Ar group was converted to a chloromethyl group; (xx) was obtained in 44 % yield. As with the method by Kaschig & Lohmann¹⁴⁸, (Scheme 2.3) the phosphonium salt (xxi) was synthesised and converted, via the ylid (xv) and betaine (xvi), to the target molecule (ii).



KEY

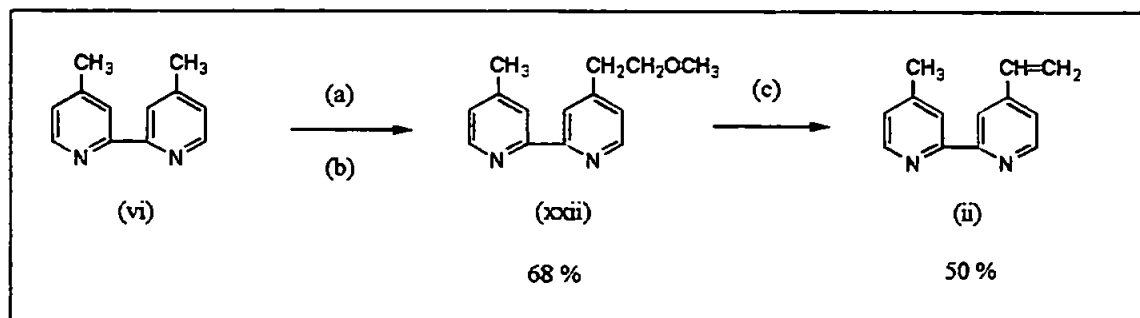
(a) Addition of 80 % *m*-chloroperbenzoic acid / CHCl_3 at 0 °C, (b) Left for 18 hrs at ambient temp., (c) Satd. aq. NaHCO_3 , (d) Tosyl chloride / dioxane, (e) Reflux, 3 hrs, (f) 5 % HCl, (g) Ph_3P (1 eq.), reflux, dry toluene, 18 hr, (h) 0.70 M methanolic soln. of KOMe, (i) Paraformaldehyde / dry MeOH slurry, 0.70 M methanolic soln of KOMe, stir for 1 hr.

(xx) 4-chloromethyl-4'-methyl-2,2'-bipyridine, (xxi) 4-(methylenetriphenylphosphonium)-4'-methyl-2,2'-bipyridine chloride

Scheme 2.4: Synthesis of (ii) using the method reported by Pitt *et al.*¹⁵⁰

(e) Abruña et al., 1985¹⁴⁹

Abruña *et al.*¹⁴⁹ published a modification of the original Ghosh & Spiro method¹⁴⁵, as shown in Scheme 2.5;



KEY

(a) LDA in THF, 0°C, under N₂, stir for 15 min., (b) CMME in dry THF, stir at 0 °C for 30 min.,

(c) t-BuOK, THF, -78°C, under N₂, stir for 90 min. at -78 °C, 15 min. at rm. temp.

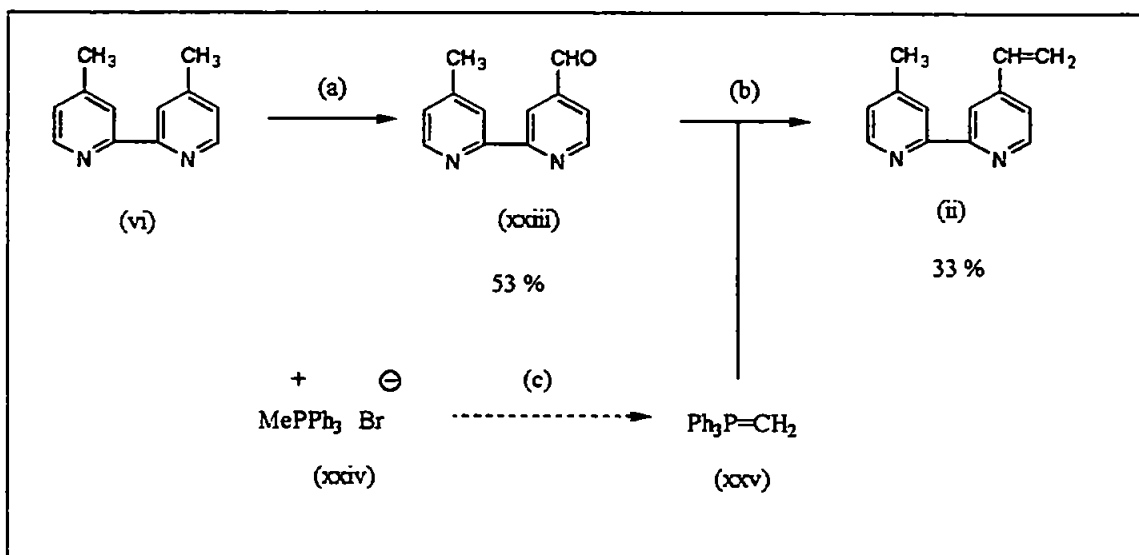
(xxii) 4-methoxyethyl-4'-methyl-2,2'-bipyridine

Scheme 2.5: Synthesis of (ii) using the method reported by Abruña *et al.*¹⁴⁹

In the first stage, conversion of a methyl group to a methoxyethyl group was effected by use of chloromethyl methyl ether (CMME). Elimination using a strong base, potassium tert-butoxide, produced (ii) in a 35 % overall yield from (vi).

(f) Leasure et al., 1996¹⁵²

In 1996, Leasure *et al.*¹⁵² proposed the route shown in Scheme 2.6 overleaf. Synthesis of (xxiii) was originally reported by Peek *et al.*¹⁵³. Selenium dioxide was used to oxidise one methyl group of (vi) to an aldehyde. Leasure *et al.*¹⁵² reported the final stage, which, once again, was a Wittig-type reaction. (xxv) was produced *in situ* by reaction of (xxiv) with *n*-butyllithium in hexanes. (xxiii) was added to this solution at -78 °C in a dry ice / acetone bath to produce the desired target molecule (ii).



KEY

(a) SeO_2 / 1,4-dioxane. reflux 24 hrs (b) -78°C / THF, (c) 2.5 M *n*-butyllithium in hexanes / THF at 0°C .

Stirred for 30 mins

(xxiii) 4-carboxaldehyde-4'-methyl-2,2'-bipyridine (xxiv) Methyltriphenylphosphonium bromide, (xxv)

Methylenetriphenylphosphorane

Scheme 2.6: Synthesis of (ii) using the method reported by Leasure *et al.*¹⁵²

All of the above methods led to the synthesis of (ii). For the present project, the method by Furue *et al.*¹⁴⁶ was discarded due to the lack of equipment necessary to withstand high pressure and the unavailability of a magnetic autoclave. Of the other five methods, the overall percentage yield of (ii) from (vi) was calculated. The steps for the synthesis of (vi) were not counted as this compound was commercially available. The figures are shown in Table 2.1 overleaf. Furue *et al.*'s method¹⁴⁶ was included for comparison.

LITERATURE METHOD	NUMBER OF SYNTHETIC STEPS FROM (vi)	OVERALL % YIELD OF (ii) FROM (vi)	REF.
Ghosh & Spiro	2	53	145
Furue <i>et al.</i>	2	20	146
Kaschig & Lohmann	6	3	148
Pitt <i>et al.</i>	5	15	150
Abruña <i>et al.</i>	2	34	149
Leasure <i>et al.</i>	2	17	152

Table 2.1: Comparison of efficiency of literature methods for the synthesis of (ii)

From these results it appeared that Ghosh & Spiro's method¹⁴⁵ produced the highest yield of (ii). As the method has been used by a number of other workers^{111,112,123}, it became the first method of choice for this study.

(2.2) SYNTHESIS OF 4-HYDROXYETHYL-4'-METHYL-2,2'-BIPYRIDINE (v) USING THE GHOSH & SPIRO METHOD¹⁴⁵

(2.2.1) Introduction

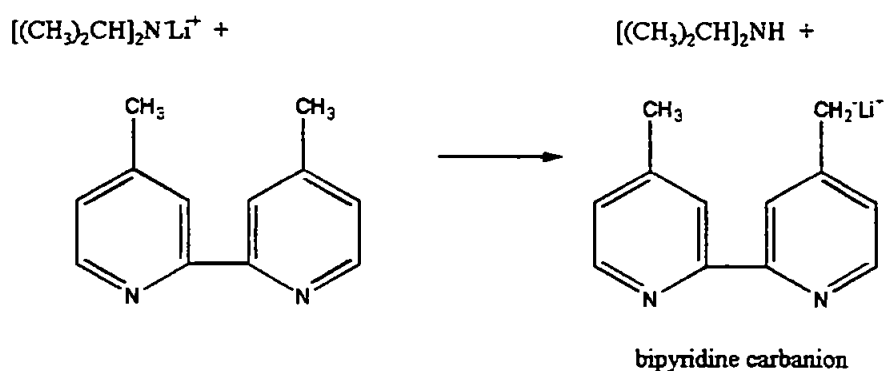
The synthetic route proposed by Ghosh & Spiro¹⁴⁵ has been given previously on page 57 (Scheme 2.1). Synthesis of 4,4'-dimethyl-2,2'-bipyridine (vi) was found to be unnecessary as it was available commercially. The synthesis of 4-hydroxyethyl-4'-methyl-2,2'-bipyridine (vii) was thought to occur by the reaction mechanism described below. It can be divided into four stages:

(a) Generation of the base;

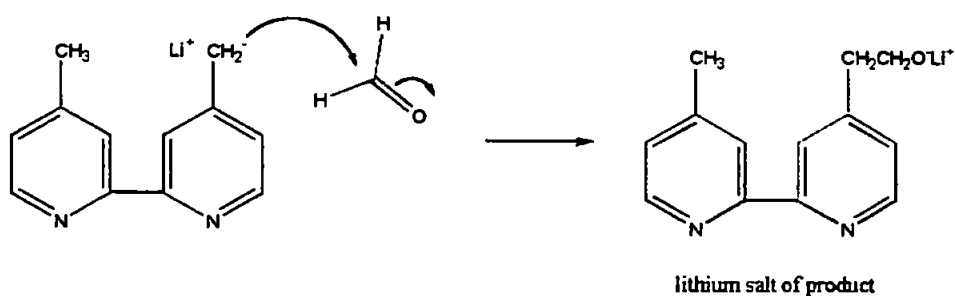


Diisopropylamine (a secondary amine) was reacted with *n*-butyllithium (a strong base) at low temperatures in an aprotic solvent, in this case THF. This produced the even stronger base, lithium diisopropylamide (LDA) which was required for the second stage.

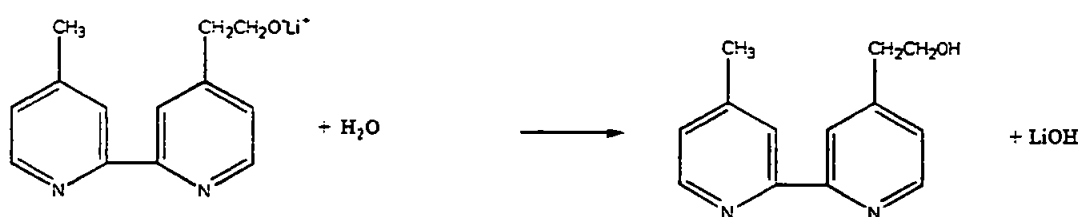
(b) Proton abstraction by LDA from one methyl group to form the bipyridine carbanion;



(c) Nucleophilic attack by the carbanion upon the formaldehyde;



(d) Quenching of the reaction using iced water;



(2.2.2) Experimental Procedure

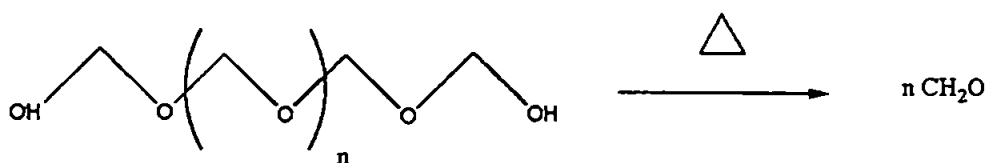
Due to the sensitivity of *n*-butyllithium to air and water, the entire experiment was conducted under an inert nitrogen atmosphere using glassware preheated for a minimum of 3 hours at 115°C. The nitrogen was dried by passing it through a calcium chloride drying tube.

Bipyridine Carbanion Generation

THF (30 ml) was added to a 250 ml 3-necked round-bottomed flask. At 0 °C, diisopropylamine (8ml, 56.7 mmol) was dispensed from its septum-sealed bottle via cannula lines and a glass syringe into the reaction flask. *n*-butyllithium in hexanes (1.6 M, 35 ml, 56.4 mmol) was also cannulated into the reaction flask via glass tubes which had been pre-calibrated, sealed with rubber septa and purged. The clear pale yellow solution was left to stir for 15 minutes and the reaction flask was covered with aluminium foil due to the photo-sensitivity of *n*-butyllithium. 4,4-dimethyl-2,2'-bipyridine (vi) (9.99 g, 54.2 mmol) was pre-prepared in THF solution (280 ml) and added dropwise to the reaction mixture from a pressure-equalising dropping funnel. This turned to a brown-orange solution, showing the production of the bipyridine carbanion. The solution was stirred for 2 hours.

Formaldehyde Generation

Formaldehyde gas was generated *in-situ* by heating the polymer paraformaldehyde;



The gas was transferred quantitatively using a specially designed piece of glassware as shown in Plate 2.1 overleaf.

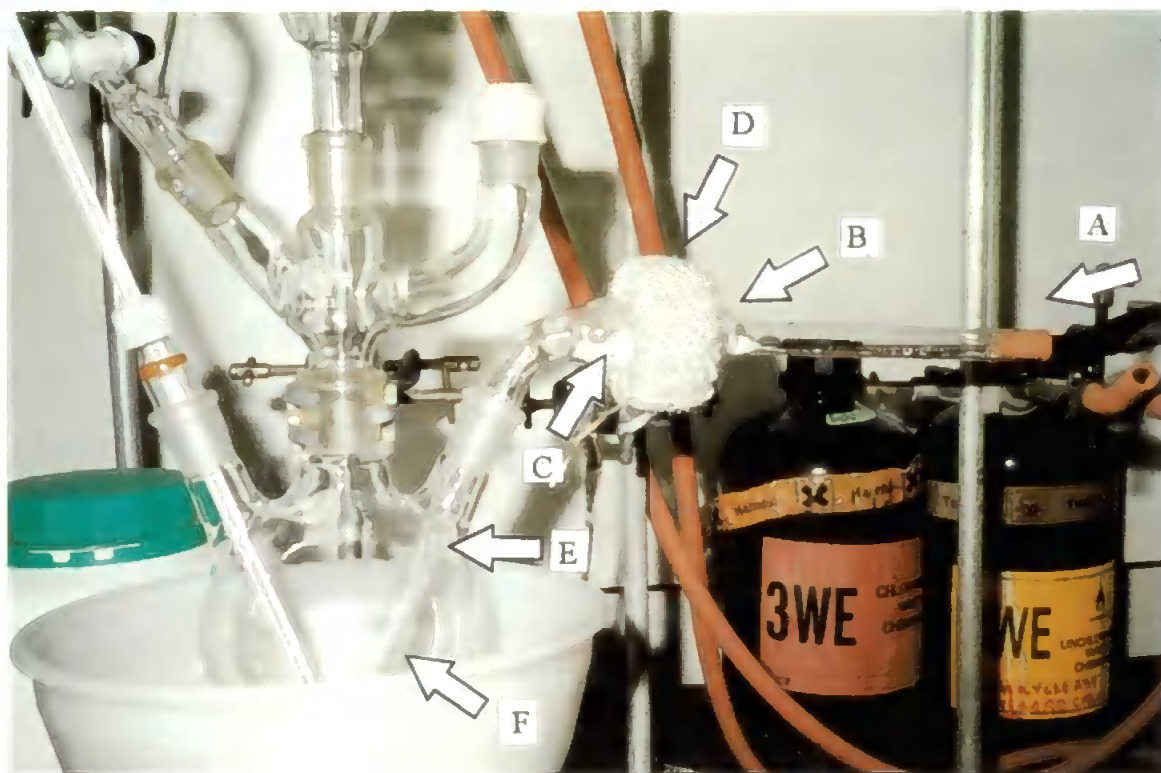


Plate 2.1: The paraformaldehyde unit

- A Flow of nitrogen into unit
- B Bulb of pyrolysis unit
- C Paraformaldehyde
- D 'Variac' controlled heating collar
- E Inlet Tube
- F Bell-shaped end to prevent tube blockage by resolidified formaldehyde gas

Paraformaldehyde (1.95 g, 65.0 mmol) was placed in the bulb of the unit. A 'Variac' controlled heating collar was fitted around the bulb and heated slowly. Upon pyrolysis of the paraformaldehyde, the arm of the inlet tube was heated with a hot air gun to prevent re-condensation of the vapour. The formaldehyde gas was added to the reaction mixture over a period of 1½ hrs at 60 - 120 °C. This proved to be problematic despite thorough heating of the pyrolysis unit, as the inlet tube of the unit led directly to the reaction flask which was being kept at 0 °C. A lot of material condensed around the exit and blocked the passage of gas. However, enough reached the reaction vessel for the colour of the reaction mixture to change to a very dark green. This was left to stir for ¾ hr and the reaction was then quenched with iced distilled water (250 ml). The resulting bright yellow solution was added to more iced water (120 ml) in a 1 litre conical flask.

Isolation and Purification of Product

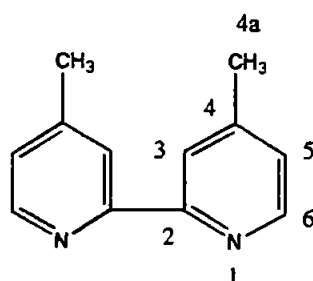
The work-up of the reaction mixture involved extraction into diethyl ether (3 x 250 ml), drying over magnesium sulfate, filtration under reduced pressure and rotary evaporation. This yielded a mixture of a yellow oil and a pale yellow-white solid. A small amount of ether was purposely left mixed with the oil to reduce its viscosity and aid its separation from the solid.

The oil was carefully removed using a Pasteur pipette. However, some solid was retained within the collected oil. In order to remove this, the oil was centrifuged at 3000 r.p.m. and the supernatant collected by Pasteur pipette. The final traces of solvent were then removed under vacuum and the oil was analysed. An attempt was made to purify it by dissolving it in diethyl ether, chilling the solution in ice and separating the oil by filtration under reduced pressure.

For the purposes of GC-MS analysis, the alcoholic group of the product was derivatized using bis(trimethylsilyl)trifluoroacetamide (BSTFA). BSTFA (50 μ l) and pyridine (50 μ l) were added to 10 mg of the sample in a vial, sealed and heated at 60 $^{\circ}$ C for 20 - 30 min. Any solvent remaining was then removed using a stream of nitrogen and a 0.1 mg/ml solution of the derivatized sample was made up in dichloromethane, unless otherwise specified. Derivatization led to better resolution of GC signals and also resulted in characteristic fragmentation in the mass spectrum.

(2.2.3) Results & Discussion

Properties & Spectral Data of 4,4'-dimethyl-2,2'-bipyridine ((vi), starting material)



(vi)

Physical appearance - a pale yellow, crystalline solid

Mp 171.6 - 173 $^{\circ}$ C (lit. 171 - 172 $^{\circ}$ C)¹⁵⁴

GC

t_R 23.02 min

NMR

1H NMR (270 MHz, $CDCl_3$); δ (ppm) 8.5 (d, 2H, H-6), 8.2 (s, 2H, H-3), 7.1 (d, 2H, H-5), 2.4 (s, 6H, H-4a)

Lit.¹⁴⁵; (60 MHz, $CDCl_3$); δ (ppm) 8.3 (d, 2H), 8.06 (s, 2H), 6.95 (d, 2H), 2.33 (s, 6H)

^{13}C NMR (68 MHz, CDCl_3); δ (ppm) 155.8 (C-2), 148.7 (C-6), 147.9 (C-4), 124.4 (C-5), 121.8 (C-3), 21.0 (C-4a)

DEPT (68 MHz, CDCl_3); δ (ppm) 148.7, 124.5, 121.8, 21.0 as CH / CH_3

Lit.¹⁵⁵; 156.4 (C-2), 149.2 (C-6), 148.5 (C-4), 125.0 (C-5), 122.4 (C-3), 21.5 (C-4a)

IR

(KBr disk); ν 3050 (ar. C-H ring str.), ν 2920 (alip. C-H str.), ν 1589 (C=N str.), ν 1450 & ν 1366 (C=C str.), δ 1450 (CH_3 bend), δ 1042, δ 980, δ 910 (in-plane C-H bend), δ 819, δ 661, δ 511 (out-of-plane C-H bend) cm^{-1}

Properties & Spectral Data of the Crude Product Prior to Centrifugation

Recovered Solid

IR

This matched the IR of the starting material (vi).

Decanted Oil

Mass of oil / ether decanted = 5.52 g

GC

Injection volume: 0.5 μl of 0.02 mg/ml in DCM

t_{R} (vi) 23.63 min, 25 %, t_{R} (vii) 32.95 min, 65 %, 10% impurities.

% crude yield ~ 30 % (lit. yield¹⁴⁵ = 70 %)

TLC

Mobile phase 50 / 50 ethyl acetate & petroleum spirit (40 - 60 $^{\circ}\text{C}$) + 1 % TEA

R_{F} (vi) 0.33, R_{F} (products) 0.18, 0.35

Small amount of tailing of spots observed.

Solubilities of starting material and decanted oil

Both the starting material and decanted oil were soluble in hot and cold dichloromethane, chloroform, THF, ethyl acetate and toluene and insoluble in hot and cold petroleum spirit (40 - 60 °C), water and hexane. The only solubility difference was that the product was readily soluble in hot and cold diethyl ether whereas the starting material was only sparingly soluble.

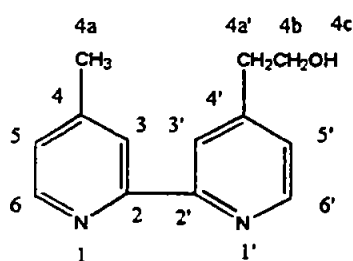
Complete removal of solvent by rotary evaporation had previously yielded a yellow-white solid covered with a small amount of very viscous oil which proved virtually impossible to separate. Separation of the oil from the solid in this experiment was facilitated by leaving a small volume of ether which dissolved all the oil and only a little solid. This solid was established by IR as being unreacted starting material. Using GC, the decanted oil was found to consist of (vii) and (vi) in the proportions 65 %:25 %, with 10 % impurities. The results from the GC were limited by the fact that it was unable to take into account the volume of solvent present. This meant that the crude yield of desired product was calculated as less than 30 %, much lower than the 70 % reported in the literature¹⁴⁵.

The IR analysis of the oil showed signals corresponding to the desired product but this was ambiguous as both it and the starting material were structurally very similar. The presence of starting material was more evident in the NMR spectra but the signals due to both compounds overlapped or were not properly resolved. Also present were small amounts of impurities.

Various methods of separation were attempted at this stage. A suitable solvent system for chromatographic separation proved hard to find due to the structural similarity

of the compounds. Many solvent systems were tried, including, amongst others, different combinations of ethyl acetate or absolute alcohol and petroleum spirit (40 - 60 °C). Streaking between the spots was observed for a great number of these systems. Solvent systems where separation of the compounds was significant were prone to tailing, even at low concentrations, although the use of 1 % triethylamine (TEA) helped with this problem. The best system was with 50:50 ethyl acetate: petroleum spirit (40 - 60 °C) and 1 % TEA. This was used for future experiments but was still not considered to be entirely satisfactory and was used only as an indication of the composition of the reaction mixture. Centrifugation was employed to separate the remaining solid from the oil.

Properties and Spectral Data of Oil Obtained after Centrifugation and Removal of Final Traces of Solvent



(vii)

Mass of oil = 2.33 g (10.9 mmol)

GC

Injection volume: 0.5 µl of 0.2 mg/ml in DCM

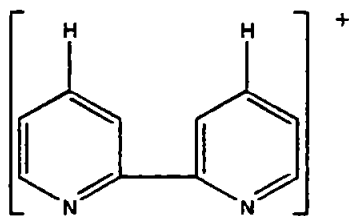
t_R (vii) 33 %, >99 % pure. % Yield = 20 % (lit. yield¹⁴⁵ 70 %)

GC-MS

t_R (vi) 20.57 min, 1.2 %

m/z 184, (M⁺ ion), 181 (M⁺ - [loss of protons from Me group]), 169, (M⁺ - CH₃),

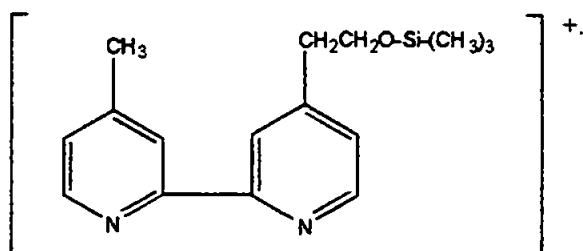
m/z 156,



m/z 92

t_R (vii) 29.67 min, 95.3 %;

m/z 286;



Trimethylsilyl derivative of the molecular cation radical of (vii)

m/z 271 ($[M+\text{trisilyl}]^+ - \text{CH}_3$), 255 ($[M+\text{trisilyl}]^+ - 2 \text{ Me groups and a proton}$), 241 (loss of 3 Me groups), 197 (loss of $-\text{SiMe}_3$), 183 ($M^+ - \text{H}$),

m/z 103, m/z 73 ($[\text{SiMe}_3]^+$)

% Yield by GC-MS = 19 %

NMR

^1H NMR (270 MHz, CDCl_3); δ (ppm) 8.5 (d, 1H) & 8.45 (d, 1H), (H-6 & H-6'), 8.2 (s, 1H) & 8.15 (s, 1H), (H-3 & H-3'), 7.1 (d, 1H) & 7.05 (d, 1H), (H-5 & H-5'), 4.2 (broad s, 1H, H-4c), 3.9 (t, 2H, H-4b), 2.9 (t, 2H, H-4a'), 2.4 (s, 3H, H-4a)

Ghosh & Spiro¹⁴⁵ reported the following data: (60 MHz, CDCl_3); δ (ppm) 8.0 (2H), 7.75 (2H), 6.7 (2H), 4.35 (s, 1H), 3.45 (t, 2H), 2.45 (t, 2H), 1.95 (s, 3H)

Daire *et al.*¹⁵⁶ reported: (CDCl_3); δ (ppm) 8.51 (d, 2H), 8.21 (s, 2H), 7.11 (m, 2H), 4.78 (s, 1H), 3.90 (t, 2H), 2.95 (t, 2H), 2.41 (s, 3H)

^{13}C NMR (68 MHz, CDCl_3); δ (ppm) 155.7 & 155.6 (C-2 & C-2'), 149.2 & 148.1 (C-4 & C-4'), 148.8, 148.5, 124.5, 124.4, 122.0, 121.6 (C-3, C-3', C-5, C-5', C-6 & C-6'), 61.8 (C-4b), 38.5 (C-4a'), 21.0 (C-4a)

DEPT (68 MHz, CDCl_3); δ (ppm) 148.8, 148.5, 124.5, 124.4, 122.0, 121.6, 21.0 as CH / CH_3 , 61.8 & 38.5 (inverted, CH_2)

IR

(KBr disk); ν 3425 (broad H-bonded O-H str.), ν 3054 (ar. =C-H str.), ν 2968 & ν 2867 (alip. C-H str.), ν 1596 & 1459 (C=C ring str.), ν 1459 (CH_2 methylene group), ν 1376 (CH_3 absorption), ν 1064 (C-O str.), δ 906 & 829 (out-of-plane C-H bend) cm^{-1}

After centrifugation and removal of the remaining solvent, the purity of the oil was much higher. However, NMR and GC-MS still showed the presence of some starting material. Purification of the oil (vii) using diethyl ether was very difficult as the starting material (vi) was sparingly soluble in (vii). Attempts to obtain a pure product resulted in substantial losses, thus decreasing the yield even more.

This synthesis was repeated a number of times, with a reproducibly low yield being achieved each time. Optimization of this step was clearly necessary to improve the yield and purity of the target molecule.

(2.2.4) Investigation of Paraformaldehyde Decomposition

The low yield of the reaction described in section 2.2.2 (page 71), was attributed to a large quantity of the formaldehyde gas re-condensing on the sides of the pyrolysis unit and therefore not actually reaching the reaction mixture. An improved crude yield of 59 % was achieved using 2.5 times the stoichiometric amount of paraformaldehyde.

However, this still did not match the yield reported in the literature¹⁴⁵. Unfortunately, during the course of the experiment, the excess gas again condensed, causing partial blockage of the inlet tube. Also, the presence of what appeared to be 'condensation' was noticed at the head of the inlet tube; the paraformaldehyde had been thoroughly dried over phosphorus pentoxide prior to use and therefore water should not have been present. As a result of this observation, investigations were made into the quality of the formaldehyde produced.

Schiff's and Brady's A reagents were used to confirm the production of formaldehyde gas. Both reagents gave positive results. A deep magenta colour was formed with the use of the former and formaldehyde 2,4-dinitrophenylhydrazone was produced with the latter.

Rodd¹⁵⁷ reported that trioxan, (trioxymethylene, 1,3,5-trioxane), a stable cyclic polymer of formaldehyde *'is prepared from paraformaldehyde by heating in a sealed tube at 115 °C with a trace of sulphuric acid or by heating in a stream of nitrogen.'* These conditions were very similar to those created in the experiment for production of (vii) and it was postulated that perhaps the formation of trioxan was the reason for the low yields obtained. An experiment was set up to mimic the conditions in the actual synthesis with just the paraformaldehyde. The solid which re-condensed at the end of the inlet tube was analysed but the results were inconclusive. Once again, 'condensation' was observed during the course of this experiment.

Further investigation yielded the following: paraformaldehyde *'is generally prepared as 91 or 95 % by weight formaldehyde with the remainder being free and combined water. The combined water is the terminating agent for the paraformaldehyde chains'*¹⁵⁸. Although the 'free' water was removed by drying over phosphorus pentoxide,

water was still bound up within the structure of the polymer, only to be released on heating. This could account for the 'condensation' seen in previous experiments. In addition, this would react with the bipyridine carbanion to reform the starting material.

Further investigations were undertaken to limit this water production. A mixture of paraformaldehyde with phosphorus pentoxide, a drying agent, was heated. This was successful in its aim as no condensation was observed, however, the reaction was terminated fairly quickly as the paraformaldehyde/P₂O₅ mixture began to char, became very exothermic and copious white fumes were emitted.

Walker¹⁵⁹ reported that formaldehyde gas produced from paraformaldehyde '*is contaminated with water, formic acid, methanol, methylal and methyl formate*'. These were all potential contaminants which could interfere with the course of the reaction. A proposed solution to this problem was to mix the paraformaldehyde with an inert solvent, diglyme (2-methoxyethyl ether), to trap these impurities. Upon heating, formaldehyde gas would be generated and pass into the reaction mixture and the impurities would remain in the gently refluxing inert medium. The experiment replicated that described in section 2.2.2 (page 67) except that the pyrolysis unit was replaced by reflux apparatus containing the paraformaldehyde and inert solvent. A drying tube containing phosphorus pentoxide came from the top of the condenser and lead into the main reaction flask via an inlet tube. Formaldehyde gas was best produced by cooling the inert solvent, adding paraformaldehyde and heating the mixture quickly; otherwise most of the gas condensed over the walls of the reflux apparatus and did not reach the reaction mixture. 3.4 times the stoichiometric amount of paraformaldehyde was necessary as so much vapour condensed on the reflux apparatus.

A poor yield was again obtained. Although the use of the diglyme may have been beneficial in removing some of the impurities, it was out-weighed by the fact that a lot of gas produced condensed upon the reflux apparatus before even reaching the reaction mixture.

One reason for the failure of the experiment to produce a good yield was attributed to the use of paraformaldehyde. Thus, alternative methods of production of formaldehyde gas, which would avoid the use of the pyrolysis unit and the subsequent problem of re-condensation, were sought.

Formaldehyde is traditionally used in the gaseous form or in its aqueous solution. As the Ghosh & Spiro method¹⁴⁵ involved moisture sensitive compounds, the latter was not an option. Other methods of producing formaldehyde gas all suffer from the disadvantages of low and uncontrolled addition of the reagent in unknown quantities^{157,160-3}. In addition, they do not avoid the problem of the strong tendency of the formaldehyde to re-polymerise.

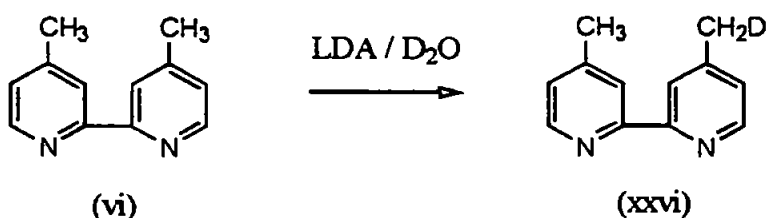
(2.2.5) Investigation of Carbanion Production

Evidence from previous experiments showed that formaldehyde gas was produced but an insufficient amount was reaching the reaction mixture. Low yields were still obtained and attention was also directed toward the formation of the carbanion. If this were not being produced in sufficient quantity, this could account for the gas being unable to react and form the desired product.

(2.2.5.1) Use of Deuterated Water to Quantify Carbanion Production

Introduction

The following experiments were performed as described in section 2.2.2 (page 67) using stoichiometric and excess quantities of LDA. However, instead of adding formaldehyde gas to the carbanion produced, deuterated water (D_2O) was used.



The ratio of the deuterated product (xxvi) and unreacted starting material (vi) could be determined, allowing the amount of carbanion formed to be calculated. In this experiment, the THF was cannulated to further avoid possible water ingress.

Experimental Procedure

An equimolar amount of D_2O in THF was cannulated into a 10 ml pressure equalising dropping funnel and added dropwise to the reaction mixture. The colour changed from dark brown to clear, then to clear green / yellow on stirring for 1 hour.

Results

Mp 169.7 - 171.2 °C (lit.¹⁵⁴ (vi) 171 - 172 °C)

GC

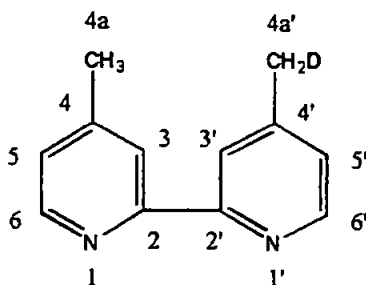
t_R (mix of (xxvi) and (vi)) 8.76 min

[10 mg/ml in DCM, Temp. Prog. 150 - 225 °C @ 2.5 °C/min, 225 - 300 °C @ 15 °C/min, 5 min @ 300 °C]

t_R (vi) = 8.82 min [10 mg/ml in DCM, same conditions as above]

NMR

^1H NMR (270 MHz, CDCl_3); δ (ppm) 8.5 (d, 2H, H-6 & H-6'), 8.2 (s, 2H, H-3 & H-3'), 7.1 (d, 2H, H-5 & H-5'), 2.4 (s, 5.46 H,^{*} H-4a)



^{13}C NMR (68 MHz, CDCl_3); δ (ppm) 155.8 (C-2), 148.7 (C-6), 147.9 (C-4), 124.4 (C-5), 121.8 (C-3), 20.9, 20.7, 20.4 (C-4a & C-4a')^{*}

DEPT (68 MHz, CDCl_3); δ (ppm) 148.7, 124.4, 121.8, 22.0^{*} as CH / CH_3 , 20.7, 20.4^{*} inverted, CH_2 .

* See discussion

IR

Matches that of (vi)

Discussion

The spectral data obtained supported the fact that the deuterated and undeuterated products were structurally very similar. As would be expected, the IR spectrum of the products matched that of 4,4'-dimethyl-2,2'-bipyridine (vi). Co-elution of the undeuterated and deuterated products occurred using GC, even with a slow ramp rate.

Therefore the relative proportions could not be ascertained by this method. However, both the proton and carbon-13 NMR could be used to calculate the relative percentages of product and starting material.

The only structural difference between the two compounds (vi) and (xxvi) is that one proton of one methyl group of (xxvi) has been replaced by deuterium. In the case of proton NMR spectra, integration values are usually integers. However, in the proton NMR spectrum in this case, the integration value of the signal at 2.4 ppm will therefore vary depending on the proportion of each compound. For a sample of pure (vi), the integration value will be 6 as there are 3 protons on each of the two methyl groups. For a sample of pure (xxvi), the integration value will be 5, three protons from one methyl group and two from the $-\text{CH}_2\text{D}$ group. A mixture of the two compounds, as obtained in this case, leads to an intermediate value which can be used to calculate the percentage purity. The equation below can be used to calculate the actual percentage of product:

$$\text{Percentage Yield of (xxvi)} = (6 - \text{integration value}) \times 100$$

The integration value of the methyl signal in this case was recorded as 5.46, thus the compound obtained consisted of 54 % product and 46 % starting material.

The presence of deuterium on one of the methyl groups of the product has an affect on the methyl carbon signal. Figures 2.1 & 2.2 overleaf show the signals at 20 - 21 ppm in the ^{13}C and DEPT spectra. The percentages of (vi) and (xxvi) can be calculated from the intensity of the signal at 20 - 21 ppm in the ^{13}C spectrum. The signal comprises the following:

- A single signal due to the two methyl groups of (vi)
- A single signal due to the undeuterated methyl group of (xxvi)

- A triplet with three parts of equal intensity due to the presence of deuterium in CH₂D

Figure 2.1 shows that the two single peaks overlap each other and also overlap one part of the triplet. This triplet signal is used as a basis for the calculation and thus the intensity of the part of the triplet overlapped by the singlet must be subtracted from the overall intensity of the singlet.

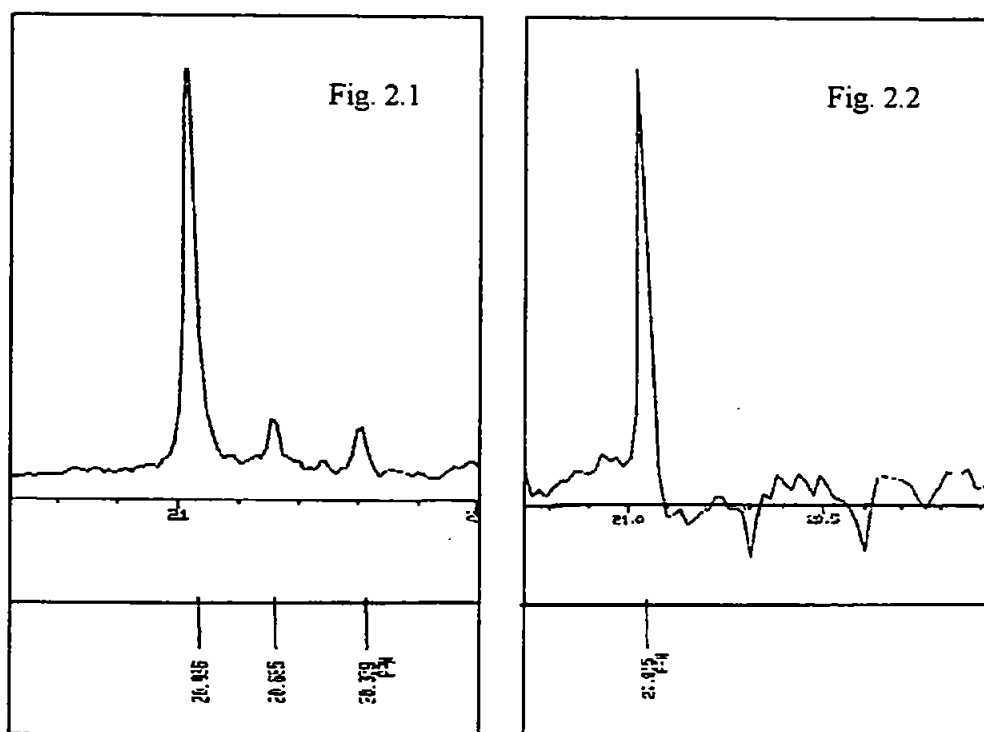


Figure 2.1: Enlargement of ¹³C NMR signal at 20 - 21 ppm,
Figure 2.2: Enlargement of DEPT NMR signal at 20 - 21 ppm

Table 2.2 shows the intensity values of the signal at 20 - 21 ppm:

¹³ C NMR SIGNAL (ppm)	% INTENSITY OF SIGNAL	RELATIVE % INTENSITY OF SIGNAL
20.9	45.9	81.1
20.7	5.8	10.2
20.4	4.9	8.7

Table 2.2: Percentage intensity values for the ¹³C NMR methyl carbon signal at 20.4 - 20.9 ppm

The percentage intensities of the two visible parts of the triplet are used to calculate an average intensity which is considered to be the intensity of the hidden third of the triplet:

$$(10.2 + 8.7) / 2 = 9.45 \quad (1)$$

In addition, the intensity of the singlet due to the undeuterated methyl group of the product also needs to be subtracted from the total signal intensity. This value equals the intensity due to the total CH₂D signal:

$$3 \times 9.45 = 28.35 \quad (2)$$

Therefore

$$\begin{aligned} \% \text{ Intensity due to the methyl groups of (vi)} &= \text{total signal intensity} - (1) - (2) \\ &= (81.1 - 9.45 - 28.35) \% \\ &= 43.3 \% \end{aligned}$$

As a percentage of the total signals;

$$\% \text{ undeuterated product (vi)} = \left[\frac{\% \text{ due to methyl groups of (vi)}}{\text{Total \% of signals at 20 - 21 ppm}} \right] \times 100$$

$$\% \text{ undeuterated product (vi)} = \left[\frac{43.3}{(81.1 + 10.2 + 8.7)} \right] \times 100 = 43 \%$$

Thus the percentage of (xxvi) was 100 % - 43 % = 57 %

(2.2.5.2) Investigation of the Effect of Using Excess Amounts of D₂O and LDA on the Percentage of Deuterated Product.

Experimental Procedure

The experimental procedure was carried out as described in section 2.2.5.1 (page 79), using a 2:1 ratio of LDA to bipyridine and 1.9 M excess of D₂O. No colour change was observed on addition of D₂O to carbanion solution.

Results

Mp 168.7 - 170.4 °C (lit.¹⁵⁴ (vi) 171 - 172 °C)

NMR

¹H NMR (270 MHz, CDCl₃); δ (ppm) 8.5 (d, 2H, H-6 & H-6'), 8.2 (s, 2H, H-3 & H-3'), 7.1 (d, 2H, H-5 & H-5'), 2.4 (s, 5.27 H,^{*} H-4a)

¹³C NMR (68 MHz, CDCl₃); δ (ppm) 155.9 (C-2), 148.8 (C-6), 148.0 (C-4), 124.5 (C-5), 121.9 (C-3), 21.0, 20.8, 20.5 (C-4a & C-4a')^{*}

¹³ C NMR SIGNAL (ppm)	% INTENSITY OF SIGNAL	RELATIVE % INTENSITY OF SIGNAL
21.0	36.1	72.1
20.8	6.5	13.0
20.5	7.5	15.0

Table 2.3: Percentage intensity values for the ¹³C NMR methyl group signal at 20.5 - 21.0 ppm for the experiment using excess D₂O and LDA

DEPT (68 MHz, CDCl₃); δ (ppm) 148.8, 124.5, 121.9, 21.0^{*} as CH / CH₃, 20.8, 20.5^{*} inverted, CH₂

* See discussion

Discussion

The percentage intensities of deuterated product and starting material using ¹H and ¹³C NMR were calculated as 73 % and 84 % respectively, using the methods described in the previous section. The discrepancy in these particular values is attributed to the fact that integration errors can occur if the baseline is not level due to the presence of small impurities or background noise. Nevertheless, this method was useful to establish

a good estimate of relative values and it appeared from these results that the experiment had been successful in its aim to increase the yield of (xxvi).

On addition of the stoichiometric amount of D₂O, the brown colour of the carbanion remained. More D₂O was added as any product containing deuterium would show up on NMR whereas if any unreacted carbanion was quenched with H₂O, it would be classed as unreacted starting material. However, even with excess D₂O, the colour still remained. Another hypothesis postulated was that the D₂O quenched the excess unreacted LDA first, as it is a stronger base than the carbanion, and then added to the carbanion. An additional problem was that now excess LDA was being used, there could also be production of dianion. There appeared to be some conflict within the literature as to whether this was a significant problem. Kelly-Basetti *et al.* reported that monolithiation of (vi) at low temperature, followed by quenching with an appropriate electrophile 'generally produces a mixture of unreacted 4,4'-dimethyl-2,2'-bipyridine, along with products arising from the the desired monolithiation and undesired dilithiation.'¹⁶⁴ Griggs & Smith reported that the reaction of (vi) with 2.5 equivalents of LDA in THF generated the bright orange dianion¹⁶⁵. Ellison and Iwamoto¹⁶⁶ successfully synthesised the symmetrical 4,4'-diheptadecyl-2,2'-bipyridine using the Ghosh & Spiro method¹⁴⁵ but with double the amount of LDA and n-hexadecylbromide. Della Ciana *et al.*¹⁶⁷ also reported that upon lithiating (vi) with *n*-butyllithium, the resulting equilibrium mixture consisted of mono-, di- and unlithiated (vi). However, in a later paper, in which the group deliberately attempted to synthesise 4,4'-divinyl-2,2'-bipyridine, it was reported that simple elimination procedures, useful for the synthesis of the monovinyl compound (ii), produced only traces of the divinylbipyridine¹⁴¹. The reason for this was attributed to the high tendency of divinylbipyridine to polymerize under the reaction conditions. On the

basis of this, it was unknown whether the production of the dianion was a significant problem in this study. Excess LDA was applied to the Ghosh & Spiro method¹⁴⁵ in an attempt to increase the yield of product.

(2.2.5.3) Effect of Using Excess LDA on the Yield of the Ghosh & Spiro Reaction¹⁴⁵

This experiment was carried out as described in section 2.2.2 (page 67), but incorporated two modifications. Formaldehyde was generated using the inert solvent apparatus described in section 2.2.4 (page 75). However, this was later exchanged for the pyrolysis unit due to blockage of the inlet tube to the reaction mixture. 9.5 times the stoichiometric amount of paraformaldehyde had been used as so much condensed on the sides of the reflux apparatus.

Excess LDA was used in the hope that this would increase the yield of product. In addition to the usual work-up of the organic layer, attention was also focused upon the aqueous layer to investigate if it contained any product or starting material. The aqueous layer and washings were taken and acidified with conc. hydrochloric acid to pH 6. These layers were then washed with diethyl ether (4 x 200 ml), left to dry over sodium sulfate and stripped of solvent. The resulting product was analysed.

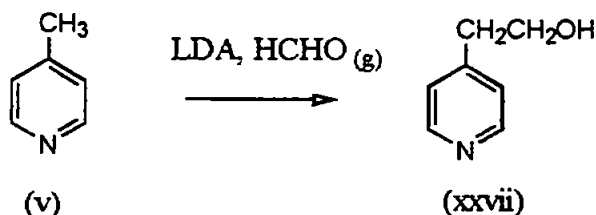
Results & Discussion

The GC and GC-MS data showed that the aim of increasing the relative percentage of product to starting material was successful. However, the crude yield was much lower in terms of mass. It was thought that maybe some product or starting material remained in the aqueous layer. This layer and washings from the reaction had been acidified so that any lithium hydroxide, produced when the reaction was quenched with water and thus making the mixture very alkaline (~ pH 10 - 11), was converted to lithium

chloride. Acidification of the mixture should have isolated any bipyridine as its unionised form. Care was taken not to acidify the mixture too much as this would convert the bipyridine to its hydrochloride salt. A pH of 6 was chosen as the pKa of pyridine is 5.19¹⁶¹. Analysis of the aqueous layers showed that some product was present but this comprised only 15 % of the theoretical yield.

A possible improvement of this method based upon the result would be to quench the reaction with strong acid to completely protonate the product, slowly raise the pH and then extract with ether. This may ensure that all the product was in the same form and give a higher yield. This had been carried out successfully in a similar method which described the synthesis of 2-(β -hydroxypropyl)pyridine reported by Walter¹⁶⁸.

(2.2.6) Analogous Reaction Using 4-Methylpyridine (v); Synthesis of 4-Hydroxyethylpyridine (xxvii)



The reaction described in section 2.2.2 (page 67) was performed using 4-methylpyridine instead of 4,4'-dimethyl-2,2'-bipyridine. The data obtained showed that although the desired product had been synthesised, unreacted (v) was also present. The overall yield was less than that obtained with the same reaction using bipyridine and because of this, it was not worth purifying the crude product. However, it was an improvement upon the literature yield¹⁶⁹ of 1.5 %. This experiment showed that the

reaction was unsuccessful with another member of the pyridine family, not just the bipyridine molecule.

(2.2.7) Excerpts of Personal Communications Related to the Ghosh & Spiro Method¹⁴⁵

The above experiments highlighted a number of problems related to the first stage of the Ghosh & Spiro method¹⁴⁵. Direct contact with Ghosh¹⁷⁰ was established to enquire if there were any suggestions he could make to improve the result of the reaction. His reply included the following points;

- *'There is some difficulty in obtaining satisfactory results' in trying to reproduce this synthesis. 'I must say that this experiment has occasionally failed in my hands as well.'*
- *'There are three things to look out for in particular:
(1) that moisture is rigorously excluded (even drying the paraformaldehyde is important),
(2) that the anion is being formed and
(3) that formaldehyde is indeed "seeing" the reaction mixture. It occasionally does happen that the formaldehyde resolidifies in the inlet tube. You may consider heating the inlet tube with electric tape. Also the rate at which the paraformaldehyde decomposes should ideally be controlled.'*¹⁷⁰

The above points had been fully explored. Further correspondence¹⁷⁰ included a more detailed description of the synthesis than was described in the published literature. Additional points included;

- *'excess paraformaldehyde was used'*
- *'The crude product was taken in ca. 10 - 20 ml of ether and yellowish coloured material came into the ether layer while some undissolved white residue remained. The ether layer was separated from the residue and evaporated to obtain 0.8 g of viscous yellow liquid. The isolated yield of pure product was, therefore, 35 %. Please note that only crude yields were given in the original JACS paper of Ghosh & Spiro.'*

Again, these details had already been included in the reaction procedure. The most important point from the above was that the maximum amount of product (35 % instead of 70 % as reported in the literature¹⁴⁵) was being obtained in this study.

Difficulties in the preparation of many common bipyridine analogues similar to (vii) have been reported in the literature^{164,171}. Separation of mixtures of such compounds has also been reported as difficult and any resulting metal complexes challenging to purify^{164,171}.

Further information pertaining to the Ghosh & Spiro reaction¹⁴⁵ was forwarded by Kotkar¹⁷², a colleague of Ghosh. Spectral details which supported the findings of this study confirmed that the solid mixed with the oil in the crude product was unreacted starting material. Another colleague of Ghosh¹⁷³ also sent information related to the synthesis. He had had problems with re-condensation of the formaldehyde gas and low yields and suggested using a modification¹⁴⁹ of the original Ghosh & Spiro method¹⁴⁵. Abruña *et al.*¹⁴⁹ reported that preparation of (ii) was difficult to execute and this modification resulted in the ability to prepare multigram quantities of (ii). Therefore this method¹⁴⁹ was adopted for the purposes of the present study.

(2.3) SYNTHESIS OF 4-METHOXYETHYL-4'-METHYL-2,2'-BIPYRIDINE (xxii) FROM 4,4'-DIMETHYL-2,2'-BIPYRIDINE (vi)

*Abruña et al., Inorg. Chem., 1985, 24, 7, 987-8*¹⁴⁹

Scheme 2.5 (page 63) shows the synthetic route for this method¹⁴⁹.

(2.3.1) Experimental Procedure

All glassware was dried at 150 °C overnight, assembled while hot and purged with nitrogen which had been dried by passing it through a calcium chloride tube. 4,4'-dimethyl-2,2'-bipyridine (vi) (7.5 g, 40.7 mmol) was added to a 250 ml stoppered conical flask, which was then sealed and purged with nitrogen. THF (215 ml) was cannulated and the mixture shaken well. THF (45 ml) was cannulated into the 500 ml

3-necked round-bottomed flask and cooled to 0 °C using a salt-ice bath. Diisopropylamine (5.7 ml, 40.4 mmol) was syringed into the reaction flask, followed by cannulation of *n*-butyllithium (1.6 M, 25 ml, 40.4 mmol). The cloudy yellow mixture was stirred well.

The bipyridine in THF solution was added dropwise from a pressure-equalising dropping funnel and the resulting dark brown solution was left for 15 mins. Chloromethyl methyl ether (CMME) (3.45 ml, 45.4 mmol) was mixed with THF (30 ml) and also added from a pressure-equalising dropping funnel to the main reaction mixture, which was gently swirled manually to aid mixing. This was left for half an hour. Further CMME (0.5 ml, 6.6 mmol) in THF (10 ml) was added to complete the colour change from dark green to pale yellow-green and left for 15 mins.

The reaction mixture was quenched with water (45 ml) and partitioned between saturated sodium hydrogen carbonate (25 ml) and diethyl ether (200 ml). Following additional ether extractions (2 x 75 ml), the combined ethereal layers were dried over magnesium sulfate. After filtration under reduced pressure and rotary evaporation of the filtrate, a clear orange oil mixed with a yellow solid was obtained. This was left to stand for a few days.

The oil was pipetted into a 50 ml round-bottomed flask. A small amount of ether was used to wash the remaining amount of solid and oil which was transferred to 2 x 10 ml glass centrifuge tubes and centrifuged for 5 mins at 5000 r.p.m. The liquid was added to the oil already separated and ether removed by application of a vacuum for an hour. The final product was a clear yellow-orange oil.

(2.3.2) Results

Mass of crude product (mixture of yellow solid and clear orange oil) = 9.0 g

GC of crude product

t_R (vi) 22.54 min, 30 %, t_R (xxii) 29.50 min, 63 %, 7 % impurities

% crude yield of (xxii) = 61% (Lit. 68 %) ¹⁴⁹

TLC

Mobile phase: 50:50 ethyl acetate: 40 - 60 °C petroleum spirit, + 1 % triethylamine

R_F (vi) 0.48

R_F (product) 0.07 & 0.55

Heavy streaking observed for both compounds.

Comparison of Solubilities of Starting Material & Decanted Oil

The starting material (vi), and the decanted oil were both soluble in hot and cold dichloromethane, THF, methanol, ethyl acetate and toluene and were not soluble in either hot or cold petroleum spirit (40 - 60 °C), water, hexane or cyclohexane. The only solubility difference was that the oil was soluble in hot or cold diethyl ether, whereas (vi) was soluble only in excess diethyl ether.

Mass of purified product (clear orange oil) = 4.0 g (17.5 mmol)

GC of purified oil

t_R (vi) 22.74 min, 5 %, t_R (xxii) 32.97 min, 89 %, 6 % impurities.

% Yield = 38 % (lit. 68 %) ¹⁴⁹

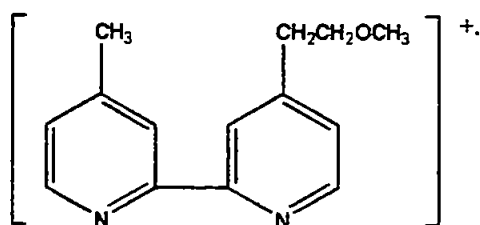
GC-MS

t_R (vi) 20.58 min

Assignments as described in section 2.2.3 (page 73-74)

t_R (xxii) 27.32 min

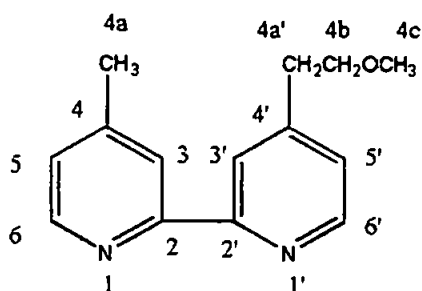
m/z 228;



Molecular cation radical

m/z 213 ($M^+ - CH_3$), m/z 198, m/z 184, m/z 170, m/z 154 (loss of the 2 ring substituents, the methoxy and methyl groups), m/z 92, m/z 77

NMR



(xxii)

1H NMR (270 MHz, $CDCl_3$); δ (ppm); 8.6 (d, 1H) & 8.5 (d, 1H), (H-6 & H-6'), 8.3 (s, 1H) & 8.2 (s, 1H), (H-3 & H-3'), 7.2 (d, 1H) & 7.1 (d, 1H), (H-5 & H-5'), 3.7 (t, 2H, $J = 6.8$ Hz, H-4b), 3.3 (s, 3H, H-4c), 3.0 (t, 2H, $J = 6.8$ Hz, H-4a'), 2.4 (s, 3H, H-4a)

Lit.¹⁴⁹; (100 MHz, $CDCl_3$ relative to TMS internal standard) δ (ppm); 8.50 (br t, 2H), 8.19 (br s, 2H), 7.11 (br t, 2H), 3.63 (t, 2H), 3.30 (s, 3H), 2.91 (t, 2H), 2.37 (s, 3H)

^{13}C NMR (68 MHz, $CDCl_3$); δ (ppm); 156.0 & 155.7 (C-2 & C-2'), 148.9 & 148.7 (C-6 & C-6'), 149.0 & 148.0 (C-4 & C-4'), 124.5, 124.2, 121.9, 121.4 (C-3, C-3', C-5 & C-5'), 72.0 (C-4b), 58.5 (C-4c), 35.5 (C-4a'), 21.0 (C-4a)

DEPT (68 MHz, CDCl₃); δ (ppm); 148.9, 148.7, 124.5, 124.2, 121.9, 121.4, 58.5, 21.0 as CH / CH₃, 72.0 & 35.5 inverted, CH₂

IR

(KBr) ν 3004, 2979 (=C-H alip.), ν 2925, 2871 (=C-H ar.), ν 1596 (C=C), ν 1461 (C=C ring str., CH₂ methylene group), 1375 (CH₃), ν 1109 (C-O), δ 1000, 898, 828 (out-of-plane C-H) cm⁻¹

(2.3.3) Discussion

The red-brown colour of the carbanion of (vi) was formed as for the Ghosh & Spiro method¹⁴⁵. Then, instead of addition of formaldehyde, chloromethyl methyl ether (CMME) was added to convert one of the methyl groups to a methoxyethyl group. The colour of the reaction mixture changed from brown to green through to yellow. CMME is very volatile (bp 55 - 57 °C)¹⁶¹ and some did not reach the reaction mixture, especially with a high nitrogen flow rate. Therefore a slight excess of CMME was added in comparison to that described in the literature¹⁴⁹. Surridge *et al.* reported the use of α ,4-dichloroanisole in place of CMME¹⁷⁴. This compound has a higher boiling point (120 - 124 °C/18 mm¹⁷⁵, 240 °C/760 mm) which would overcome this problem of loss due to volatility, however, no further details of the success of the reaction in terms of percentage yields were given.

Following concentration of the product *in vacuo* after extraction with ether, Abruña *et al.*¹⁴⁹ reported that the oil was filtered through flash grade silica gel. This was thought to be for the purpose of decolourising the product as the oil later isolated was colourless¹⁴⁹. The oil obtained in this study was orange and was filtered as described in the literature¹⁴⁹ but despite changing the polarity of the solvent used for elution, a poor

recovery of the product was obtained. Although some colour was retained on the column, the procedure was inefficient and an alternative method was sought to remove the colour from the oil. The product was taken, dissolved in chloroform and then boiled with decolourising charcoal. A better recovery was achieved but the colour, probably due to polymeric impurities present in quantities too small to be observed by NMR, still remained. Further attempts to remove the colour were abandoned to avoid further loss of product. Nallas & Brewer¹⁷⁶, who described a modification of the Abruña method¹⁴⁹ made no mention of the filtration stage and isolated the product as a pale yellow oil which was used successfully in the next stage of the reaction.

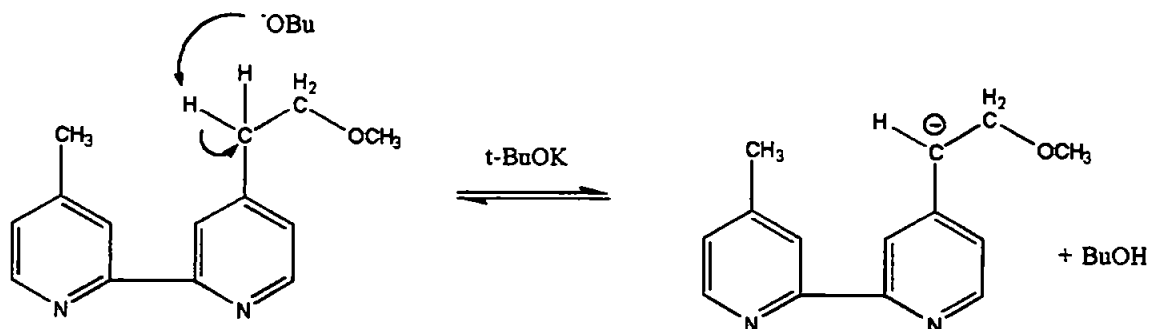
The crude mixture obtained consisted of a higher proportion of product than had been obtained with the Ghosh & Spiro reaction¹⁴⁵. The mixture was left to stand for an extra few days upon the advice of Professor Abruña¹⁷⁷ to allow the majority of the solid to precipitate. Again, separation was a problem as the two compounds were structurally very similar. Filtration through a Hirsch funnel was attempted, but the oil was too viscous. Separation of the product from the starting material by TLC proved to be unsuccessful. However, the solubilities of the two compounds were investigated and diethyl ether was used to separate the oil from the solid. The oil dissolved well, and with a minimum amount of ether, the solid was left as a fine white powder. With the aid of centrifugation, separation was successful. GC showed that only a small percentage of starting material remained. It was decided to continue with the next stage of the reaction as the presence of this small amount was considered unlikely to interfere with the course of the next step.

(2.4) SYNTHESIS OF 4-METHYL-4'-VINYL-2,2'-BIPYRIDINE (ii) FROM 4-METHOXYETHYL-4'-METHYL-2,2'-BIPYRIDINE (xxii)

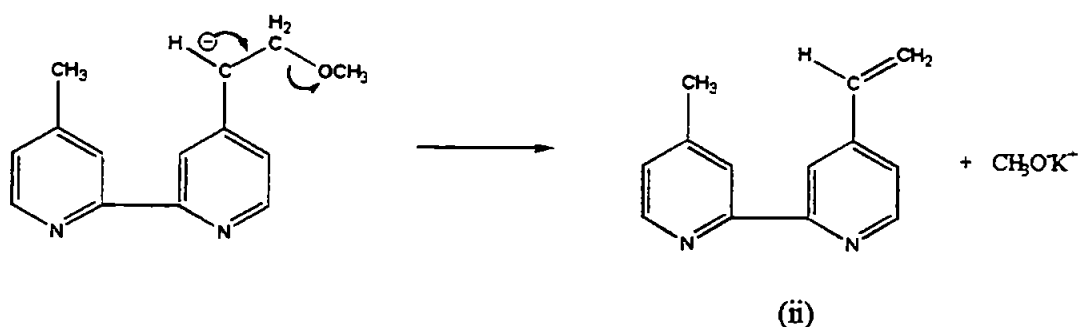
Abruña et al., Inorganic Chemistry, 1985, 24, 7, 987-988¹⁴⁹

(2.4.1) Introduction

The mechanism for this reaction is termed as a hydro-alkoxy elimination, or cleavage of an ether to give an alkene and proceeds via the E1cB mechanism, i.e. a unimolecular elimination of a conjugate base¹⁷⁸. The first stage of the reaction was the production of a carbanion. This was as a result of the abstraction of a proton from the β -carbon using potassium tert-butoxide as a strong base.



The next stage involved the elimination of -OCH₃ and the formation of a double bond;



Upon quenching the reaction mixture, the potassium methoxide was converted to methanol and the solution became very alkaline due to the presence of potassium hydroxide;



(2.4.2) Experimental Procedure

All apparatus was dried at 105 °C overnight, assembled while hot and purged with nitrogen. The reaction mixture was protected from light and stirred throughout the experiment. THF (90 ml) was added via cannulation to 4-methoxyethyl-4'-methyl-2,2'-bipyridine (xxii) (3.2 g, 14.2 mmol) in a 250 ml 3-necked round-bottomed flask. The reaction mixture was cooled to -78 °C using a butyl acetate/liquid nitrogen slush bath and then t-BuOK (3.2 g, 28.6 mmol) dissolved in THF (100 ml) was added dropwise. The dark brown-orange solution was left to stir for 1.5 hr at -78 °C and then allowed to return to room temperature over a period of 25 min.

The mixture was quenched with water (40 ml) and the resulting orange-yellow mixture extracted thrice with 75 ml portions of ether. The combined ethereal layers were dried over magnesium sulfate, followed by filtration under reduced pressure and rotary evaporation. The viscous orange-yellow oil was kept under vacuum for 1 hr, to yield orange-yellow crystals in a small amount of oil. Both the crystals and oil were dissolved in dry ether. The clear yellow liquid was filtered, under reduced pressure through a column of 2 - 3 inches of 40 - 63 µm silica gel (ether eluent), to remove polymeric impurities. This was repeated, leaving a yellow-orange residue on the column and yielding a clear pale yellow liquid. Rotary evaporation gave yellow crystals which were purified by mixed

solvent recrystallisation using ether/hexane. The product was collected by filtration under reduced pressure using ice-cold ether for washing.

(2.4.3) Results

Mass of crude product (yellow crystals) = 2.1 g (10.7 mmol, 75 % yield)

Mp 79.9 - 89.2 °C (lit. 85 - 88 °C)¹⁷⁹

Mass of pure product (white crystals) = 1.4 g (7.13 mmol)

Mp 85.3 - 89.3 °C

GC of pure product

t_R (vi) 22.93 min, 5 %, t_R (ii) 25.50 min, 95 %.

% Yield = 49 % (lit. 50 %)¹⁴⁹

GC-MS

t_R (vi) 20.53 min

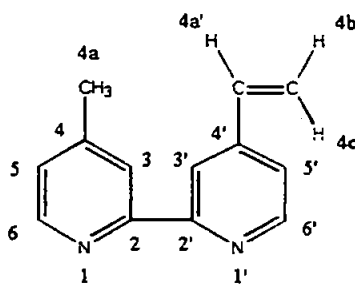
m/z 184 (M^+ ion), 183 ($M^+ - H$), m/z 78;

t_R (ii) 23.00 min

m/z 197 ($M^+ + 1$ ion), 196 (M^+ ion), 195 ($M^+ - H$ ion), 181 ($M^+ - CH_3$), m/z 170, m/z 167

(loss of $CH=CH_2$), 154 (loss of $CH=CH_2$ and CH_3), m/z 92, m/z 77

NMR



(ii)

The solvent acetone- d_6 was used for all NMR measurements. ^1H NMR was performed at 270 MHz and ^{13}C and DEPT NMR at 68 MHz. The signals were assigned with further information from 2D NMR methods. Table 2.4 overleaf gives full details of these assignments.

IR

(KBr); ν 3052 (=C-H str., ar. and vinyl), ν 2923 (-C-H str., alip.), ν 1588, 1544, (C=C ring str. ar.), 1455 (CH_2 methylene group), 1362 (CH_3 methyl group), δ 986, 927 (=C-H out-of-plane bend, indicative of monosubstituted double bond), δ 986, 927, 906, 830, 809 (=C-H out-of-plane bend, -C-H out-of-plane bend) cm^{-1}

UV

Solvent: CHCl_3

$\lambda_{\text{max}} = 282 \text{ nm}$, $\epsilon = 12477 \text{ mol}^{-1}\text{dm}^3\text{cm}^{-1}$ (lit. 281 nm, $\epsilon = 10600 \text{ mol}^{-1}\text{dm}^3\text{cm}^{-1}$, solvent CHCl_3)¹⁴⁸

TLC

R_F (xxii) 0.78 (& 0.19, faint trace of (vi))

R_F (ii) 0.83 (& 0.23, faint trace of (vi))

(2.4.4) Discussion

Vinyl groups are known to polymerise very easily, so the exclusion of light during the course of the reaction and also throughout the work-up stages was necessary to prevent the polymerization of the product.

The solution of the methoxyethyl compound (xxii) in THF was a clear orange solution. On addition of potassium tert-butoxide, the colour changed to a dark orange-brown colour, and then to orange-yellow when water was added.

¹ H NMR δ (ppm)	Integration	Multiplicity	Assignment	¹³ C NMR δ (ppm)	DEPT	COMMENTS
2.4	3	s	4a	21.6	CH/CH ₃	Only aliphatic carbon in ¹³ C NMR
6.8	1	dd	4a'	136.5	CH/CH ₃	Carbon assignment from VCHSHF $J_{cis} = 11$, $J_{trans} = 17.5$ Hz
5.5	1	d	4b	119.5	CH ₂	Coupling constant < that of 4c ($J_{cis} = 11$ Hz)
6.1	1	d	4c	119.5	CH ₂	Coupling constant > that of 4b ($J_{trans} = 17.5$ Hz)
8.5	1	s	3'	119.1	CH/CH ₃	Singlet overlaps signal at 8.5 ppm in ¹ H NMR, shifted downfield from 3 because of conjugation with ring and vinyl group. Carbon assignment from VCHSHF
8.2	1	s	3	122.7	CH/CH ₃	Carbon assignment from VCHSHF
8.6	1	d	6'	150.8	CH/CH ₃	Doublet shifted downfield because of conjugation with ring and vinyl group.
8.55	1	d	6	150.2	CH/CH ₃	Carbon assignment from VCHSHF
7.4	1	d	5'	121.8	CH/CH ₃	Signal shifted further downfield than that for 5 because of conjugation with ring and vinyl group. Carbon assignment from VCHSHF

Table 2.4: Full NMR Interpretation for 4-methyl-4'-vinyl-2,2'-bipyridine (II)

¹ H NMR δ (ppm)	Integration	Multiplicity	Assignment	¹³ C NMR δ (ppm)	DEPT	COMMENTS
7.1	1	d	5	126.0	(CH/CH ₃)	Carbon Assignment from VCHSHF
-	-	-	2'	157.9	-	Of the four quarternary carbons, it is shifted furthest downfield due to close proximity of nitrogen in the ring and also because of conjugation with the ring and the vinyl group.
-	-	-	2	156.9	-	Signal shifted downfield due to close proximity of nitrogen in the ring.
-	-	-	4'	149.1	-	Signal shifted further downfield than that for 4 due to conjugation with the ring and the vinyl group.
-	-	-	4	146.8	-	Only quarternary of the four which remains unassigned.

Lit.¹⁴⁵ ¹H NMR (60 MHz, CDCl₃); δ (ppm) 8.45 - 8.05 (4H), 7.15 - 6.80 (2H), 6.65 - 5.25 (3H, vinylic protons), 2.30 (s, 3H)

Pitt *et al.* reported¹⁵⁰: ¹H N.M.R (CDCl₃); δ (ppm) 8.63 - 7.14 (6H, Ar.), 6.77 (q, 10, 17, 1H, CH=C), 6.09 (d, 17, 1H, CH-CH₂), 5.52 (d, 10, 1H, C-CH₂), 2.44 (s, 3H, CH₃)

Lewis & Miller reported¹⁸⁰: ¹H NMR (300 MHz, CDCl₃); δ (ppm) 8.59 & 8.5 (d, 6,6'-py H), 8.38 & 8.21 (d, 3,3'-py H), 7.26 & 7.11 (d, 5,5'-py H), 6.75, 6.72, 6.69 & 6.66 (q, CH=CH₂), 6.07, 6.01, 5.48 & 5.45 (q, CH-CH₂), 2.37 (s, CH₃)

¹³C NMR (CDCl₃); δ (ppm) 156.43 (C-2'), 155.59 (C-2), 152.01 (C-6'), 150.53 (C-6), 148.26 (C-4'), 145.8 (C-4), 134.85 (C-5'), 124.63 (C-5), 122.01 (C-3'), 120.56 (C-3), 118.83 (CH=CH₂), 118.44 (CH=CH₂), 29.38 (CH₃)

cont...

Table 2.4: Full NMR Interpretation for 4-methyl-4'-vinyl-2,2'-bipyridine (II)

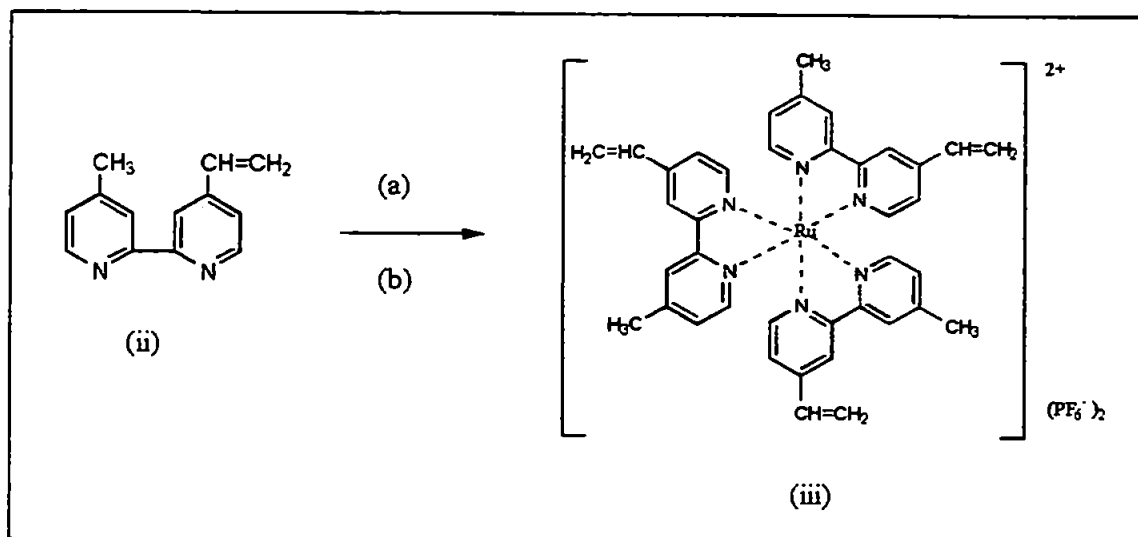
Upon filtration of an ether solution of the crude product through silica gel, the yellow colour was retained on the column and a good recovery of pale yellow crystals was collected. Following recrystallization, analysis by GC showed that the product was pure apart from a small amount of (vi) that was still present. This was also observed in the NMR spectrum where slight overlapping and incomplete resolution of the signals was observed. However, the disappearance of the -OH stretch and C-O stretch in the IR spectrum showed that no (xxii) was present. This was supported by the TLC results. The starting material showed a faint trace of (vi) present, which was also present in the product. There was a small amount of streaking between otherwise well-separated spots.

(2.5) SYNTHESIS OF RUTHENIUM TRIS(4-METHYL-4'-VINYL-2,2'-BIPYRIDINE) BIS(HEXAFLUOROPHOSPHATE) (iii)

Bommarito *et al.*, *Inorg. Chem.*, 1992, 31, 3, 495-502¹⁸¹

(2.5.1) Introduction

Initially the aim was to incorporate one vinyl ligand into the tris ruthenium complex, however, the literature showed that this would not polymerize well¹¹⁰. Incorporation of three vinyl ligands would facilitate the eventual aim of electropolymerization. The reasons for this are discussed later. Therefore, the method reported by Bommarito *et al.*¹⁸¹ was used to synthesise ruthenium tris(4-methyl-4'-vinyl-2,2'-bipyridine) bis(hexafluorophosphate), (iii) as shown in Scheme 2.7 overleaf.



KEY

(a) RuCl_3 , 1:1 EtOH / H_2O , reflux, 3hrs under N_2 , (b) Aq. satd. NH_4PF_6

(iii) Ruthenium tris(4-methyl-4'-vinyl-2,2'-bipyridine) bis(hexafluorophosphate), $[\text{Ru}(\text{vbpy})_3]^{2+}$

Scheme 2.7: Synthesis of (iii) using the method reported by Bommarito *et al.*¹⁸¹

(2.5.2) Experimental Procedure

Throughout the reaction, the mixture was protected from light. 25 ml of a 1:1 ethanol:water mix was added to ruthenium trichloride (0.34 g, 1.64 mmol) and 4-methyl-4'-vinyl-2,2'-bipyridine (ii) (1.08 g, 5.5 mmol) in a 50 ml two-necked round-bottomed flask. This was left to stir and purge with nitrogen for 20 mins and then heated at reflux for 3 hrs. After cooling, saturated ammonium hexafluorophosphate (1 ml) was added to precipitate the complex and this was stood in ice for 10 mins. The crystals were isolated by filtration under reduced pressure. The complex was isolated easily. The red solid was washed with diethyl ether to dissolve any impurities.

(2.5.3) Results

Mass of product (red solid) = 0.87 g (0.89 mmol)

The percentage yield was based upon the number of moles of $\text{RuCl}_3 \cdot x\text{H}_2\text{O}$. The value of x , the number of moles of waters of crystallization, was calculated as 1.55 by heating a sample of ruthenium trichloride and measuring the mass lost due to water.

% Yield = 61 % [No lit. yield given]

Solubility: Soluble in DMSO and acetone, insoluble in diethyl ether, water and chloroform.

UV

Solvent: MeCN, λ (max) / nm, (ϵ / $\text{mol}^{-1}\text{dm}^3\text{cm}^{-1}$); 211.0 (39743), 247.0 (43561), 296.0 (44088), 466.0 (13142), (lit. 216, 248, 296, 466 +/- 2 nm)¹⁸¹

IR (KBr Disk); ν 3116.0 (=C-H ar.str.), ν 2925.6 (-C-H alip. str.), ν 1617.2, 1480.7 (C=C ar. & vinyl str.), δ 1423.7, 1399.0 (CH_3 bend), δ 1301.1, 1238.6, 1120.7, 1034.4, 993.9, 942.5 (in-plane C-H bend), δ 1034.4, 993.9, 942.5 (C=H vinyl out-of-plane bend), δ 841.0 (=C-H out-of-plane bend, v. strong)

NMR

The hydrogens and carbons of (iii) were labelled as for the free ligand (ii) (page 97). The solvent acetone- d_6 was used for all NMR measurements. ^1H NMR was performed at 270 MHz and ^{13}C and DEPT NMR at 68 MHz. The signals were assigned with further information from 2D NMR methods. Table 2.5 overleaf gives full details of these assignments.

(2.5.4) Discussion

The ruthenium trichloride and vinylbipyridine mixture was an intense dark brown colour. After refluxing followed by addition of saturated ammonium hexafluorophosphate, the colour changed to a deep red and crystals began to precipitate.

¹ H NMR δ (ppm)	Integration	Multiplicity	Assignment	¹³ C NMR δ (ppm)	DEPT	COMMENTS
2.4	3	s	4a	21.6	CH/CH ₃	Only aliphatic signal
6.3	1	d	4c	123.1	CH ₂	$J_{cis} = 11$ Hz, $J_{trans} = 16$ Hz. Carbon assignment from VCHSHF spectrum.
6.9	1	dd	4a'	134.7	CH/CH ₃	$J_{cis} = 11$ Hz, $J_{trans} = 16$ Hz. Carbon assignment from VCHSHF spectrum.
-	-	-	4'	147.7	-	VCHSHF shows no correlation. VCOLOC spectrum shows 3-bond correlation to 4b.
5.7	1	d	4b	123.1	CH ₂	$J_{cis} = 11$ Hz. Carbon assignment from VCHSHF spectrum. Further evidence for assignment comes from VCOLOC spectrum - 3 bond coupling to 4'.
-	-	-	4	151.6	-	VCOLOC spectrum shows 4a coupling with 3 carbons. VCHSHF spectrum shows signal at 151.63 ppm to be a quaternary carbon, thus in VCOLOC spectrum, correlation at 151.63 is a two-bond coupling.
8.9	1	s	3'	122.3	CH/CH ₃	VCOLOC spectrum shows 3-bond coupling with proton 4a'. VCHSHF spectrum gives carbon assignment.
8.7	1	s	3	126.5	CH/CH ₃	VCHSHF gives carbon assignment.

Table 2.5: Full NMR interpretation for Ru(vbpy)₃²⁺, (III)

¹ H NMR δ (ppm)	Integration	Multiplicity	Assignment	¹³ C NMR δ (ppm)	DEPT	COMMENTS
7.6	1	d	5'	125.6	CH/CH ₃	VCOLOC spectrum shows 3-bond coupling with proton 4a'. VCHSHF gives carbon assignment.
7.4	1	d	5	129.9	CH/CH ₃	VCHSHF gives carbon assignment.
7.8	1	d	6	153.0	CH/CH ₃	COSY shows correlation of proton 6 with proton 5. VCHSHF gives carbon assignments.
7.9	1	d	6'	152.1	CH/CH ₃	VCHSHF gives carbon assignments.
-	-	-	2, 2'	158.1, 158.9	-	Cannot assign which is which

cont...

Table 2.5: Full NMR Interpretation for Ru(vbpy)₃²⁺, (III)

Purification of the crude product was attempted using chromatographic separation, as described by Bommarito *et al.*¹⁸¹. However, this was not successful as no definite spot on the TLC plate was observed for this compound. Streaking was apparent and was attributed to the presence of the different vinyl complexes (see Figure 2.3, page 107). For the purpose of this study at this stage, the presence of the other complexes was considered not to be a problem, so the separation procedure was abandoned.

Mixed solvent recrystallization was attempted but not found to be successful. In addition, the intense colour of the product made it difficult to see when the product had begun to crystallise. Use of diethyl ether to wash the complex of any impurities was more suitable and the result was a fine crystalline powder.

The UV data was the only literature-reported data for this compound and the results obtained agreed with those reported¹⁸¹.

McWhinnie and Miller reported that incorporation of substituted bipyridines into metal complexes does not lead to any significant perturbations of the spectroscopic properties of the bipyridine complexes as the co-ordination sphere of the metal centre remains intact¹⁵. It is interesting to note that some IR values obtained obey the general rule outlined by these authors;

The spectra of the free ligands undergo slight modification on co-ordination to a metal ion; in particular, the ring frequencies 1600 - 1000 cm⁻¹ tend to undergo small but observable shifts to higher wavenumber¹⁵.

The proton NMR data obtained showed a number of interesting features. The chemical shifts for the vinyl and aromatic protons were different from the free ligand, verifying that complexation had taken place. No trace of signals due to the free ligand was observed. However, as well as the signals due to the complex, there were some small signals, particularly in the vinylic region, present as shoulders to the main signals. The

^{13}C and DEPT spectra of the compound also showed some additional resonances, present as shoulders to the main peaks. An interpretation of this was that as the 4-methyl-4'-vinyl-2,2'-bipyridine ligand had been contaminated with a small amount of 4,4'-dimethyl-2,2'-bipyridine, some of this could have been incorporated into the complex. There would then be competition between the two types of ligands for incorporation into the complex. This would mean that as well as the ruthenium tris(4-methyl-4'-vinyl-2,2'-bipyridine) bis(hexafluorophosphate) complex, there would also be amounts of three other complexes, as shown in Figure 2.3:

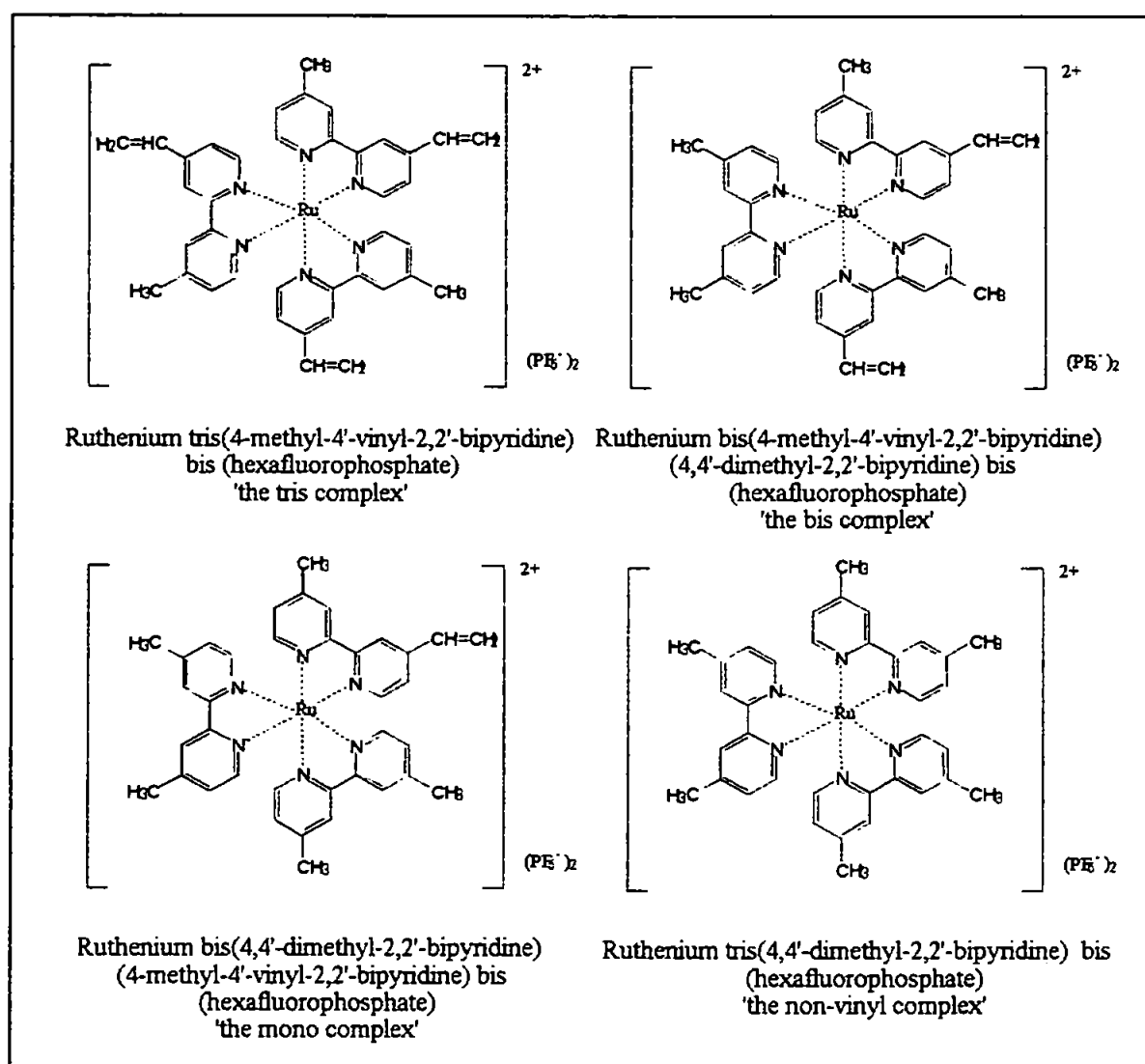


Figure 2.3: The four possible ruthenium complexes obtained by complexing a mixture of the ligands 4-methyl-4'-vinyl-2,2'-bipyridine (ii) and 4,4'-dimethyl-2,2'-bipyridine (vi).

The shoulder signals could be due to either the bis or mono complexes. It was possible, from the proton NMR integrations, to calculate the proportion of tris to bis complexes. The assumption was made that the shoulder signals were due the bis complex; any mono complex present would be of a smaller percentage and would show up as very small signals due to the fact that it would have only three vinylic protons present per molecule compared with 6 and 9 of the bis and tris complexes respectively. The complex ruthenium tris(4,4'-dimethyl-2,2'-bipyridine) bis(hexafluorophosphate) contains no vinyl groups and therefore would exhibit no signals in this particular region.

(2.5.4.1) Calculation of the Ratio of Tris and Bis Complexes

The following calculation has been based upon the assumption that due to the chemical similarity of the ligands, the relative rates of reaction of the ligands 4-methyl-4'-vinyl-2,2'-bipyridine (ii) and 4,4'-dimethyl-2,2'-bipyridine (vi) are equal.

The signal at 5.7 ppm was assigned to proton 4b. A shoulder signal is present at 5.8 ppm.

Integration value due to main signal (tris complex) = 1.021 (a)

Integration value due to 'shoulder' signal (bis complex) = 0.117 (b)

The ratio of signals due to tris and bis complexes is 1.021 : 0.117. However, to obtain figures relating to the composition of the mixture, value (b) has to be multiplied by a factor of 1.5 as the tris complex has three protons compared with two protons of the bis complex contributing to this signal.

The molecular ratio of tris to bis complex is now 1.021 : 0.176 = 5.82 : 1.00

Therefore,

$$\% \text{ tris complex} = \left(\frac{5.82}{(5.82 + 1.00)} \right) \times 100$$

% tris complex = 85 %

% bis complex = 15 %

The integrations of the other signals in the proton spectrum can be compared with what would be expected for a mixture of complexes composed of the above percentages.

Table 2.6 shows the number of protons for a mixture of the tris and bis complexes in a 5.82 : 1.00 ratio:

NO. OF MOLECULES OF COMPLEX	AROMATIC PROTONS (Ar)	4b VINYLIC PROTONS (V)	METHYL PROTONS (Me)
1 TRIS	18	3	9
5.82 TRIS	104.76	17.46	52.38
1 BIS	18	2	12
TOTAL (5.82 TRIS + 1 BIS)	122.76	19.46	64.38

Table 2.6: Proton ratios in a mixture of tris and bis complexes

From these figures, the theoretical ratio of aromatic protons to vinylic protons is calculated as follows;

Aromatic protons : vinylic protons = 122.76 : 19.46 = 6.3 : 1.0

Similarly, the theoretical ratio of aromatic to methyl protons is 1.9:1.0 and vinyl to methyl protons is 1.0 : 3.3. These calculated values are tabulated overleaf and compared with the experimentally determined ratio obtained directly from the proton NMR spectrum.

PROTON RATIO	RATIO FOR PURE TRIS COMPD.	RATIO FOR PURE BIS COMPD.	CALCULATED RATIO (AS ABOVE) FOR A MIXTURE OF 85% TRIS & 15% BIS COMPLEXES	EXPERIMENTALLY DETERMINED RATIO FROM THE PROTON NMR SPECTRUM
Ar:V	6 : 1	9 : 1	6.3 : 1	6.6 : 1
Ar:Me	2 : 1	1.5 : 1	1.9 : 1	1.8 : 1
V:Me	1 : 3	1 : 6	1 : 3.3	1 : 3.6

Table 2.7: Proton ratios for the mixture of ruthenium vinylbipyridine complexes

It can be seen that the values correlate very well. The figures show that if there were some bis complex present, then the ratio of vinyl protons to aromatic protons would be smaller than expected for the pure tris complex, and the ratios of methyl to aromatic and methyl to vinyl protons would be greater than for the pure tris complex. This was the case. The above calculations have shown that the integration values have given a good indication of the purity of the compound synthesised. In spite of the presence of some bis complex, the percentage of tris complex was considered to be high enough to continue with the next step of electropolymerization, described in Chapter 3.

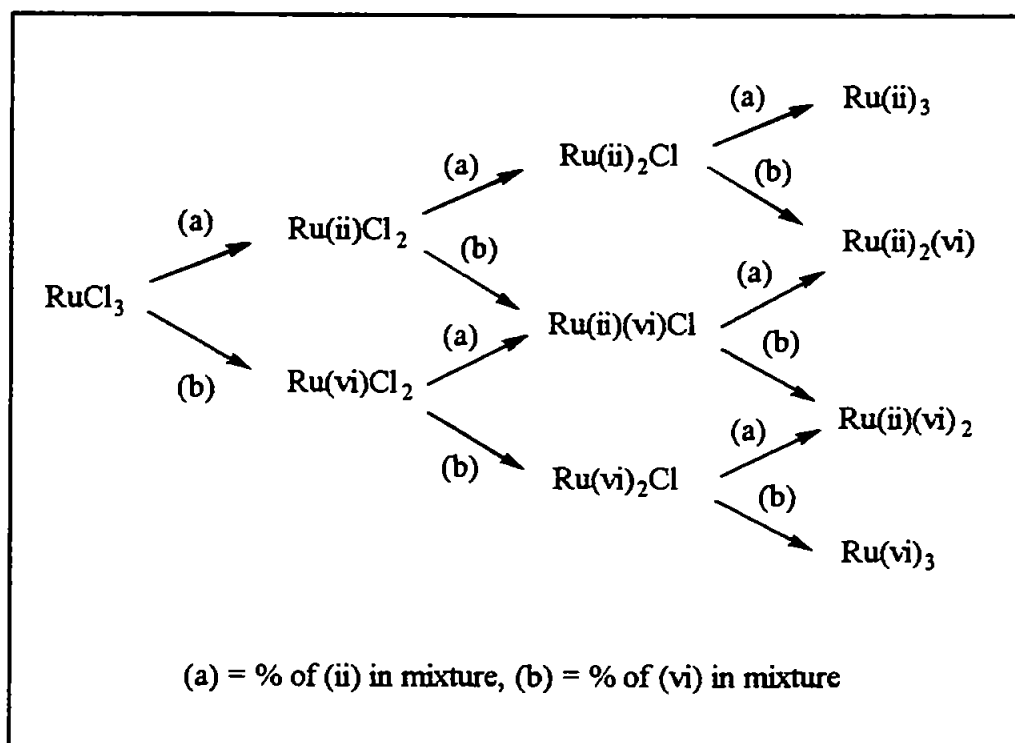
Denisevich *et al.* stated that electropolymerization was most successful with the maximum number of vinyl ligands per complex molecule¹¹⁰. The reasons for this have been discussed in Chapter 1. Therefore, for the purposes of this study, a high percentage of the tris complex was desired. Ideally, experiments would be carried out using the 4-methyl-4'-vinyl-2,2'-bipyridine ligand with varying amounts of 4,4'-dimethyl-2,2'-bipyridine, and the composition of the complex observed. However, this would be very time-consuming and so a mathematical model has been developed which shows the complex composition, based upon ligand purity. Details of this model are described below, and in the paper by Williams *et al.*¹⁸²

(2.5.4.2) Mathematical Model for Prediction of the Percentage Composition of a Mixture of Ruthenium tris(vinylbipyridine) Complexes

A mathematical model has been created which predicts the theoretical relative percentages of $RuL_nL'_{3-n}$ ($L = 4\text{-methyl-4'-vinyl-2,2'-bipyridine (ii)}$, $L' = 4,4'\text{-dimethyl-2,2'-bipyridine (vi)}$ and $n = 0, 1, 2, \text{ or } 3$) within the complex based upon the purity of (ii) before the synthesis is even attempted¹⁸³.

If the precursor ligand contains 100 % of (ii), then it follows that the complex will be 100 % tris-vinyl complex. Likewise, if the ligand contains 0 % of (vi), the complex will contain no vinyl ligands. If the composition of the ligand is a mixture, then the composition of the complex is based upon statistical probabilities.

Scheme 2.8 shows the different products, the routes via which they can be obtained and the probabilities of addition of each ligand. As with the calculation in section 2.5.4.1 (page 108), it is based upon the assumption that because both ligands are chemically very similar, the relative rates of reaction of both ligands will be equal.



Scheme 2.8: Probabilities of formation of ruthenium vinylbipyridine complexes

The three ligands are each substituted successively for a chlorine and there is the possibility of four different products, shown previously on page 107. Two of these products can be formed via three different routes. For example, to obtain $Ru(ii)_2(vi)$, two vinyl ligands and a non-vinyl ligand are required. The percentage of this complex present in the final product, using a ligand precursor of 85 % (ii) and 15 % (vi), is therefore 85 % x 85 % x 15 %. However, these may not necessarily substitute into the complex in this order. The percentage probability of the approach of these three ligands is therefore tripled, giving an overall percentage of 33 % bis complex. Table 2.8 overleaf shows the percentage of each complex for all purities of the 4-methyl-4'-vinyl-2,2'-bipyridine ligand. These results are depicted graphically below in Figure 2.4:

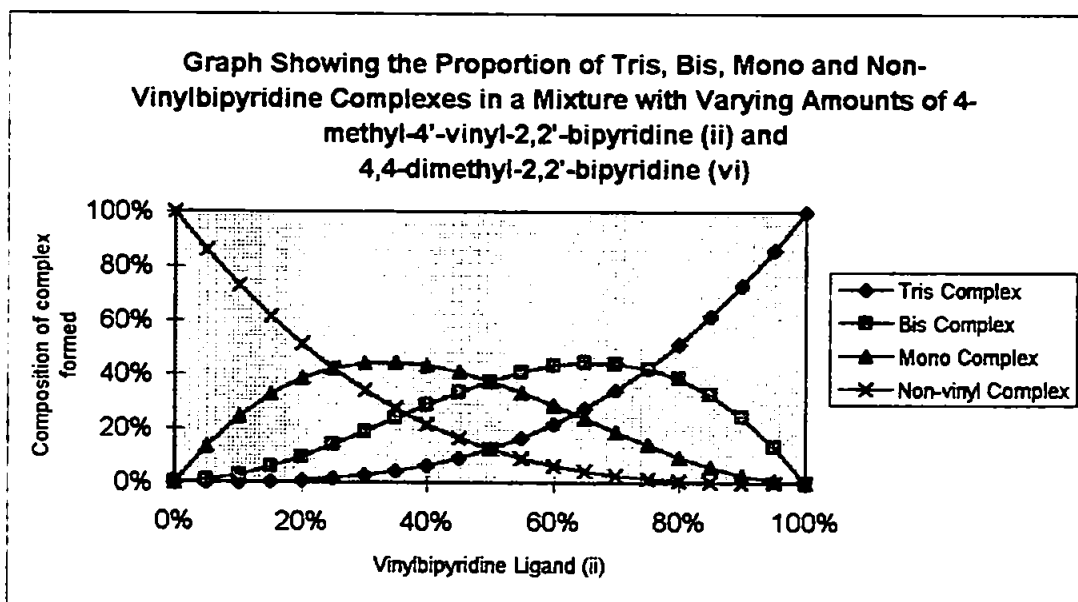


Figure 2.4: Graph of relative percentages of ruthenium vinylbipyridine complexes based upon relative percentages of ligands (ii) and (vi)¹⁸³

VINYL LIGAND (%)	DIMETHYL LIGAND (%)	TRIS-VINYL COMPLEX (%)	BIS-VINYL COMPLEX (%)	MONO-VINYL COMPLEX (%)	NON-VINYL COMPLEX (%)
100	0	100	0	0	0
95	5	86	14	1	0
90	10	73	24	3	0
85	15	61	33	6	0
80	20	51	38	10	1
75	25	42	42	14	2
70	30	34	44	19	3
65	35	27	44	24	4
60	40	22	43	29	6
55	45	17	41	33	9
50	50	13	38	38	13
45	55	9	33	41	17
40	60	6	29	43	22
35	65	4	24	44	27
30	70	3	19	44	34
25	75	2	14	42	42
20	80	1	10	38	51
15	85	0	6	33	61
10	90	0	3	24	73
5	95	0	1	14	86
0	100	0	0	0	100

Table 2.8: Composition of a ruthenium vinylbipyridine complex based upon varying percentages of ligands (II) and (VI).¹⁸³

From this model it would be expected that with a ratio of 95 % (ii): 5 % (vi) as is obtained in this study for (ii), the complex should be composed of 86 % tris, 14 % bis and 1 % mono-vinyl complex. NMR supports this prediction; integration values of the tris and bis complexes indicate that there is 85 % tris complex. The model shows in particular that the gradual increase in the amount of (vi) compared with (ii) results in a rapid percentage decrease of the tris complex. In fact, 20 % of (vi) decreases the percentage tris complex to 51 %. It is therefore important to have good separation of product from starting material in the early syntheses of the ligand precursors.

Another interesting feature about the ruthenium tris(4-methyl-4'-vinyl-2,2'-bipyridine) bis(hexafluorophosphate) complex is that it can exist as two complexes, a facial (Fac) form with C_3 symmetry and meridional (Mer) form with C_1 symmetry. These are shown in Figure 2.5 below.

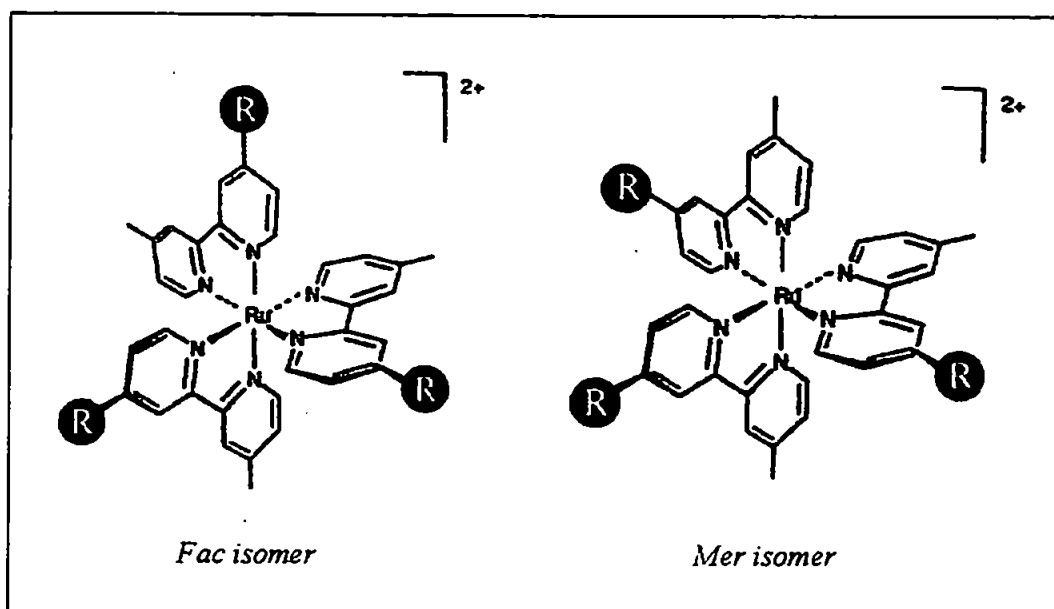


Figure 2.5: Facial (Fac) & meridional (Mer) isomers of (iii)

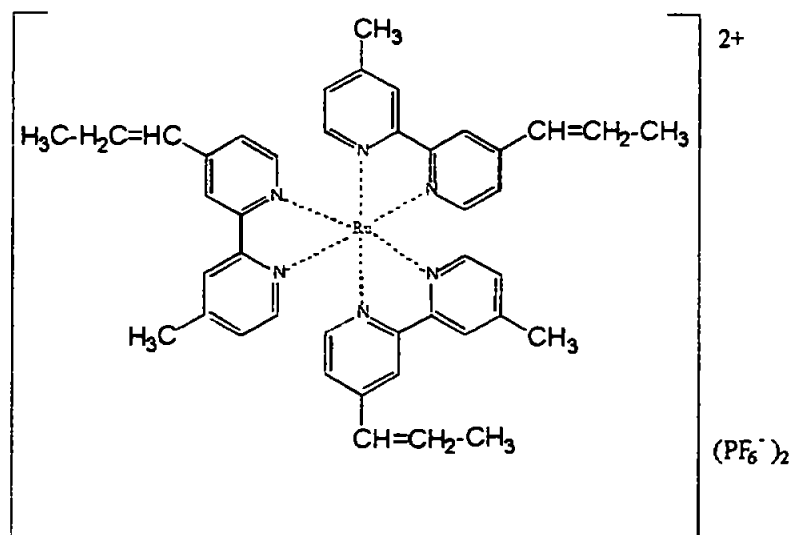
Slightly different proton NMR spectra have been recorded for these two individual isomers¹⁸⁴. The chelated ligands are equivalent in the Fac isomer but non-equivalent within the Mer isomer¹⁸⁵. The Fac isomer therefore exhibits a proton NMR spectrum of

higher symmetry than that of the Mer isomer. SurrIDGE *et al.* reported the synthesis of $[\text{Os}(\text{vbpy})_3][\text{PF}_6]_2$ which involved substitution of the ligands of an osmium complex for the ligand (ii), followed by precipitation of the product¹⁸⁶. This was similar to the synthesis described by Bommarito *et al.* for (iii)¹⁸¹. The splitting observed in the proton NMR spectrum of $\text{Os}(\text{vbpy})_3^{2+}$ was consistent with the statistically preferred Mer isomer, with no evidence for the Fac isomer. The incomplete resolution of the resonances in this present study was, therefore, probably caused by the presence of the former isomer of $\text{Ru}(\text{vbpy})_3^{2+}$. However, the isomeric composition of the complex in terms of these two isomers is not thought to be important for the purposes of this study.

Almost all the signals in the proton, ^{13}C and DEPT spectra were fully assigned with the aid of 2D NMR (Table 2.5, p 104-105). This data is thought to be previously unreported in the literature.

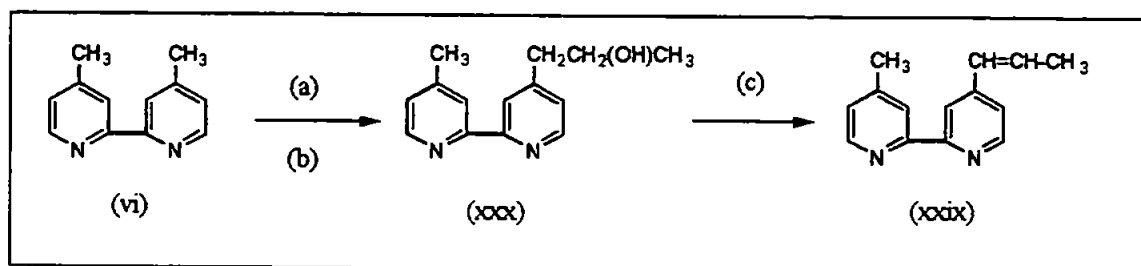
(2.6) SYNTHESIS OF RUTHENIUM TRIS(4-METHYL-4'-(E-PROP-2-ENYL)-2,2'-BIPYRIDINE) BIS(HEXAFLUOROPHOSPHATE)

(2.6.1) Introduction



(xxviii), $\text{Ru}(\text{ppbpy})_3^{2+}$

Research was extended to produce the complex shown on the previous page, ruthenium tris(4-methyl-4'-(*E*-prop-2-enyl)-2,2'-bipyridine) bis(hexafluorophosphate) (xxviii). The Ghosh and Spiro method¹⁴⁵ was used successfully to produce the 4-methyl-4'-(*E*-prop-2-enyl)-2,2'-bipyridine ligand, (xxix) as shown in Scheme 2.9 below. Again, Bommarito's method¹⁸¹ was used to produce the tris complex from this ligand.



KEY

(a) LDA / THF, (b) CH₃CHO, 1 eq., (c) P₂O₅ / Xylene, reflux

(xxix) 4-methyl-4'-(*E*-prop-2-enyl)-2,2'-bipyridine, (xxx) 4-(2-hydroxypropyl)-4'-methyl-2,2'-bipyridine

Scheme 2.9: Synthesis of (xxix) using the method reported by Ghosh & Spiro¹⁴⁵.

To the best of the author's knowledge, the compounds (xxx), (xxix) and (xxviii) are novel and previously unreported in the literature.

(2.6.2) Synthesis of 4-(2-hydroxypropyl)-4'-methyl-2,2'-bipyridine (xxix) from 4,4'-dimethyl-2,2'-bipyridine (vi)

(2.6.2.1) Experimental Procedure

All glassware was dried at 150 °C overnight, assembled while hot and purged with nitrogen which had been passed through a calcium chloride tube. 4,4'-dimethyl-2,2'-bipyridine (vi) (10.19 g, 55 mmol) was added to a 500 ml stoppered conical flask, which was then sealed and purged with nitrogen. THF (250 ml) was cannulated and the mixture shaken well. THF (30 ml) was cannulated into the 500 ml 3-necked round-

bottomed flask and cooled to 0 °C using a salt-ice bath. Diisopropylamine (8.0 ml, 61 mmol) was syringed into the reaction flask, followed by cannulation of *n*-butyllithium (1.6 M, 36 ml, 57.6 mmol). The cloudy yellow mixture was stirred well for 15 mins.

The bipyridine in THF solution was added dropwise from a pressure-equalising dropping funnel and the resulting deep red-black solution was left for 2 hours at 0 °C. Light was excluded during this period. Ethanal (3.19 ml, 57.1 mmol) was syringed into a 25 ml septum-sealed conical flask containing THF (15 ml). This mixture was added from a pressure-equalising dropping funnel to the main reaction mixture, which was gently swirled manually to aid mixing. This was left for one hour.

The yellow-green reaction mixture was quenched with water (200 ml) and the resulting clear, light orange solution was stirred for 15 minutes. The product was thrice extracted with 100 ml portions of diethyl ether and the combined ethereal layers dried over magnesium sulfate. After filtration under reduced pressure and rotary evaporation of the filtrate, a vivid yellow-orange solid mixed with a brown oily liquid was obtained. Traces of remaining ether were removed at low pressure. Purification was achieved using column chromatography. A column of dimensions 7.5 x 10 cm was used, the mobile phase consisted of 95 % DCM: 5 % methanol. 2 % by volume of triethylamine was added. The final product was a clear yellow oil.

(2.6.2.2) Results

Properties & Spectral Data of ethanal (acetaldehyde)

Physical appearance - a clear colourless liquid

Bp 21 °C ¹⁷⁵

GC

Ethanal was analysed using a packed column because of its very low boiling point.

GC details (3) as described in experimental section 2.7.1 (page 128)

1 % solution of ethanal in water.

t_R 1.82 min, > 99 % pure

Properties & Spectral Data of Crude Product

Crude product (brown oily liquid mixed with a yellow solid) = 13.1 g

GC of crude product

t_R (vi) 22.65 min, 27 %, t_R (xxx) 31.02 min, 65 %, 8 % impurities.

% crude yield by GC = 68 %

Mass of pure product (yellow-orange oil) = 4.6 g (20.1 mmol)

GC of purified product

t_R (vi) 26.57 min, 5 %, t_R (xxx) 34.15 min, 87 %, 8 % impurities. % yield by GC = 32 %

GC-MS

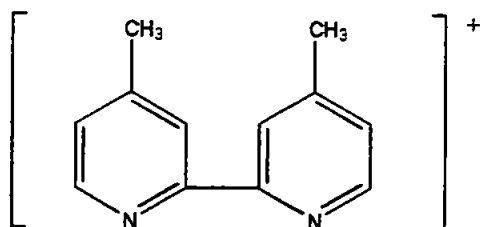
t_R (vi) 20.56 min

Assignments as for section 2.2.3 (page 73-74)

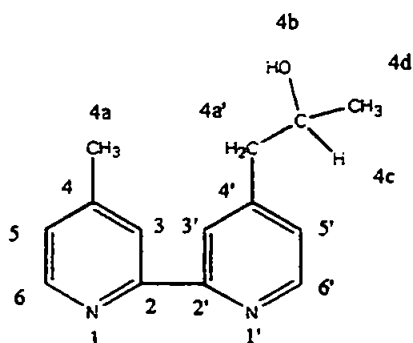
t_R (xxx) 28.75 min

m/z 227 ($M^+ - H$), 213 ($M^+ - CH_3$),

m/z 184;



NMR



(xxx)

^1H NMR (270 MHz, CDCl_3); δ (ppm) 8.55 (d, 1H) & 8.5 (d, 1H) (H-6 & H-6'), 8.2 (s, 1H) & 8.15 (s, 1H) (H-3 & H-3'), 7.2 (d, 1H) & 7.1 (d, 1H) (H-5 & H-5'), 4.1 (m, 1H, H-4c), 2.8 (d, 2H, H-4a'), 2.4 (s, 3H, H-4a), 1.2 (d, 3H, H-4d)

^{13}C NMR (68 MHz, CDCl_3); δ (ppm) 155.9 & 155.7 (C-2 & C-2'), 148.8 & 148.7 (C-6 & C-6'), 149.1 & 148.2 (C-4 & C-4'), 124.9, 124.6, 122.1, 122.0 (C-3, C-3', C-5 & C-5'), 67.7 (C-4b), 45.9 (C-4a'), 23.1 (C-4d), 21.0 (C-4a)

DEPT (68 MHz, CDCl_3); δ (ppm) 148.8, 148.7, 124.9, 124.6, 122.1, 122.0, 67.7, 23.1, 21.04as CH/ CH_3 , 45.9 (inverted CH_2)

IR

(KBr disk); ν 3368 (broad O-H str. [H-bonded]), ν 3055 (=C-H ar. & vinyl str.), ν 2970 (C-H str.), ν 1596 (C=C ring str.), ν 1461 (CH_2 group, C=C str.), 1377 (CH_3 deformation), ν 1120 (C-O str.), δ 984, 946, 909, 744 (=C-H out-of-plane bend) cm^{-1}

TLC

R_F (vi) 0.66

R_F (xxx) 0.50

Although there was sufficient separation to carry out column chromatography, there was slight streaking between spots.

(2.6.2.3) Discussion

This reaction had been performed successfully using the pyridine analogue¹⁸⁷ and was then applied to 4,4'-dimethyl-2,2'-bipyridine (vi) in this study. 4-(2-hydroxypropyl)-4'-methyl-2,2'-bipyridine (xxx) was synthesised by a modification of the Ghosh & Spiro method¹⁴⁵. The difficulties encountered previously with the addition of formaldehyde gas to the carbanion were not observed when ethanal was used. This was reflected in the result - a crude yield of 68 % was obtained. This was much higher than the results for production of the hydroxyethyl compound (vii), where a typical yield was of 30 %. Separation was more successful this time, not only because a higher proportion of oil to solid was produced, but also a suitable system for column chromatography was found. The percentage yield dropped upon purification and as with the production of the methoxyethyl compound (xxii), separation was not entirely complete, a small percentage of (vi) remained. However, it was considered that this would not interfere too much with the next stage. The spectral data obtained was consistent with the structure of the desired product.

(2.6.3) Synthesis of 4-methyl-4'-(*E*-prop-2-enyl)-2,2'-bipyridine (xxix) from 4-(2-hydroxypropyl)-4'-methyl-2,2'-bipyridine (xxx)

(2.6.3.1) Experimental Procedure

Light was excluded throughout this experiment. All glassware was dried at 150 °C overnight, assembled while hot and purged with nitrogen which had been passed through

a calcium chloride tube. Xylene (35 ml) was added to 4-(2-hydroxypropyl)-4'-methyl-2,2'-bipyridine (xxx) (1.48 g, 6.48 mmol) in a 250 ml round-bottomed flask. The resulting clear yellow solution was cannulated into a 250 ml three-necked round-bottomed flask. Phosphorus pentoxide (4.83 g, 34 mmol) was added carefully and the reaction mixture refluxed for two hours.

The mixture, a clear yellow liquid with yellow-orange solid, was left to cool to room temperature and then to 5 °C using a salt-ice bath. Crushed ice was added to decompose any excess phosphorus pentoxide and then the mixture was twice extracted with 50 ml portions of water and the aqueous layers combined. The pH was adjusted to 5.0, the product extracted with DCM (3 x 40 ml) and dried over magnesium sulfate. After filtration under reduced pressure and rotary evaporation, the crude product was a pale yellow-cream solid. A minimum amount of diethyl ether was used to dissolve impurities, leaving a fine white powder which was collected by filtration under reduced pressure.

(2.6.3.2) Results

Mass of crude product (pale cream-yellow solid) = 1.0 g

GC of crude product

t_R (xxix) 31.67 min (90 %), t_R (xxx) 34.09 min (2 %), 8 % impurities.

% crude yield by GC = 66 %

Mass of pure product = 0.3 g (1.43 mmol)

GC of pure product

Injection volume: 0.5 μ l 10 mg/ml in DCM. Attenuation 8.

t_R (vi) 25.64 min, 0.3 %, t_R (xxix) 31.70 min, 96 %, t_R (xxx) 34.17 min, 0.2 %.

% Yield of pure product by GC = 21 %

GC-MS

t_R (vi) 19.49 min, 0.7 %. Assignments of MS fragments as described in section 2.2.3 (page 73-74).

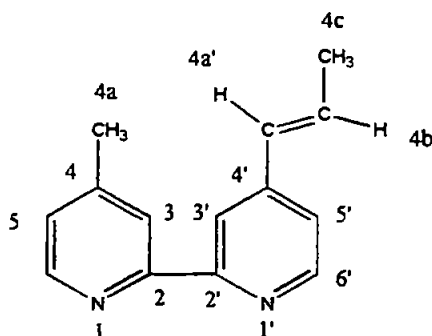
t_R (xxix) 25.49 min, 89 %

m/z 209 ($M^+ - H$), m/z 195, m/z 181 (loss of methyl group from prop-2-enyl group), m/z 170, m/z 154 (loss of allyl and CH_3 from M^+ ion), m/z 92 ((v) - H)

Solubilities

The product was found to be soluble in ethyl acetate and warm methanol and also warm DMSO. It was insoluble in water, hexane and diethyl ether.

NMR



(xxix)

1H NMR (270 MHz, $CDCl_3$); δ (ppm) 8.55 (d, 1H) & 8.5 (d, 1H) (H-6 & H-6'), 8.3 (s, 1H) & 8.2 (s, 1H) (H-3 & H-3'), 7.2 (d, 1H) & 7.1 (d, 1H) (H-5 & H-5'), 6.6 (dq, 1H, H-4b, $J_{trans} = 16$ Hz), 6.5 (d, 1H, H-4a', $J_{trans} = 16$ Hz), 2.4 (s, 3H, H-4a), 1.9 (d, 3H, H-4c)

^{13}C NMR (68 MHz, CDCl_3); δ (ppm) 156.6 & 155.9 (C-2 & C-2'), 148.2 & 146.3 (C-4 & C-4'), 149.3, 148.9, 131.3, 129.2, 124.7, 122.0, 120.5, 118.1 (C-3, C-3', C-5, C-5', C-4a' & C-4b), 21.2 (C-4a), 18.7 (C-4c)

DEPT (68 MHz, CDCl_3); δ (ppm) 149.3, 148.9, 131.3, 129.2, 124.7, 122.0, 120.5, 118.1, 21.2 & 18.7 all CH/ CH_3

IR

(KBr Disk) ν 3003.1, 2968.1, 2930.0, 2909.7 (=C-H alkenic and ar. str.), ν 1589.0, 1542.7, 1461.9 (C=C ring str.), δ 1461.9, 1368.7 (CH_3 in-plane bend), δ 986.3 - 797.9 (series of peaks, =C-H out-of-plane bends, indicative of m-disubstituted rings), δ 966.4 (trans-1,2-disubstituted double bond) cm^{-1} .

(2.6.3.3) Discussion

The spectral data obtained was consistent with the structure of the desired compound. A low yield of high purity product was obtained, with a very small amount of bipyridine (vi) having been carried through to this stage. 4-methyl-4'-(prop-2-enyl)-2,2'-bipyridine is capable of exhibiting *E/Z* isomerism. The *E* form would be expected to be the predominant isomer as this is the sterically favoured form. The *Z* form is energetically less favoured due to interference of the end methyl group of the prop-2-enyl group with the hydrogen atom at the 5' position of the pyridine ring.

This predominance of the *E* form was confirmed by NMR spectroscopy. For the signals due to protons 4a' and 4b, the coupling constant (J) was measured as 16 Hz. This figure is consistent with that expected for the *E* isomer. The value of J for the *Z* isomer lies between 2 - 15 Hz and there is no apparent evidence from the NMR data that any amount of this isomer had been formed.

(2.6.4) Synthesis of Ruthenium tris(4-methyl-4'-(E-prop-2-enyl)-2,2'-bipyridine) bis(hexafluorophosphate) (xxviii).

Bommarito et al., *Inorg. Chem.*, 1992, 31, 3, 495-502¹⁸¹

(2.6.4.1) Experimental Procedure

Throughout the reaction, the mixture was protected from light. 6.5 ml of a 1:1 ethanol:water mix was added to ruthenium trichloride (0.08 g, 0.40 mmol) and 4-methyl-4'-(E-prop-2-enyl)-2,2'-bipyridine (xxix) (0.24 g, 1.16 mmol) in a 50 ml two-necked round-bottomed flask. This was left to stir and purge with nitrogen for 20 mins and then heated at reflux for 3 hrs. The mixture, which changed during this period from dark brown yellow to dark red-orange, was then left to cool. Saturated ammonium hexafluorophosphate (1 ml) was added to precipitate the complex and this was stood in ice for 10 mins. The crystals were isolated by filtration under reduced pressure using a Hirsch funnel.

(2.6.4.2) Results

Mass of product (orange solid) = 0.21 g (0.21 mmol)

% Yield = 59 %

UV

Solvent: MeCN, λ (max)/nm ($\epsilon/\text{mol}^{-1}\text{dm}^3\text{cm}^{-1}$); 211 (50062), 250 (71106), 296 (72675), 468 (20602)

IR

(KBr Disk); ν 3119.2, 3080.1, 3028.6 (=C-H ar. and vinyl str.), ν 2964.6, 2928.3 (-C-H alip. str.), ν 1614.8, 1479.7 (C=C ring str.), δ 1379.9 (CH₃ bend), δ 1309.7, 1240.0,

969.9 (in-plane C-H bend), δ 969.9, 908.9, 839.6, 795.3, 743.8 (=C-H out-of-plane bend) cm^{-1}

NMR

The hydrogens and carbons of (xxviii) were labelled as for the free ligand (xxix). The solvent acetone- d_6 was used for all NMR measurements. ^1H NMR was performed at 270 MHz and ^{13}C and DEPT NMR at 68 MHz. The signals were assigned with further information from 2D NMR methods. Table 2.9 overleaf gives full details of these assignments.

(2.6.4.3) Discussion

The yield of ruthenium tris(4-methyl-4'-(*E*-prop-2-enyl)-2,2'-bipyridine) bis(hexafluorophosphate) complex was very similar to the yield of ruthenium tris(4-methyl-4'-vinyl-2,2'-bipyridine bis(hexafluorophosphate) (iii). The spectral data was also similar, as would be expected. A full set of NMR data was collected (Table 2.9), which allowed almost complete structural elucidation and confirmation that the desired product had been synthesised.

¹ H NMR δ (ppm)	Integration	Multiplicity	Assignment	¹³ C NMR δ (ppm)	DEPT	COMMENTS
2.4	3	s	4a	21.6	CH/CH ₃	Carbon assignment from VCHSHF spectrum.
1.9	3	d	4c	19.4	CH/CH ₃	Carbon assignment from VCHSHF spectrum.
-	-	-	4	151.5	-	Carbon assignment from VCOLOC spectrum - 2-bond coupling with 4a. No other couplings with protons in either VCHSHF or VCOLOC spectra.
-	-	-	4'	148.2	-	Carbon assignment by direct comparison with ¹³ C spectrum of Ru(vbpy) ₃ ²⁺
-	-	-	2, 2'	158.5, 158.2	-	Carbon assignment by direct comparison with ¹³ C spectrum of Ru(vbpy) ₃ ²⁺ . Cannot assign which is which.
6.5	1	d	4a'	136.7	CH/CH ₃	<i>J</i> _{trans} = 16. Carbon assignment by direct comparison with ¹³ C spectrum of Ru(vbpy) ₃ ²⁺
6.9	1	dq	4b	128.9	CH/CH ₃	Carbon assignment from VCHSHF spectrum.
7.85	1	d	6	152.6	CH/CH ₃	Carbon assignment by direct comparison with ¹³ C spectrum of Ru(vbpy) ₃ ²⁺
7.75	1	d	6'	152.0	CH/CH ₃	Carbon assignment by direct comparison with ¹³ C spectrum of Ru(vbpy) ₃ ²⁺

Table 2.9: Full NMR interpretation for Ru(ppbp)₃²⁺, (xxviii)

¹ H NMR δ (ppm)	Integration	Multiplicity	Assignment	¹³ C NMR δ (ppm)	DEPT	COMMENTS
7.4	1	d	5	129.9	CH/CH ₃	Carbon assignment by direct comparison with ¹³ C spectrum of Ru(vbpy) ₃ ²⁺ Carbon assignment from VCHSHF spectrum.
7.5	1	d	5'	125.2	CH/CH ₃	Carbon assignment by direct comparison with ¹³ C spectrum of Ru(vbpy) ₃ ²⁺ Carbon assignment from VCHSHF spectrum.
8.65	1	s	3	126.4	CH/CH ₃	Carbon assignment by direct comparison with ¹³ C spectrum of Ru(vbpy) ₃ ²⁺ Carbon assignment from VCHSHF spectrum.
8.70	1	s	3'	121.8	CH/CH ₃	Carbon assignment by direct comparison with ¹³ C spectrum of Ru(vbpy) ₃ ²⁺ Carbon assignment from VCHSHF spectrum.

cont...

Table 2.9: Full NMR interpretation for Ru(ppbpy)₃²⁺, (xxviii)

(2.7) EXPERIMENTAL APPENDIX

(2.7.1) Instrumentation and Techniques Used for Analysis

Infra-red (IR) Analysis; (1) Bruker FT-IR IFS-66, 16 scans (2) Perkin-Elmer 298 IR Spectrophotometer. Scan range 4000 - 650 cm^{-1} , scan time 4 min, medium slit programme, abscissa expansion 0.5.

Solid samples - KBr disks, liquid / oil samples, NaCl windows.

Nuclear Magnetic Resonance (NMR) Analysis; Jeol EX270 MHz FT-NMR Spectrometer

Proton (^1H) NMR spectra were recorded at 270 MHz using a 45° pulse, carbon-13 (^{13}C) NMR at 68 MHz using a 45° pulse and DEPT spectra at 68 MHz using a three pulse sequence. Samples were dissolved in either chloroform- d_1 (containing 0.1 v/v tetramethylsilane, (TMS)) or acetone- d_6 . Using the former deuterated solvent, ^1H NMR resonances were referenced to TMS at 0 ppm and to the residual protio solvent peaks at 77.0 ppm in ^{13}C spectra. Using deuterated acetone, resonances were referenced to the residual protio solvent peaks at 2.0 ppm and 30.3 ppm for the ^1H and ^{13}C NMR spectra respectively.

Gas Chromatography (GC) Analysis; (1) Carlo Erba Strumentazione, hydrogen carrier gas, 2 ml/min, FID (2) Carlo-Erba HRGC 5300 Mega Series, hydrogen carrier gas, FID, detector temp. 300 °C. Both columns DB5, 30m x 0.32 mm i.d., 0.25 μm film thickness. Temperature programme 40 - 300 °C @ 5 °C/min, 10 min @ 300 °C, attenuation 5 unless otherwise stated. For each run, 0.5 μl 0.1 mg/ml on-column injection of sample was made. (3) Perkin Elmer Gas Chromatograph 8600, FID, injector temp. 50 °C, detector temp. 250 °C. C-20M glass-packed column, 6 m x 2 mm i.d. Temp. Prog.; 40 °C, isothermal, 20 min. 1 μl injections were made.

G.C. analysis was performed using (1) or (2) were used unless otherwise stated.

Gas Chromatography-Mass Spectrometric (GC-MS) Analysis; Hewlett Packard 5890 Series (II) Chromatograph, Hewlett Packard 7673 Injector, Hewlett Packard 5970 Series Mass Selective Detector, HP1 Column, 12 m x 0.2 mm i.d. Helium Carrier Gas, pressure 40 kPa

Mass Spectrometry (MS); Kratos MS-25

UV-VIS Spectrophotometry; Hewlett Packard 8453 Photodiode Array UV-VIS 190 - 1100 nm Spectrophotometer.

Melting Point Apparatus; (1) Electrothermal Mp Apparatus 9200 (2) Kofler Heizbank, Austria.

Thin Layer Chromatography (TLC) performed on aluminium backed plates; stationary phase silica gel 60F₂₅₄. Visualised under UV light at 254 nm.

pH Meters; (1) Hanna Instruments HI9025 Microcomputer pH meter (2) HI931402 Microprocessor pH meter

pH electrode; BDH Gelplas General Purpose Combination Cat. No. 309/1050/03

(2.7.2) Chemicals Used in This Study

Key, AS = used as supplied

CHEMICAL (ABBREVIATION USED IN TEXT)	SUPPLIER	PREPARATION PRIOR TO USE
Acetic acid, glacial	BDH	Diluted - ~ 50 %
Acetone- <i>d</i> ₆ 100 atom % D	Aldrich	AS
Aluminium oxide, 60G. Neutral, Type E	Merck	AS
Ammonium hexafluorophosphate, 99.99 %	Aldrich	AS
Bis(trimethylsilyl)trifluoro- acetamide {BSTFA}	Aldrich	Refrigerated
<i>n</i> -Butyllithium, 1.6 M in hexanes. Packaged under nitrogen	Aldrich	Refrigerated. Care, pyrophoric.
Chloroform- <i>d</i> , 99.8 atom %D (+0.1 % v/v TMS)	Aldrich	Refrigerated
Chloromethyl methyl ether, tech. {CMME}	Aldrich	Dried over magnesium sulfate for half an hour, stored under nitrogen. Refrigerated.
Diethyl ether	Rathburns	Stored over Na wire
Deuterium Oxide, 99.9 atom % D {D ₂ O}	Aldrich	Refrigerated
Diglyme (2-methoxyethyl ether), 99+ %, spectrophotometric grade	Aldrich	AS
Diisopropylamine, redistilled, 99.5 % Packaged under nitrogen	Aldrich	Refrigerated
4,4'-Dimethyl-2,2'-dipyridyl, 99 % {bpy}	Aldrich	Stored over P ₂ O ₅ under vacuum for a minimum of 24 hours
Ethanal (acetaldehyde)	Aldrich	Dried over sodium sulfate in an inert atmosphere, stored under nitrogen and refrigerated.
Glyme (1,2-dimethoxyethane)	Rathburns	AS

Table 2.10: Table of chemicals and their preparation for use in this study

CHEMICAL {ABBREVIATION USED IN TEXT}	SUPPLIER	PREPARATION PRIOR TO USE
Magnesium sulfate, GPR	BDH	AS
4-Methylpyridine, 98 % {Mepy}	Aldrich	Distilled over KOH, then stored under nitrogen and refrigerated.
Nitrogen gas (white spot) <5 ppm O ₂ , < 2ppm H ₂ O	Air Products plc	Dried by passing through a calcium chloride guard tube.
Nitrogen cryogenic liquid	BOC Gases	AS
Paraformaldehyde, 95 %	Aldrich	Stored under vacuum over P ₂ O ₅ under vacuum for a minimum of 24 hours
Phosphorus pentoxide, 97 %	Aldrich	AS
Potassium tert-butoxide, 97 %	Lancaster	Moisture sensitive - stored over P ₂ O ₅ under vacuum for a minimum of 24 hours
Pyridine, GPR	BDH	AS
Ruthenium trichloride	Aldrich	Very hygroscopic. Stored over P ₂ O ₅ under vacuum for a minimum of 24 hours
Schiff's Reagent (Fuschin aldehyde reagent.)	BDH	Refrigerated
Silica gel for Flash Chromatography. Particle Size 40 - 63 μm	BDH	AS
Sodium hydrogen carbonate	BDH	AS
Sodium sulfate, GPR	BDH	AS
Tetrachloromethane	Aldrich	AS
Tetrahydrofuran {THF}	BDH	Distilled over sodium wire, stored over sodium wire under nitrogen [bp 66 °C, lit. 65 - 67 °C] ¹⁷⁵
Trifluoroacetic acid {TFA}	Aldrich	AS
Xylene (Dimethylbenzene xylol)	Rathburns	Dried over sodium wire

cont... Table 2.10: Table of chemicals and their preparation for use in this study

Additional solvents not included in Table 2.10, unless otherwise stated, were from either Rathburns or BDH and were used as supplied. Purified water from a Milli-Q system was used throughout. The resistivity was greater than $18 \text{ M}\Omega\text{cm}^{-1}$ in all cases.

Addresses of Chemical Suppliers

Air Products plc, Basingstoke, Hants., England

Aldrich Chemical Co. Ltd., Gillingham, Dorset, England

BDH Chemicals Co., Poole, Dorset, England

BOC Gases, Worsley, Manchester, England

Lancaster Synthesis Ltd., Morecambe, Lancashire, England

Merck Ltd., Poole, Dorset, England

Rathburn Chemicals Ltd., Peeblesshire, Scotland

CHAPTER 3

PREPARATION, DEVELOPMENT AND INVESTIGATION OF CHEMICALLY MODIFIED ELECTRODES COATED WITH RUTHENIUM TRIS(BIPYRIDINE) RELATED POLYMERS

(3.1) ELECTROPOLYMERIZATION

(3.1.1) Introduction

Chemically Modified Electrodes (CME's) based on the polymer poly-[ruthenium tris(4-methyl-4'-vinyl-2,2'-bipyridine) bis(hexafluorophosphate)] (poly-[Ru(vbpy)₃²⁺]) were required in this study for chemiluminescence (CL) analysis. These were obtained by the reductive electropolymerization of the monomer Ru(vbpy)₃²⁺ in acetonitrile solution, using the method by Denisevich *et al.*¹¹⁰

(3.1.2) Initial Electropolymerization Procedure

Introduction

The following sections describe the optimization of the production of CME's for the purpose of this study. All potentials in this work are quoted relative to a Standard Calomel Electrode (SCE).

Experimental Procedure

The initial experimental arrangement is shown in Figure 3.1 overleaf.

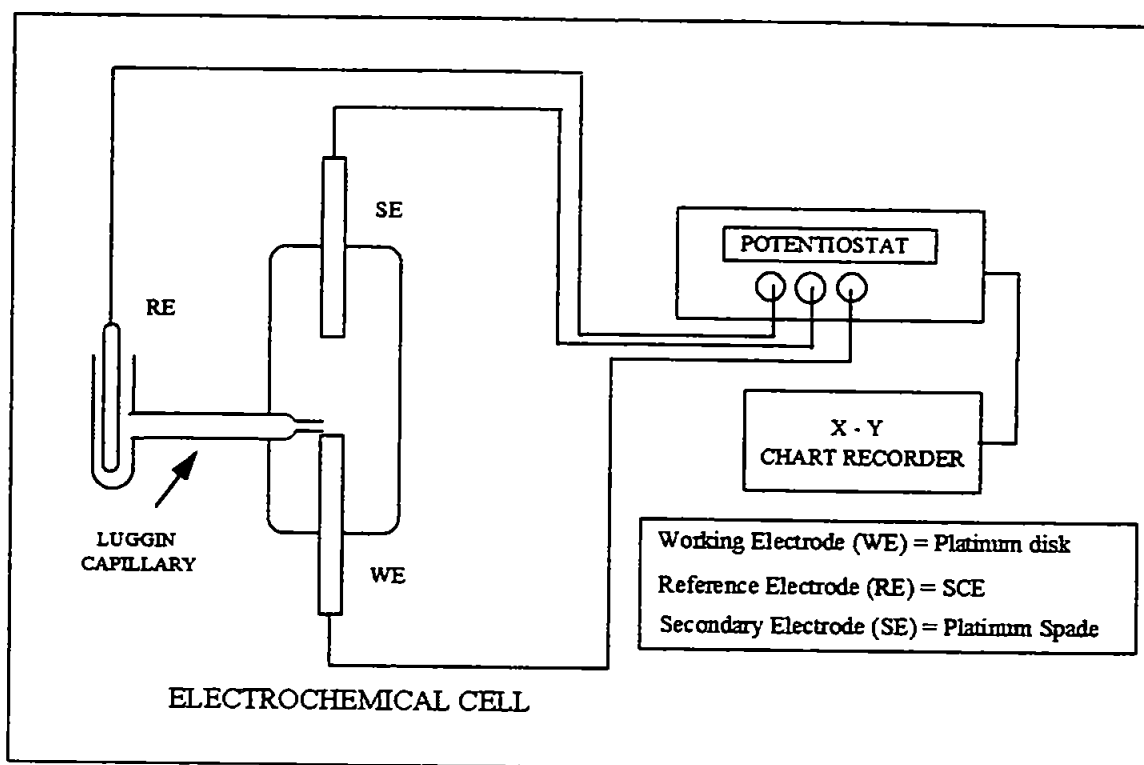


Figure 3.1: Initial experimental arrangement for electropolymerization

An electrochemical cell was designed as a completely sealed system in order to eliminate the presence of air and water. The platinum disk working electrode (WE), of surface area 0.64 cm^2 , was incorporated into the cell so that the metal surface faced upwards. This was to facilitate the uniform formation and adsorption of a polymer film. The SE, a platinum disk electrode similar to the WE, was positioned parallel to and opposite the WE. This would provide a uniform current density over the entire surface of the WE, allowing for more homogeneous film growth. The RE was a small calomel reference electrode which could 'sit' in the Luggin capillary. Platinum electrodes were cleaned with conc. sulphuric acid and then Milli-Q water prior to use. All chemicals were dried before use, as described in section 3.6.2 (pages 191-192).

The cell was prepared by heating it to above $100 \text{ }^\circ\text{C}$ for 3 hours, allowing it to cool, and then filling it with 0.1 M tetraethylammonium perchlorate (TEAP) in acetonitrile (MeCN). 100 ml of solution was syringed into the cell whilst in the horizontal

position (Plate 3.1, overleaf) and then a nitrogen stream, passing through a sinter, created fine bubbles which purged the system of oxygen. This was performed for 20 minutes prior to the cyclic voltammetry experiment. This solution of supporting electrolyte alone was used to check for the presence of any electrochemistry occurring between the two potential limits by recording a cyclic voltammogram (CV), a plot of the change in current with varying potential.

The cell was then filled with a solution of 0.1 mM $\text{Ru}(\text{vbpy})_3^{2+}$ in MeCN and 0.1 M TEAP and the purging process repeated. The cell was sealed and turned to the vertical position (Plate 3.2, page 137) during the electropolymerization procedure, which took place over a two hour period. Once again, progress was monitored by recording a CV. Light was excluded throughout due to the photosensitive nature of $\text{Ru}(\text{vbpy})_3^{2+}$. The electrode potential was scanned at 0.1 V/s between the potential limits chosen and selected scans were recorded. The resulting CME was washed with acetonitrile before placing it back in the cell with fresh supporting electrolyte to test for the presence of a conducting film. After analysis, the CME was stored in MeCN.

In later experiments, TEAP became unavailable commercially and was replaced by tetra-*n*-butylammonium perchlorate (TBAP).

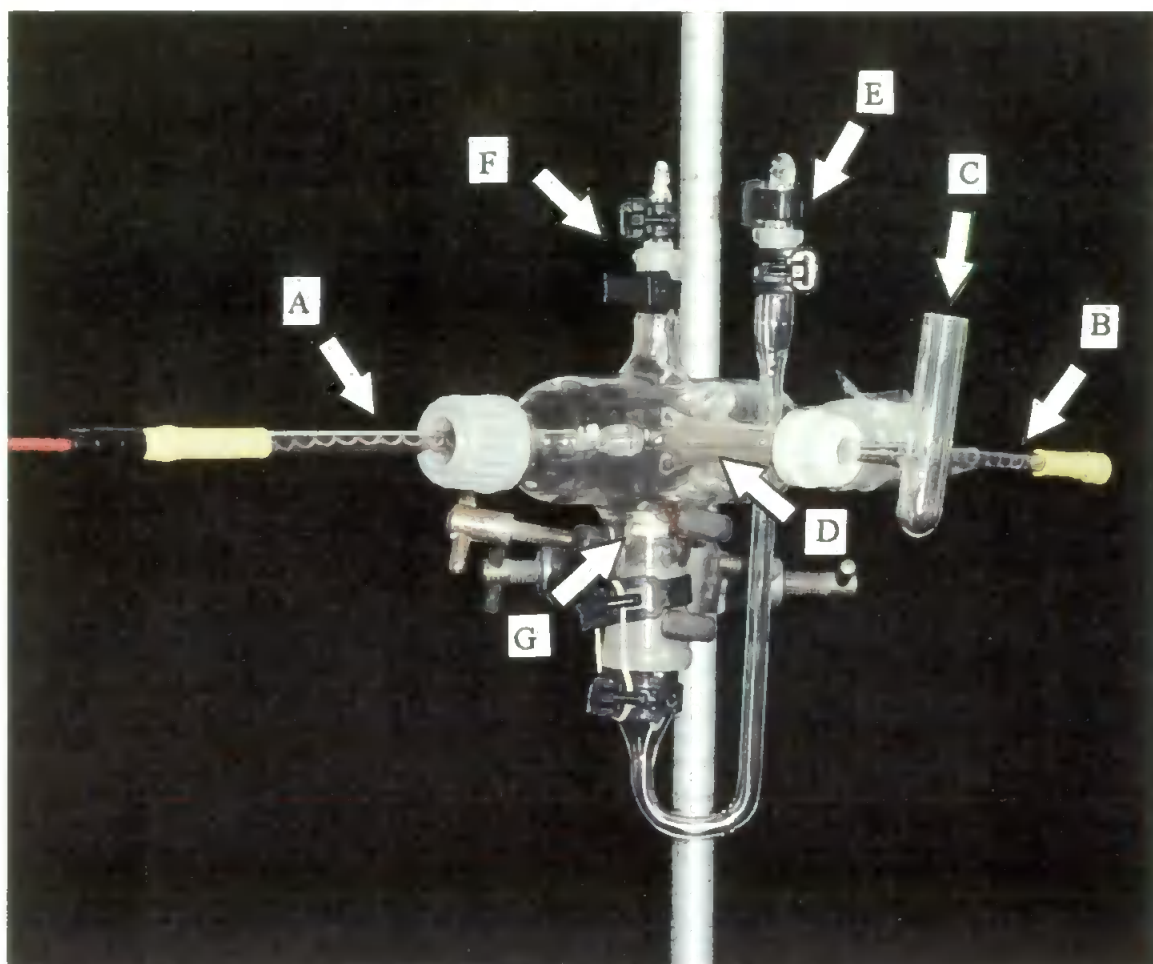


Plate 3.1: Empty electrochemical cell used for electropolymerization, horizontal position

- A Platinum disk Working Electrode (WE)
- B Platinum disk Secondary Electrode (SE)
- C Pocket for Reference Electrode (RE)
- D Luggin Capillary
- E Stoppered opening for filling cell
- F Stoppered opening for purging cell
- G Sintered frit

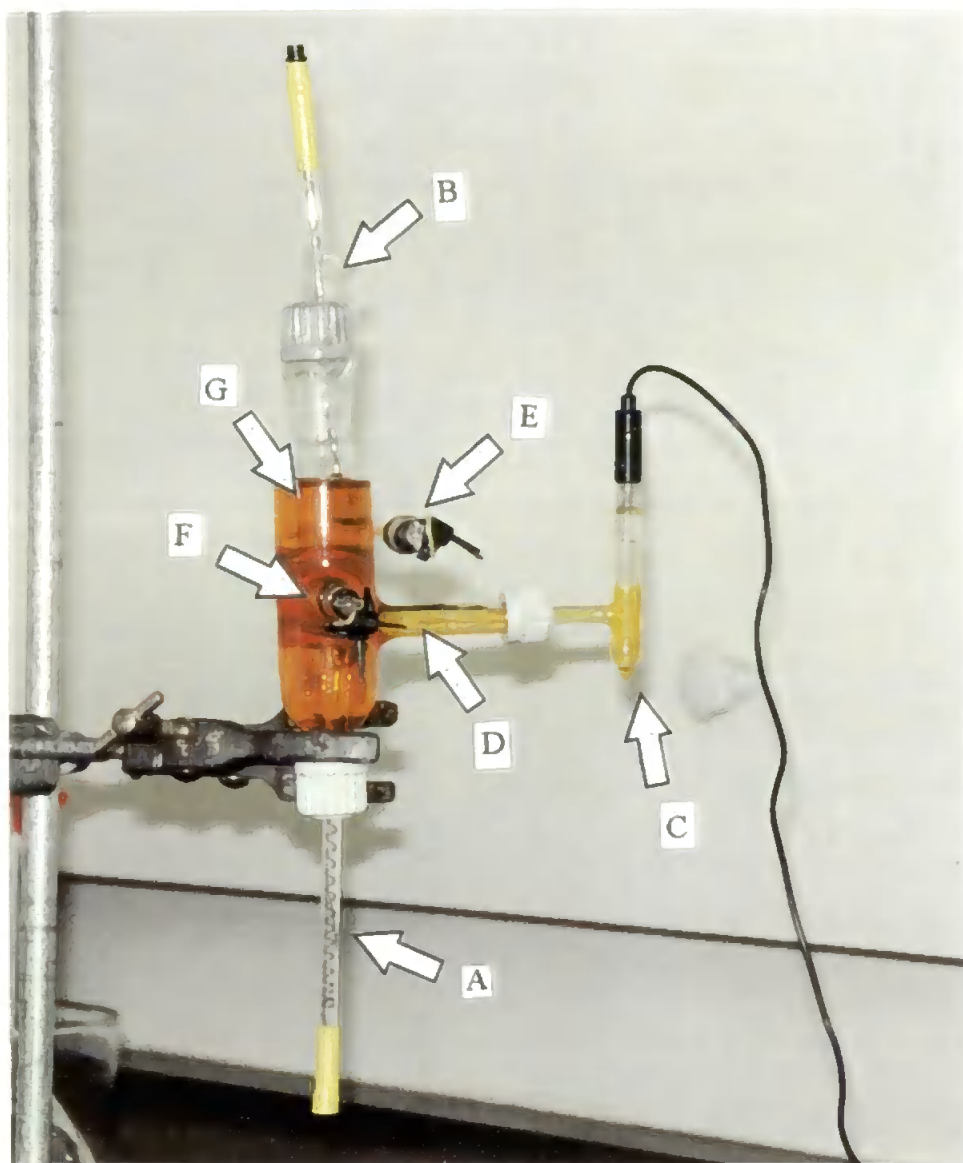


Plate 3.2: Electrochemical cell used for electropolymerization, vertical position.

- A Platinum disk Working Electrode (WE)
- B Platinum disk Secondary Electrode (SE)
- C Pocket containing Reference Electrode (RE)
- D Luggin Capillary
- E Stoppered opening for filling cell
- F Stoppered opening for purging cell
- G 0.1 mM Ruthenium tris(4,4'-vinyl-2,2'-bipyridine) bis(hexafluorophosphate) in acetonitrile solution, containing 0.1 M TEAP as supporting electrolyte.

Results & Discussion

The CV of 0.1 M TEAP in MeCN solution, recorded prior to purging, indicated that some electrochemistry was occurring at the more negative potentials. This was attributed to the presence of oxygen as no electrochemistry was observed between the limits required for electropolymerization after purging with nitrogen for ten minutes. The shape of the CV was maintained after a period of half an hour without further purging, proving that the cell was well-sealed.

Electropolymerization performed using 0.1 mM $\text{Ru}(\text{vbpy})_3^{2+}$ /0.1 M TEAP in MeCN resulted in the formation of an orange-brown film on the electrode surface. Increasing waves on the CV were observed but the peaks were not particularly well-defined (Figure 3.2, overleaf).

The CV of the conductance of the resulting CME in supporting electrolyte alone (Figure 3.3, page 140) was not satisfactory. This was attributed to the fact that the glassware, solution and electrodes were exposed to air prior to testing as the filling solution was changed from $\text{Ru}(\text{vbpy})_3^{2+}$ /TBAP in MeCN to fresh supporting electrolyte. Hence electrochemistry due to oxygen was obscuring the current arising from the conductance of the polymer.

It was clear that although the cell was designed to eliminate the presence of air and water, this aim had not fully been achieved and more work was required to improve the quality of the CME's produced.

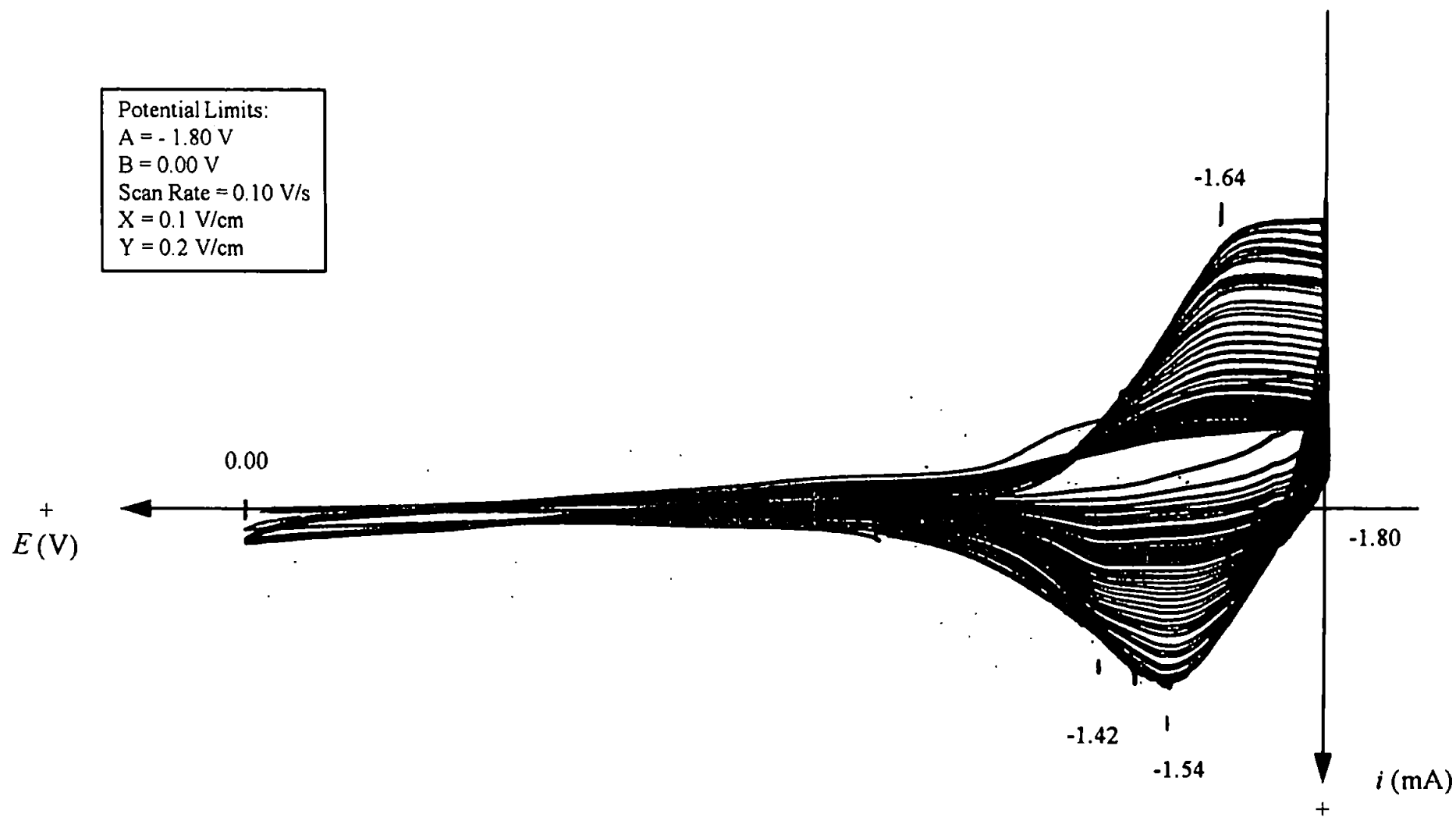
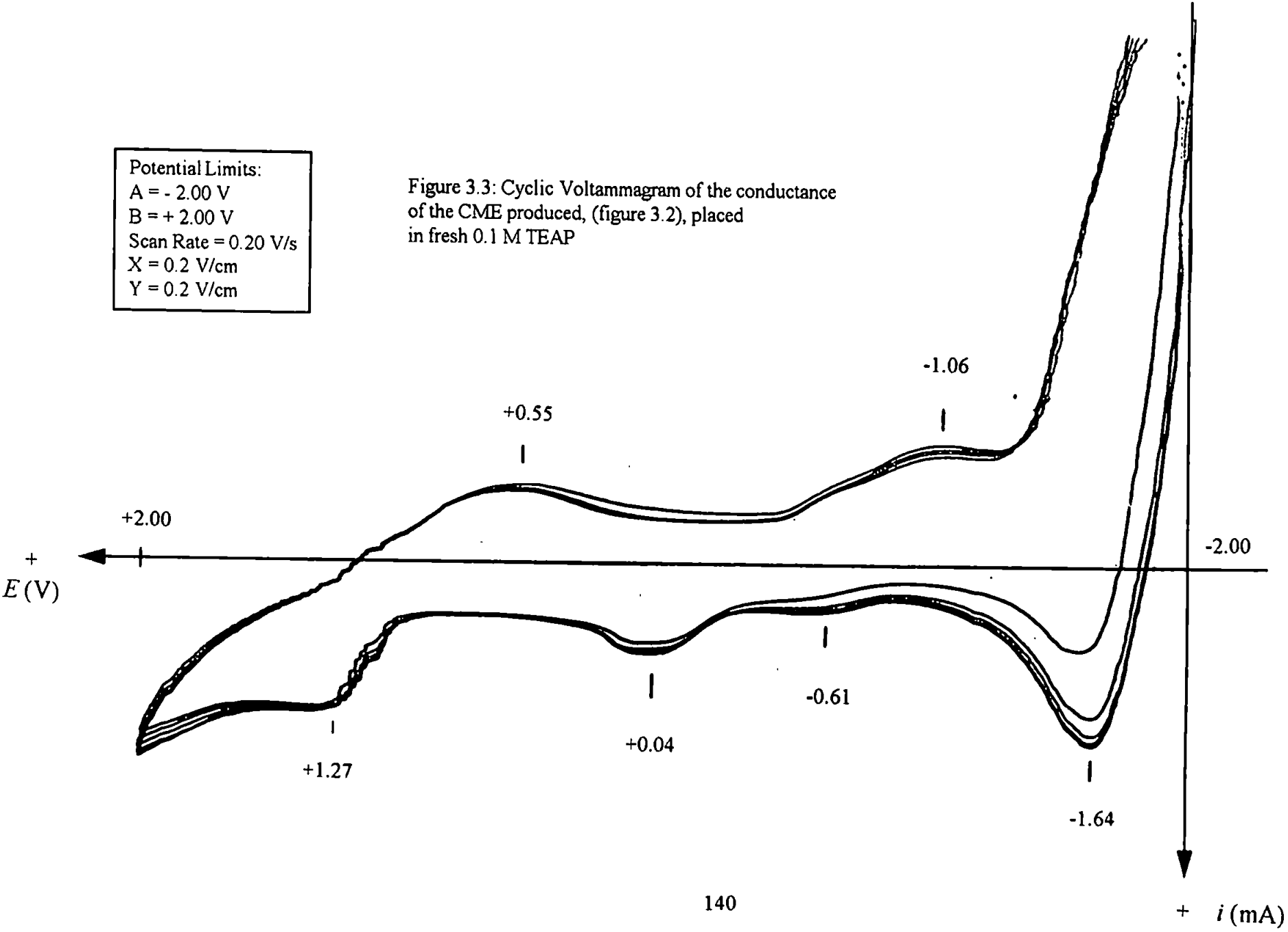


Figure 3.2: Cyclic Voltammogram obtained from the electropolymerization of 0.1 mM $\text{Ru}(\text{vbpy})_3^{2+}$ in 0.1 M TEAP in acetonitrile

Potential Limits:
A = - 2.00 V
B = + 2.00 V
Scan Rate = 0.20 V/s
X = 0.2 V/cm
Y = 0.2 V/cm

Figure 3.3: Cyclic Voltammogram of the conductance of the CME produced, (figure 3.2), placed in fresh 0.1 M TEAP



(3.1.3) Electropolymerization Within A Glove Box

Introduction

It was decided that use of a glove box was the only way to achieve the inert atmosphere required. Many authors reported the use of a glove-box to preclude any reaction of reduced monomer or polymer with oxygen^{134,136,137,188,189}. For example, Surridge *et al.*¹⁷⁴ performed co-polymerizations under nitrogen, either in an inert (dry N₂) atmosphere enclosure or in cells under nitrogen purge and reported that the former technique was more reliable.

In order that the whole of the electropolymerization experiment could be carried out inside the glove box, the length of the working electrode was shortened to 10 cm. The sintered frit was removed from the assembly as it was considered unnecessary. Connectors were added to both sides of the glove-box's metal casing so that the cell could be connected to the potentiostat whilst inside the glove box.

Experimental Procedure

The electrodes were cleaned by sonication for 20 minutes in DCM or chloroform, followed by conc. sulphuric acid and UV-irradiated Milli-Q water. The glove box was prepared before each electropolymerization by purging with nitrogen and drying with phosphorus pentoxide.

All glassware was heated and loaded directly into the glove box main chamber, together with the chemicals and the rest of the equipment. The inner door was kept open during loading because the size of the cell meant that it could not be transferred in the assembled state from the transfer chamber to the main chamber. Hence, an extended purging period was required. After purging for one night, the monomer solution was

made up as described in section 3.1.2 (page 133) and the cell filled inside the glove box. Purging was continued throughout this period.

Results & Discussion

Despite performing the electropolymerization procedure within the glove box, a poor CV was obtained. Definite peaks were not observed and there was little evidence of a growing film. There were two possible explanations for this. Either electropolymerization had failed to take place or, once again, the current from the electrochemical reactions of oxygen and water was considered to be masking the current resulting from the electropolymerization reaction. The first suggestion was disproved as a thick, flaky but uniform film had been deposited on the electrode surface. Further modifications of the electropolymerization conditions were, therefore, still required for complete elimination of the presence of air and water.

(3.1.4) Final Modifications of the Electropolymerization Procedure

Experimental Procedure

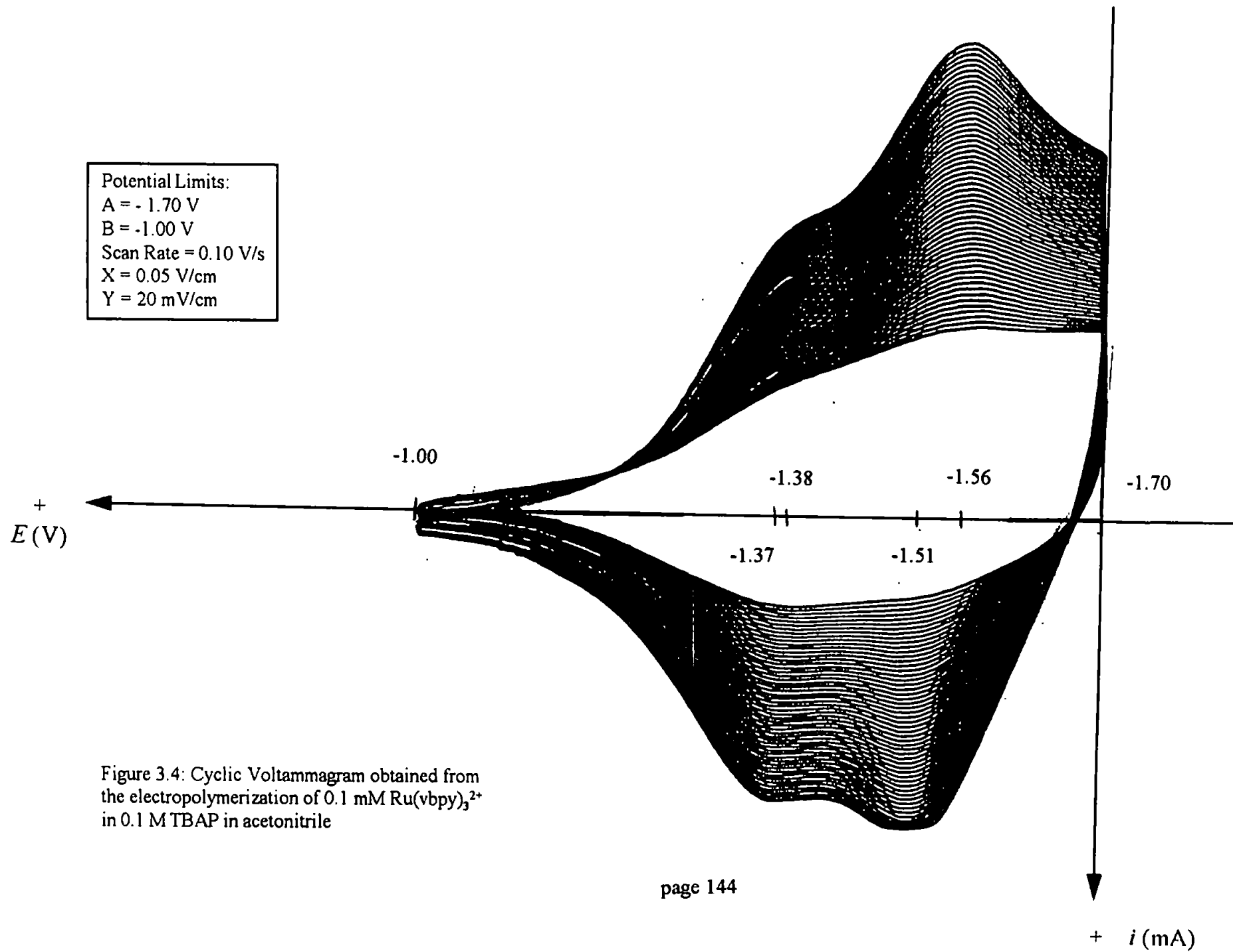
The glove-box containing the cell and equipment needed for electropolymerization was purged for 72 hours in an attempt to fully eliminate any air or water. The wires connecting the potentiostat to the glove box were screened and earthed to the glove box to reduce electrical noise. The electropolymerization procedure was performed and the conductance of the electrode was tested as described previously in section 3.1.2 (page 133).

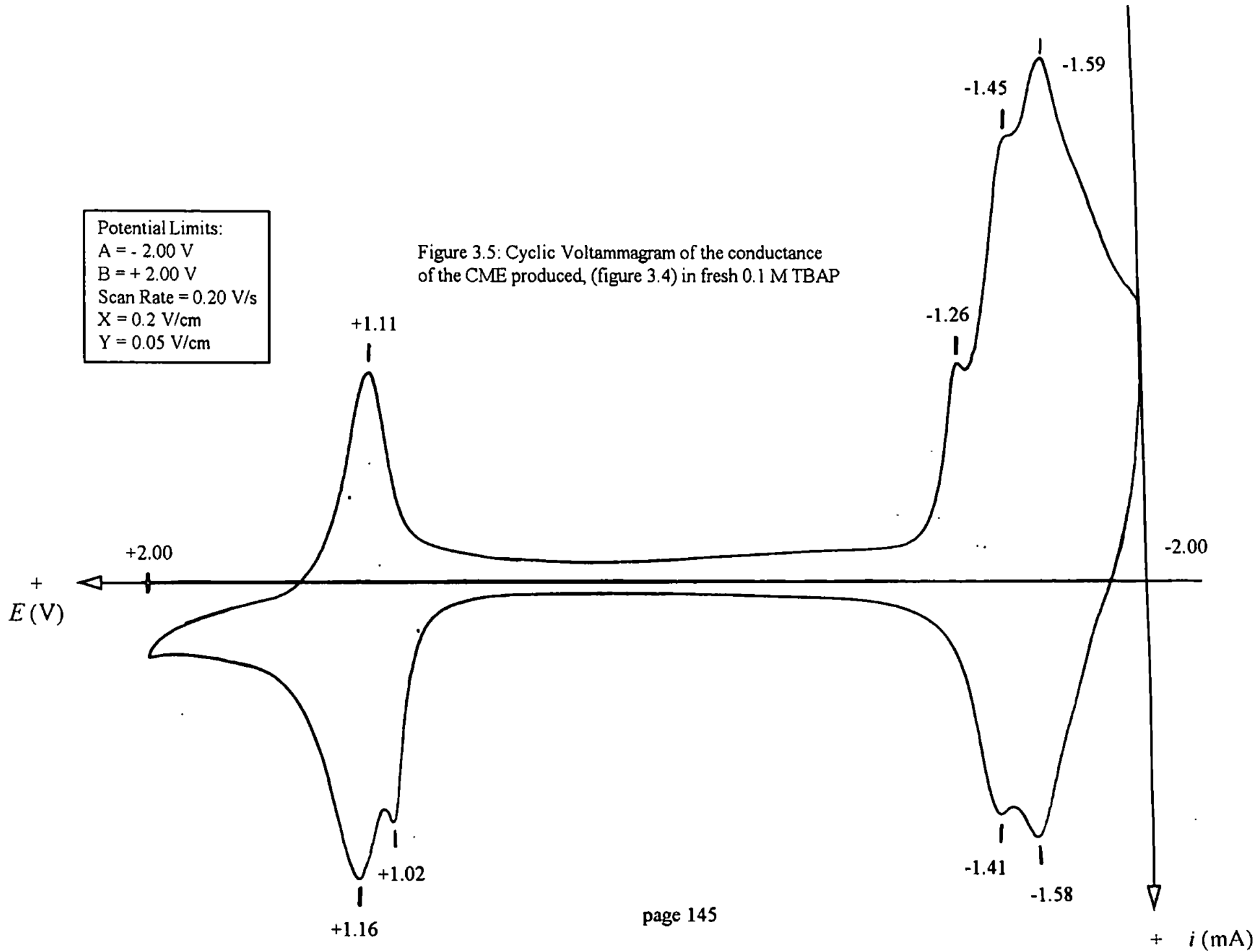
Results & Discussion

Figure 3.4 overleaf shows the resultant CV which matched that reported in the literature¹¹⁰. There are two main features. The peaks represent the change in oxidation state of the ruthenium centres and appear at -1.4 V and -1.5 V for the $[\text{Ru}(\text{vbpy})_3]^{2+/1+}$ and $[\text{Ru}(\text{vbpy})_3]^{1+/0}$ couples respectively. Secondly, there is clear indication from the increasing current waves that an electroactive polymer film was growing on the electrode surface. The growing film itself also electrocatalytically reduces fresh inward-diffusing solution complex. The currents obtained were initially quite small. This effect is explained by the fact that since the concentration of $[\text{Ru}(\text{vbpy})_3]^{2+}$ was small (0.1 mM), diffusion to the electrode surface was low. The currents then became much larger than is accountable by diffusion-controlled electrochemistry. This is attributed to the expanding surface area of the polymer film and the electrochemistry of the increasing number of redox active centres within the film.

The CV showing the conductance of the resulting CME (Figure 3.5, page 145) also mirrored that in the literature¹¹⁰. The $[\text{Ru}(\text{vbpy})_3]^{2+/1+}$ and $[\text{Ru}(\text{vbpy})_3]^{1+/0}$ reduction waves remained observable and the $[\text{Ru}(\text{vbpy})_3]^{3+/2+}$ oxidation wave appeared at +1.1 V vs SCE. The quality of the film produced also improved - the electrode surface was covered with an adherent orange material, indicative of a thin film. In contrast, films obtained in previous experiments were thick, opaque and flaky.

The reason for the significant improvement in CV and film appearance was attributed mainly to the extra 48 hours of purging required for creation of a completely inert atmosphere. However, upon repeating the experiment even with the stringent conditions described above, results were not always satisfactory. Further investigations were necessary to render the experiment entirely reproducible, but due to time constraints, the problems encountered were not entirely resolved.





(3.1.5) Electropolymerization of Ruthenium tris(4-methyl-4'-(E-prop-2-enyl)-2,2'-bipyridine) bis(hexafluorophosphate)

Introduction

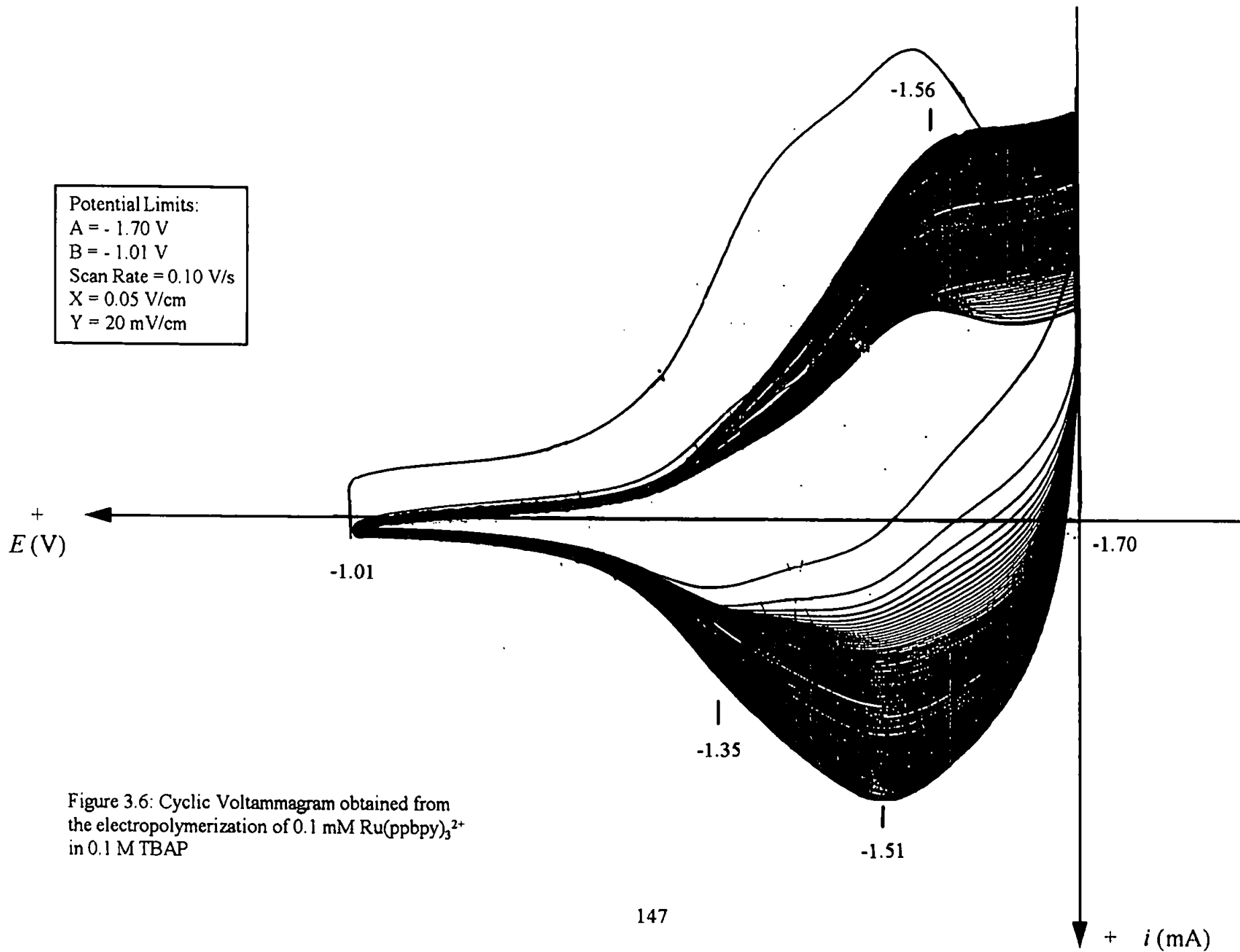
The monomer complex ruthenium tris(4-methyl-4'-(E-prop-2-enyl)-2,2'-bipyridine) bis(hexafluorophosphate), $\text{Ru}(\text{ppbpy})_3^{2+}$, has not been previously reported in the literature. Electropolymerization of this monomer produced a novel polymer which formed the basis of a novel polymer modified electrode.

Experimental Procedure

The electropolymerization technique used for the preparation of CME's coated with poly- $[\text{Ru}(\text{vbpy})_3^{2+}]$, as described in section 3.1.4, (page 142) was applied to the formation of films of poly- $[\text{Ru}(\text{ppbpy})_3^{2+}]$ from 0.1 mM $\text{Ru}(\text{ppbpy})_3^{2+}$ in 0.1 M TBAP in MeCN.

Results & Discussion

The CV obtained (Figure 3.6, overleaf) shows that there were only two main peaks at -1.51 V scanning anodically and -1.56 V scanning cathodically. These peaks were not particularly well defined. However, a growing polymer film was observed and a dark orange brown film obtained on the electrode surface. This proved that the modified monomer structure does not significantly alter the ability of the compound to electropolymerize.



(3.1.6) Overall Discussion of the Electropolymerization Procedure

It is apparent that the elimination of all traces of air and water is crucial to the success of this step, the appearance of the CV and the quality of the film. Rigorous conditions, utilising a glove-box, were required. As a result of this stringent procedure, only one CME was able to be produced per experiment.

The final procedure was used many times. However, on occasions, problems were still experienced in obtaining reproducible CV's. The cause of this is unknown and was attributed to the very sensitive nature of the procedure. In contrast, successful experiments produced CME's which were stable to air, water and light.

(3.2) MICROSCOPE IMAGES OF CHEMICALLY MODIFIED ELECTRODES

(3.2.1) Microscopy

Plate 3.3 overleaf shows the surface of a preliminary CME. The film coverage was uneven and the platinum surface was clearly visible. The polymer was observed to be composed of red-brown clusters deposited on the electrode. As the electropolymerization technique was modified, the appearance of the CME's improved. Plate 3.4 shows the surface of a further developed CME and a more even coating of polymer is observed. The most recent electrodes showed no visible clusters at all at this magnification, merely a colouration of the platinum surface.

(3.2.2) Scanning Electron Microscopy

To place the polymer in the microscope, the coated electrode surface was pressed against an adhesive carbon disk mounted on a steel stub and the resulting structure sputtered with gold. Thus the image produced (Plate 3.5, page 151) was of the polymer surface at the electrode-polymer interface.

It can be seen that the polymer is a network of microspheres with large pores within this structure. Without sputtering, the polymer was visible, indicating the conducting nature of the material. However, the use of gold created a clearer image. Similar results were obtained for poly-[Ru(ppbpy)₃]²⁺, again showing a conducting polymeric network with many pores (Plate 3.6, page 152).

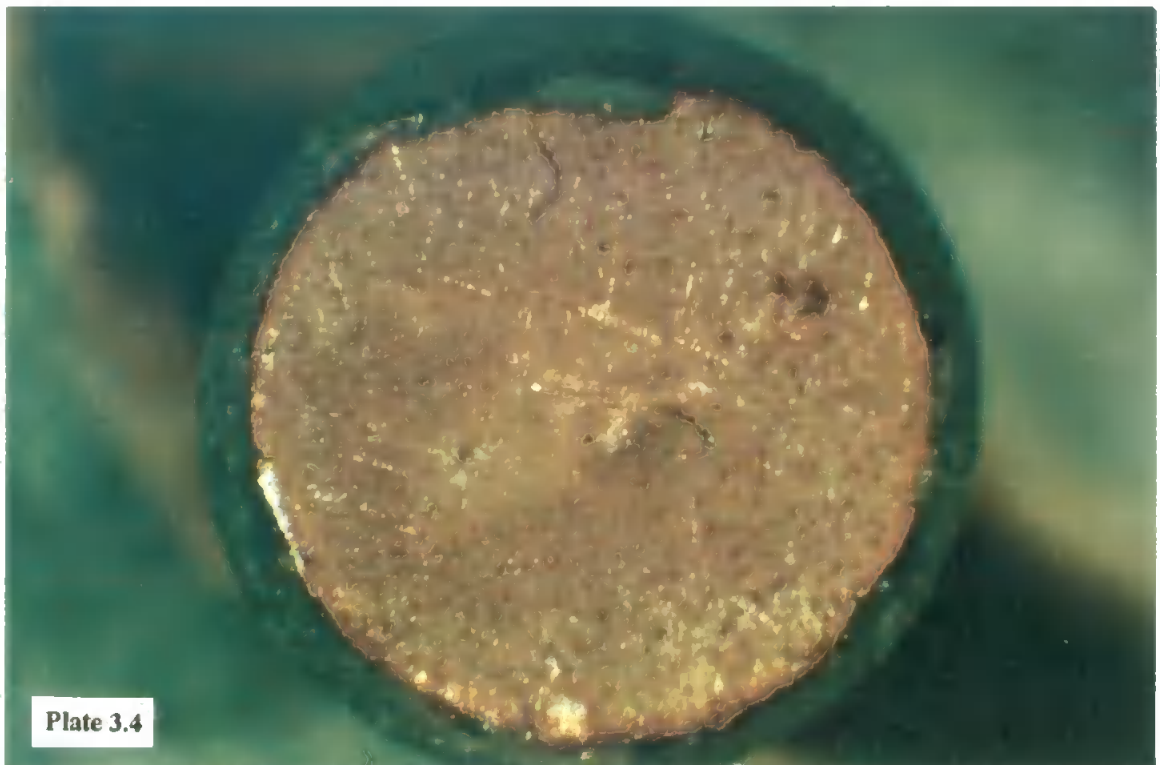
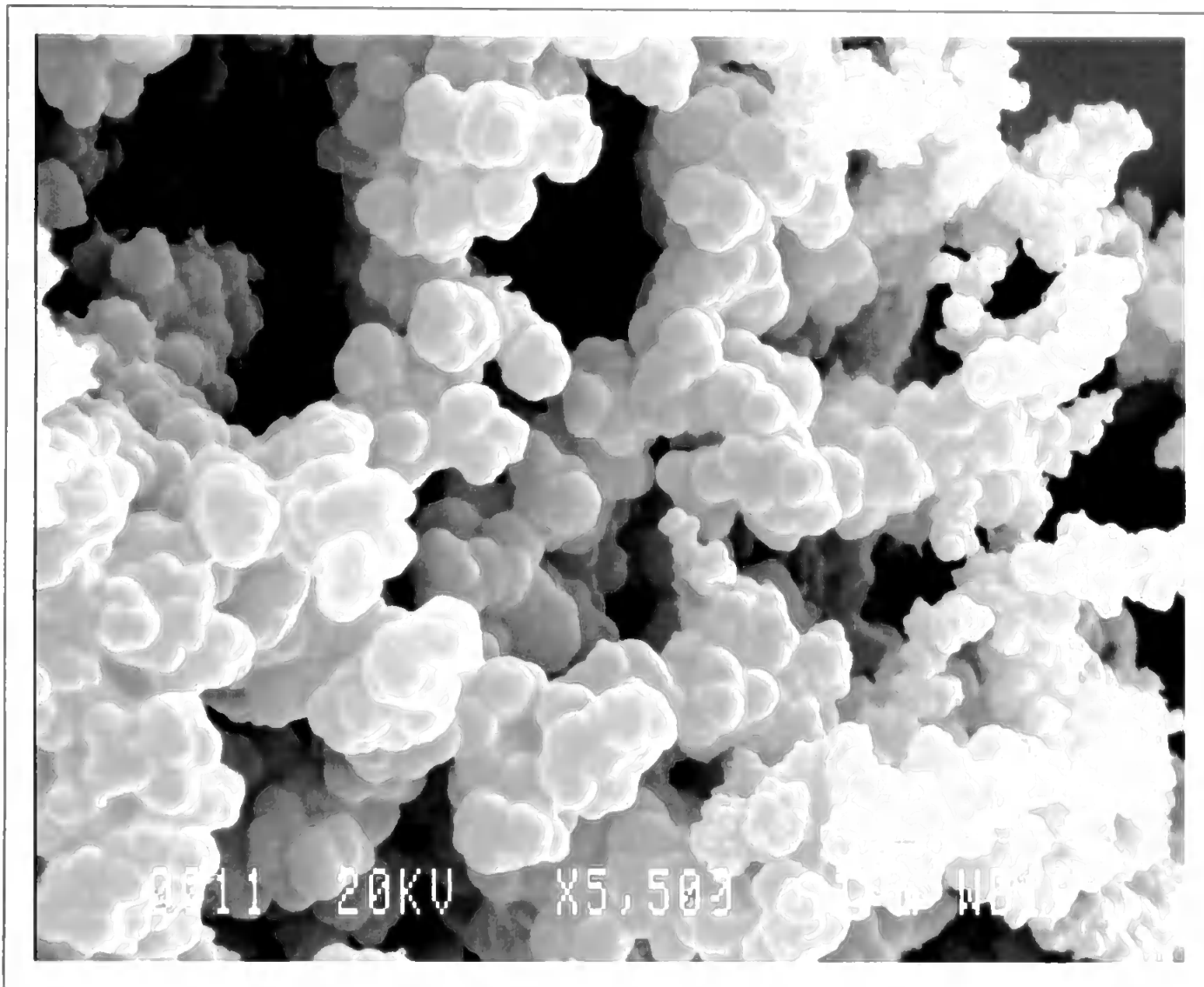


Plate 3.3: Microscope image of a preliminary CME
Plate 3.4: Microscope image of a more developed CME



**Plate 3.5: Scanning Electron Microscope Image of
poly-[ruthenium tris(4-methyl-4'-vinyl-
2,2'-bipyridine) bis(hexafluorophosphate)]**

**x 5500 magnification, accelerating voltage of
the electron beam, 20 kV**

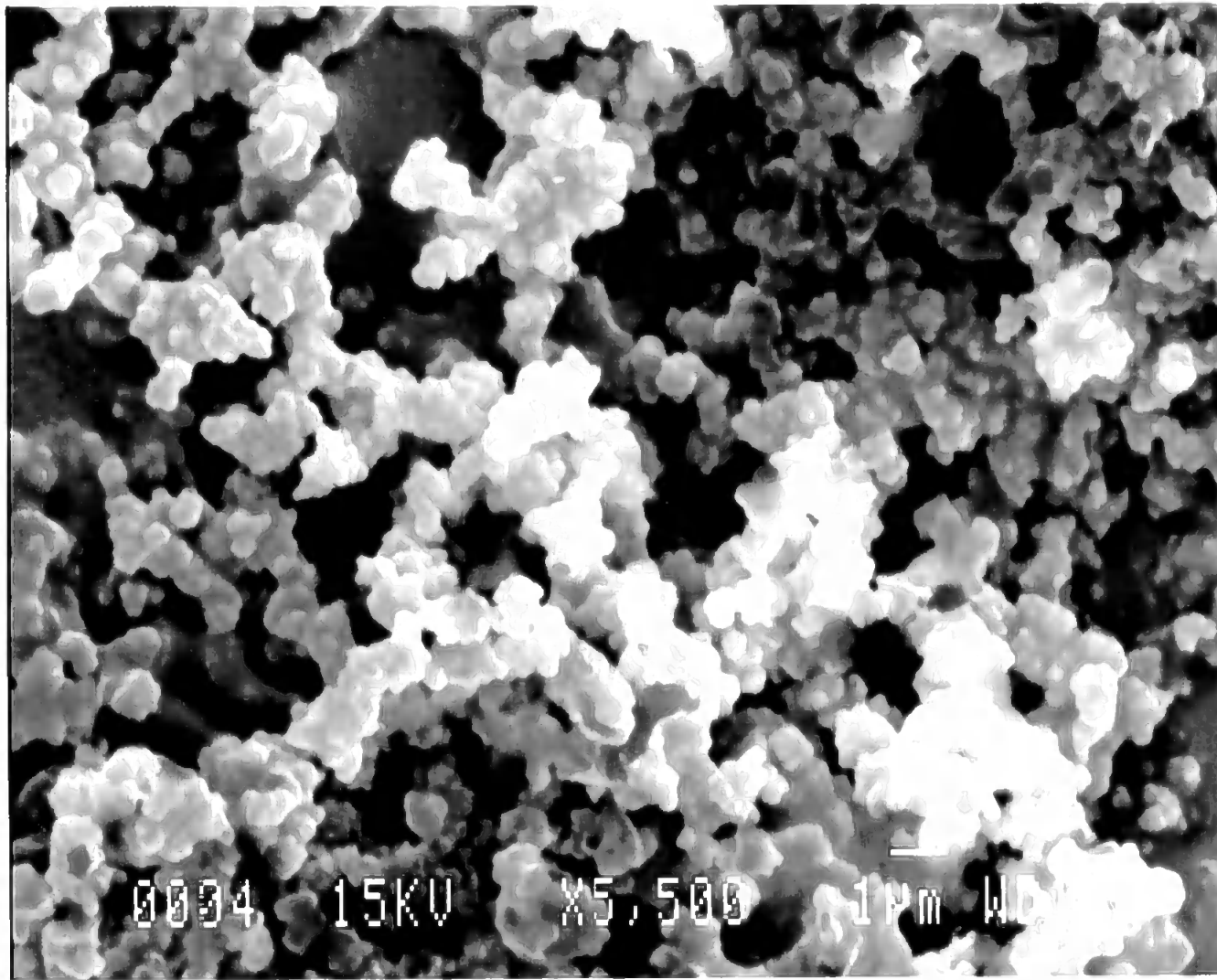


Plate 3.6: Scanning Electron Microscope image of poly-[ruthenium tris(4-methyl-4'-(*E*-prop-2-enyl)-2,2'-bipyridine) bis(hexafluorophosphate)]

x 5500 magnification, accelerating voltage of the electron beam, 15 kV

(3.3) ELECTROCHEMICAL PROPERTIES & ANALYTICAL APPLICATIONS OF RUTHENIUM TRIS(2,2'-BIPYRIDINE) SOLUTION ($\text{Ru}(\text{bpy})_3^{2+}$)

(3.3.1) Investigation of Chemiluminescence Emission from 0 mM, 0.1 mM and 0.1 M Oxalate Solutions

Introduction

The $\text{Ru}(\text{bpy})_3^{2+}$ solution/oxalate redox system has been well-documented in the literature^{38,42,45,46,80}. Research presented in this study used this system as a model to optimize various experimental parameters. These were later employed to investigate the electrochemical properties of the CME's produced via the electropolymerization technique described in section 3.1.4 (page 142).

Experimental Procedure

Figure 3.7 overleaf shows the complete instrumental arrangement. A conventional three-electrode arrangement was attached to a potentiostat. The cell was enclosed in a light-tight box to exclude any stray light. CL was detected using a photomultiplier tube (PMT), which was powered by 0.7 kV from a high voltage power supply (HVPS). The CME was placed as close to the bottom of the beaker as possible but ensuring that there was sufficient room for the analyte solution to pass beneath the electrode. The PMT was situated directly underneath the CME to maximise detection of any CL produced.

The output from the PMT was recorded in millivolts on the Y-axis of a chart recorder which could function as either an X-Y or Y-t recorder. Since the intensity of light is directly proportional to the rate of electron transfer, these plots are essentially CV's and can be interpreted as such.

0.1 mM and 0.1 M oxalate solutions in 0.1 M acetate buffer containing 1 mM $\text{Ru}(\text{bpy})_3^{2+}$ were made up and the pH adjusted to 6.0, in agreement with the literature⁴². 1 mM $\text{Ru}(\text{bpy})_3^{2+}$ in 0.1 M acetate buffer was used as the blank.

Each of the three solutions was scanned between the potential limits of -1.0 to +2.5 V at scan rates of 5, 25 and 100 mV/s. Between each analysis, the solutions were stirred and left for a five minute period.

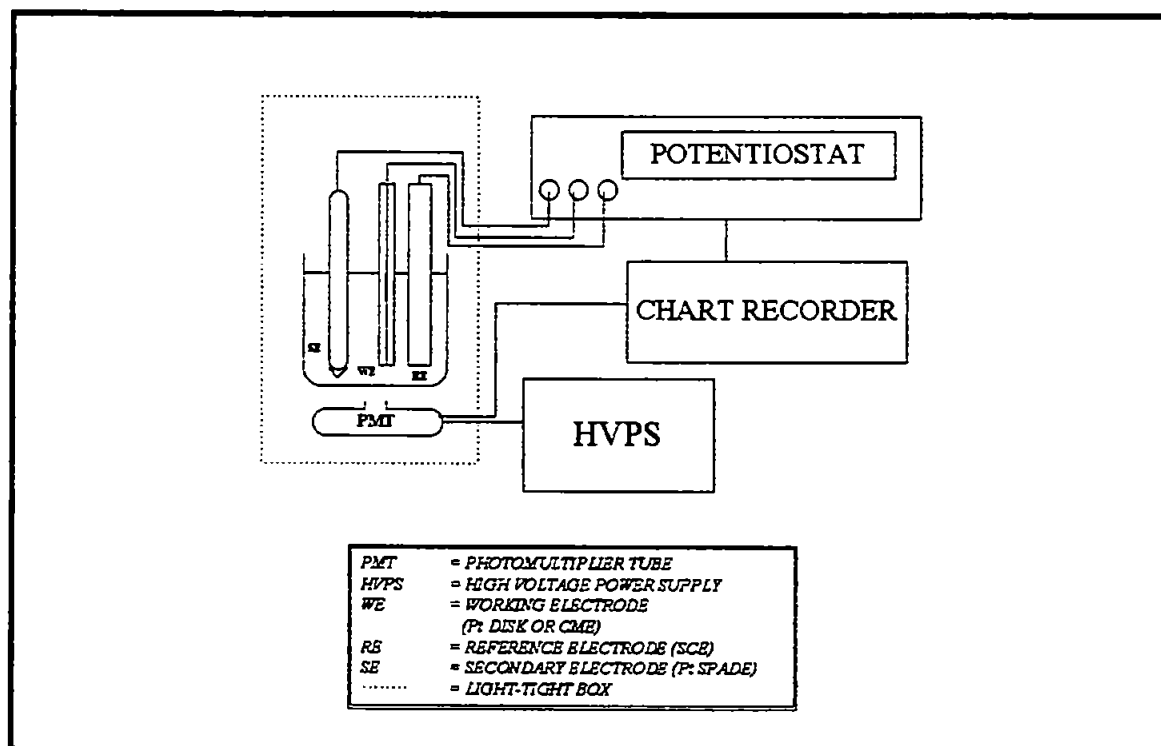


Figure 3.7: Experimental arrangement for chemiluminescence detection

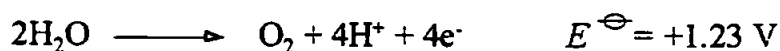
Results & Discussion

Figure 3.8 (page 156) shows the CL response of the solution containing no oxalate. As the anodic scan rate was increased, the small peaks at approximately +1, +2 and +2.5 V also increased in intensity. These peaks were attributed to electrochemistry of contaminants within the blank acetate solution.

A definite response was observed for the 0.1 mM oxalate solution. Figure 3.9 (page 157), shows the results of increasing the scan rate using this solution. Some electrochemistry was observed at the more negative potentials, but one main signal occurred at +1.2 V for all three traces.

The use of 0.1 M oxalate solution resulted in a larger main signal when scanning anodically, as shown in Figure 3.10 (page 158). The signal increased in intensity with increasing scan rate as before. The higher oxalate concentration also resulted in the appearance of another signal which occurred upon scanning cathodically - this had not been apparent with the 0.1 mM oxalate concentration (Figure 3.9, page 157). This signal decreased with increasing scan rate and this may be explained as follows. At a low scan rate, more time is spent at positive potentials, thus more electrochemical products are created. Therefore, on the reverse (cathodic) scan, more reduction of the products is possible. Upon scanning more quickly, not much time is spent at these higher potentials and thus a smaller amount of product forms. The peak is therefore smaller when scanning cathodically.

The formation of bubbles was observed at the electrode surface at the more positive potentials. This was attributed to the splitting of water releasing oxygen as follows;



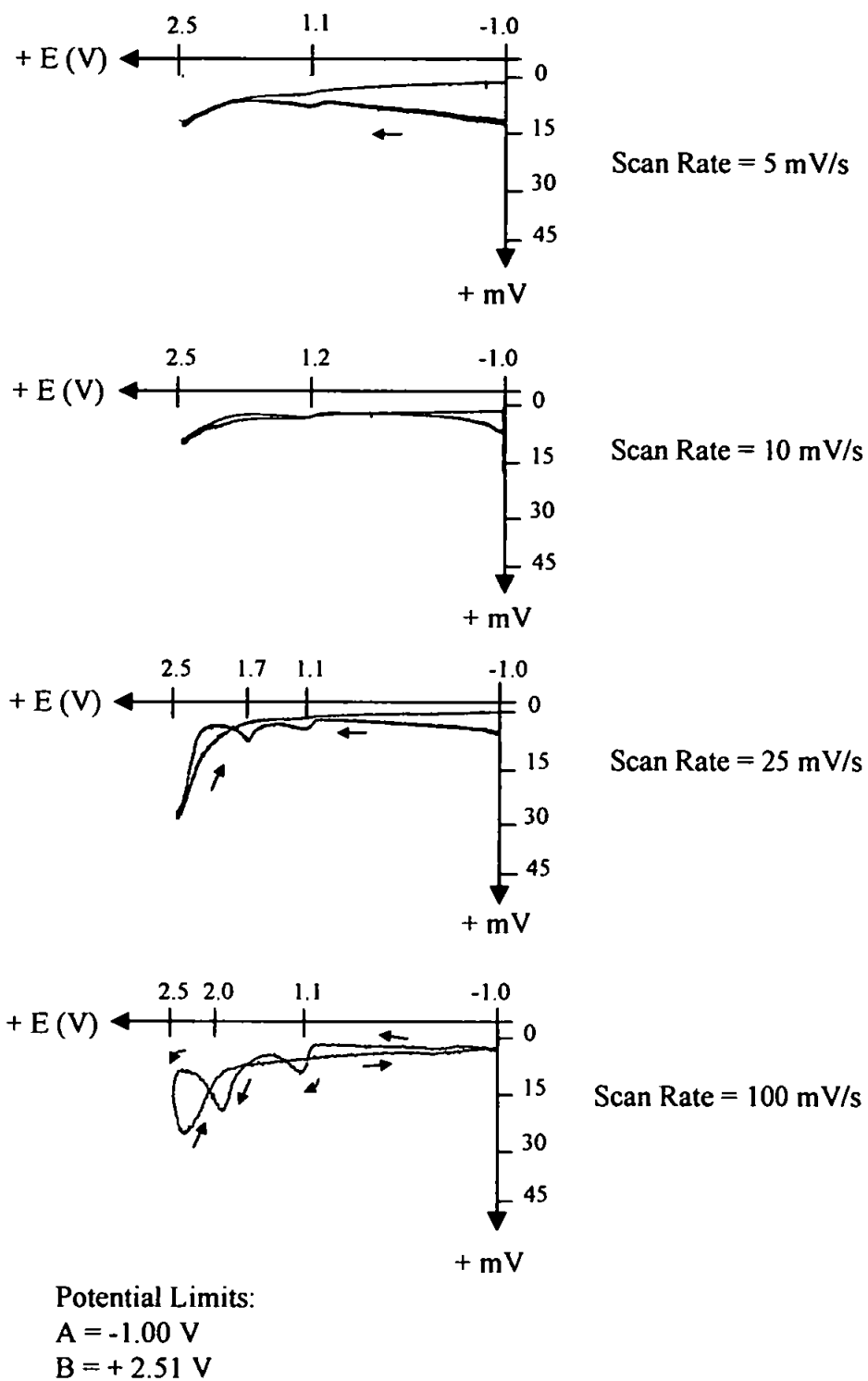
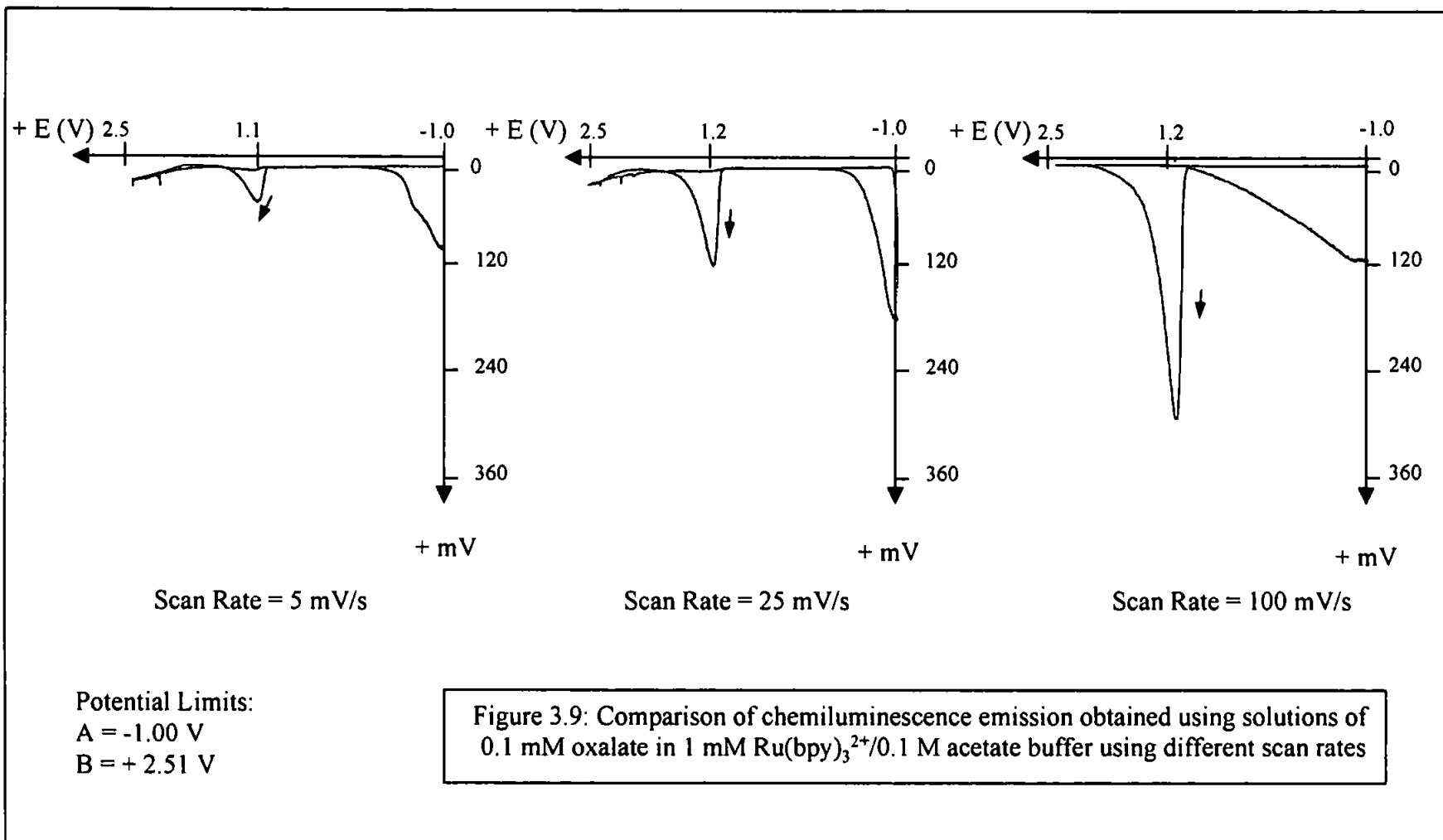
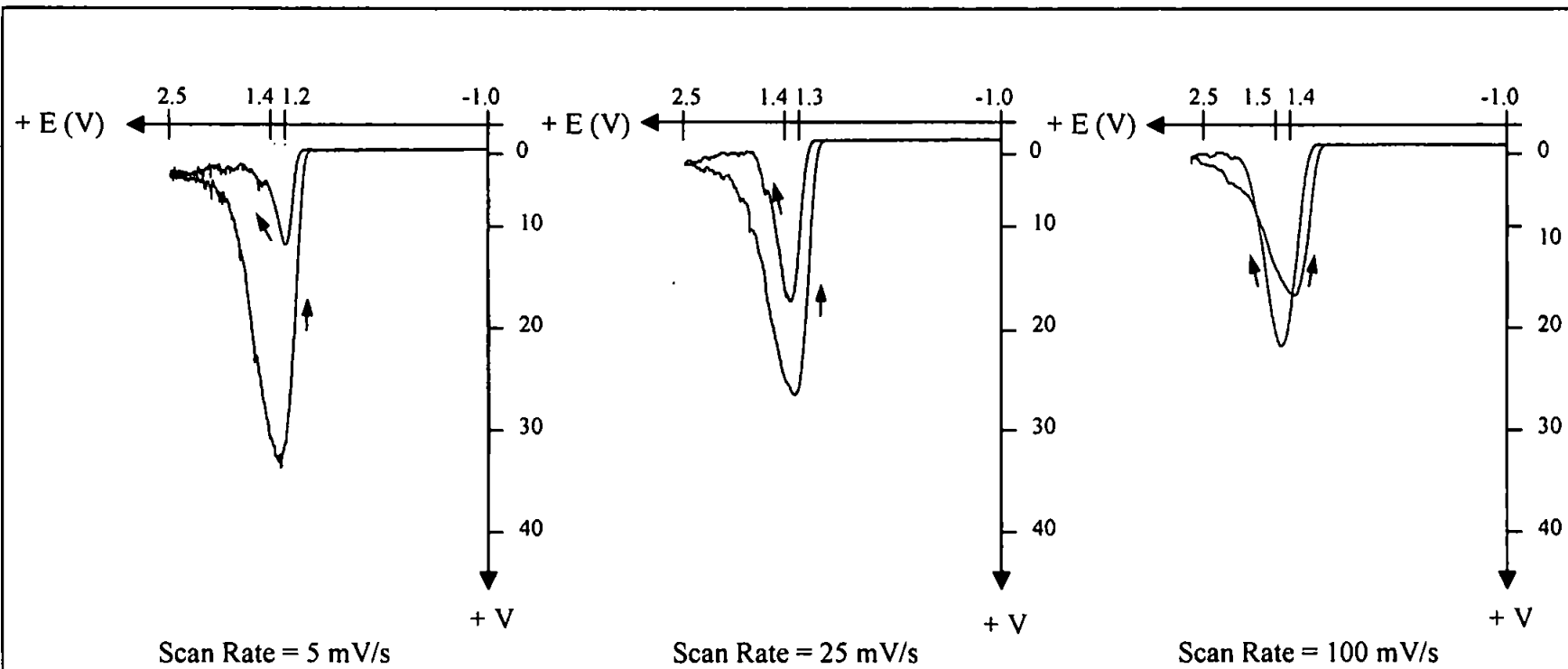


Figure 3.8: Comparison of chemiluminescence emission obtained using solutions of 1 mM Ru(bpy)₃²⁺ in 0.1 M acetate buffer using different scan rates. [0 M oxalate]





Potential Limits:
 A = -1.00 V
 B = +2.51 V

Figure 3.10: Comparison of chemiluminescence emission obtained using solutions of 0.1 M oxalate in 1 mM Ru(bpy)₃²⁺/0.1 M acetate buffer using different scan rates

(3.3.2) Investigation of Chemiluminescence Emission For 0 mM, 0.1 mM and 0.1 M Oxalate Solutions Using a Reduced Potential Range

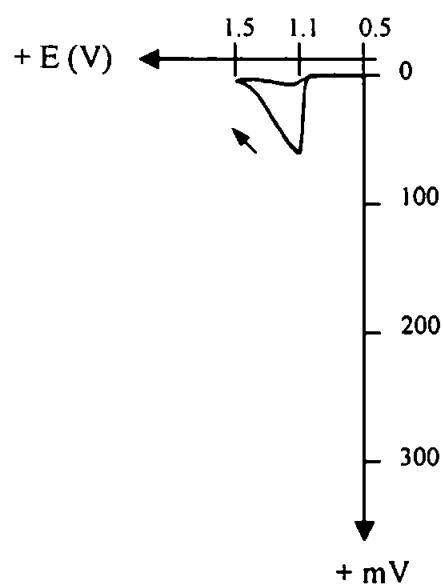
Experimental Procedure

The above experiments were repeated with the same three solutions used in section 3.3.1 (page 153), but using a narrower potential window, from +0.5 to +1.5 V. This potential range was considered to be more suitable for this redox system as the main signal due to the CL emission from the oxalate was within this range and other signals were excluded.

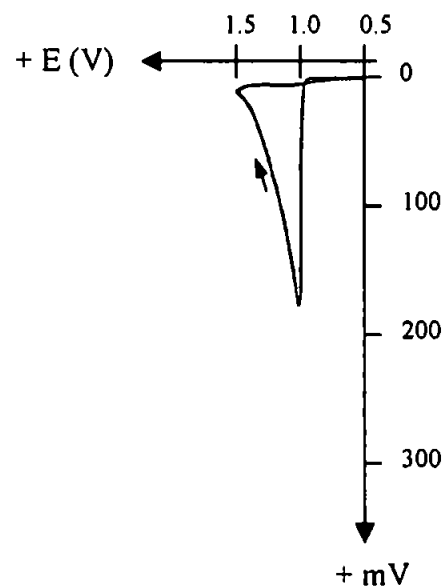
Results & Discussion

In the blank solution, negligible ECL was observed. Figure 3.11 overleaf shows the signals obtained using 0.1 mM oxalate. Although the signal at a scan rate of 100 mV/s was off-scale, this was the optimum scale for comparison of peak height and it can be seen that the signals increased in intensity with increasing scan rate. This was also the case when using a 0.1 M solution of oxalate, shown in figure 3.12 (page 161). In this case, the signal observed when scanning cathodically was less intense than when scanning anodically, a reversal of the results obtained previously using a wider potential range (Figure 3.10, page 158). This could be explained by the earlier discussion in section 3.3.1 (page 155). The system did not reach such positive potentials as before because of the smaller potential range. Therefore the amount of electrochemical products and hence the signal upon scanning cathodically were reduced.

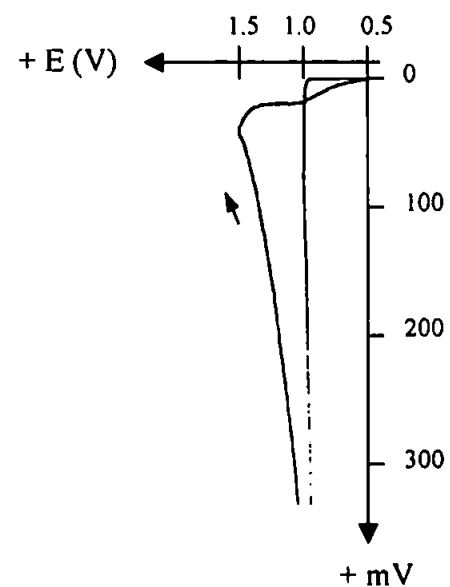
From the results presented above, a faster scan rate increased the intensity of the signal due to the oxalate. The final parameters for the optimum CL signal were potential limits of +0.5 and +1.5 V and a scan rate of 0.1 V/s. Higher scan rates were beyond the capabilities of the instrumentation used.



Scan Rate = 5 mV/s



Scan Rate = 25 mV/s



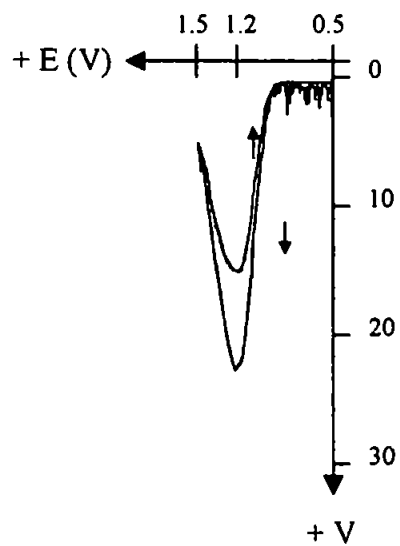
Scan Rate = 100 mV/s

Potential Limits:

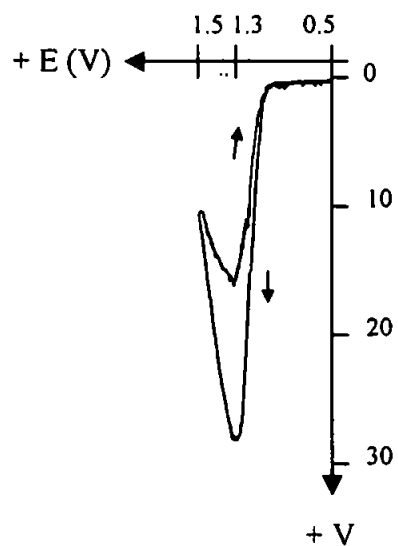
A = + 0.50 V

B = + 1.50 V

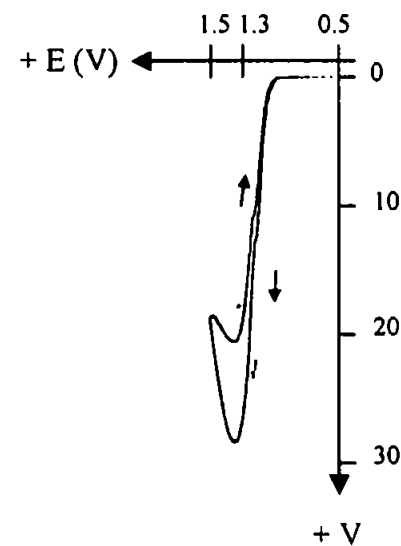
Figure 3.11: Comparison of chemiluminescence emission obtained using solutions of 0.1 mM oxalate in 1 mM $\text{Ru}(\text{bpy})_3^{2+}$ /0.1 M acetate buffer using different scan rates and a reduced potential range



Scan Rate = 5 mV/s



Scan Rate = 25 mV/s



Scan Rate = 100 mV/s

Potential Limits:
 A = + 0.50 V
 B = + 1.50 V

Figure 3.12: Comparison of chemiluminescence emission obtained using solutions of 0.1 M oxalate in 1 mM Ru(bpy)₃²⁺/0.1 M acetate buffer using different scan rates and a reduced potential range

(3.4) ELECTROCHEMICAL PROPERTIES & ANALYTICAL APPLICATIONS OF CHEMICALLY MODIFIED ELECTRODES

(3.4.1) Electrochemiluminescence of poly-[Ru(vbpy)₃²⁺]

One of the most important characteristics of the CME based on poly-[Ru(vbpy)₃²⁺] is its ability to emit electrochemiluminescence (ECL), as reported by Abruña & Bard¹¹². In the present study, this was utilised for the detection of various analytes. The optimum parameters, previously established by using the Ru(bpy)₃²⁺/oxalate system as a model, were used to investigate and optimize the electrochemical properties of the CME. The CME was then tested using a wider range of analytes, including amines.

(3.4.2) Effect of Film Quality upon Electrochemical Properties

Section 3.1 (page 133), described the development of the electropolymerization method which led to a gradual but significant improvement in the quality of the CME's produced. This section reports the use of these CME's for analysis. As the nature of the polymer film changed throughout the study, results involving different films could not be directly compared. In addition, some experiments have been carried out using only one set of results as investigation of reproducibility was limited by the time required to produce a CME. However, the results presented give an indication of the capabilities of the electrodes.

(3.4.3) Investigation and Optimization of the Electrochemical Properties of CME's Using the Oxalate Redox System

Introduction

The optimum parameters used for the $\text{Ru}(\text{bpy})_3^{2+}/\text{oxalate}$ system were applied to this system, in which the $\text{Ru}(\text{bpy})_3^{2+}$ complex in solution was replaced by a CME. Splitting of water was shown to occur at higher potentials and it was necessary to avoid this particularly in this experiment for two reasons. Firstly, the signals could interfere with those due to the reaction of the oxalate producing CL and secondly, bubbles of oxygen produced within the pores of the polymer could damage the delicate film.

Experimental Procedure

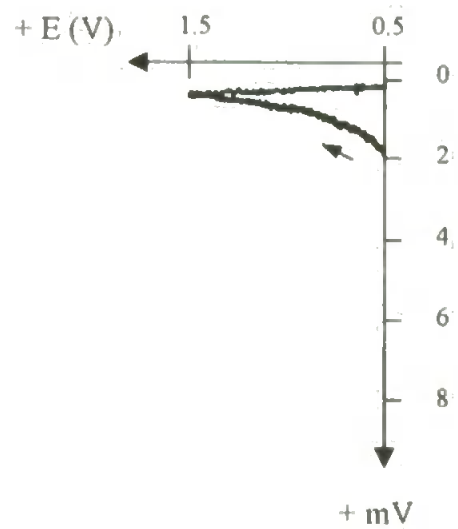
0.1 mM and 0.1 M oxalate solutions were made up in 0.1 M acetate buffer at pH 6.0. A bare platinum electrode was placed in oxalate solution and scanned between the potential limits of +0.5 V to +1.5 V, to check for the absence of any electrochemical response. This platinum disk was then replaced by a CME and the blank solution and two oxalate solutions were scanned at rates of 5, 25 and 100 mV/s between the selected potential limits. The solutions were stirred and left for a 15 minute period before the next analysis. Previously, stirring of the $\text{Ru}(\text{bpy})_3^{2+}/\text{oxalate}$ solution had allowed fresh complex and analyte to form a homogeneous solution. In the case of a porous film, further time was required to allow fresh analyte to diffuse into the film and also to allow reacted products within the structure of the film to diffuse out.

Results & Discussion

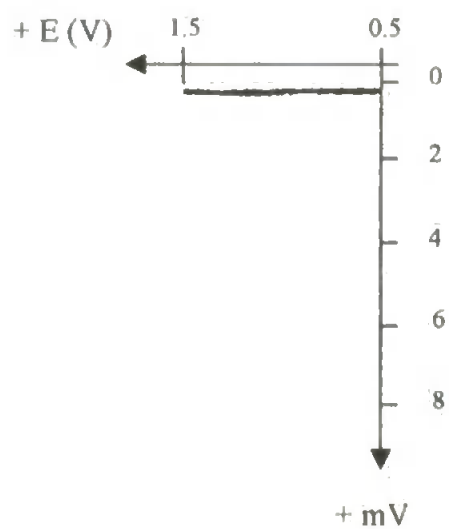
No electrochemical response was observed when the bare platinum electrode was placed in oxalate solution. This proved that no reaction took place and that any signals obtained in the following experiments were due to the ruthenium centres in the polymer film reacting with the oxalate solution.

When using the CME, no signal was observed for the blank solution (Figure 3.13, overleaf). Even when maximum sensitivity was employed, very little response was observed upon analysis of the 0.1 mM solution (Figure 3.14, page 166). However, a definite signal was recorded for the 0.1 M oxalate solution (Figure 3.15, page 167) when scanning anodically. No signal was observed when scanning cathodically.

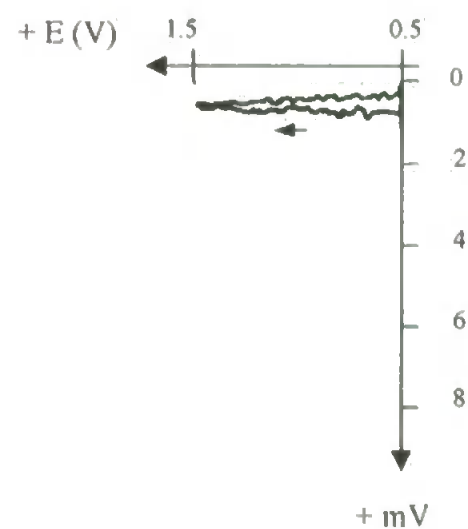
The results showed that the CME was able to detect the presence of oxalate in solution, although at this stage, it was much less sensitive in comparison with using $\text{Ru}(\text{bpy})_3^{2+}$ in solution.



Scan Rate = 5 mV/s



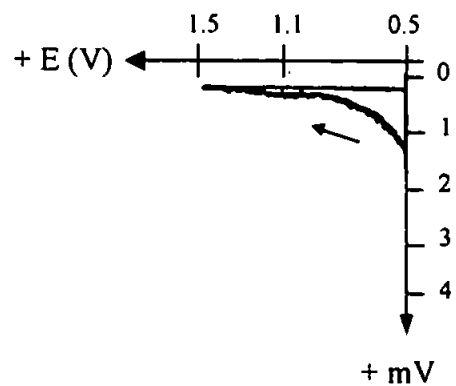
Scan Rate = 25 mV/s



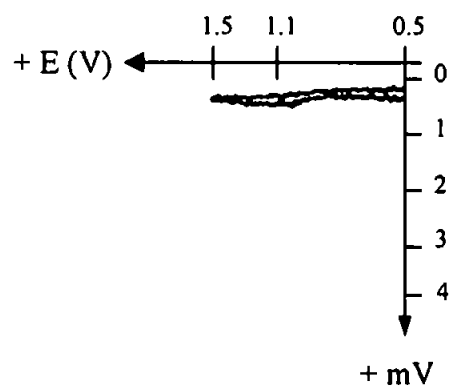
Scan Rate = 100 mV/s

Potential Limits:
 A = + 0.50 V
 B = + 1.50 V

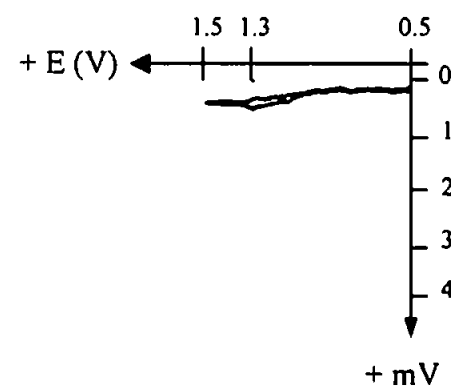
Figure 3.13: Comparison of chemiluminescence emission obtained using a CME in 0.1 M acetate buffer using different scan rates. [0 M oxalate]



Scan Rate = 5 mV/s



Scan Rate = 25 mV/s



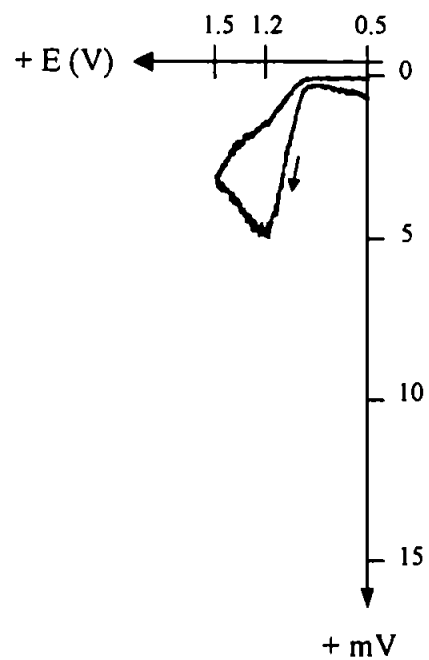
Scan Rate = 100 mV/s

Potential Limits:

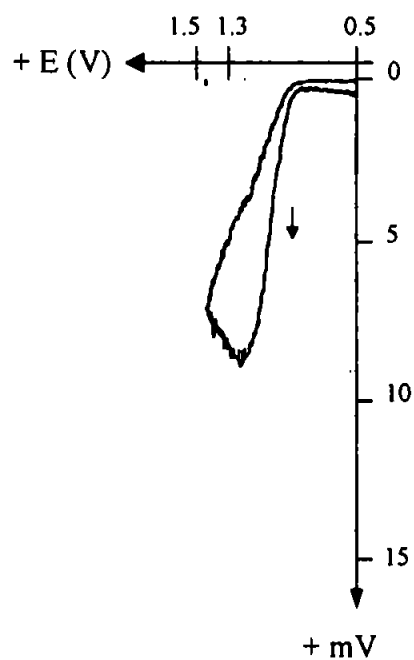
A = + 0.50 V

B = + 1.50 V

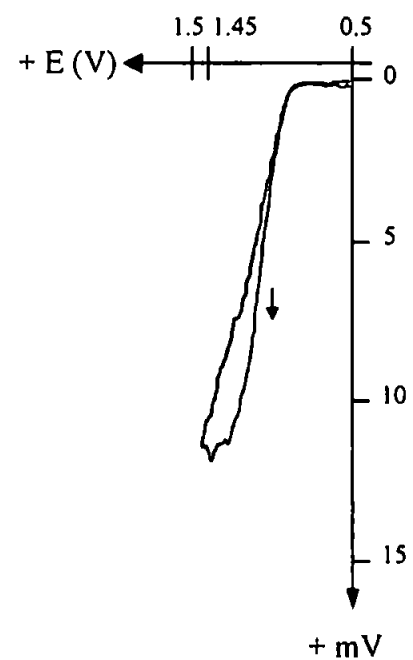
Figure 3.14: Comparison of chemiluminescence emission obtained using a CME in a solution of 0.1 mM oxalate in 0.1 M acetate buffer using different scan rates



Scan Rate = 5 mV/s



Scan Rate = 25 mV/s



Scan Rate = 100 mV/s

Potential Limits:

A = + 0.50 V

B = + 1.50 V

Figure 3.15: Comparison of chemiluminescence emission obtained using a CME in a solution of 0.1 M oxalate in 0.1 M acetate buffer using different scan rates

(3.4.4) Effect of pH on Intensity of Chemiluminescence Emission

Introduction

The aim of this experiment was to observe the change in CL emission over a wide pH range. However, the use of extreme pH values could have a detrimental effect on the film quality and so the reproducibility of the CME was tested by reversing the change in pH.

Experimental Procedure

0.1 M oxalate solution was made up using Milli-Q water and the pH was adjusted using hydrochloric acid or potassium hydroxide solutions. The oxalate solution was scanned at 0.1 V/s from +0.5 V to +1.5 V and the CL emission was recorded at unit increments between pH 3 to 11. The solution was then stirred and left for 5 minutes in between each analysis. The procedure was repeated at each of the pH values using a blank solution.

Results & Discussion

Figure 3.16 overleaf shows the CL emission as the pH was varied so that it became increasingly alkaline and then reversed to become acidic. Negligible emissions were recorded for blank solutions at all pH values. As can be seen, once in oxalate solution, CL was emitted at every pH value from 3 to 11 and demonstrated the stability of the film over this wide pH range. This electrode stability can be contrasted with that of the ruthenium complex in solution. $\text{Ru}(\text{bpy})_3^{3+}$ is very stable in acidic solution but reduction to $\text{Ru}(\text{bpy})_3^{2+}$ is promoted by alkaline conditions, thus reducing its lifetime as an active chemiluminescent reagent¹⁹⁰.

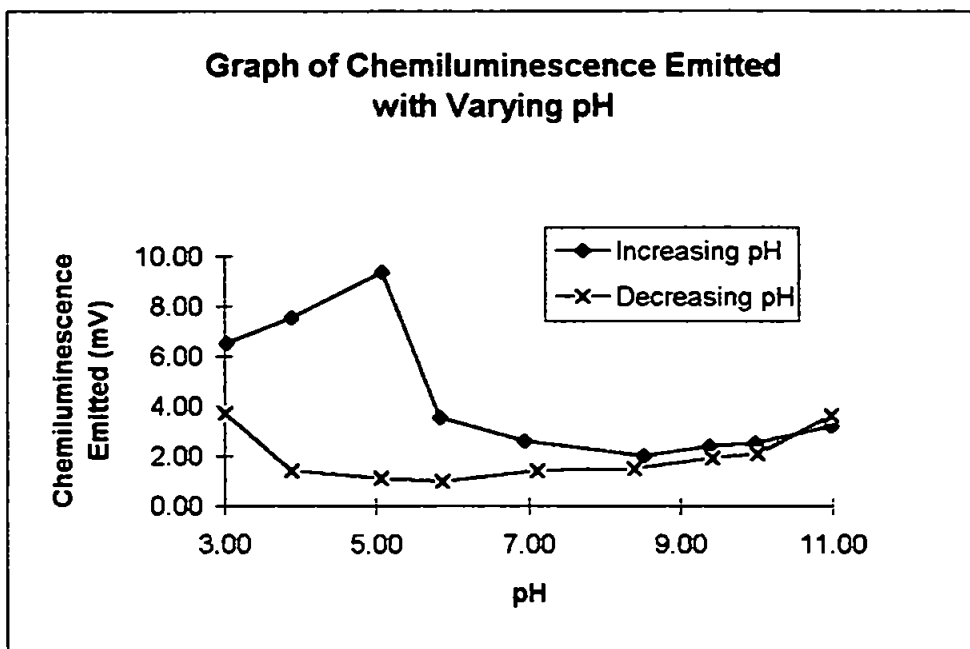


Figure 3.16: Change in chemiluminescence emission with varying pH

For the first data series in this study (increasing pH), the maximum emission occurred at acidic pH values and the optimum was recorded at pH 5. This fell sharply at pH 6 and was constant until a slight increase in emission at very alkaline pH values. Upon using solutions of decreasing pH, the luminescence fell. The optimum observed previously did not occur. This was attributed to the quality of the film diminishing during the experiment, either because the high pH values had had a detrimental effect on the film or because of repeated use of the electrode. A narrower pH range was therefore chosen to discover which of these two theories was correct.

(3.4.4.1) Effect of pH on Intensity of Chemiluminescence Emission Using a Narrow pH Range

Experimental Procedure

The method described in the previous section was repeated using a fresh CME but focused upon a narrower pH range of 4 - 7 at 0.5 pH unit increments. A repeat analysis was performed the following day using the same electrode.

Results & Discussion

The results are shown in Figure 3.17:

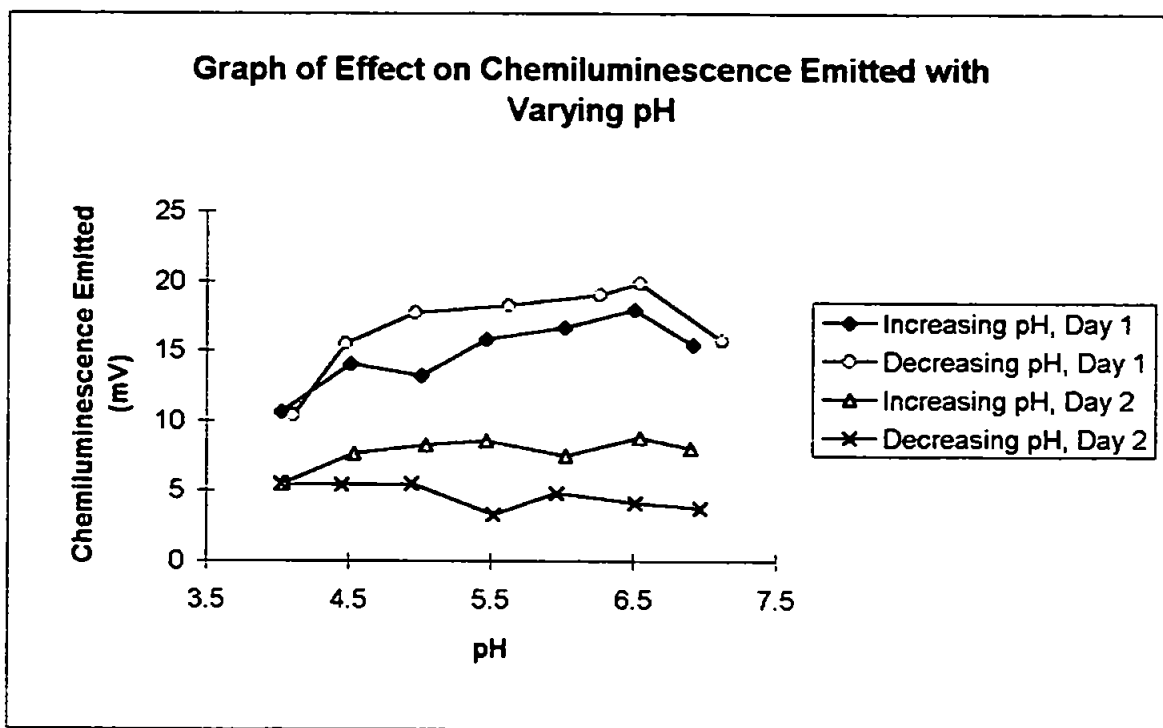


Figure 3.17: Change in chemiluminescence emission with varying pH (narrow range)

Once again, no CL was observed for any of the blank solutions at the corresponding pH values. A reproducible set of results was collected which showed that the CL emission increased with increasing pH to a maximum at pH 6.5.

The signals for the second series of results on day one were slightly higher than for the first series. A reason for this could be that for the first few analyses performed, the oxalate ions had not had chance to diffuse far into the film structure. A period of time could be required for the film to become completely equilibrated with oxalate. Generally, however, for each data series, the emissions became comparatively lower. This is attributed to deterioration of film quality with an increasing number of evaluations. For the fourth series, the emission changed very little throughout the pH range.

Further oxalate studies were performed at the optimum pH of 6.5. This is shifted slightly from the optimum pH of 5.8 observed using ruthenium tris(2,2'-bipyridine) in solution and the oxalate redox system⁴².

(3.4.5) Calibration & Limit of Detection Results

(3.4.5.1) Ru(bpy)₃²⁺ Solution Calibration Data

Introduction

This experiment was performed using Ru(bpy)₃²⁺ in solution to test the capabilities of the instrumentation. Previous results have shown that maximum sensitivity is achieved at high scan rates therefore scanning between the two potentials was performed at 0.1 V/s as before and also at 10 V/s.

Experimental Procedure

The technique of standard additions from the lowest to the highest concentration of oxalate was used. The pH was maintained at 6.5 using solutions of potassium hydroxide and hydrochloric acid. The solution was scanned between the potential limits of +0.5 to +1.5 V. For each change in concentration, three measurements were taken at

scan rates of both 0.1 and 10 V/s. After each measurement, the solution was stirred and left for five minutes. Signals were recorded using a Y-t recorder when using a scan rate of 10 V/s.

Results & Discussion for a Scan Rate of 0.1 V/s

Figure 3.18 overleaf shows the calibration graph obtained. As CL emission was observed over a large concentration range, a log-log graph enabled all values to be seen clearly. This method of showing results was justified as the literature⁴² has shown that the CL emission from the reaction of oxalate with $\text{Ru}(\text{bpy})_3^{2+}$ is directly proportional to concentration. The mean of the three values for each oxalate standard was plotted. A concentration of 0 M oxalate could not be plotted on a log-log graph and therefore the response was subtracted from each value. The error bars were calculated as the log of two times the standard deviation of the three values for each standard. A linear relationship was observed for the concentration range 1×10^{-6} to 2.5×10^{-1} M. This indicated that the CL emission was directly proportional to oxalate concentration. The limit of detection was 10^{-6} M; CL emission for oxalate concentrations below this value did not follow the linear trend.

Results & Discussion for a Scan Rate of 10 V/s

Once again, a linear relationship was observed, this time for the concentration range 1×10^{-7} to 2.5×10^{-1} M oxalate (Figure 3.19, overleaf). Calculation of peak height was easier using this method as a definite sharp peak was observed in comparison with the broader peak obtained when scanning between two potentials. This results in a slightly lower margin of error. The limit of detection for this method was 10^{-7} M.

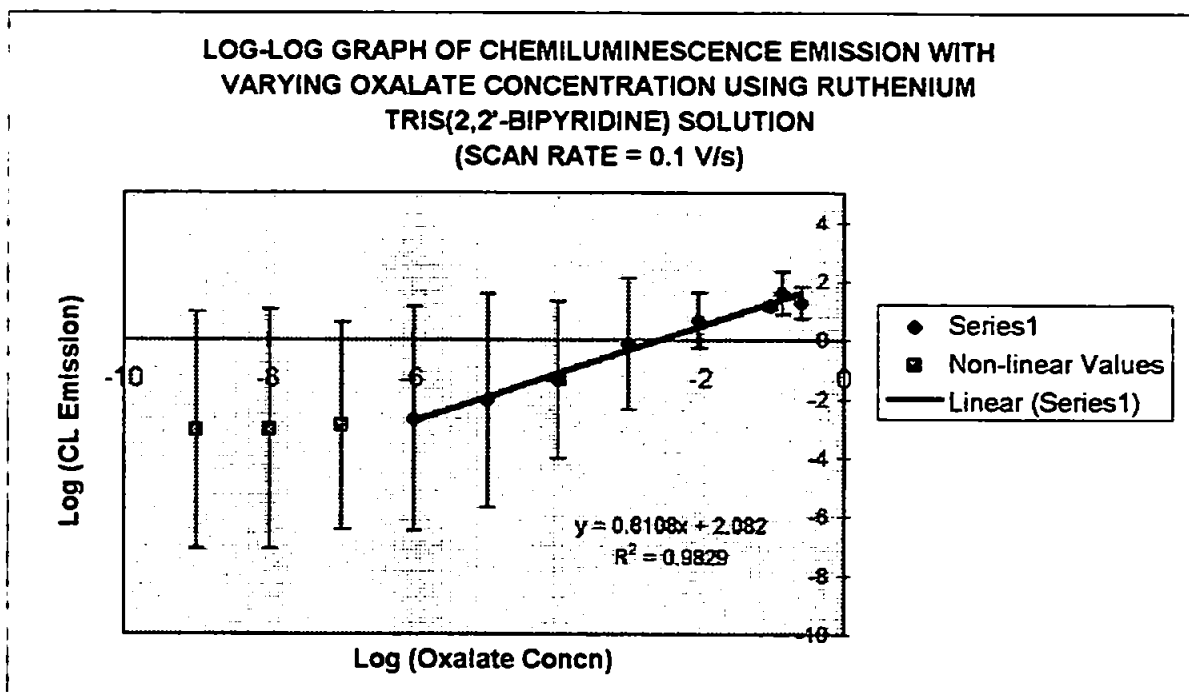


Figure 3.18: Calibration graph for Ru(bpy)₃²⁺/oxalate system, scan measurements performed at 0.1 V/s

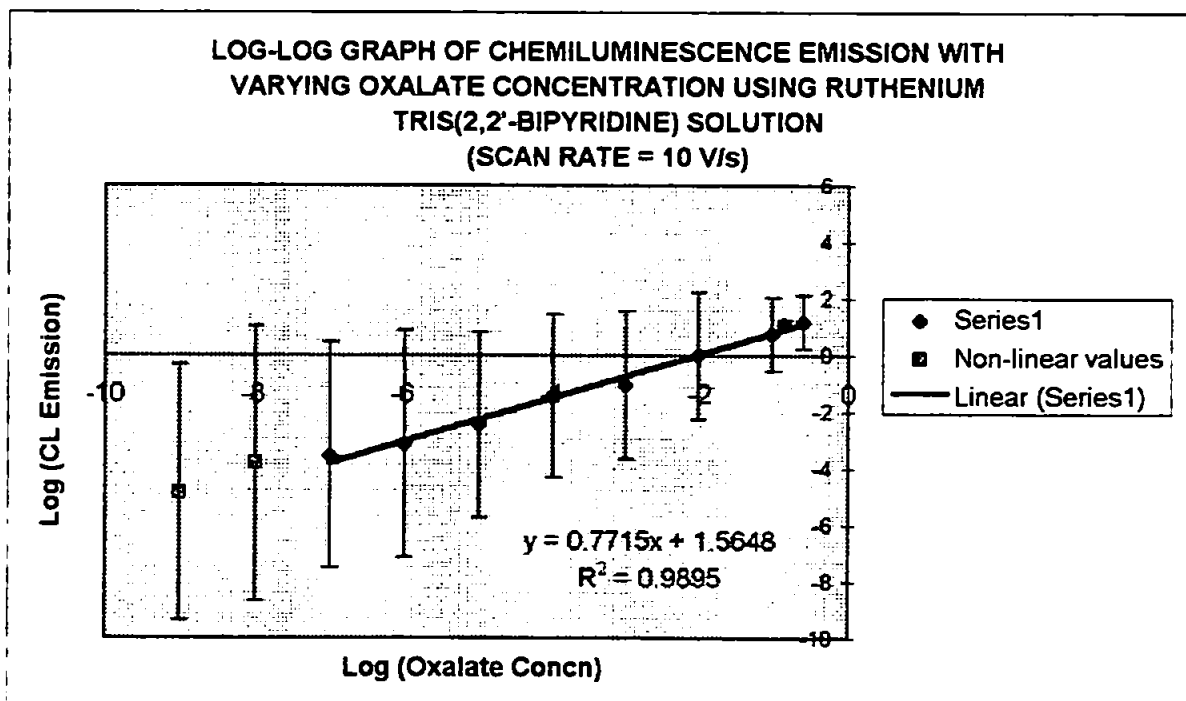


Figure 3.19: Calibration graph for Ru(bpy)₃²⁺/oxalate system, scan measurements performed at 10 V/s

(3.4.5.2) CME Calibration Data

Within the polymer films is a high density of electroactive sites which have the potential to emit CL, whereas only a small amount of available complex in solution is in contact with the working electrode and is converted to the +3 reactive state. For this reason, it was hoped that the sensitivity of the CME's produced in this study would be greater in comparison to the $\text{Ru}(\text{bpy})_3^{2+}$ complex in solution.

Over the course of improving the technique of electropolymerization, the films produced varied in quality in terms of thickness, appearance and adsorption to the electrode. Preliminary CME's produced had thick films which deteriorated quickly after a few analyses. More developed CME's tended to be thinner but more adherent. Both types of CME were analysed in the next section and the results compared.

(3.4.5.2.1) Investigation of a Preliminary CME.

Experimental Procedure

A 0.1 M oxalate solution in 0.1 M acetate buffer at pH 6.0 was prepared and volumes of this solution were added using the method of standard addition to 100 ml of the buffer solution. The oxalate concentration ranged from 1×10^{-5} to 1×10^{-2} M. After each measurement, the solution was stirred and left for five minutes. For measurements at 0.1 V/s, the potential limits were -1 to +1.25 V at a scan rate of 0.1 V/s. For measurements at 10 V/s, signals were recorded using a Y-t recorder.

Results & Discussion for a Scan Rate of 0.1 V/s

Figure 3.20 (page 176), shows the calibration graph obtained for the CME. CL emission was only observed over a narrow concentration range so a log-log plot was not required, unlike the $\text{Ru}(\text{bpy})_3^{2+}$ solution calibration data in section 3.4.5.1 (page 173).

This enabled a value for 0 M oxalate to be plotted and it was shown that the range was linear over one order of magnitude. Using the CME, CL emission was observed to be proportional to oxalate concentration, as was the case for the ruthenium tris(2,2'-bipyridine) complex in solution. Values below 1×10^{-3} M were not visible above the background noise. Replicate values were not obtained as the film had visibly deteriorated by the end of the experiment.

The standard addition method was used, using serially diluted standards. This was done for the following reasons. Firstly, the same solution could be used throughout as opposed to having to keep taking the CME out and placing it in a fresh solution. It had been noticed in previous analyses that this tended to cause deterioration of the film. Serial dilution also avoided the possibility of oxalate remaining in the polymer film from the previous analysis and an artificially high reading would be obtained, so-called 'memory effects'.

Results & Discussion for a Scan Rate of 10 V/s

The same experiment was performed using the same electrode and Figure 3.21 overleaf shows the calibration graph obtained.

This graph demonstrates very similar characteristics to Figure 3.20. Despite a much higher scan rate, the measured intensity was similar to that at a scan rate of 0.1 V/s.

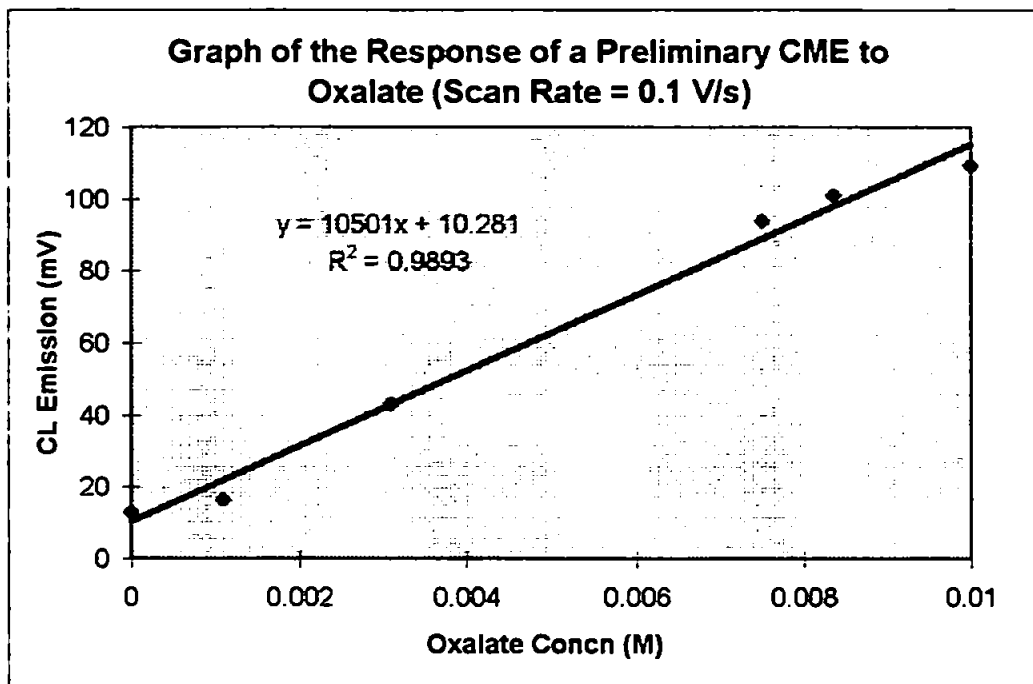


Figure 3.20: Calibration graph for a preliminary CME, scan measurements performed at 0.1 V/s

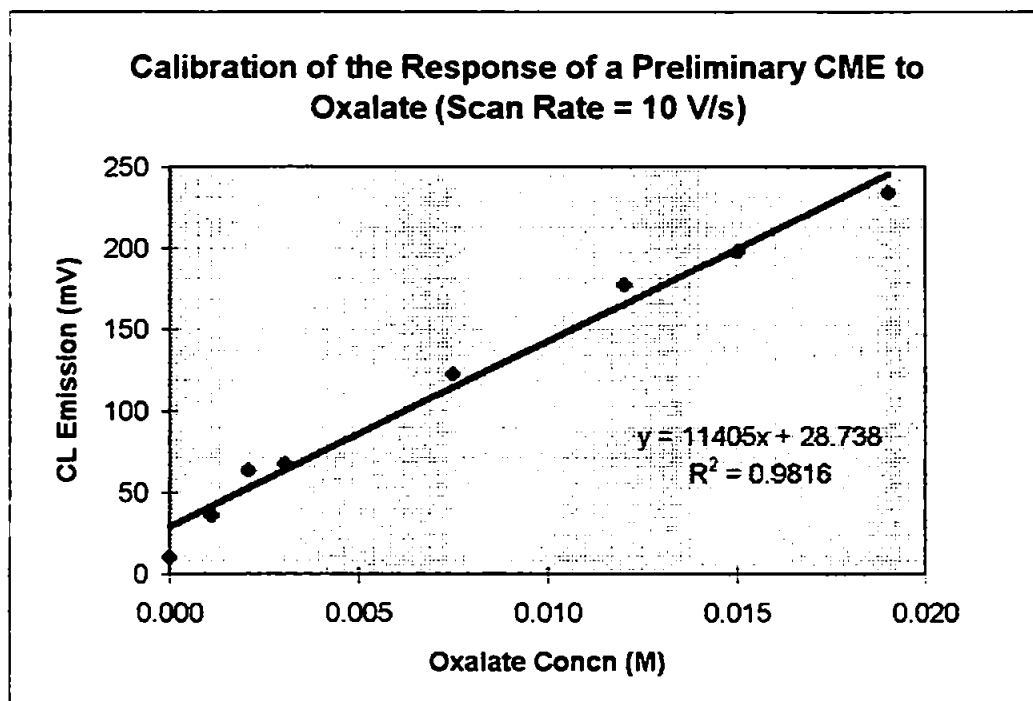


Figure 3.21: Calibration graph for a preliminary CME, scan measurements performed at 10 V/s

(3.4.5.2.2) Investigation of a More Developed CME

Experimental Procedure

The calibration experiment was later repeated over a much larger oxalate concentration range (1×10^{-9} to 0.1 M) with a higher quality film. As before, the technique of standard addition was used but was not suitable for producing high oxalate concentrations, therefore for the two highest concentrations at 0.01 and 0.1 M, separate standards were used. As a result of the optimization procedure since performed in section 3.4.3 (page 163) a narrower potential range from +0.5 to +1.5 V was used and the solution was scanned between these potentials at a scan rate 10 V/s. Between each measurement, the solution was stirred and left for 25 mins. This longer period was chosen as experiments had shown that the film often required time to 'recover' between subsequent analyses. The pH was adjusted to pH 6.5, no buffer was required.

Results & Discussion

No response was observed between concentrations 10^{-9} to 10^{-3} M. Chemiluminescence was only observed when the electrode was placed directly in the 0.01 M and 0.1 M standards. From this and the previous experiments, it was concluded that the CME's exhibited a linear response to oxalate solution but only over a narrow concentration range. However, these results are preliminary investigations and there is scope for improvement.

(3.4.6) Electrode Lifetime Study

Experimental Procedure

This experiment tested the performance over a period of time of a CME with a thin film. The electrode was produced as described in section 3.1.4 (page 142) and electropolymerization took place over one hour. The performance was tested using 0.1 M oxalate solution at pH 6.5. The electrode was scanned at a rate of 10 V/s between the potential limits of +0.5 and +1.5 V and the emission recorded. The solution was then stirred and left for 30 minutes to ensure diffusion of fresh solution to the electrode and diffusion of reacted oxalate away from it. The procedure was then repeated. This was continued for a twelve hour period and the electrode was then stored in acetonitrile overnight. The process was repeated the next day. The following night, the electrode was stored in a solution of the analyte to see the effect upon the initial readings on the third day.

The electrode was stored in acetonitrile for one week and the performance investigated once again. The electrode was then stored in 0.1 M oxalate for another week and re-investigated. The performance of the electrode was investigated at varying intervals over a period of 24 weeks (six months).

Results & Discussion

Figure 3.22 overleaf shows a plot of the results obtained for days 1, 2, 3, 8, 9 and 168 (24 weeks).

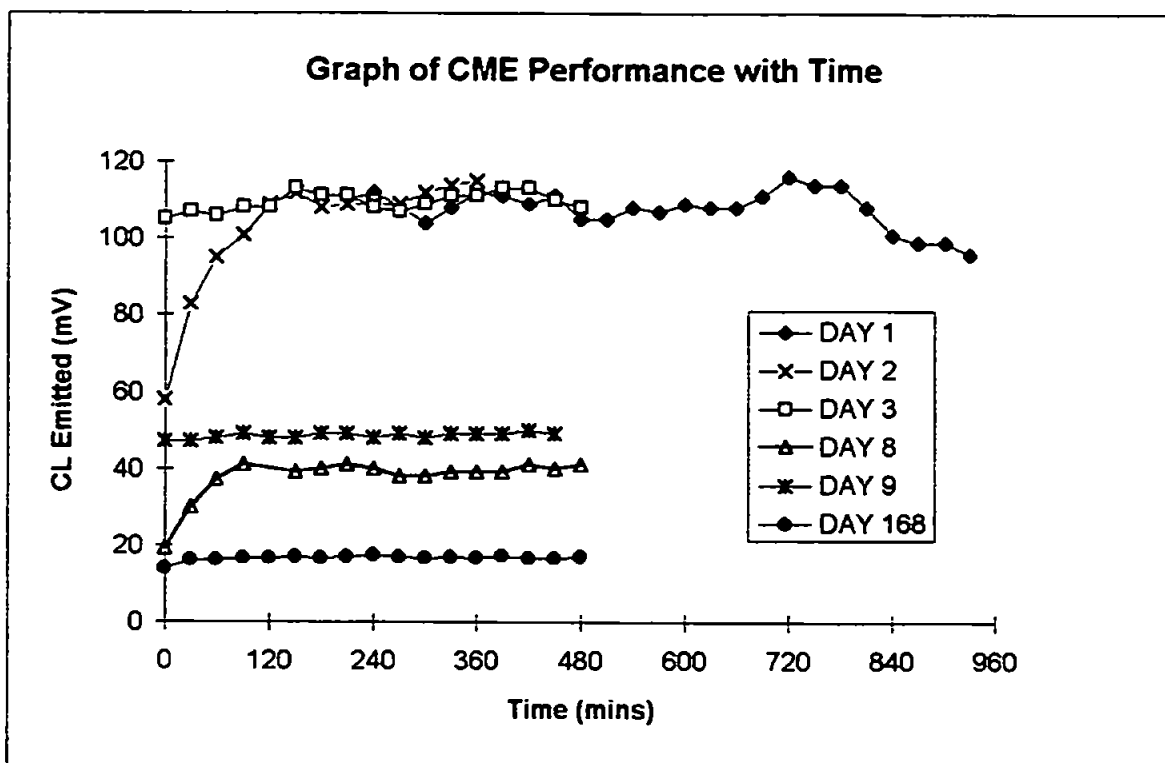


Figure 3.22: Graph of electrode performance over a period of time

The electrode was analysed in the presence of 0.1 M oxalate every half an hour for a twelve hour period on the first day. A stable response was obtained from the electrode with a slight decrease towards the end of the period. No values were recorded during the first 240 minutes as the lack of electrode response to a blank solution was confirmed.

The response for the second day was lower initially but increased and equalled the levels obtained from the first day. The electrode had been stored in acetonitrile solution overnight and the first few low responses were attributed to the time necessary for oxalate to diffuse into the film. The results for day three supported this hypothesis. This time, the electrode had been stored in 0.1 M oxalate solution overnight and therefore this initial 'normalizing period' was not observed. The same pattern was noticeable from the results for day 8, when the electrode had been stored in acetonitrile and day 9, when it was stored in 0.1 M oxalate. As a result of this observation, the electrode was stored in the

latter solution for the rest of the study. A stable response was obtained throughout for each set of results, even after a six month period.

Figure 3.23 below shows the average response for each day the electrode was analysed. The average response for the first three days was steady but there was a rapid fall after the first week to almost half the initial response. The response increased slightly for week 9, but from then on, there was a gradual decrease in the signal.

This decrease was attributed to the depletion of the ruthenium redox centres within the polymer film. The presence of these centres is necessary for the reaction of the film with the analyte of interest to produce CL. As the film was not chemically bound to the platinum surface, it is possible that the whole polymer was slowly desorbing from the electrode.

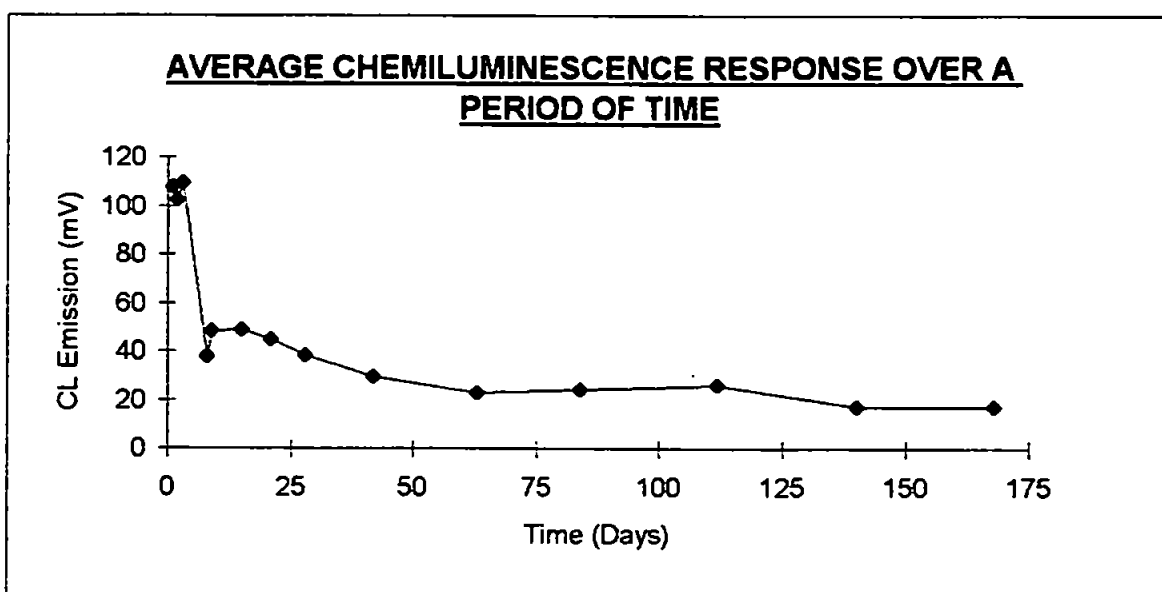


Figure 3.23: Average chemiluminescence response over a period of days

In addition, although ruthenium is co-ordinated to the bipyridine ligands within the polymeric structure, oxalate is also a bidentate ligand. Therefore, the oxalate itself could have been leaching ruthenium from the film. More importantly, although it was

discovered that storage of the electrode in oxalate solution facilitated the stability of the initial electrode responses after a period of not being used, this would probably exacerbate the leaching problem. Despite this, the electrode was still capable of detecting oxalate after a six month period, although the efficiency of the electrode had fallen greatly. The results presented here contradict Lee who claimed that the analytical performance of a poly-[Ru(vbpy)₃²⁺]-modified electrode was limited³⁵. The reason given was that the ECL intensity gradually decreased due to some decomposition of the polymer film. This was found to occur in this study but nevertheless, the electrode was able to be regenerated over 200 times. The aim of this study, to produce an electrochemically regenerable chemically modified electrode for CL analysis, had therefore been achieved.

(3.4.7) Detection of a Range of Analytes

(3.4.7.1) Introduction

Chapter 1 contains a review demonstrating the variety of analytes which can be detected using the ruthenium tris(2,2'-bipyridine) complex in solution and immobilized within a membrane. The aim of this experiment was to investigate the ability of the CME's produced in this study to detect some of these analytes. For each analyte, the literature method was followed as closely as possible, except that use of the Ru(bpy)₃²⁺ solution was replaced by using a CME.

(3.4.7.2) Experimental Procedure

The experimental arrangement described in section 3.3.1 (page 153), for the CL detection of oxalate was employed. A CME was used as the working electrode. Unless

otherwise stated, the scan rate was 0.1 V/s. The potential limits are given in the results section.

Table 3.1 below shows the analyte solutions used in this study.

ANALYTE CONCENTRATION	BUFFER	CORRESPONDING LITERATURE METHOD FOR ANALYTE WITH Ru(bpy) ₃ ²⁺
0.1 M sodium oxalate	-	42
0.1 M & 1 M ascorbic acid	0.2 M NaAc-AcH	67
0.1 M citric acid	-	67
10 mM DL-Tryptophan	1:1 MeOH / H ₂ O	62
0.1 M DL-Valine	0.025 M K ₂ HPO ₄	41
0.1 M ethylamine	10 mM NaAc	40, 52, 191
0.1 M diethylamine	10 mM NaAc	40, 52, 191
0.1 M triethylamine	10 mM NaAc	40, 52, 191
0.1 M propylamine	10 mM NaAc	40, 52, 191

Table 3.1: Parameters used for the detection of the analytes determined in this study.

100 ml solutions of the analytes were made up with Milli-Q water. pH was altered by using dilute solutions of hydrochloric acid and potassium hydroxide. The blank solutions used in each case were 100 ml of buffer or the solvent at the same pH as the analyte solution. Between each analysis, the solution was stirred and then left for 15 mins.

If detection of an analyte resulted in no CL response, the ability of the CME to detect ECL was checked by using the oxalate system, which is known to produce a signal.

(3.4.7.3) Results & Discussion

(3.4.7.3.1) Detection of Ascorbic and Citric Acid

The work in this section was based on the results of Chen & Sato, who reported the determination of ascorbic acid in soft drinks and apple juice⁶⁷. HPLC was employed as the separation technique and the eluted ascorbic acid was mixed with $\text{Ru}(\text{bpy})_3^{2+}$ solution⁶⁷. This solution was then oxidised and the resulting CL detected. The optimum potential range was +1.40 to +2.0 V.

The initial results from the present study using the CME were not encouraging. Therefore, changes were made in an attempt to detect ascorbic acid, as shown in Table 3.2:

ASCORBIC ACID CONCEN (M)	pH OF ANALYTE SOLUTION	POTENTIAL LIMITS (V)	SIGNAL?
0.1	7.8	+0.50 to +1.75	×
0.1	7.8	0 to +1.75	×
1	7.8	0 to +1.75	×
1	7.2	0 to +1.75	×
1	5.0	0 to +1.75	×

Table 3.2: Variation of parameters for detection of ascorbic acid

The potential limits in this study were extended further than that used for the oxalate redox system, but not too far because of the problem of interference from the blank and the decomposition of water. The ascorbic acid concentration was increased and the solution analysed at three different pH values. pH 7.8 was used initially as this was the pH of the reagent solution used in the literature⁶⁷. This was changed to pH 7.2, the pH of the buffer solution alone⁶⁷ and then to pH 5.0. The first redox potential of ascorbic acid at

this latter pH should occur at +0.127 V¹⁶¹. However, no electrochemical response due to ascorbic acid was observed.

Chen & Sato also examined the (ECL) intensities of a number of compounds which, in their study, were classed as interferents⁶⁷. Some of these emitted a significant amount of ECL and one of these, citric acid, also studied by Zhike *et al.*,⁶⁸ was investigated in this study. 0.1 M citric acid solution was scanned between +0.25 and +1.75 V at a scan rate of 0.1 V/s. The solution was analysed at pH values of 2.3, 7.2 and 9.75 but no electrochemical response was observed at any of these three values.

(3.4.7.3.2) Detection of Amines

Chemiluminescent detection of amines using tris(2,2'-bipyridine) ruthenium (III) in solution¹⁹¹ and immobilised within Nafion on an electrode surface⁷⁶ has been reported. Noffsinger & Danielson carried out a study comparing the relative CL emission intensity of primary, secondary and tertiary amines¹⁹¹. The aim of the experiment discussed here was determine if a similar pattern was observed using the CME. In this study, the primary, secondary and tertiary ethylamines were analysed.

In the present study, 0.1 M solutions of ethylamine, diethylamine and triethylamine in 10 mM sodium acetate buffer were analysed between the potential limits of +0.5 V and +1.5 V. Each amine solution was analysed at pH 5.8 and 11. pH 11 was the pH of the amine solution in buffer solution, pH 5.8 was the pH used by Noffsinger & Danielson^{52,191}. A solution of *n*-propylamine was also analysed. Table 3.3 overleaf shows the results of this experiment.

AMINE CONCENTRATION (M)	CL EMISSION INTENSITY AT pH 5.8 (mV)	CL EMISSION INTENSITY AT pH 11.0 (mV)
0.1 M ethylamine	0	0.53
0.1 M diethylamine	0	0.69
0.1 M triethylamine	0	3.51
0.1 M <i>n</i> -propylamine	-	0.23

Table 3.3: Chemiluminescence observed for the detection of amines

No emission was recorded for any of the amines at pH 5.8. This did not agree with the results obtained by Noffsinger and Danielson¹⁹¹, who quoted this pH as the optimum value for maximum CL.

However, signals were observed at pH 11. These results were in agreement with those of Brune & Bobbitt⁴¹, who reported that the CL emission for triethylamine was greater at more alkaline pH values, the optimum emission occurring at pH 9. A possible explanation for this apparent contradiction between the two papers was suggested by Brune & Bobbitt⁴¹. It appeared that in the study by Noffsinger and Danielson¹⁹¹, the Ru(bpy)₃³⁺ concentration may have been affected by the pH of the solution. Uchikura & Kirisawa¹⁹², who detected alicyclic tertiary amines using tris(2,2'-bipyridine) ruthenium (II), reported that the pH values at maximum CL intensities were shifted to the upper range, generally pH 8 and above, which also correlates with the results obtained in this study.

Noffsinger & Danielson⁵² compared the intensity of the CL emitted when electrogenerated Ru(bpy)₃³⁺ was reacted with primary, secondary and tertiary amines. The signal response of trialkylamines was a factor of 100 and 1000 greater than that for secondary and primary amines, respectively. This was attributed to the differences in the first ionization potentials of the different classes of compounds¹⁹¹. In the current research,

CL emitted followed the trend tertiary > secondary > primary, although the factors between the three ethylamines were significantly less than reported. In addition, Knight & Greenway⁵⁴ give a detailed discussion about the stabilising or destabilising effects of substituents (depending upon their nature and size) upon the radical intermediates formed in the reaction.

The chemiluminescent sensor used in this study, although not as sensitive as for the oxalate redox system, successfully detected aliphatic amines at pH 11 and was regenerated a number of times throughout the analysis.

(3.4.7.3.3) Detection of Amino Acids

Tryptophan and Valine, shown below, were selected for detection using a CME.

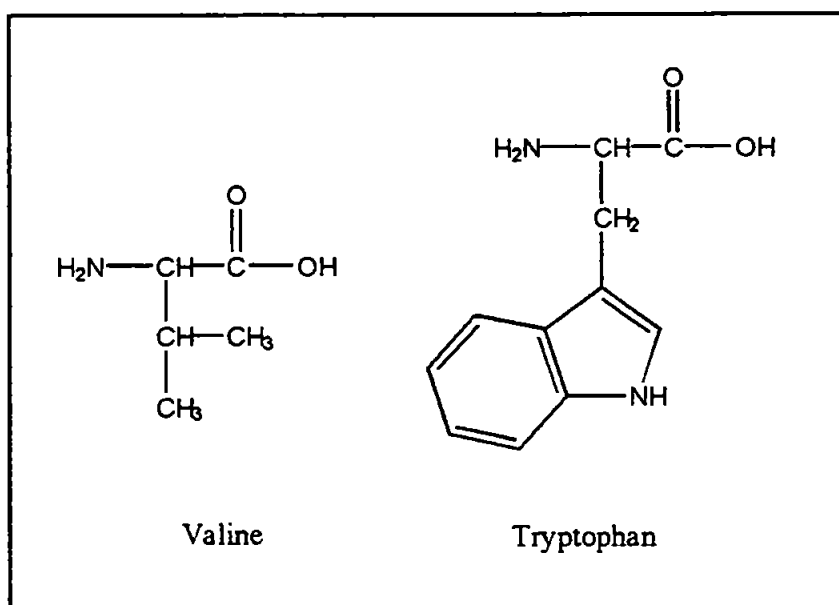


Figure 3.24: Structure of the two amino acids, valine (Val) and tryptophan (Trp)

The potential limits used were 0 V and + 1.75 V. The results for the detection of these two amino acids are given overleaf in Table 3.4.

pH	CL INTENSITY FOR 10 mM Trp (mV)	CL INTENSITY FOR 0.1 M Val (mV)
1.5	0	-
8.1	-	0
9.7	0	-
11.0	-	0.2
12.0	0	+VE 0.5, -VE 2.3

Table 3.4: Chemiluminescence observed for the detection of the amino acids Trp and Val

No CL was detected for the blank solutions at any of the pH values selected. Emission was observed for Val at very alkaline pH values, in agreement with the literature⁴¹. The increase in emission for Val with increasing pH and at a maximum of 11.0 was reported. No electrochemical response was observed at any pH for Trp in this study. The reason for this lack of reactivity is unknown. Detection using Ru(bpy)₃³⁺ in solution has been well reported in the literature^{53,61-63,193}. One possible reason is that the concentration used in this study was too low - the CME and associated apparatus has been proved to be less sensitive than Ru(bpy)₃²⁺ throughout these analyte detection studies and the concentration of Trp was only 10 mM due to its lack of solubility in the solvent chosen, as opposed to the usual concentration of 0.1 M. Another possible reason was due to the size of the molecule. Trp has a bulky indole group compared with the isopropyl group of Val. Thus, the 'pores' of the polymer on the electrode surface may be too small for the molecule to infiltrate the structure and react with the ruthenium centres. Although some reaction would have taken place at the electrode-solution interface, the light emission might not have been enough to be detected.

(3.5) CHEMILUMINESCENCE OF POLY-[RUTHENIUM TRIS(4-METHYL-4'-(E-PROP-2-ENYL)-2,2'-BIPYRIDINE) BIS(HEXAFLUOROPHOSPHATE)]

Introduction

The aim of this experiment was to investigate the properties of a novel CME coated with the polymer poly-ruthenium tris(4-methyl-4'-(E-prop-2-enyl)-2,2'-bipyridine) bis(hexafluorophosphate) and to examine its performance as a CL sensor.

Experimental Procedure

The electropolymerization of the novel complex ruthenium tris(4-methyl-4'-(E-prop-2-enyl)-2,2'-bipyridine) bis(hexafluorophosphate), $\text{Ru}(\text{ppbpy})_3^{2+}$, was described in section 3.1.5 (page 146). The resulting CME was analysed using 0.1 M oxalate solution at pH 6.5 by scanning between the potentials +0.5 to +1.5 V at a scan rate of 0.1 V/s.

Results & Discussion

The CME gave no response when immersed in the blank solution (Figure 3.25). Figure 3.26 shows the CL response of the electrode to oxalate. Subsequent analyses showed a diminished response. As only one set of results for this electrode have been obtained, the experiment needs to be repeated. However, from these preliminary investigations, this electrode has shown to be equally as sensitive as electrodes based upon poly-[$\text{Ru}(\text{vbpy})_3^{2+}$]. The difference in structure of the monomer has not altered its ability to electropolymerize and the fundamental properties of the film (conductance, chemiluminescence) also remain unchanged. The results obtained here prove that an electrochemically regenerable CME has been produced.

Figure 3.25

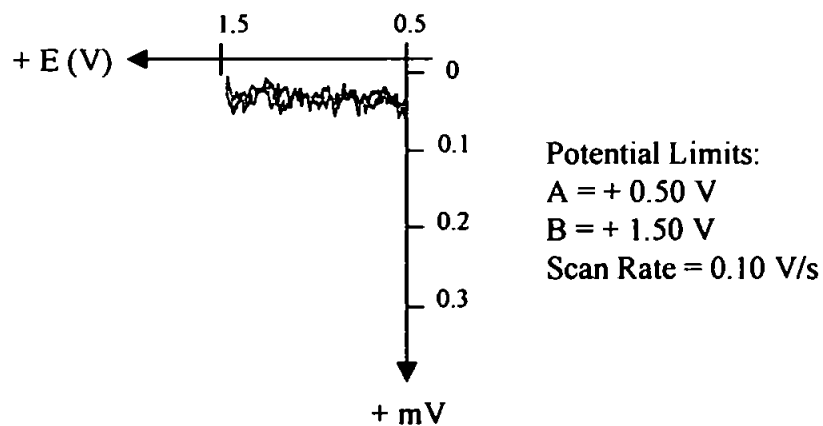


Figure 3.25: Chemiluminescent response of CME coated with poly-[Ru(ppbpy)₃²⁺] in a solution containing 0 M oxalate

Figure 3.26

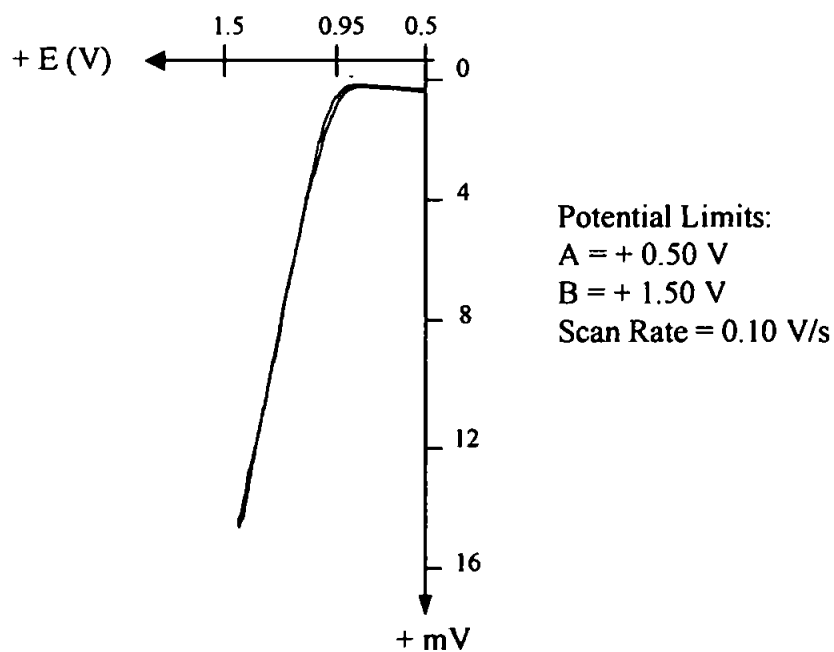


Figure 3.26: Chemiluminescent response of CME coated with poly-[Ru(ppbpy)₃²⁺] in a solution containing 0.1 M oxalate

(3.6) EXPERIMENTAL APPENDIX

(3.6.1) Instrumentation and Techniques Used for Analysis

Potentiostat; (1) Sycopel Scientific Scanning Ministat

Chart Recorders; (1) Recorderlab X-Y Recorder (2) CR Curken Y-T Recorder

PhotoMultiplier Tube (PMT); Oriel Corporation Company, Stamford, Comm.

Extended UV range, number 7062

High Voltage Power Supply (HVPS); EM1 Electron Tube Division Type PM 28B

pH Meters; (1) Hanna Instruments HI9025 Microcomputer pH meter (2) HI931402

Microprocessor pH meter

pH electrode; BDH Gelplas General Purpose Combination Cat. No. 309/1050/03

Optical Microscope; Olympus Technoscope with fibre-optic light source

Scanning Electron Microscope; Jeol JSM-6100

(3.6.2) Chemicals Used in This Study

Key; AS = Used as supplied

CHEMICAL (ABBREVIATION USED IN TEXT)	SUPPLIER	PREPARATION PRIOR TO USE
Acetic acid, glacial	BDH	Diluted - ~ 50 %
Acetonitrile HPLC Grade {ACN}	BDH	Dried by shaking with 4A Molecular Sieves ^{194,195} . Stored under nitrogen and filtered before use
Citric Acid, Analar	BDH	AS
Diethylamine, GPR	BDH	AS
Di-potassium hydrogen orthophosphate	BDH	AS
Ethylamine, 70 Wt. % Soln. in Water	Aldrich	AS
Molecular Sieve Type 4A, 1/16" pellets, Crystalline Sodium Aluminosilicate	BDH	Washed well with acetonitrile, allowed to dry, heated at 260 °C for 3 hrs, cooled over silica gel in desiccator. [Pellets reusable]
Nitrogen gas (white spot) < 5 ppm O ₂ , < 2 ppm H ₂ O	Air Products plc	Dried by passing through a calcium chloride guard tube.
Phosphorus pentoxide, 97 %	Aldrich	AS
Propylamine, Lab. Reagent	Sigma	AS
Ruthenium tris(2,2-bipyridine) dichloride. Water content 6 mol/mol. {Ru(bpy) ₃ } ²⁺	Sigma	Light sensitive - stored in the dark and refrigerated.
Sodium acetate anhyd. 99.0%, Analar	BDH	AS
Sodium oxalate, 99.5+%	Aldrich	AS
Tetra- <i>n</i> -butylammonium perchlorate > 98% (T), {TBAP}	Fluka	Stored over P ₂ O ₅ under vacuum for minimum of 24 hours
Tetraethylammonium perchlorate, 98%. Contains up to 10% water {TEAP}	Acros	Thrice recrystallised from water, stored over P ₂ O ₅ under vacuum for minimum of 24 hours

Table 3.5: Table of chemicals and their preparation for use in this study

CHEMICAL (ABBREVIATION USED IN TEXT)	SUPPLIER	PREPARATION PRIOR TO USE
Triethylamine, 99+ % {TEA}	Aldrich	AS
DL-Tryptophan, Sigma Grade	Sigma	AS
DL-Valine, 99+ %	Aldrich	AS

cont..

Table 3.5: Table of chemicals and their preparation for use in this study

Additional solvents not included in Table 3.5, unless otherwise stated, were from either Rathburns or BDH and used as supplied. Purified water from a Milli-Q system was used throughout. The resistivity was greater than $18 \text{ M}\Omega\text{cm}^{-1}$ in all cases.

Addresses of Suppliers

Acros (Fisher Scientific UK Ltd.), Loughborough, Leicestershire

Air Products plc, Basingstoke, Hants., England

Aldrich Chemical Co. Ltd., Gillingham, Dorset, England

BDH Chemicals Co., Poole, Dorset, England

Fluka (Sigma-Aldrich Co. Ltd.), Gillingham, Dorset, England

Sigma (Sigma-Aldrich Co. Ltd.), Poole, Dorset, England

CHAPTER 4

CONCLUSIONS & FURTHER WORK

(4.1) SUMMARY

The research in this study has covered three different areas. Firstly, the synthesis of the ruthenium tris(4-methyl-4'-vinyl-2,2'-bipyridine) bis(hexafluorophosphate) complex. The method by Abruña *et al.*¹⁴⁹ was used to obtain a good yield of the ligand 4-methyl-4'-vinyl-2,2'-bipyridine, which was then incorporated successfully into the ruthenium complex¹⁸¹. This route was then applied to the synthesis of the analogous ruthenium tris(4-methyl-4'-(*E*-prop-2-enyl)-2,2'-bipyridine) bis(hexafluorophosphate) complex. This complex and its precursor are novel compounds.

The second stage involved electropolymerization of the ruthenium tris(vinylbipyridine) monomer complex to immobilize the polymer poly-[ruthenium tris(4-methyl-4'-vinyl-2,2'-bipyridine) bis(hexafluorophosphate)] onto an electrode surface. Many of these chemically modified electrodes were produced and were used in the third stage, a preliminary investigation of the analytical capabilities of these electrodes.

The ability of the polymer films to exhibit chemiluminescence was studied by comparison with the ruthenium tris(2,2'-bipyridine) complex in solution, using the oxalate redox system as a model⁴². The effects of changing parameters such as potential, scan rate and pH upon the performance of the CME were all investigated and optimized to produce maximum CL emission. After each analysis, the redox centres within the polymer were regenerated for continued use of the electrode. The selected parameters were then used in studies of electrode lifetime, dynamic range and limit of detection for

the oxalate system. The electrodes were also used for the detection of a number of other analytes over a wide range of pH values.

The polymer poly-[ruthenium tris(4-methyl-4'-(*E*-prop-2-enyl)-2,2'-bipyridine) bis(hexafluorophosphate)] was produced using the same electropolymerization procedure as described for the formation of the analogous ruthenium tris(vinylbipyridine) polymer¹¹⁰. The resulting CME was used successfully for the detection of oxalate. Both the polymer and the CME are thought to be previously unreported in the literature.

In conclusion, this research fulfilled the aim of producing two electrochemically regenerable chemically modified electrodes for chemiluminescence analysis.

(4.2) FUTURE WORK

The aim of this research has been achieved but investigations have only touched upon the surface of an extensive area of chemistry. There is much scope for further studies.

The electropolymerization procedure for the manufacture of CME's is successful but there appears to be a lack of consistency in film quality and further work is clearly required to achieve fully reproducible polymer films. The optimum film thickness could be determined by studying CL emission as a result of varying the electropolymerization time. The surface coverage (Γ) of a complex on an electrode can be determined by studying the slow scan CV obtained when the electrode is placed in fresh electrolyte-containing solution. The value of Γ is estimated by integration of the charge under the voltammetric wave in a CV^{137,188}. The use of an electrochemical quartz crystal microbalance could also be used to determine the amount of polymer on the electrode

surface. The mass of the film present would give an indication of the number of redox-active centres present.

It is unclear at this stage exactly how the film thickness would affect the performance of the electrode. A thin film might improve the speed of response as less time may be required for anions to infiltrate the polymer. In contrast, a thicker film, containing more redox centres, may lower the limit of detection. However, there may be the disadvantage of problems with adherence of the polymer to the electrode.

Two further issues were encountered in the current research. Firstly, the degradation of the polymer film, as observed in the lifetime study. This study proved very successful but the lifetime of the electrode could be further extended if the degradation could be minimized. The decomposition was attributed either to the ruthenium centres becoming inactive over a period of time, perhaps because of a change in structure, or because of the possible leaching of ruthenium from the film. As a result of the latter suggestion, it is proposed that storage in oxalate may be a contributory factor but this had been employed to avoid the initial low chemiluminescence responses of the electrode. An alternative method of leaving the electrodes exposed to air is suggested. Ikeda *et al.* reported that electrodes still functioned after being stored in air in a closed vial¹²¹. It has also been shown that, provided care was taken to avoid damaging the thin films, coated electrodes could be stored in air for several weeks¹¹⁰. This could solve the problem of both low initial responses and leaching of redox active centres encountered in this study.

The main problem, however, is the narrow dynamic range and high limit of detection of the CME's produced. The focus of further research needs to be directed towards enhancing the chemiluminescence ability of electrodes and improving the instrumental set-up to allow for more sensitive detection.

To address the former issue, one of the possible variables in this study is the anion of the electrolyte. Although no electrolyte was used with oxalate, acetate was used for ascorbic acid and amines and hydrogen orthophosphate for valine. The effect of using different electrolytes upon the CL emission could be investigated. The size of the anion could be a contributory factor - a smaller anion may easily diffuse in and out of the polymer, enabling the analyte to diffuse more quickly into the polymer and increase the CL emission. This proposed investigation is based upon the research already published which studied the ability of a heptyl-thiol derivative of ruthenium tris(2,2'-bipyridine), adsorbed onto indium tin oxide substrates, to emit CL upon reaction with oxalate⁸². The identity of the electrolyte anion was discovered to have an effect on CL intensity. Use of perchlorate compared with sulfate or nitrate diminished the signal. It was postulated that ion-pairing of perchlorate with the adsorbed complex could have occurred and that an electroactive organic 'film' might have formed, which would not be penetrated by the oxalate anions. In addition, the perchlorate ion could be quenching the electronic excited state of the adsorbed complex.

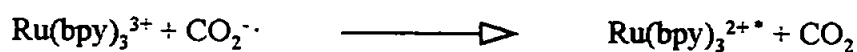
Stirring the analyte solution would enhance diffusion of the species to the electrode surface and might improve the CL intensity. A disadvantage of this could be that the motion of the solution may affect the adherence of the film to the electrode. Heating the analyte solution would also increase diffusion and could cause the polymer film to swell. This would increase the size of the pores within the polymer network, allowing for more rapid diffusion of analyte into the film and enhanced CL emission. However, the film might part from the platinum surface. Moreover, a number of reports in the literature¹⁹⁶⁻¹⁹⁹ have shown that the luminescence lifetime and quantum yield of $\text{Ru}(\text{bpy})_3^{2+}$ in solution increases with *decreasing* temperature. There is clearly the

potential for investigation of the temperature dependency of the ECL intensity from the CME.

Two further approaches for enhancement of CL emission have been considered. Firstly, ultrasound could be employed for this purpose. A marked increase in emission intensity (together with an improvement in reproducibility and stability) has been observed by irradiation of the $\text{Ru}(\text{bpy})_3^{2+}$ /oxalate system with ultrasound in the 40 and 60 kHz frequency range in two different reaction media²⁰⁰. Secondly, the use of a surfactant could also achieve this aim. Xu *et al.* noted an increase in ECL signal from the same system by using a certain amount of the surfactant Triton-X, which stabilized oxalate radical intermediates in solution²⁰¹. Both of these methods could be used in an attempt to increase the CL signal from the immobilised complex, although they may have a detrimental effect upon the stability of the polymer film.

As discussed in the introduction, the ruthenium tris(2,2'-bipyridine) complex in solution is capable of detecting a plethora of species. An investigation into how many of these could be detected using the CME is required. In addition, a study of a range of solvents could extend the analytical utility of the CME. The ruthenium complex in solution is usually dissolved in water or acetonitrile whereas when using the CME, only the analyte and not the complexed redox centres need to be soluble in the solvent.

The work in this study has focused upon the reduction of the ruthenium from the 3+ to the 2+ excited state using a reducing agent, for example, the oxalate anion radical ($\text{CO}_2^{\cdot-}$);



The effect of using an oxidizing agent is unknown but is considered to be a viable option.

The oxidizing agent chosen would be used to convert the ruthenium centres from the +1

to +2 excited state. Whether the potential used to generate the +1 state would affect the film in any way (either directly or by inducing undesired background electrochemistry) would have to be investigated. This suggestion of using an oxidizing agent certainly has potential, particularly considering the results from the study by White & Bard⁶⁹. The strongly oxidizing intermediate, $\text{SO}_4^{\cdot-}$, was generated during reduction of $\text{S}_2\text{O}_8^{2-}$ and successfully produced CL when reacted with electrogenerated $\text{Ru}(\text{bpy})_3^+$;



It was shown that the CL intensity obtained from this system was reported to be several times larger than that of previously reported systems based on $\text{Ru}(\text{bpy})_3^{2+}$. Use of $\text{SO}_4^{\cdot-}$ as a reductant may increase the chemiluminescence intensity from the CME's in this present study.

There is conflicting evidence in the literature about the effect of oxygen on the ECL intensity of luminescent transition metal complexes. Some consider this not to be an issue, however, it has been noted^{87,193} that molecular oxygen quenches excited states of luminescent transition metal complexes. However, continuous purging of the sample with argon⁸⁷ or nitrogen¹⁹³ improved the CL emission. The effect of purging of analyte solutions in this current study could be investigated as a possible method for improving the chemiluminescence intensity.

Once the intensity of the ECL emission of the CME was optimised, the system could be coupled with an analytical technique such as flow injection analysis (FLA), high performance liquid chromatography (HPLC) or capillary electrophoresis (CE). An on-line, automated system, possibly incorporating a separation step prior to detection could be produced for the sensitive determination of analytes in solution.

Use of a flow cell system should significantly improve sensitivity. Bowie *et al.* described how a simple FI-CL manifold could maximize the CL emission intensity measured by the detector⁹. By optimising the dimensions of the mixing and detector coils, flow rates, pH, temperature and reagent concentrations, a highly sensitive yet compact, inexpensive system would be capable of giving rapid and reproducible results. For a technique such as this, in-line chemical and physical treatment of the sample and removal of matrix interferences is possible for improved detection of the desired species. Various detectors are available for CL detection but PMT's are still the most common choice and probably the most sensitive. Cooling the PMT housing (typically -10 to -20 °C) can reduce dark current and minimize baseline noise⁹.

Finally, the research could extend into the realms of altering the structure of the monomer complex. The polymerizable moiety has already been lengthened - the prop-2-enyl group has been added to the bipyridine ligand instead of the vinyl group. The resulting novel ruthenium complex was successfully electropolymerized and the CME was able to detect oxalate. Optimization of potential, scan rate, dynamic range, limit of detection and pH, together with the study of electrode lifetime and the detection of various analytes, which were all performed on the tris-vinylbipyridine coated electrode, could then be applied to this and other novel CME's.

As long as a polymerizable group is present upon the ligand, there is the potential for electropolymerization to occur. There is some debate over whether the size of the vinyl-containing ligand is important. The ability of a variety of ligands to electropolymerize has been studied and no particular inhibition of film formation was observed when the vinyl-containing ligand had greater steric bulk¹⁴⁰. However, for some complexes, steric crowding of 4,4'-substituents on a bipyridine ligand resulted in less

efficient electropolymerization¹²⁸⁻¹³⁰. This issue needs to be considered in further studies. The manufacture of a whole range of different CME's is nevertheless feasible, with the possibility of improved electrode performance.

The analytes able to be detected currently by the CME's produced in this study have possible applications in many different fields, for example, in food analysis or for environmental monitoring purposes. The ultimate aim would be to miniaturise the CME. If only a small volume of liquid were required to pass by the detector, it could be placed very close to the electrode surface, minimising the amount of chemiluminescence reflected and subsequently lost. This would maximise the amount of light detected and hopefully improve the limit of detection. If miniaturisation were successful, this would have particular impact in the area of biomedical science. The rapid response is certainly a desirable feature for this type of application in comparison with techniques which require lengthy analysis. Miniaturisation could also enable the system to be portable and therefore be used in the field, *e.g.* for measuring levels of analytes in water.

In conclusion, this research has yielded a valuable contribution in the study of chemiluminescent sensors. A regenerable detection system has been created which, with further development, could be a serious competitor in the development of robust and re-usable yet low-cost and easy-to-operate sensors.

REFERENCES

- (1) Gafney, H.D. & Adamson, A.W., *J. Chem. Ed.*, 1975, 52, 7, pp 480-481
'Chemiluminescence. An Illuminating Experiment.'
- (2) Robards, K. & Worsfold, P.J., *Analytica Chimica Acta*, 1992, 266, pp 147-173
Review. 'Analytical Applications of Liquid-phase Chemiluminescence.'
- (3) Kricka, L.J. & Thorpe, G.H.G., *The Analyst*, 1983, 108, pp 1274-1296
'Chemiluminescence and Biological Methods in Analytical Chemistry.'
- (4) Hurtubise, R.J. in
'Encyclopaedia of Analytical Science', 1995, Vol. 5, pp 2733-2756, Academic Press,
Editor-in-chief, Townshend, A.
- (5) Kankare, J. in
'Encyclopaedia of Analytical Science', 1995, Vol. 1, pp 608-632, Academic Press,
Editor-in-chief, Townshend, A.
- (6) Cotton, F.A., Wilkinson, G. & Gaus, P.L.
'Basic Inorganic Chemistry', 1987, 2nd Edition, John Wiley & Sons, Inc, New York
- (7) Skoog, D.A. & Leary, J.J.
'Principles of Instrumental Analysis', 1992, 4th Edition, Saunders College Publishing
- (8) Suppan, P.,
'Chemistry and Light', 1994, The Royal Society of Chemistry
- (9) Bowie, A.R., Sanders, M.G. & Worsfold, P.J., *J. Biolumin. Chemilumin.*, 1996, 11,
pp 61-90
'Analytical Applications of Liquid Phase Chemiluminescence Reactions - A Review.'

(10) Knight, A.W., *Trends in Analytical Chemistry*, 1999, 18, 1, pp 47-62

'A Review of Recent Trends in Analytical Applications of Electrogenerated Chemiluminescence.'

(11) Jirka, G.P. & Nieman, T.A., *Mikrochimica Acta*, 1994, 113, 3-6, pp 339-347

'Modulated Potential Electrogenerated Chemiluminescence of Luminol and $\text{Ru}(\text{bpy})_3^{2+}$.'

(12) Rozhitskii, N.N., *Russian Journal of Analytical Chemistry USSR*, (English Translation), 1992, 47, pp 1288-1310

'Electrochemiluminescence Analysis of Solutions.'

(13) Knight, A.W. & Greenway, G.M., *The Analyst*, 1994, 119, pp 879-890

'Occurrence, Mechanisms and Analytical Applications of Electrogenerated Chemiluminescence.' A Review.

(14) Brandt, W.W., Dwyer, F.P. & Gyarfas, E.C. in

Chemistry Reviews, 1954, 54, from page 960

'Chelate Complexes of 1,10-Phenanthroline and Related Compounds.'

(15) McWhinnie, W.R. & Miller, J.D. in

Advances in Inorganic Chemistry and Radiochemistry, 1969, 12, from page 135, Academic Press, Eds., Emeléus, H.J. & Sharpe, A.G.

'The Chemistry of Complexes Containing 2,2'-Bipyridyl, 1,10-Phenanthroline, or 2,2',6',2"-Terpyridyl as Ligands.'

(16) Summers, L.A. in

Advances in Heterocyclic Chemistry, 1984, 35, from page 282, Academic Press, Ed., Katritsky, A.

'The Bipyridines'

(17) Burstall, F.H., *J. Chem. Soc.*, 1936, pp 173-175

'Optical Activity Dependent on Co-ordinated Bivalent Ruthenium.'

(18) Juris, A., Barigelletti, F., Campagna, S., Balzani, V., Belser, P., von Zelewsky, A. in *Coordination Chemistry Reviews*, 1988, **84**, pp 85-277

'Ruthenium (II) Polypyridine Complexes - Photophysics, Photochemistry, Electrochemistry and Chemiluminescence.'

(19) Krausz, E. & Ferguson, J. in

'Progress in Inorganic Chemistry', 1989, Vol. 37, pp 293-390, J. Wiley & Sons, Inc., Ed. Lippard, S.J

'The Spectroscopy of the $[\text{Ru}(\text{bpy})_3]^{2+}$ System.'

(20) Balzani, V., Bolletta, F., Gandolfi, M.T. & Maestri, M., in

Topics in Current Chemistry; 'Organic Chemistry & Theory', 1978, No. 75, Ed., Dewar

'Biomolecular Electron Transfer Reactions of the Excited States of Transition Metal Complexes.'

(21) Watts, R.J., *J. Chem. Ed.*, 1983, **60**, 10, 834-842

'Ruthenium Polypyridyls. A Case Study.'

(22) Balzani, V. & Bolletta, F., *Comments Inorg. Chem.*, 1983, **2**, pp 211-226

'Transition Metal Complexes as Mediators in Photochemical and Chemiluminescence Reactions.'

(23) Kalyanasundaram, K. in

Coordination Chemistry Reviews, 1982, **46**, pp 159-244, Elsevier Scientific Publishing Company, Amsterdam

'Photophysics, Photochemistry and Solar Energy Conversion with Tris(bipyridyl) Ruthenium (II) and its Analogues.'

- (24) Kalyanasundaram, K.,
'Photochemistry of Polypyridine and Porphyrin Complexes', 1992, Academic Press Ltd.
- (25) Seddon, E.A. & Seddon, K.R.,
'The Chemistry of Ruthenium', 1984, Elsevier
- (26) Balzani, V., Bolletta, F., Ciano, M. & Maestri, M., *J. Chem. Ed.*, 1983, **60**, *6*,
pp 447-450
'Electron Transfer Reactions Involving Light.'
- (27) Paris, J.P. & Brandt, W.W., *J. Am. Chem. Soc.*, 1959, **81**, pp 5001-5002
'Charge Transfer Luminescence of a Ruthenium (II) Chelate.'
- (28) Hercules, D.M. & Lytle, F.E., *J. Am. Chem. Soc.*, 1966, **88**, *20*, pp 4745-4746
'Chemiluminescence from Reduction Reactions.'
- (29) Tokel, N.E. & Bard, A.J., *J. Am. Chem. Soc.*, 1972, **94**, *8*, pp 2862-2863
'Electrogenerated Chemiluminescence. IX. Electrochemistry and Emission from Systems
Containing Tris(2,2'-bipyridine) ruthenium (II) Dichloride.'
- (30) Gerardi, R.D., Barnett, N.W. & Lewis, S.W., *Analytica Chimica Acta*, 1999, **378**,
pp 1-41
'Analytical applications of tris(2,2'-bipyridyl) ruthenium (III) as a chemiluminescent
reagent.'
- (31) Barnett, N.W., Bowser, T.A., Gerardi, R.D. & Smith B., *Analytica Chimica Acta*,
1996, **318**, pp 309-317
'Determination of Codeine in Process Streams Using Flow-Injection Analysis with
Chemiluminescence Detection.'

(32) Sutin, N. & Creutz, C., *Adv. Chem. Ser.*, 1978, 168, pp 1-27

'Properties and Reactivities of the Luminescent Excited States of Polypyridine Complexes of Ruthenium (II) and Osmium (II).'

(33) Tokel-Takvoryan, N.E., Hemingway, R.E. & Bard, A.J., *J. Am. Chem. Soc.*, 1973, 95, 20, pp 6582-6589

'Electrogenerated Chemiluminescence. XIII. Electrochemical and Electrogenerated Chemiluminescence Studies of Ruthenium Chelates.'

(34) Bolletta, F. & Bonafede, S., *Pure & Applied Chem.*, 1986, 58, 9, pp 1229-1232

'Chemiluminescence and Electrochemiluminescence of Co-ordination Compounds.'

(35) Lee, W.-Y., *Mikrochimica Acta*, 1997, 127, 1-2, pp 19-39

Fundamental Review. 'Tris (2,2'-bipyridyl) ruthenium (II) Electrogenerated Chemiluminescence in Analytical Science.'

(36) Gerardi, R.D., Barnett, N.W. & Jones, P., *Analytica Chimica Acta*, 1999, 388, 1-2, pp 1-10

'Two Chemical Approaches for the Production of Stable Solutions of Tris(2,2'-bipyridyl) Ruthenium (III) for Analytical Chemiluminescence.'

(37) Lytle, F.E. & Hercules, D.M., *Photochemistry and Photobiology*, 1971, 13, pp 123-133

'Chemiluminescence from the Reduction of Aromatic Amine Cations and Ruthenium (III) Chelates.'

(38) Rubinstein, I. & Bard, A.J., *J. Am. Chem. Soc.*, 1981, 103, pp 512-516

'Electrogenerated Chemiluminescence. 37. Aqueous Ecl Systems Based on Ru(2,2'-Bipyridine)₃²⁺ and Oxalate or Organic Acids.'

- (39) Nonidez, W.K. & Leyden, D.E., *Analytica Chimica Acta*, 1978, 96, pp 401-404
'Effect of Reducing Agents of Pharmacological Importance on the Chemiluminescence of Tris-(2,2'-Bipyridine) Ruthenium (II).'
- (40) Brune, S.N. & Bobbitt, D.R., *Anal. Chem.*, 1992, 64, 2, 166-170
'Rôle of Electron-Donating / Withdrawing Character, pH, and Stoichiometry on the Chemiluminescence Reaction of Tris(2,2'-bipyridyl) ruthenium (III) with Amino Acids.'
- (41) Brune, S.N. & Bobbitt, D.R., *Talanta*, 1991, 38, 4, pp 419-424
'Effect of pH on the Reaction of Tris(2,2'-Bipyridyl) Ruthenium (III) with Amino-Acids: Implications for their Detection.'
- (42) Rubinstein, I., Martin, C.R. & Bard, A.J., *Anal. Chem.*, 1983, 55, pp 1580-1582
'Electrogenerated Chemiluminescent Determination of Oxalate.'
- (43) Lee, W.-Y. & Nieman, T.A., *Anal. Chem.*, 1995, 67, pp 1789-1796
'Evaluation of Use of Tris(2,2'-Bipyridyl) ruthenium (III) as a Chemiluminescent Reagent for Quantitation in Flowing Streams.'
- (44) Sharma, S., Nath, R. & Thind, S.K., *Scanning Microscopy*, 1993, 7, 1, pp 431-441
'Recent Advances in Measurement of Oxalate in Biological Materials.'
- (45) Chang, M.-M., Saji, T. & Bard, A.J., *J. Am. Chem. Soc.*, 1977, 99, 16, pp 5399-5403
'Electrogenerated Chemiluminescence. 30. Electrochemical Oxidation of Oxalate Ion in the Presence of Luminescers in Acetonitrile Solutions.'
- (46) Rubinstein, I. & Bard, A.J., *J. Am. Chem. Soc.*, 1981, 103, 17, pp 5007-5013
'Polymer Films on Electrodes. 5. Electrochemistry and Chemiluminescence at Nafion-Coated Electrodes.'

(47) Uchikura K., *Bunseki Kagaku*, 1990, 39, pp 323-326

'Determination of Oxalate by FIA with Electrogenerated Chemiluminescence Detection.'

(48) Saka Amiri, M.A. & Vallon, J.J., *Analytica Chimica Acta*, 1994, 299, 1, pp 75-79

'Comparison of Performances and Analytical Applications of Two Immobilized Oxalate Oxidase Sensors.'

(49) Skotty, D.R., Lee, W.-Y. & Nieman, T.A., *Anal. Chem.*, 1996, 68, pp 1530-1535

'Determination of Dansyl Amino Acids and Oxalate by HPLC with Electrogenerated Chemiluminescence Detection Using Tris(2,2'-Bipyridyl) Ruthenium (II) in the Mobile Phase.'

(50) Skotty, D.R. & Nieman, T.A., *J. Chrom. B*, 1995, 665, pp 27-36

'Determination of Oxalate in Urine and Plasma Using Reversed-Phase Ion-Pair High-Performance Liquid Chromatography with Tris(2,2'-Bipyridyl) Ruthenium (II)-Electrogenerated Chemiluminescence Detection.'

(51) Barnett, N.W., Bowser, T.A. & Russell, R.A., *Analytical Proceedings Including Analytical Communications*, 1995, 32, 2, pp 57-59

'Determination of Oxalate in Alumina Process Liquors by Ion Chromatography with Post Column Chemiluminescence Detection.'

(52) Noffsinger, J.B. & Danielson, N.D., *J. Chrom.*, 1987, 387, pp 520-524

'Liquid Chromatography of Aliphatic Trialkylamines with Post-Column Chemiluminescent Detection Using Tris(2,2'-Bipyridine) Ruthenium (III).'

(53) Bolden, M.E. & Danielson, N.D., *J. Chrom. A.*, 1998, 828, pp 421-430

'Liquid Chromatography of Aromatic Amines with Photochemical Derivatization and Tris(Bipyridine) ruthenium (III) Chemiluminescence Detection.'

(54) Knight, A.W. & Greenway, G.M., *The Analyst*, 1996, 121, pp 101R-106R

'Relationship Between Structural Attributes and Observed Electrogenerated Chemiluminescence (ECL) Activity of Tertiary Amines as Potential Analytes for the Tris(2,2-Bipyridine) Ruthenium (II) ECL Reaction.' A Review.

(55) Holeman, J.A. & Danielson, N.D., *J. Chrom. A*, 1994, 679, pp 277-284

'Liquid Chromatography of Antihistamines Using Post-Column Tris(2,2'-Bipyridine) ruthenium (III) Chemiluminescence Detection.'

(56) Targove, M.A. & Danielson, N.D., *J. Chromatographic Science*, 1990, 28, pp 505-509

'High-Performance Liquid Chromatography of Clindamycin Antibiotics Using Tris(Bipyridine)-ruthenium (III) Chemiluminescence Detection.'

(57) Danielson, N.D., He, L., Noffsinger, J.B. & Trelli, L., *Journal of Pharmaceutical and Biomedical Analysis*, 1989, 7, 11, pp 1281-1285

'Determination of Erythromycin in Tablets and Capsules Using Flow Injection Analysis with Chemiluminescence Detection.'

(58) Monji, H., Yamaguchi, M., Aoki, I. & Ueno, H., *J. Chrom. B*, 1997, 690, 1-2, pp 305-313

'Highly Sensitive High-Performance Liquid Chromatographic Determination Method for a New Erythromycin Derivative, EM523, and its Major Metabolites in Human Plasma and Urine Using Post-Column Tris(2,2'-bipyridine) ruthenium (III) Chemiluminescence Detection.'

(59) Greenway, G.M., Knight, A.W. & Knight, P.J., *The Analyst*, 1995, 120, pp 2549-2552

'Electrogenerated Chemiluminescent Determination of Codeine and Related Alkaloids and Pharmaceuticals with Tris(2,2'-bipyridine) ruthenium (II).'

(60) Barnett, N.W., Hindson, B.J., Lewis, S.W. & Purcell, S.D., *Analytical Communications*, 1998, 35, 10, pp 321-324

'Determination of Codeine, 6-Methoxycodone and Thebaine Using Capillary Electrophoresis with Tris(2,2'-bipyridyl) ruthenium (II) Chemiluminescence Detection.'

(61) He, L., Cox, K.A. & Danielson N.D., *Anal. Letts.*, 1990, 23, 2, pp 195-210

'Chemiluminescence Detection of Amino Acids, Peptides, and Proteins Using Tris-2,2'-Bipyridine Ruthenium (III).'

(62) Uchikura, K. & Kirisawa, M., *Chem. Letts.*, 1991, pp 1373-1376

'Chemiluminescence of Tryptophan with Electrogenerated Tris(2,2'-Bipyridine) Ruthenium (III).'

(63) Uchikura, K. & Kirisawa, M., *Anal. Sci.*, 1991, 7, pp 971-973

'Electrochemiluminescence Determination of D-, L-Tryptophan Using Ligand-Exchange High-Performance Liquid Chromatography.'

(64) Hijikata, Y., Hara, K., Shiozaki, Y., Murata, K. & Sameshima, Y., *J. Clin. Chem. Clin. Biochem.*, 1984, 22, 4, pp 291-299

'Determination of Free Tryptophan in Plasma and Its Clinical Applications.'

(65) Chen, X., Jia, L., Wang, X. & Hu, G., *Anal. Sci.*, 1997, 13 Supplement, pp 71-75

'Study of the Electrochemiluminescence Based on the Reaction of Hydroxyl Compounds with Ruthenium Complex.'

- (66) Chen, X., Sato, M. & Lin, Y., *Microchemical Journal*, 1998, 58, 1, pp 13-20
'Study of the Electrochemiluminescence Based on Tris(2,2'-bipyridine) ruthenium (II) and Alcohols in a Flow Injection System.'
- (67) Chen, X. & Sato, M., *Anal. Sci.*, 1995, 11, 5, pp 749-754
'High-Performance Liquid Chromatographic Determination of Ascorbic Acid in Soft Drinks and Apple Juice Using Tris(2,2'-bipyridine) ruthenium (II) Electrochemiluminescence.'
- (68) Zhike, H., Hua, G., Liangjie, Y., Shaofang, L., Hui, M., Xiaoyan, L. & Yun'e, Z., *Talanta*, 1998, 47, pp 301-304
'Pulse Injection Analysis with Chemiluminescence Detection: Determination of Citric Acid Using Tris-(2,2'-Bipyridine) Ruthenium (II).'
- (69) White, H.S. & Bard, A.J., *J. Am. Chem. Soc.*, 1982, 104, 25, pp 6891-6895
'Electrogenerated Chemiluminescence. 41. Electrogenerated Chemiluminescence and Chemiluminescence of the $\text{Ru}(2,2'\text{-bpy})_3^{2+}\text{-S}_2\text{O}_8^{2-}$ System in Acetonitrile-Water Solutions.'
- (70) Blackburn, G.F., Shah, H.P., Kenten, J.H., Leland, J., Kamin, R.A., Link, J., Peterman, J., Powell, M.J., Shah, A., Talley, D.B., Tyagi, S.K., Wilkins, E., Wu, T.-G. & Massey R.J., *Clinical Chemistry*, 1991, 37, 9, pp 1534-1539
'Electrochemiluminescence Detection for Development of Immunoassays and DNA Probe Assays for Clinical Diagnostics.'
- (71) Ege, D., Becker, W.G. & Bard, A.J., *Anal. Chem.*, 1984, 56, pp 2413-2417
'Electrogenerated Chemiluminescent Determination of $\text{Ru}(\text{bpy})_3^{2+}$ at Low Levels.'

- (72) Hsueh, Y.-T., Smith, R.L. & Northrup, M.A., *Transducers '95, Eurosenors (IX)*, 'Proceedings from The 8th International Conference on Solid-State Sensors and Actuators, and Eurosenors (IX)', Stockholm, Sweden, June 25-29, 1995, pp 768-771
'A Microfabricated, Electrochemiluminescence Cell for the Detection of Amplified DNA.'
- (73) Liang, P., Dong, L.W. & Martin, M.T., *J. Am. Chem. Soc.*, 1996, **118**, 38, pp 9198-9199
'Light Emission from Ruthenium-Labeled Penicillins Signaling Their Hydrolysis by Beta-Lactamase.'
- (74) Liang, P., Sanchez, R.I. & Martin, M.T., *Anal. Chem.*, 1996, **68**, 14, pp 2426-2431
'Electrochemiluminescence-Based Detection of Beta-Lactam Antibiotics and Beta-Lactamases.'
- (75) Adachi, T. in
'Encyclopaedia of Analytical Science', 1995, Vol. 7, pp 4481-4487, Academic Press,
Editor-in-chief, Townshend, A.
- (76) Downey, T.M. & Nieman, T.A., *Anal. Chem.*, 1992, **64**, pp 261-268
'Chemiluminescence Detection Using Regenerable Tris(2,2'-bipyridyl) Ruthenium (II) Immobilized in Nafion.'
- (77) Martin, A.F. & Nieman, T.A., *Analytica Chimica Acta*, 1993, **281**, pp 475-481
'Glucose Quantitation Using an Immobilized Glucose Dehydrogenase Enzyme Reactor and a Tris(2,2'-Bipyridyl) ruthenium (II) Chemiluminescent Sensor.'
- (78) Egashira, N., Kumasako, H. & Ohga, K., *Anal. Sci.*, 1990, **6**, 6, pp 903-904
'Fabrication of a Fiber-Optic-Based Electrochemiluminescence Sensor and Its Application to the Determination of Oxalate.'

(79) Egashira, N., Kumasako, H., Kurauchi, Y. & Ohga, K., *Anal. Sci.*, 1994, 10, 3, pp 405-408

'Selective Determination of Oxalate with a Ruthenium (II) Complex / Nafion-Modified Electrode Combined with a Carbon Dioxide Sensor.'

(80) Rubinstein, I. & Bard, A.J., *J. Am. Chem. Soc.*, 1980, 102, pp 6641-6642

'Polymer Films on Electrodes. 4. Nafion-Coated Electrodes and Electrogenenerated Chemiluminescence of Surface-Attached Ru(bpy)₃²⁺.'

(81) Zhang, X. & Bard, A.J., *J. Phys. Chem.*, 1988, 92, 20, pp 5566-5569

'Electrogenenerated Chemiluminescent Emission from an Organized (L-B) Monolayer of a Ru(bpy)₃²⁺-Based Surfactant on Semiconductor and Metal Electrodes.'

(82) Jackson, W.A. & Bobbitt, D.R., *Microchemical Journal*, 1994, 49, 1, pp 99-109

'Voltammetric and Chemiluminescent Characterization of a Heptyl-thiol Derivative of Ruthenium Tris Bipyridine Self-Adsorbed onto Indium Tin Oxide Substrates.'

(83) Sawaguchi, T., Ishio, A., Matsue, T., Uchida, I. & Itaya, K., *Denki Kagaku*, 1989, 57, 12, pp 1209-1210

'Electrogenenerated Chemiluminescence from Ru(bpy)₂(ndbpy) LB Monolayer and its Application to Oxalate Sensor.'

(84) Egashira, N., Kondoh, N., Kurauchi, Y. & Ohga, K., *Denki Kagaku*, 1992, 60, 12, pp 1148-1151

'Selective Determination of Oxalate Ions with a Fiber-Optic Electrochemiluminescence Sensor Having a Carbon Paste Electrode Modified with Bis(2,2'-bipyridine)-(4,4'-dinonadecyl-2,2'-bipyridine) ruthenium (II).'

(85) Zhao, C.-Z., Egashira, N., Kurauchi, Y. & Ohga, K., *Electrochimica Acta*, 1998, **43**, 14-15, pp 2167-2173

'Electrochemiluminescence Oxalic Acid Sensor Having a Platinum Electrode Coated with Chitosan Modified with a Ruthenium (II) Complex.'

(86) Zhao, C.-Z., Egashira, N., Kurauchi, Y. & Ohga, K., *Anal. Sci.*, 1998, **14**, 2, pp 439-441

'Electrochemiluminescence Sensor Having a Pt Electrode Coated with a Ru(bpy)₃²⁺-Modified Chitosan / Silica Gel Membrane.'

(87) Blanchard, R.M., Martin, A.F., Nieman, T.A., Guerrero, D.J. & Ferraris, J.P., *Mikrochimica Acta*, 1998, **130**, 1-2, pp 55-62

'Electrogenerated Chemiluminescence Using Solution Phase and Immobilized Tris(4,7-diphenyl-1,10-phenanthroline)disulfonic acid ruthenium (II).'

(88) Abruña, H.D. in

Coordination Chemistry Reviews, 1988, **86**, pp 135-189, Elsevier Science Publishers, Amsterdam

'Coordination Chemistry in Two Dimensions: Chemically Modified Electrodes.'

(89) Kaneko, M. & Wöhrlé, D., in

Advances in Polymer Science; 'Electronic Applications', 1988, **84**, from page 141, Springer-Verlag, Berlin, Heidelberg

'Polymer-Coated Electrodes: New Materials for Science and Industry.'

(90) Albery, W.J. & Hillman, A.R. in

Annual Review. C. Royal Society of Chemistry, 1981, Chapter 10, pp 377-437

'Modified Electrodes.'

(91) Redepenning, J.G., *Trends in Analytical Chemistry*, 1987, 6, 1, pp 18-22

'Chemically Modified Electrodes: A General Overview.'

(92) Faulkner, L.R., *Chemical & Engineering News*, 1984, 62, pp 28-45

'Chemical Microstructures on Electrodes.'

(93) Merz, A. in

Topics in Current Chemistry, Electrochemistry (IV), 1990, 152 from page 51, Springer-Verlag, Berlin, Ed., Dewar, M.J.S. *et al.*

'Chemically Modified Electrodes.'

(94) Murray, R. W. in

'Molecular Design of Electrode Surfaces. Techniques of Chemistry', 1992, Vol. (XXII), Chapter 1, pp 1-48, John Wiley & Sons Inc.

'Introduction to the Chemistry of Molecularly Designed Electrode Surfaces.'

(95) Calvert, J.M., Sullivan, B.P. & Meyer, T.J. in

'Chemically Modified Surfaces in Catalysis and Electrocatalysis.', A.C.S. Symposium Series 192, 1982, Chapter 9, pp 158-183, American Chemical Society, Washington D.C., Ed., Miller, J.S.

'Reductive Chloride Ion Loss and Electropolymerization Techniques in Preparing Metallopolymer Films on Electrode Surfaces.'

(96) Murray, R. W., in

'Electroanalytical Chemistry, A Series of Advances', 1984, 13, from page 192, Marcel Dekker Inc., Ed., Bard, A.J.

'Chemically Modified Electrodes.'

(97) Murray, R. W., *Acc. Chem. Res.*, 1980, 13, pp 135-141

'Chemically Modified Electrodes.'

(98) IUPAC Recommendations 1997, *Pure and Applied Chemistry*, 1997, **69**, *6*, pp 1317-1323

‘Chemically Modified Electrodes: Recommended Terminology and Definitions.’

(99) Dong, S. & Wang, Y., *Electroanalysis*, 1989, **1**, pp 99-106

Review Article: ‘The Application of Chemically Modified Electrodes in Analytical Chemistry.’

(100) Murray, R.W., Ewing, A.G. & Durst, R.A., *Anal. Chem.*, 1987, **59**, *5*, 379A-390A

‘Chemically Modified Electrodes. Molecular Design for Electroanalysis.’

(101) Bergbreiter, D.E. in

‘Chemically Modified Surfaces in Catalysis and Electrocatalysis.’, A.C.S. Symposium Series 192, 1982, Chapter 1, American Chemical Society, Washington D.C., Ed., Miller, J.S.

‘Chemically Modified Surfaces in Catalysis.’

(102) Abruña, H.D., Calvert, J.M., Denisevich, P., Ellis, C.D., Meyer, T.J., Murphy Jr., W.R., Murray, R.W., Sullivan, B.P. & Walsh, J.L. in

‘Chemically Modified Surfaces in Catalysis and Electrocatalysis.’, A.C.S. Symposium Series 192, 1982, Chapter 8, pp 132-157, American Chemical Society, Washington D.C., Ed., Miller, J.S.

‘Transfer of Solution Reactivity Properties to Electrode Surfaces.’

(103) Baldwin, R.P. & Thomsen, K.N., *Talanta*, 1991, **38**, *1*, pp 1-16

‘Chemically Modified Electrodes in Liquid Chromatography Detection: A Review.’

(104) Lane, R.F. & Hubbard, A.T., *The Journal of Physical Chemistry*, 1973, 77, 11, pp 1401-1410

'Electrochemistry of Chemisorbed Molecules. I. Reactants Connected to Electrodes through Olefinic Substituents.'

(105) Lane, R.F. & Hubbard, A.T., *The Journal of Physical Chemistry*, 1973, 77, 11, pp 1411-1421

'Electrochemistry of Chemisorbed Molecules. II. The Influence of Charged Chemisorbed Molecules on the Electrode Reactions of Platinum Complexes.'

(106) Lenhard, J.R. & Murray, R.W., *J. Electroanal. Chem.*, 1977, 78, pp 195-201

'Chemically Modified Electrodes. Part VII. Covalent Bonding of a Reversible Electrode Reactant to Pt Electrodes Using an Organosilane Reagent.'

(107) Ghosh, P.K. & Spiro, T.G., *J. Electrochem. Soc.: Electrochemical Science & Technology*, 1981, 128, 6, pp 1281-1287

'Electroactive Coatings of Tris(bipyridyl)- and Tris(*o*-phenanthroline)-Ruthenium (II) Attached to Electrodes via Hydrosilylation or Electropolymerization of Vinyl Derivatives.'

(108) Murray, R.W., *Ann. Rev. Mater. Sci.*, 1984, 14, pp 145-169

'Polymer Modification of Electrodes.'

(109) Kaneko, M., Yamada, A., Tsuchida, E. & Kurimura, Y., *J. Polymer Science, Polymer Letters Edition*, 1982, 20, 11, pp 593-597

'Preparation and Photochemical Reactivity of Poly(styrene-co-Vinylbipyridine) Pendant Ru(bpy)₃²⁺ Complex.'

(110) Denisevich, P., Abruña, H.D., Leidner, C.R., Meyer, T.J. & Murray, R.W., *Inorg. Chem.*, 1982, 21, pp 2153-2161

'Electropolymerization of Vinylpyridine and Vinylbipyridine Complexes of Iron and Ruthenium: Homopolymers, Copolymers, Reactive Polymers.'

(111) Abruña, H.D., Denisevich, P., Umaña, M., Meyer, T.J. & Murray, R.W., *J. Am. Chem. Soc.*, 1981, 103, 1, pp 1-5

'Rectifying Interfaces Using Two-Layer Films of Electrochemically Polymerized Vinylpyridine and Vinylbipyridine Complexes of Ruthenium and Iron on Electrodes.'

(112) Abruña, H.D. & Bard, A.J., *J. Am. Chem. Soc.*, 1982, 104, pp 2641-2642

'Electrogenerated Chemiluminescence. 40. A Chemiluminescent Polymer Based on the Tris(4-vinyl-4'-methyl-2,2'-bipyridyl) ruthenium (II) System.'

(113) Wier, L.M., Guadalupe, A.R. & Abruña, H.D., *Anal. Chem.*, 1985, 57, 9, pp 2009-2011

'Multiple-Use Polymer-Modified Electrodes for Electroanalysis of Metal Ions in Solution.'

(114) Cha, S.K. & Abruña, H.D., *Anal. Chem.*, 1990, 62, pp 274-278

'Determination of Copper at Electrodes Modified with Ligands of Varying Coordination Strength: A Preamble to Speciation Studies.'

(115) Cha, S.K., Kasem, K.K. & Abruña, H.D., *Talanta*, 1991, 38, 1, pp 89-93

'Effects of Competitive Binding on the Amperometric Determination of Copper with Electrodes Modified with Chromotrope 2B.'

(116) Cha, S.K., Ahn, B.K., Hwang, J.-U. & Abruña, H.D., *Anal. Chem.*, 1993, 65, pp 1564-1569

‘Determination of Mercury at Electrodes Modified with Polymeric Films of [Ru(vbpy)₃]²⁺ Incorporating Amino Acids.’

(117) Kasem, K.K. & Schultz, F.A., *Journal of Inorganic and Organometallic Polymers*, 1994, 4, 4, pp 377-390

‘Ion Exchange and Charge Transport Properties of Polymeric Tris(4-vinyl-4'-methyl-2,2'-bipyridine) Ruthenium (II) Films.’

(118) Kasem, K.K. & Schultz, F.A., *Canadian Journal of Chemistry*, 1995, 73, 6, pp 858-864

‘Electrochemistry of Polyoxometalates Immobilized in Ion Exchange Polymer Films.’

(119) Ontko, A.C., Armistead, P.M., Kircus, S.R. & Thorp, H.H., *Inorg. Chem.*, 1999, 38, 8, pp 1842-1846

‘Electrochemical Detection of Single-Stranded DNA Using Polymer-Modified Electrodes.’

(120) Albarelli, M.J., White J.H., McMillan, M., Bommarito, G.M. & Abruña, H.D. in A.C.S. Symposium Series (Electrochemical Surface Science: Molecular Phenomenon Electrode Surface), 1988, 378, Chapter 15, pp 216-232

‘In situ Surface Extended X-Ray Absorption Fine Structure at Chemically Modified Electrodes.’

(121) Ikeda, T., Schmehl, R., Denisevich, P., Willman, K. & Murray, R.W., *J. Am. Chem. Soc.*, 1982, 104, 10, pp 2683-2691

‘Permeation of Electroactive Solutes through Ultrathin Polymeric Films on Electrode Surfaces.’

(122) Ewing, A.G., Feldman, B.J. & Murray, R.W., *J. Phys. Chem.*, 1985, 89, 7, pp 1263-1269

'Permeation of Neutral, Cationic, and Anionic Electrode Reactants Through a Polycationic Polymer Film as a Function of Electrolyte Concentration.'

(123) Hurrell, H.C. & Abruña, H.D., *Mol. Cryst. Liq. Cryst.*, 1988, 160, pp 377-388

'Conductivity Studies of Metal Coordination Polymers of Cobalt, Iron, Ruthenium, and Osmium Vinylbipyridine Complexes.'

(124) Leidner, C.R. & Murray, R.W., *J. Am. Chem. Soc.*, 1985, 107, 3, pp 551-556

'Estimation of the Rate of Electron Transfers between Two Contacting Polymer Surfaces.'

(125) Leidner, C.R., Sullivan, B.P., Reed, R.A., White, B.A., Crimmins, M.T., Murray, R.W., & Meyer, T.J., *Inorg. Chem.*, 1987, 26, 6, pp 882-891

'Synthesis and Electropolymerization of Distyrylbipyridine and Methylstyrylbipyridine Complexes of Iron, Ruthenium, Osmium, Rhenium, and Cobalt.'

(126) Beer, P.D., Kocian, O. & Mortimer, R.J., *J. Chem. Soc., Dalton Trans.*, 1990, pp 3283-3288

'Novel Mono- and Di-ferrocenyl Bipyridyl Ligands: Syntheses, Electrochemistry, and Electropolymerisation Studies of Their Ruthenium (II) Complexes.'

(127) Beer, P.D., Kocian, O., Mortimer, R.J. & Ridgway, C., *J. Chem. Soc., Chem. Comm.*, 1991, pp 1460-1463

'Syntheses, Co-ordination, Spectroscopy and Electropolymerisation Studies of new Alkynyl and Vinyl Linked Benzo- and Aza-crown Ether-Bipyridyl Ruthenium (II) Complexes. Spectrochemical Recognition of Group IA / IIA Metal Cations.'

(128) Beer, P.D., Kocian, O., Mortimer, R.J. & Ridgway, C., *The Analyst*, 1992, 117, 1247-1249

'Surface Modification with Macrocyclic-Containing Redox-Active Polymers: Towards the Design of Novel Spectroelectrochemical Group IA/IIA Metal Cation Sensors.'

(129) Beer, P.D., Kocian, O., Mortimer, R.J. & Ridgway, C., *J. Chem. Soc., Dalton Trans.*, 1993, 17, pp 2629-2638

'New Alkynyl- and Vinyl-Linked Benzo- and Aza-crown Ether-bipyridyl Ruthenium (II) Complexes which Spectrochemically Recognize Group IA and IIA Metal Cations.'

(130) Beer, P.D., Kocian, O., Mortimer, R.J. & Ridgway, C., *J. Chem. Soc., Faraday Trans.*, 1993, 89, 2, pp 333-338

'Cyclic Voltammetry of Benzo-15-crown-5 Ether-vinyl-bipyridyl Ligands, their Ruthenium (II) Complexes and Bismethoxyphenyl-vinyl-bipyridyl Ruthenium (II) Complexes.'

(131) Beer, P.D., Kocian, O., Mortimer, R.J. & Ridgway, C. & Stradiotto, N.R., *J. Electroanal. Chem.*, 1996, 408, pp 61-66

'Electrochemical Polymerisation Studies of Aza-15-crown-5 vinyl-2,2'-bipyridine Ruthenium (II) Complexes.'

(132) Beer, P.D., Mortimer, R.J., Szemes, F. & Weightman, J.S., *Anal. Comm.*, 1996, 33, 365-366

'Selective Fluorimetric Recognition of Dihydrogen Phosphate Over Chloride Anions by a Novel Ruthenium (II) Bipyridyl Receptor Complex.'

(133) Beer, P.D. & Cadman, J., *New Journal of Chemistry*, 1999, 23, 4, pp 347-349

'Phosphate Anion Binding and Luminescent Sensing in Aqueous Solution by Ruthenium (II) Bipyridyl Polyaza Receptors.'

(134) Elliott, C.M., Baldy, C.J., Nuwaysir, L.M. & Wilkins, C.L., *Inorg. Chem.*, 1990, 29, pp 389-392

'Electrochemical Polymerization of 4-Methyl-4'-vinyl-2,2'-bipyridine-Containing Metal Complexes: Polymer Structure and Mechanism of Formation.'

(135) Guarr, T.F. & Anson, F.C., *J. Phys. Chem.*, 1987, 91, 15, pp 4037-4043

'Electropolymerization of Ruthenium Bis(1,10-phenanthroline)(4-methyl-4'-vinyl-2,2'-bipyridine) Complexes through Direct Attack on the Ligand Ring System.'

(136) Gould, S., Earl, C., Sullivan, B.P. & Meyer, T.J., *J. Electroanal. Chem.*, 1993, 350, pp 143-159

'Reductive Electropolymerization of Complexes Containing an Aldehyde-Substituted Derivative of 2,2'-Bipyridine.'

(137) Gould, S., Strouse, G.F., Meyer, T.J. & Sullivan, B.P., *Inorg. Chem.*, 1991, 30, 14, pp 2942-2949

'Formation of Thin Polymeric Films by Electropolymerization. Reduction of Metal Complexes Containing Bromomethyl-Substituted Derivatives of 2,2'-Bipyridine.'

(138) Fussa-Rydel, O., Zhang, H.-T., Hupp, J.T. & Leidner, C.R., *Inorg. Chem.*, 1989, 28, 8, pp 1533-1537

'Electrochemical Assembly of Metallopolymeric Films via Reduction of Coordinated 5-Chlorophenanthroline.'

(139) Moss, J.A., Argazzi, R., Bignozzi, C.A. & Meyer, T.J., *Inorg. Chem.*, 1997, 36, 5, pp 762-763

'Electropolymerization of Molecular Assemblies.'

(140) Calvert, J.M., Schmehl, R.H., Sullivan, B.P., Facci, J.S., Meyer, T.J. & Murray, R.W., *Inorg. Chem.*, 1983, 22, 15, pp 2151-2162

'Synthetic and Mechanistic Investigations of the Reductive Electrochemical Polymerization of Vinyl-Containing Complexes of Iron (II), Ruthenium (II), and Osmium (II).'

(141) Della Ciana, L., Dressick, W.J. & von Zelewsky, A., *J. Heterocyclic Chemistry*, 1990, 27, 2, pp 163-165

'Synthesis of 4,4'-Divinyl-2,2'-bipyridine.'

(142) Baldy, C.J., Morrison, D.L. & Elliott, C.M., *Langmuir*, 1991, 7, 10, pp 2376-2379

'Electrostatic Interaction Effects on the Rate of Reductive Polymerization for Vinylbipyridine-Containing Metal Complexes.'

(143) Dalton, E.F., Surridge, N.A., Jernigan, J.C., Wilbourn, K.O., Facci, J.S. & Murray, R.W., *Chemical Physics*, 1990, 141, 1, pp 143-157

'Charge Transport in Electroactive Polymers Consisting of Fixed Molecular Redox Sites.'

(144) Baizer, M.M.,

'Organic Electrochemistry', 1973, Vol. (V), Marcel Dekker, New York, Ed. Baizer, M.M.

(145) Ghosh, P.K. & Spiro, T.G., *J. Am. Chem. Soc.*, 1980, 102, 17, pp 5543-5549

'Photoelectrochemistry of Tris(bipyridyl) ruthenium (II) Covalently Attached to n-Type SnO₂.'

(146) Furue, M., Sumi, K. & Nozakura, S., *J. Polymer Science: Polymer Letters Edition*, 1982, 20, pp 291-295

'Preparation of Poly(vinyl-2,2'-bipyridine) and Complex Formation with Various Metal Ions.'

(147) Case, F.H., *J. Am. Chem. Soc.*, 1946, 68, pp 2574-2577

'The Synthesis of Certain Substituted 2,2'-Bipyridyls.'

(148) Kaschig J. & Lohmann, D., *United States Patent*, Jan. 3rd, 1984, Patent No. 4,424,359

'Vinyl-Substituted 2,2'-Bipyridine Compounds.'

(149) Abruña, H.D., Breikss, A.I. & Collum, D.B., *Inorg. Chem.*, 1985, 24, 7, pp 987-988

'Improved Synthesis of 4-Vinyl-4'-methyl-2,2'-bipyridine.'

(150) Pitt, C.G., Bao, Y. & Seltzman, H.H., *Journal of Polymer Science: Polymer Letters Edition*, 1986, 24, pp 13-16

'The Synthesis of Polymers Containing the 2,2'-Bipyridine Ligand.'

(151) Rodd in

'Rodd's Chemistry of Carbon Compounds', 1976, Vol. (IV), Part F, Chapter 24, p 67, 2nd Edition, Elsevier, Amsterdam, Ed. Coffey, S.

(152) Leasure, R.M., Ou, W., Moss, J.A., Linton, R.W. & Meyer T.J., *Chemistry of Materials*, 1996, 8, 1, pp 264-273

'Spatial Electrochromism in Metallopolymeric Films of Ruthenium Polypyridyl Complexes.'

- (153) Peek, B.M., Ross, G.T., Edwards, S.W., Meyer, G.J., Meyer, T.J., & Erickson, B.W., *Int. J. Peptide Protein Res.*, 1991, **38**, pp 114-123
'Synthesis of Redox Derivatives of Lysine and Related Peptides Containing Phenothiazine or Tris(2,2'-bipyridine) ruthenium (II).'
- (154) CRC Handbook of Data on Organic Compounds, 1985, Vol. 1, CRC Press Inc., Eds. Weast, R.C. & Astle M.J.
- (155) Marker, A., Canty, A.J. & Brownlee, R.T.C., *Austrian Journal of Chemistry*, 1978, **31**, pp 1255-1263
'Carbon-13 Chemical Shifts of Some Pyridines, 2,2'-Bipyridyls and 1,10-Phenanthrolines.'
- (156) Daire, F., Bedioui, F., Devynck, J. & Bied-Charreton, C., *J. Electroanal. Chem.*, 1986, **205**, pp 309-318
'Electropolymerisation and Redox Properties of Bipyridyl-polypyrrole and Cu(II) Bipyridyl-polypyrrole Film Electrodes.'
- (157) Rodd in
'Rodd's Chemistry of Carbon Compounds', 1965, Vol. (I), Part C, Chapter 8, p 21, 2nd Edition, Elsevier, Amsterdam, Ed. Coffey, S.
- (158) Sigma-Aldrich Company Ltd., Personal Communication
- (159) Walker, J.J.
'Formaldehyde', 1975, 4th Edition, Krieger, Huntington, New York,
- (160) Corey, E.J. & Suggs, J.W., *Tetrahedron Letters*, 1975, **31**, pp 2647-2650
'Pyridinium Chlorochromate. An Efficient Reagent for Oxidation of Primary and Secondary Alcohols to Carbonyl Compounds.'

- (161) The Merck Index, An Encyclopaedia of Chemicals and Drugs, 1996, 12th Edition, Merck & Co. Inc., Ed. Budavari, S.
- (162) Finar, LL.
'Organic Chemistry, The Fundamental Principles', Vol. 1, 1973, 6th Edition, Longman Group U.K. Ltd.
- (163) McMurray, J.
'Organic Chemistry', 1988, 2nd Edition, Brooks/Cole Publishing Co.,
- (164) Kelly-Basetti, B.M., Krodkiewska, I., Sasse, W.H.F., Savage, G.P. & Simpson, G.W., *Tetrahedron Letters*, 1995, **36**, 2, pp 327-330
'Synthesis of Unsymmetrically 4-Substituted 2,2'-Bipyridines.'
- (165) Griggs, C.G. & Smith, D.J.H., *J. Chem. Soc., Perkin Trans. 1*, 1982, pp 3041-3043
'An Improved Synthesis of Amphiphilic 4,4'-Disubstituted 2,2'-Bipyridines.'
- (166) Ellison, D.K. & Iwamoto, R.T., *Tet. Letts.*, 1983, **24**, 1, pp 31-32
'Synthesis of Unsymmetrical 4,4'-Dialkyl-2,2'-Bipyridines.'
- (167) Della Ciana, L., Hamachi, I. & Meyer, T.J., *J. Org. Chem.*, 1989, **54**, pp 1731-1735
'Synthesis of Side-Chain Derivatives of 2,2'-Bipyridine.'
- (168) Walter, L.A. in
'Organic Syntheses', Coll. Volume 3, 1955, pp 757-759
- (169) Brown, H.C. & Eldred, N.R., *J. Am. Chem. Soc.*, 1949, **71**, pp 445-450
'Studies in Stereochemistry. XIV. Reaction of Triethylamine and Quinuclidine with Alkyl Halides; Steric Effects in Displacement Reactions.'
- (170) Ghosh, P.K., Personal Communication

(171) Collins J.E., Lamba, J.J.S., Love, J.C., McAlvin, J.E., Ng, C., Peters, B.P., Wu, X. & Fraser, C.L., *Inorg. Chem.*, 1999, 38, 9, pp 2020-2024

'Ruthenium (II) α -Diimine Complexes with One, Two, and Three 4,4'-Bis(hydroxymethyl)-2,2'-bipyridine and 4,4'-bis(chloromethyl)-2,2'-bipyridine Ligands: Useful Starting Materials for Further Derivatization.'

(172) Kotkar, D., Personal Communication

(173) Achar, S., Personal Communication

(174) Surridge, N.A., Keene, F.R., White, B.A., Facci, J.S., Silver, M. & Murray, R.W., *Inorg. Chem.*, 1990, 29, 24, pp 4950-4955

'Site Dilution of Osmium Polypyridine Complexes in Three Electron-Hopping Conductive Polymer Films on Electrodes by Electrochemical Copolymerization of Osmium with Ruthenium and with Zinc Complexes.'

(175) Aldrich Catalogue Handbook of Fine Chemicals, 1999-2000

(176) Nallas, G.N.A. & Brewer, K.J., *Inorganica Chimica Acta*, 1997, 257, 1, pp 27-35

'Chemically Modified Electrodes Incorporating Ruthenium Complexes of Polyazine Bridging Ligands.'

(177) Abruña, H.D., Personal Communication

(178) March, J.

'Advanced Organic Chemistry', 1985, p 904, 3rd Edition, John Wiley & Sons, Inc.

(179) Sumi, K., Furue, M. & Nozakura, S., *Journal of Polymer Science: Polymer Chemistry Edition*, 1984, 22, pp 3779-3788

'Preparation and Luminescence Properties of Tris(Bipyridine) Ruthenium (II)-Containing Vinyl Polymers: $\text{Ru}(\text{bpy})_2(\text{Poly-6-Vinyl-2,2'-Bipyridine})\text{Cl}_2$ and $\text{Ru}(\text{bpy})_2(\text{Poly-4-Methyl-4'-Vinyl-2,2'-Bipyridine})\text{Cl}_2$.'

(180) Lewis, A.L. & Miller, J.D., *J. Mater. Chem.*, 1993, 3, 8, pp 897-902

'Synthesis, Characterisation and Complexation Behaviour of a Series of Pyridyl- and Bipyridyl-based Hydrogel Membranes.'

(181) Bommarito, S.L., Lowery-Bretz, S.P. & Abruña, H.D., *Inorg. Chem.*, 1992, 31, pp 495-502

'Synthesis and Characterization of Redox Polymers of $[M(4\text{-vinyl-4}'\text{-methyl-2,2}'\text{-bipyridine})_3](PF_6)_2$ ($M = Ru, Os$).'

(182) Williams, C.E., Lowry, R.B., Braven, J. & Belt, S.T., *in press*;

'Novel Synthesis and Characterisation of Ruthenium tris(4-methyl-4'-vinyl-2,2'-bipyridine) Complexes.'

(183) Lowry, R.B., Personal Communication

(184) Rutherford, T.J., Reitsma, D.A. & Keene, F.R., *J. Chem. Soc., Dalton Trans.*, 1994, 24, pp 3659-3666

'Stereochemistry in Tris(bidentate ligand) ruthenium (II) Complexes Containing Unsymmetrical Polypyridyl Ligands.'

(185) Cook, M.J., Lewis, A.P. & McAuliffe, G.S.G., *Organic Magnetic Resonance*, 1984, 22, 6, pp 388-394

'Luminescent Metal Complexes. 4 - ^{13}C NMR Spectra of the Tris Chelates of Substituted 2,2'-Bipyridyls and 1,10-Phenanthrolines with Ruthenium (II) and Osmium (II).'

(186) Surridge, N.A., Zvanut, M., Keene, F.R., Sosnoff, C.S., Silver M. & Murray, R.W., *J. Phys. Chem.*, 1992, 96, 2, pp 962-970

'Effects of Mixed-Valent Composition and Bathing Environment on Solid-State Electron Self-Exchanges in Osmium Bipyridine Redox Polymer Films.'

(187) Morrish, J., unpublished results

(188) Gould, S., O'Toole, T.R. & Meyer, T.J., *J. Am. Chem. Soc.*, 1990, 112, 26, pp 9490-9496

'Photochemical Ligand Loss as a Basis for Imaging and Microstructure Formation in a Thin Polymeric Film.'

(189) Guadalupe, A.R., Chen, X., Sullivan, B.P. & Meyer, T.J., *Inorg. Chem.*, 1993, 32, 24, pp 5502-5512

'Oxo Complexes, pH Effects, and Catalysis in Films Formed by Electropolymerization.'

(190) Ghosh, P.K., Brunschwig, B.S., Chou, M., Creutz, C. & Sutin, N., *J. Am. Chem. Soc.*, 1984, 106, 17, pp 4772-4783

'Thermal and Light-Induced Reduction of $\text{Ru}(\text{bpy})_3^{3+}$ in Aqueous Solution.'

(191) Noffsinger, J.B. & Danielson, N.D., *Anal. Chem.*, 1987, 59, pp 865-868

'Generation of Chemiluminescence upon Reaction of Aliphatic Amines with Tris(2,2'-Bipyridine) Ruthenium (III).'

(192) Uchikura, K. & Kirisawa, M., *Anal. Sci.*, 1991, 7, 803-804

'Generation of Chemiluminescence upon Reaction of Alicyclic Tertiary Amines with Tris(2,2'-Bipyridine) Ruthenium (II) Using Flow Electrochemical Reactor.'

(193) Jackson, W.A. & Bobbitt, D.R., *Analytica Chimica Acta*, 1994, 285, pp 309-320

'Chemiluminescent Detection of Amino Acids Using in situ Generated $\text{Ru}(\text{bpy})_3^{3+}$.'

(194) Leonard, J., Lygo, B. & Procter G.,

'Advanced Practical Organic Chemistry', 1995, 2nd Edition, Blackie Academic & Professional

(195) Perrin, D.D. & Amarego, W.L.F.

'Purification of Organic Chemicals', 1988, 3rd Edition, Pergamon Press

(196) Lytle, F.E. & Hercules, D.M., *J. Am. Chem. Soc.*, 1969, **91**, 2, pp 253-257

'The Luminescence of Tris(2,2'-bipyridine) ruthenium (II) Dichloride.'

(197) Itoh, K. & Honda, K., *Chem. Letts.*, 1979, pp 99-102

'Temperature Dependence of ECL Efficiency of Tris(Bipyridine) Ruthenium (II) Complex.'

(198) Van Houten, J. & Watts, R.J., *J. Am. Chem. Soc.*, 1976, **98**, 16, pp 4853-4858

'Temperature Dependence of the Photophysical and Photochemical Properties of the Tris(2,2'-bipyridyl) ruthenium (II) Ion in Aqueous Solution.'

(199) Wallace, W.L. & Bard, A.J., *J. Phys. Chem.*, 1979, **83**, 10, pp 1350-1357

'Electrogenerated CL. 35. Temperature Dependence of the Electrochemiluminescence Efficiency of Ru(bpy)₃²⁺ in Acetonitrile and Evidence for Very High Excited State Yields from Electron Transfer Reactions.'

(200) Walton, D.J., Phull, S.S., Bates, D.M., Lorimer, J.P. & Mason, T.J., *Electrochimica Acta*, 1993, **38**, 2/3, pp 307-310

'Ultrasonic Enhancement of Electrochemiluminescence.'

(201) Xu, G., Cheng, L. & Dong, S., *Anal. Letts.*, 1999, **32**, 11, pp 2311-2326

'Effects of Heteropoly Acids and Surfactant on Electrochemiluminescence of Tris(2,2'-bipyridine) Ruthenium (II).'

BIBLIOGRAPHY

- Brett, C.M.A. & Brett, A.M.O.
'Electrochemistry. Principles, Methods, and Applications', 1998, Oxford University Press
- Joule, J.A., Mills, K. & Smith, G.F.
'Heterocyclic Chemistry', 1995, 3rd Edition, Chapman & Hall
- Katritzky, A.R.,
'Handbook of Heterocyclic Chemistry', 1985, Pergamon Press Ltd.
- Morrison, R.T. & Boyd, R.N.
'Organic Chemistry', 1992, 6th Edition, Prentice-Hall Inc.
- Norman, R.O.C. & Coxon, J.M.
'Principles of Organic Synthesis', 1993, 3rd Edition, Blackie Academic & Professional
- Pavia, D.L., Lampman, G.M. & Kriz Jr., G.S.,
'Introduction to Spectroscopy, A Guide for Students of Organic Chemistry', 1979, Saunders College Publishing.
- Vogel's Textbook of Practical Organic Chemistry, 1989, 5th Edition, Longman Group U.K. Ltd., Eds. Furniss, B.S., Hannaford, A.J., Smith, P.W.G. & Tatchell, A.R.
- Wayne, R.P.
'Photochemistry', 1970, Butterworth & Co. Ltd., London
- Dictionary of Chemistry, 1981, Intercontinental Book Productions Ltd., Series Ed. Daintith, J.